DOE/ET/10159-T22

WD-TR-81/015-004
DRAFT

DOE/ET/10159--T22

DE83 000822

COMPARISON OF FISCHER-TROPSCH REACTOR SYSTEMS

PHASE I -- FINAL REPORT

MASTER

Gregory J. Thompson
Mary L. Riekena
Anthony G. Vickers

DISCLAIMER

This report was prepared as an account of work sponsored by an agency of the United States Government. Neither the United States Government nor any agency thereof, nor any of their employees, makes any warranty, express or implied, or assumes any legal liability or responsibility for the accuracy, completeness, or usefulness of any information, apparatus, product, or process disclosed, or represents that its use would not infringe privately owned rights. Reference herein to any specific commercial product, process, or service by trade name, trademark, manufacturer, or otherwise, does not necessarily constitute or imply its endorsement, recommendation, or favoring by the United States Government or any agency thereof. The views and opinions of authors expressed herein do not necessarily state or reflect those of the United States Government or any agency thereof.

September 1981

PREPARED FOR THE
UNITED STATES DEPARTMENT OF ENERGY

UNDER CONTRACT NO. DE-AC01-78ET10159
(Formerly ET-78-C-01-3117)

UOP/SDC, A JOINT VENTURE
7929 WESTPARK DRIVE
MCLEAN, VIRGINIA 22102
(703) 790-9850

DISTRIBUTION OF THIS DOCUMENT IS UNLIMITED

DISCLAIMER

This report was prepared as an account of work sponsored by an agency of the United States Government. Neither the United States Government nor any agency Thereof, nor any of their employees, makes any warranty, express or implied, or assumes any legal liability or responsibility for the accuracy, completeness, or usefulness of any information, apparatus, product, or process disclosed, or represents that its use would not infringe privately owned rights. Reference herein to any specific commercial product, process, or service by trade name, trademark, manufacturer, or otherwise does not necessarily constitute or imply its endorsement, recommendation, or favoring by the United States Government or any agency thereof. The views and opinions of authors expressed herein do not necessarily state or reflect those of the United States Government or any agency thereof.

DISCLAIMER

Portions of this document may be illegible in electronic image products. Images are produced from the best available original document.

DISCLAIMER

This report was prepared as an account of work sponsored by the United States Government. Neither UOP, nor the United States, nor the United States Department of Energy, nor any of their employees, makes any warranty, express or implied, or assures any legal liability or responsibility for the accuracy, completeness, or usefulness of any information, apparatus, product, or process disclosed, or represents that its use would not infringe privately owned rights. Reference herein to any specific commercial product, process, or service by trade name, mark, manufacturer, or otherwise, does not necessarily constitute or imply its endorsement, recommendation, or favoring by the United States Government or any agency thereof.

FOREWORD

This report describes work performed between March, 1979 and December, 1980. This work was authorized as UOP/SDC Task Order No. 15, sponsored by the United States Department of Energy (DOE) under Contract No. DEAC01-78ET10159 (formerly ET-78-C-01-3117). The DOE task monitor is Mr. R. E. Hildebrand. The UOP/SDC liquefaction program manager is Mr. J. E. Gantt. The UOP task manager is Mrs. M. L. Riekena.

ACKNOWLEDGMENTS

The following individuals contributed to the execution of the program and the preparation of the report material.

George J. Czajkowski
David S. Hacker*
Edward C. Haun
Robert C. Koltz
Paul R. Lamb
Daniel J. O'Leary
Peter R. Pujado

* Consultant, University of Illinois, Chicago Circle Campus

TABLE OF CONTENTS

SECTION 1 -- SUMMARY

Franz Fischer and Hans Tropsch are credited with the discovery, in the 1920's, that carbon monoxide and hydrogen can be converted in the presence of a metal catalyst to a variety of hydrocarbon products. Just prior to and during World War II the "Fischer-Tropsch" reaction was commercialized in Germany and used to produce military fuels in fixed bed reactors. It was recognized from the start that this reactor system had severe operating and yield limitations and alternative reactor systems were sought. In 1955 the Sasol I complex, using an entrained bed (Synthol) reactor system, was started up in South Africa. Although this reactor was a definite improvement and is still operating, the literature is filled with proponents of other reactor systems, each claiming its own advantages. This report provides a summary of the results of a study to compare the development potential of three of these reactor systems with the commercially operating Synthol-entrained bed reactor system.

1.1 DESCRIPTION OF REACTOR SYSTEMS

The three reactor systems to be evaluated are:

1) The tube-wall reactor, developed by the U.S. Bureau of Mines (1), resembling a shell and tube heat exchanger having catalyst flame-sprayed onto the cooling tubes.

2) The slurry reactor as proposed by Koelbel (2), with catalyst suspended in an inert liquid, cooled by immersed coils, with syngas bubbled through the catalyst slurry.

3) An ebullating bed reactor, which is also a liquid phase reactor, but with larger size catalyst and heat removal from a circulating liquid stream that is also used to keep the bed expanded (3).

These three reactors and the entrained bed reactor are shown in Figure 1.1-1.

The commercial Synthol reactor is used as a benchmark against which the development potential of the other three reactors can be compared. This reactor system is operated by Sasol in South Africa. However, most of the information on which this study is based was supplied by the M. W. Kellogg Co. (4). No information beyond that in the literature on the operation of the Synthol reactor system was available for consideration in preparing this study, nor were any details of the changes made to the original Synthol system to overcome the operating problems reported in the literature (5).

Because of conflicting claims and results found in the literature, it was decided to concentrate a large part of this study on a kinetic analysis of the reactor systems, in order to provide a theoretical analysis of intrinsic strengths and weaknesses of the reactors unclouded by different catalysts, operating conditions and feed compositions. The remainder of the study considers the physical attributes of the four reactor systems, and compares their respective investment costs, yields, catalyst requirements and thermal efficiencies from simplified conceptual designs.

FIGURE 1.1-1

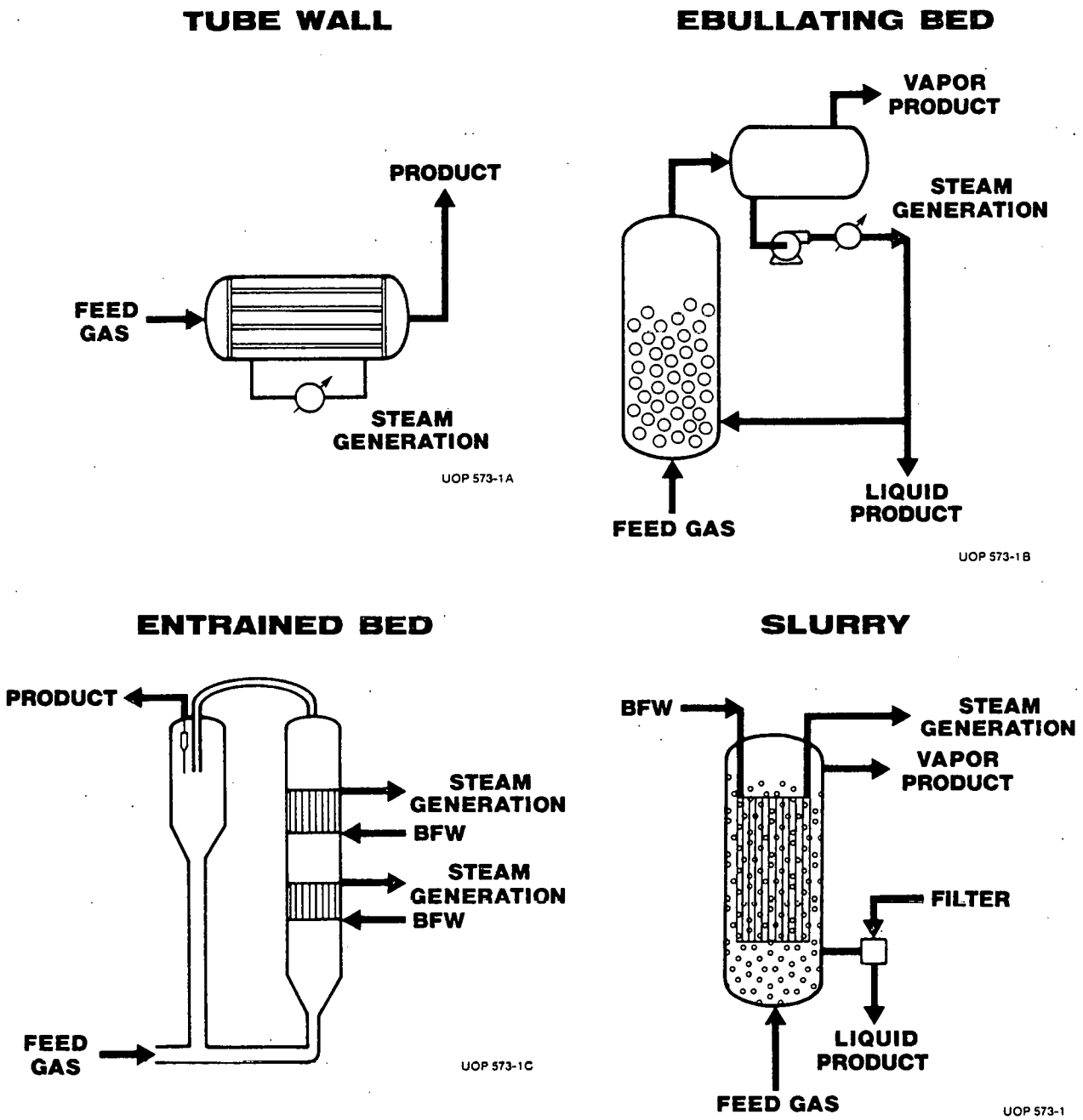
TUBE WALL
PRODUCT
FEED GAS
STEAM GENERATION
UOP 573-1A
EBULLATING BED
VAPOR PRODUCT
STEAM GENERATION
FEED GAS
LIQUID PRODUCT
UOP 573-1B
ENTRAINED BED
PRODUCT
STEAM GENERATION
BFW
STEAM GENERATION
BFW
FEED GAS
UOP 573-1C
SLURRY
BFW
STEAM GENERATION
VAPOR PRODUCT
FILTER
LIQUID PRODUCT
FEED GAS
UOP 573-1

1.2 KINETIC ANALYSIS

Before computer models for any of the reactors could be written, it was necessary to develop a mathematical description of the basic Fischer-Tropsch reactions. As none of the kinetic analyses in the literature were judged to be appropriate for this purpose, a new kinetic analysis was made which provided the basis for all of the work that followed. The mechanism selected for the basic Fischer-Tropsch reactions, shown in Figure 1.2-1, is discussed in detail in Section 4. The term "mechanism" as used here and elsewhere in this report refers to the reaction scheme used as the basis for the kinetic analysis. The principal features of this mechanism are the equilibrium between the olefin product and the catalyst sites, and the inclusion of the concentration of free catalyst sites [MH] in our assumption of steady state concentrations for all intermediates attached to the catalyst sites.

Once the steady state assumption is made, the mechanism can be analyzed by a simple mathematical definition of the reaction system that will predict the product composition from the concentrations of the reactants, and from the values of the various rate constants indicated on Figure 1.2-1. While further work is required to check the validity of this kinetic model of the Fischer-Tropsch reaction, the fact that good agreement was obtained on predicted values of rate constants when it was applied to data from different reactor systems operating under different conditions, does provide some encouragement that this rather simple analysis may be correct. Reactor models using this kinetic scheme, combined with the parallel shift reaction, were then prepared for the entrained bed, slurry and tube-wall reactors, and a considerable number of variable studies are presented in Section 4.

From consideration of the general mathematical definition of the Fischer-Tropsch reactions, combined with other reactions that may occur in parallel, the following general conclusions can be drawn regarding the best results that can be expected from this route for the liquefaction of syngas:

1) While further studies to determine if rate constants vary with carbon number are required before absolute conclusions can be drawn, it does appear that the reaction mechanism will not permit significant departure from the Schulz-Flory distribution of products, except with respect to methane and to a lesser extent light olefins (see Section 4.1).

2) Methane appears to result from at least two parallel reactions. The methane produced from the basic Fischer-Tropsch reactions will fall on a Schulz-Flory distribution with other paraffins, but considerably below a Schulz-Flory distribution for paraffins plus olefins, particularly for conditions that give high olefin-to-paraffin ratios. At high temperatures a significant increase in methane yield will result from a second route to methane, probably that suggested by Dry (6), and the methane yield will be significantly above that of a Schulz-Flory distribution.

3) The equilibrium between olefins and the catalyst site assumed in the kinetic analysis provides a basis for explaining why the light olefin yield can be below that predicted by a Schulz-Flory distribution, particularly when the light olefin concentration is increased by recycling light olefins to the reactor.

4) The shift reaction can be combined with the Fischer-Tropsch reaction in a single reactor, provided that reactor is operated at a low enough temperature to effectively eliminate free carbon formation.

5) A significant departure from the Schulz-Flory distribution could result if an additional termination step, such as aromatization of the olefins, is added to the reaction mechanism. This is not included in the scope of this paper.

6) The degree of polymerization of the product is highly dependent on CO concentration and, to a lesser extent, H_2 concentration, in addition to catalyst composition and temperature. The use of a kinetic model is, therefore, almost essential for understanding the significance of experimental data at various conversion levels and feed compositions, or when comparing results from plug flow reactors with those from a back-mixed system.

It is immediately apparent that these general kinetic conclusions support almost all of the claims made by Koelbel and co-workers (2, 7) for the superiority of the slurry reactor system. Koelbel operated his reactor at high conversion and low temperature. As this is a back-mixed reactor, these conditions resulted in a low CO concentration throughout the reactor. This in turn gave a degree of polymerization of about 4, which is close to the gasoline optimum, even at the low operating temperature. Had Koelbel operated at lower conversion at this low operating temperature, he would have had a much higher degree of polymerization and perhaps duplicated the serious problems related to the high liquid viscosity that were characteristic of Farley and Ray's work (8). The low temperature could also explain the low methane yield and lack of free carbon formation, while exploiting a simultaneous shift reaction by operating on feed gas with a low (0.7) H_2/CO ratio. The slurry reactor model also confirms Koelbel's claim that mass transfer has little influence under the operating conditions used. The only item in Koelbel's data not consistent with the kinetic model is the gasoline yield. With a Schulz-Flory product distribution, the gasoline yield peaks at about 48 wt-% of the product with a degree of polymerization of 4. The gasoline yield shown in Table 1.3-2 corresponds to 56 wt-% of the product. However, the gasoline yield for the operating conditions chosen for the slurry reactor, that does correspond to a Schulz-Flory distribution, is still substantially above that of the vapor phase reactors.

Similar application of these general conclusions to the entrained bed reactor serves to explain some of the weaknesses of this system. In this vapor phase reactor, the degree of polymerization must be held below that which would result in the condensation of liquid on the surface of the heat removal coils. It is, however, a plug flow system and the CO concentration at the entrance to the reactor will inherently be higher than in a back-mixed reactor running at high conversion. The degree of polymerization, therefore, is reduced by a combination of dilution of the feed CO with large amounts of recycle gas and by operation at high temperature. The high temperature puts the process into an operating region where free carbon formation is a substantial problem and causes deactivation and disintegration of the catalyst. To minimize free carbon formation, the

process is operated at a high hydrogen concentration. This combined with high temperature results in high methane yield. Also, the high hydrogen concentration combined with high levels of CO_2 in the recycle gas effectively eliminates the shift reaction, requiring external shift and an extra step for removal of acid gas on the syngas feed. The reactor model of this system also show it to be the least flexible of those studied due to the intermittent heat removal and the interrelation between operating variables.

FIGURE 1.2 -1

MECHANISM

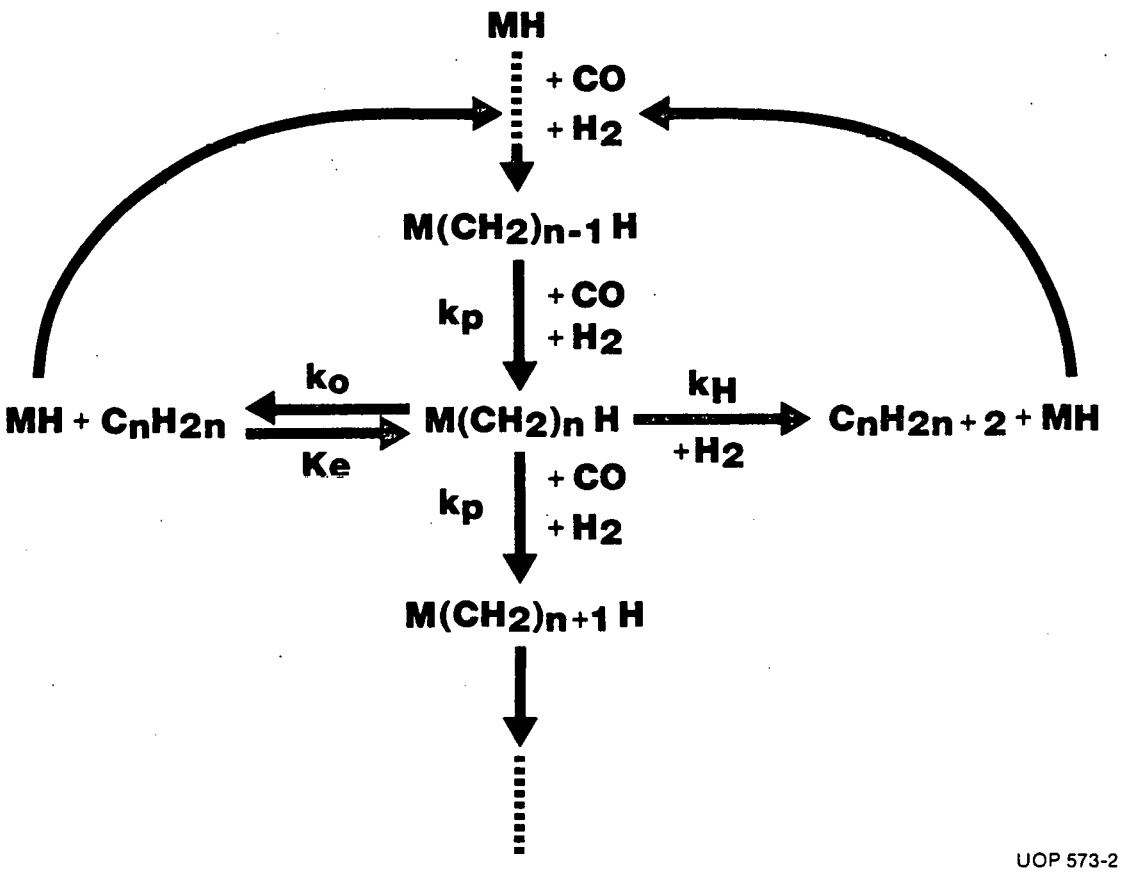

UOP 573-2

1.3 PHYSICAL COMPARISON

The basis used for physical comparison is shown in Table 1.3-1. The details of this physical comparison are presented in Section 5. The reactors were compared at the same operating pressure, but otherwise the operating parameters are those suggested in the literature for the entrained bed, slurry and ebullating bed reactors. The operating conditions for the tube-wall reactor were purposely selected to arrive at as reasonable a design as possible for this system. The tube-wall reactor model allowed a set of yields to be estimated consistent with these operating conditions. The model also showed that because of low catalyst concentration, this reactor must be operated at high temperature if the size of the reactor is to be reasonable. This will result in a high methane yield, and it is doubtful that the reactor could be operated at the conditions selected without appreciable problems with free carbon formation.

Table 1.3-2 provides a comparison of the yields claimed for Kellogg and Koelbel for the entrained bed and slurry reactors, respectively, with those estimated for the tube-wall reactor. Yields for the ebullating bed reactor would be similar to that shown for the slurry reactor. Only costs for major items of equipment are included in the cost comparison given in Table 1.1-3, where estimated costs of the three potential systems are presented as percentages of the commercially operating entrained bed system. A comparison of estimated catalyst requirements is presented in Table 1.3-4. This assumes that the cost per pound of the granular fused iron catalysts used in the entrained and ebullating bed reactors is the same. The costs per pound for the precipitated iron and flame-sprayed catalyst used in the slurry and tube-wall reactors, respectively, are estimated. Differences in energy utilization, expressed as percentages of the heat of reaction recovered, are shown in Table 1.3-5.

The results of the physical comparison indicate that two of the reactor types can be eliminated from further consideration. The tube-wall reactor can be dismissed because the investment cost and the catalyst replacement cost are more than double those of the Synthol reactor. Also, catalyst replacement is extremely laborious. The ebullating bed reactor

can be expected to show many of the advantages of the slurry system, but no catalyst is known to exist that combines physical stability with the activity assumed for this study. The catalyst replacement cost shown in Table 1.3-4 is, therefore, extremely high. The high cost of the liquid circulating system, combined with the low probability that this reactor will ever show a significant advantage over the slurry system, makes it unlikely that anyone will spend the effort required to develop a physically stable, high activity catalyst with large enough size for employing an ebullating bed reactor.

The physical comparison study shows a clear advantage for the slurry reactor over the others considered, and there is little doubt that the slurry reactor should be commercialized to provide a significant advance over the commercially operating Synthol-entrained bed reactor. The slurry reactor appears to be superior in having the lowest investment cost and catalyst requirements, combined with the highest gasoline yield and thermal efficiency and also providing the best hope for a continuously operating process. The final paragraphs of this summary briefly explain the reasons for the advantages of the slurry reactor over the entrained bed reactor.

TABLE 1.3-1 Basis for Physical Comparison

Design Rate: 28×10^6 SCFH CO + H_2 Converted
Operating Pressure: 400 psig

Reactor Type	Design Source	T_{out}, °F	GHSV, hr^{-1}	Recycle Ratio
Entrained	Kellogg	635	1100	2.3
Tube-Wall	U.S. Bureau of Mines	640	230	0.4
Slurry	Koelbel	527	480	0.1
Ebullating	Chem Systems	547	390	0.1

TABLE 1.3-2 Product Yields for Fischer-Tropsch Reactors

	Entrained Bed, lb/hr	Tube-Wall, lb/hr	Slurry, lb/hr
C_1	44,000	42,600	7,800
C_2-C_4	125,800	81,500	108,800
Gasoline (C_{5-11})	99,800	135,700	193,900
Diesel (C_{12-25})	32,800	52,100	25,100
Heavy (C_{26+})	12,100	10,400	2,300
Alcohols	27,900	13,300	5,700
Acids	4,300	5,200	-
Total	346,700	340,800	343,600

TABLE 1.3-3 Relative Investment Costs for Fischer-Tropsch Reactor Systems

	Entrained Bed	Tube-Wall	Slurry	Ebullating Bed
No. of Reactors	2	52	18	20
Reactor and Receiver	34	189	33	28
Other Vessels	30	-	<1	-
Heat Exchangers	32	15	10	21
Pumps	4	4	2	16
Total	100	208	45	65

TABLE 1.3-4 Catalyst Requirements for Fischer-Tropsch Reactors

Reactor	Entrained Bed	Tube-Wall	Slurry	Ebullating Bed
Catalyst Inventory, tons (ft^2)	900	(4.4×10^6)	100	3,000
Catalyst Usage, tons/yr (ft^2/yr)	8,400	(8.8×10^6)	950	18,000
Catalyst Cost, 10^3 $/yr	6,720	14,200	3,420	14,400

TABLE 1.3-5 Heat Recovery in Fischer-Tropsch Reactors

	Entrained Bed		Tube-Wall		Slurry	
	MM Btu/hr	% of ΔH_R	MM Btu/hr	% of ΔH_R	MM Btu /hr	% of ΔH_R
Steam Generation	690	36	1660	85	1790	91
BFW Heating	570	30	-	-	-	-
$H_{Products} - H_{Feed}$	640	34	300	15	170	9
Total Heat of Reaction ΔH_R	1900	100	1960	100	1960	100

1.4 COMPARISON OF SLURRY AND ENTRAINED BED REACTORS

The entrained bed reactor does have an advantage of scale over the other systems. For 28 MM SCFH of CO + H_2 converted, the basis used for this study, two entrained bed reactors were required in parallel compared to 18 in parallel for the slurry system. As would be expected, the cost of the reactors alone is lower for the entrained bed reactors. However, when the catalyst separation and catalyst recycle system are added, the cost advantage is completely offset. The cost of two entrained bed reactor systems, complete with catalyst separation and recycle equipment, is about equal to the cost of the 18 slurry reactors.

The vapor exiting the entrained bed system contains all of the catalyst lost due to the high rate of fracture and attrition (4.1 tons/day per reactor) (9). A quench tower is employed for the combined function of heat recovery and catalyst fines removal. This is a very expensive item that is not required for the slurry system. The heat exchange equipment is also much larger for the entrained bed system, reflecting lower temperature levels in the quench tower and higher flow rates due to the high recycle gas ratio. When the cost of all of the items included in the reactor/heat exchange envelope are added up, the entrained bed investment appears to be more than double that required for the slurry system. While it must be recognized that this was not a definitive cost analysis, this difference is large enough to show clearly that the slurry system should offer significant investment savings over the entrained bed system.

Two other points should be made in connection with this cost comparison. First, the cost comparison does not allow for any spare reactors. With 18 reactors in parallel and an apparent ability to operate continuously, it is unlikely that spare reactors would be required for the slurry system. However, the Synthol entrained bed system is apparently shut down every 50-60 days for catalyst replacement, and Sasol has reported adding an additional reactor system to Sasol I in order to maintain production rates (5). If spare reactors are required for the entrained bed system, this further increases the investment advantage of the slurry system. Second, the reactors were all compared at the same

operating pressure of 415 psig. While the entrained bed reactor is operated at 300 psig, the bulk of the work on the slurry system is at 160 psig. Although it is believed that operation of the slurry system at higher pressure could be accomplished with some modification to the catalyst composition, this requires pilot plant demonstration. If the slurry system were operated at 160 psig, more than twice the number of reactors would be required and a large portion of the investment advantage would be lost.

The higher thermal efficiency of the slurry system is readily explained by the much lower recycle gas requirements. The much lower content of water vapor in the slurry gas effluent is also a contributing factor.

The lower investment cost and higher thermal efficiency of the slurry reactor itself can be combined with further investment savings and increases in overall thermal efficiency when upstream shift and acid gas removal steps along with the downstream recycle gas system are eliminated.

While catalyst makeup requirements are not well established for the slurry system, the available data (10) indicate that the catalyst makeup requirement would be 11% of that required by the entrained bed system, if a precipitated catalyst is required.

Finally, it should be reemphasized that the above is a discussion of the potential advantage of a slurry reactor system over the commercially operating entrained bed system. The slurry system still has to be commercialized. However, a 5 foot diameter reactor was operated in the early 1950's, and scaleup to the 14 foot diameter reactor selected for this study should not be difficult. The potential advantages determined from this study for the slurry system, combined with similar conclusions arrived at in independent studies (10, 11), provide a clear incentive to justify work on its commercialization.

SECTION 2 - INTRODUCTION

This study provides an engineering evaluation of four reactor systems available for indirect liquefaction of coal via Fischer-Tropsch technology. The four reactor systems include the following:

1. The entrained bed reactor, originally developed by the M. W. Kellogg Company and operating commercially at Sasol.

2. The tube-wall reactor, developed by the U.S. Bureau of Mines.

3. The slurry reactor, developed by H. Koelbel and others.

4. The ebullating bed reactor, developed by the U.S. Bureau of Mines and also utilized by Chem Systems.

The evaluation consists of kinetic and physical comparisons. In the kinetic comparison, computer models of the first three systems are utilized to identify inherent differences in the reactors. Studies using the slurry reactor model also allow tentative conclusions regarding the ebullating bed reactor.

For the physical comparison, conceptual designs of each of the reactor systems allow estimation of investment costs, product yields, thermal efficiencies and other operational differences.

SECTION 3 - DISCUSSION OF THE FOUR REACTOR SYSTEMS

3.1 GENERAL

Task Order No. 15 required the comparison of the commercially operating entrained bed Synthol process with three other processes that have not been commercialized. This in itself created a difficulty, because processes frequently appear more attractive in the conceptual stage than after a process is put into final form following commercial experience. This study was conducted to determine if any of the three conceptual reactors appear to offer significant advantages over the commercial process. If a reactor is not attractive as a conceptual design, it probably should be dropped from further consideration. If any appears to have a significant advantage over the commercial process, the system in question deserves some further development effort prior to commercialization. Only after the process has been commercialized can a true comparison with the entrained bed process be made.

A review of the four reactor systems, prepared from data available in the literature, is presented in this section. Upon completion of this literature review, it was clear that there are many complications to preparing a comparison between these reactor systems. Although all of the reactors employed iron catalyst, results changed considerably depending on the presence of other metals or contaminants. Experiments on the various reactors were invariably carried out at widely different operating conditions (summarized in Table 3.1-1), at different conversion levels, and on different feed compositions. It was impossible to determine whether the different results reported in the literature were caused by differences between reactor systems or the choice of catalyst or operating conditions.

The problem presented by Task Order No. 15 was, therefore, approached on two fronts:

First: Carry out a fundamental kinetic study of each reactor system to sort out which of the claims in the literature with respect to yields are due to fundamental differences in the reactor systems.

Second: Make physical comparisons between the reactors, with operating conditions and yields selected in the light of the kinetic study, to determine the approximate differences in investment costs and operating efficiencies.

The results of the above two studies are presented in Sections 4 and 5, respectively, of this report.

3.2 ENTRAINED BED REACTOR

This reactor was originally developed and designed by M. W. Kellogg Company. Sasol has operated the process in Sasol I since 1955. The designs for the newer Sasol II and III projects were based on improvements developed by Sasol during operation of the first plant. Since Kellogg has published much more descriptive information on their version of the process (4), this study is largely based on the process as offered by Kellogg. Sasol has also published many papers, and these were used to supplement the Kellogg data.

There are many descriptions of the process in the literature (4, 5, 12, 14). The reactor system typically consists of three vessels in series with intercoolers. A separate vessel is required to recover the catalyst from the product vapor for recycle to the reactor. It is a vapor phase process, operated with about 75% CO conversion per pass. The process operates with considerable recycle gas (2.3/1 molar recycle/feed), consisting of 40 mol-% H_2, unconverted CO, large amounts of CO_2 and methane, and other light hydrocarbons. The feed syngas has a H_2/CO ratio of 2.4/1, and the combined feed has a H_2/CO ratio of 4.7/1. Preheated feed is introduced to the reactor at about 600°F and 365 psig. The catalyst separator runs at 635°F and 285 psig (4).

This is the only one of the reactor systems under consideration that is in commercial operation. However, no information on the performance of the commercial unit was available for the preparation of this study. Both Kellogg and Sasol regard such information as proprietary. While there is no detailed publication of Sasol's operating experience with the process, Rousseau (5) mentions that there were considerable difficulties when the plant was started up in 1955. Both conversion and selectivity were much lower than predicted by pilot plant data. Fouling of reactors was experienced, and frequent shutdowns were required for removal of deposits. Also, catalyst activity declined rapidly. A third reactor was added to the two originally built to maintain output when one reactor was down for cleaning and catalyst changing. The plant was substantially revamped in 1960 to correct deficiencies in the original design, but no details of the

changes are revealed. Hoogendoorn (12) indicates that improvement of the catalyst contributed to achieving "reasonably continuous operation". Although Kellogg designed the process for continuous catalyst addition and withdrawal, Sasol shuts down and replaces the entire load of catalyst after 50 days operation (12). In another publication, Hoogendoorn (13) also states that "It is necessary to limit the production of high boiling hydrocarbons, as a too high production of such material results in agglomeration of catalyst particles and loss of fluidization properties". There is also an indication (9) that some of the original loss of on-stream efficiency was due to mechanical problems with compressors. Perhaps the most significant information in the literature with respect to the operability of the Sasol plants is Sasol's decision to proceed with the Sasol II and III projects, which is a clear statement of their confidence that they have solved the operating problems. Sasol II was starting-up at the time of the writing this report. Publication of the start-up results is awaited with interest.

Dry (14, 15) has published interesting insights into the kinetics of the entrained bed system, particularly with respect to the effect of H_2/CO ratio on the degree of polymerization, and methane and free carbon formation. He indicates that the temperature used for the entrained bed system is above that where free carbon formation due to the Boudouard reaction ($2\ CO \rightarrow CO_2 + C$) occurs. The rate of free carbon formation can be reduced by increasing the hydrogen partial pressure, but Dry's mechanism indicates that this will result in additional methane formation in place of free carbon.

From the literature review, it can be concluded that Sasol's entrained bed system is a commercial process that can be operated successfully. The operating conditions require a high hydrogen partial pressure in the reactor in order to hold free carbon formation to a reasonable level. Free carbon formation results in loss of catalyst activity and in catalyst fracture, requiring the replacement of the catalyst inventory after 50 days operation. The operating conditions result in high methane formation, considerably above that predicted by a Schulz-Flory distribution (discussed in Section 4).

3.3 TUBE-WALL REACTOR

The concept of the tube-wall reactor originated at the U.S. Bureau of Mines. The first bench-scale studies were on methanation reactors (16) and the technique was later adapted for Fischer-Tropsch synthesis (1). In 1977 the R. M. Parsons Company published a Fischer-Tropsch Complex Conceptual Design/Economic Analysis (17), in which tube-wall reactors were to be used for the shift conversion, Fischer-Tropsch synthesis, and methanation. This study indicated the use of tube-wall reactors would result in an overall thermal efficiency for the plant of 69.7% and, in general, in a very attractive process.

The tube-wall reactor is illustrated in Figure 1-1. The concept is very simple and involves coating catalyst by a flame-spraying technique onto the surface of heat exchanger tubes. In the flame-spraying technique a high temperature flame is used to melt powdered catalyst onto a metal surface. Designs differ in the placement of catalyst either on the inside or the outside tube surface. In 1971 the C. E. Lummus Company undertook the design of a tube-wall methanator with catalyst applied to the inside of 2-inch diameter tubes (18). Parsons, in their conceptual design, chose to apply the catalyst to external fins.

In the Parsons-type design, the vapor phase reactants and products flow through the shell side of the reactor. Boiling water or oil inside the tubes carries away the heat released by the reaction. "Typical" operating conditions in a tube-wall reactor, as shown in Table 3.1-1, are a catalyst temperature of 580-640°F, pressure of 400 psig, and H_2/CO ratio in combined feed greater than 2.0. Some recycle gas is generally used, although this is not necessary for temperature control.

The major advantages claimed for the tube-wall reactor are excellent temperature control and near-isothermal operation (17). The high rate of heat transfer from the catalyst surface eliminates the possibility of hot spots forming on the catalyst surface. The catalyst surface temperature

is very near the coolant temperature and thus very nearly isothermal. It is believed that excellent temperature control will contribute to maintaining catalyst activity.

The main difficulty in applying the tube-wall reactor to Fischer-Tropsch synthesis is getting enough catalyst surface area into the reactor. Fischer-Tropsch catalysts generally show low activity and very little internal surface area; therefore, a large geometric surface area is required. At the same time, this surface area must be achieved within a configuration which allows recoating with new catalyst when the activity of the old catalyst declines.

3.4 SLURRY REACTOR

The concept of the slurry Fischer-Tropsch reactor was originated in 1951 by Koelbel and Ackermann (20). This early laboratory-scale work showed great potential when compared to existing fixed-bed technology and eventually became the performance target for subsequent research. In 1953, as part of a joint venture between Rheinpreussen and Koppers Company, a semiindustrial demonstration plant with a 5 foot diameter by 28 foot tall reactor began operation (7). Dr. H. Koelbel was also involved in this project, and the plant operated successfully until 1955.

During the postwar period other countries also began work on the slurry Fischer-Tropsch reactor. Farley and Ray operated a bench-scale reactor at the British Fuel Research Station in 1952 (21), and in 1964, a pilot plant-scale unit at Warren Spring Laboratory in Stevenage (8). From 1948 to 1953 the U.S. Bureau of Mines investigated the slurry reactor as part of a larger program investigating synthesis gas conversion (22, 23, 24). The last group to become involved was the Japanese (25). The incentive for their work, which was supported by the iron and steel industry, was to utilize the large quantities of CO-rich gas which are by-products of steel production.

In all of these investigations the basic slurry reactor concept has remained unchanged. It is illustrated in Figure 1-1. A synthesis gas feed is sparged into a reactor containing a liquid catalyst slurry. The liquid is largely paraffinic and generally inert to reaction. The reactor diameter is sized for a gas superficial velocity of 0.2 to 0.3 feet per second. This gas rate maintains the catalyst in suspension within the slurry. Since the Fischer-Tropsch reaction is highly exothermic, temperature control is maintained by heat removal through steam cooling coils located within the reactor. The major portion of products is removed overhead as vapor, with heavier products remaining in the slurry. The split between vapor and liquid depends upon the degree of polymerization of the product. If a heavy product is produced, net liquid must be removed through a filtering system in order to maintain a constant fluid level in the reactor. Liquid is added to the reactor if there is a net decrease of liquid through evaporation.

General agreement exists among the investigators on certain advantages claimed for the slurry system. These include:

1. Reactor design is simple.

2. Catalyst (usually between 1 and 40 microns in size) is easily added to or removed from the reactor without shutdown.

3. Temperature control is superior to other reactor systems.

4. Product flexibility and selectivity is superior to other reactor systems.

5. There are no erosion problems.

Koelbel's work (7) includes the following additional claims:

1. Feed gas H_2/CO ratios as low as 0.7 can be used without significant free carbon formation.

2. Single pass $CO + H_2$ conversions as high as 90% are attainable.

3. Gasoline yields in excess of those predicted by a Schulz-Flory distribution are attainable.

4. Methane yields are lower than from other types of reactors.

Although the Japanese work by Sakai and Kunugi (25) reportedly substantiate some of these claims, no other investigators have been successful in duplicating Koelbel's work. In particular, Farley and Ray (8) attempted to operate at Koelbel's operating conditions and found they could only attain 50% conversion. To maintain conversion, temperature increases were required which led to build up of free carbon followed by increased slurry viscosity and eventual gelation of the reactor contents. Schlesinger and coworkers (23, 24) at the Bureau of Mines did not have the gelation problems of Farley and Ray but did show substantially lower

conversion (70%) with product yields which closely approximated a Schulz-Flory distribution. Attempts have been made to clarify these discrepancies by suggesting that different catalysts were used (10), and that Farley and Ray were producing a much heavier product which led to the increased viscosity. It is apparent that while the Fischer-Tropsch slurry reactor may offer some significant advantages, it still requires further investigation.

3.5 EBULLATING BED REACTOR

The original oil circulation reactor contained a fixed bed of catalyst. Oil trickling down through the bed removed the heat of reaction, allowing reasonable temperature control. However, agglomeration of the catalyst particles caused a rapid increase in pressure drop across the reactor and continuous operation was not possible (19). In the 1940's the U.S. Bureau of Mines (26) revised the process to incorporate upward-flowing oil at a velocity to expand the catalyst bed by about 30%. This was the jiggling bed, later known as the ebullating bed, reactor.

Operation with an expanded catalyst bed eliminated the pressure drop problem. The new system looked sufficiently promising in bench-scale tests to justify building, in 1949, a 50 BPSD demonstration plant at Louisiana, Missouri (27). The demonstration reactor was 3 feet diameter by 30 feet tall and operated at a temperature of 500 to 524°F, a pressure of 300 to 350 psig, and a syngas H_2/CO ratio of 0.76. Methane yield was only half that of a fixed-bed reactor, and 86% of the hydrocarbon product was in the C_3+ fraction. The plant operated successfully, though only at half capacity, until 1953. At this time, due to the abundance of cheap petroleum, the synthesis of fuels from coal was no longer interesting, and the demonstration unit was shut down.

Bench-scale work on the ebullating bed reactor continued. The fused iron catalysts used at the Louisiana, Missouri facility broke up rapidly due to the constant motion in the reactor. In the search for a physically stable catalyst massive iron catalysts, including steel shot and steel lathe turnings, were tried (28). These catalysts, though better able to withstand the agitation in an ebullating bed reactor, were also less active.

Chem Systems (29) has also done considerable development work on the ebullating bed reactor, but not for Fischer-Tropsch synthesis. They have used ebullating bed reactors on a pilot plant-scale to produce methane and methanol from syngas. They also have a Department of Energy contract to build a liquid-phase reactor to demonstrate methanation.

A survey of the literature reveals that operating advantages similar to the slurry reactor can be claimed for the ebullating bed reactor. These advantages include superior temperature control, superior product flexibility and selectivity, and the use of low H_2/CO syngas. It also shares with the slurry reactor the potential problems of oil degradation and increasing viscosity, leading to reduced conversion. The unique and recurring problem in operating an ebullating bed reactor operation is that of physical stability of the catalyst. For Fischer-Tropsch synthesis, it is not clear that the problem has been solved.

TABLE 3.1-1

	Entrained Bed Reactor	Tube-Wall Reactor	Slurry Reactor	Ebullating Bed Reactor
Pressure, psig	300-400	400	150-175	300-400
Temperature, °F	600-635	580-640	500-540	500-540
GHSV, hr^{-1}	1000	20-1000	200-300	200-300
H_2/CO (fresh feed)	2.4	1.0-2.0	0.6-1.2	0.6-1.2
Recycle/Fresh Feed	2.3	1.5	0	0-1.5
Catalyst Size, microns	40	-	1-40	2000-4000

SECTION 4 - THEORETICAL COMPARISON OF REACTORS

This section is divided into five areas:

4.1 The Fischer-Tropsch Mechanism
4.2 The Reactor Models
4.3 Discussion of Results
4.4 Conclusions
4.5 Mechanism Improvements

A reasonable mathematical description of Fischer-Tropsch kinetics is essential to a successful modeling effort. Section 4.1 describes the approach taken in the development of the mechanism, the requirements and assumptions built into the mathematics, and the resultant product rate expressions.

Section 4.2 discusses the incorporation of the mechanism into the three different reactor models. The heat and weight balance equations used for each system, as well as the necessary support subroutines, are discussed in detail. A description of the capabilities built into each reactor model concludes Section 4.2.

Section 4.3 is divided as follows:

1. Data Fitting
2. Reactor Variable Studies, and
3. Reactor Comparisons

Data fitting is a very important part of any modeling effort in that it gives a direct indication of the reliability of the model. In this case, reasonable agreement of fit parameters common to all three reactor systems suggests that the equations chosen to describe the mechanism and reactor systems are good approximations. Section 4.3 describes the approach used in the selection of fit parameters and the results of the data fitting.

Confidence generated in the system equations through data fitting naturally leads to the exploration of operating parameter effects on conversion and product yield structure. These variable studies are presented for each reactor system.

The final objective of the modeling effort is to compare the Fischer-Tropsch reactor systems for inherent strengths and/or weaknesses. The end of Section 4.3 discusses these reactor comparisons and coupled with the physical comparison of reactors (Section 5) provides a foundation for the overall conclusions presented in the Summary.

Section 4.4 lists conclusions based only on the theoretical comparisons.

Although the mechanism discussed in Section 4.1 is capable of describing gross product yields and, therefore, fulfills the requirements of this report, a more in-depth understanding of Fischer-Tropsch reactor systems can be gained by the incorporation of certain mechanism improvements. Section 4.5 discusses these improvements and describes their incorporation into the original mechanism.

4.1 MECHANISM

Anderson, et al. (30), Vannice (31), Catalytica Associates, Inc. (32), Oak Ridge (33), and Ponec (34), have all given excellent reviews of the existing theories on mechanisms for the Fischer-Tropsch reaction. In general, the vast majority of the data are discussed in terms of three mechanisms: the hydroxy-carbene mechanism, the formyl mechanism, and the carbide mechanism. At various points in Fischer-Tropsch history, each of these has been generally favored over the other two, and none of them can be clearly eliminated from consideration. Even though each has its own distinctive active intermediate, there is still a great deal of commonality among the mechanisms.

This commonality is the foundation for the four <u>minimum</u> criteria that must be met to adequately describe the Fischer-Tropsch mechanism:

A. The mechanism must be a polymerization process. For the Fischer-Tropsch reaction, this involves the formation of an active species followed by propagation of alkyl chains, one carbon at a time until termination occurs by severing the catalyst-carbon bond. This, then, leaves an active species available to begin the chain propagation again.

B. The mechanism must be consistent with the generation of normal paraffins and olefins as primary products. This is consistent with the polymerization process described above, and typifies the product yields obtained from iron catalysts. The remainder of the product consists primarily of oxygenates, aromatics, and branched olefins and paraffins (30-34).

C. The mechanism must reflect the non-selective nature of the carbon number distribution as described by the Schulz-Flory analysis (35). With the exception of the light hydrocarbons, i.e., C_1-C_5, a plot of the natural log of the mole fraction of carbon numbered species versus the carbon numbers closely approximates a straight line. By making the assumption that all hydrocarbon species on the catalyst surface <u>have an equal probability</u> to add a carbon and form an oligomer one carbon longer, Schulz and Flory (35) were able to statistically predict the Fischer-Tropsch product distribution by carbon number. The above assumption led to an equation of the form:

$$X_n = p^{n-1}(1-p) \tag{1}$$

which when put in log form becomes:

$$\ln X_n = n \ln p + \ln \frac{1-p}{p} \tag{2}$$

This can be seen to be the equation of a straight line with slope, ln p, and intercept, $\frac{1-p}{p}$. Knowing p, one can now calculate a term called the "Degree of Polymerization" which is defined as:

$$DP = \frac{1}{1-p} \tag{3}$$

The degree of polymerization is a measure of the extent of the polymerization reaction. It can also be used to describe the average Fischer-Tropsch product distribution. For example, Figure 4.1-1 represents the weight fraction of C_n versus n at different degrees of polymerization (32). It should be noted that as DP increases, the product distribution becomes very broad. At a DP equal to 6, the C_6 oligomer is the most abundant species on a weight basis, but only accounts for 7 wt-% of the total product. This truly is a characteristic of the Fischer-Tropsch reaction and is an indication of the non-selective nature of the polymerization process.

D. The mechanism should incorporate an equilibrium between the olefins on the catalyst sites and the olefins in the surrounding gas or liquid (36, 37). The paraffin production is a termination reaction, and the evidence that paraffins do not initiate new chains or insert into existing chains is strong (37, 38, 39). For olefins and oxygenates, the evidence is that they are reactive and, although it is not completely clear, appear to be reactive largely through chain initiation (38-41). In explaining the mechanism of the bi-functional Fischer-Tropsch catalyst, P. D. Caesar, et al. (36), proposed that "Chain propagation by coordination of α-olefins becomes the major route in iron Fischer-Tropsch chemistry as the reaction temperature is raised from 250-350°C". It seems likely, then, that there is an equilibrium, either chemical or physical, between the olefins on the catalyst sites and the olefins in the gas or liquid surrounding the catalyst particles.

Figure 4.1-2 is a schematic representation of the mechanism used in all the reactor models. M represents an "active" metal site. Whether M is a carbide, hydroxy-carbene, or a formyl structure is not important. It is merely a location where chain propagation can occur. The polymerization process proceeds by addition of CO and hydrogen to an alkyl chain, $M(CH_2)_{n-1}H$, forming another alkyl chain one carbon longer, $M(CH_2)_nH$, while liberating H_2O. This process is continued from $M(CH_2)_nH$ to $M(CH_2)_{n+1}H$, and so forth.

Two reactions are responsible for the production of the primary products. The first is the hydrogenation of an alkyl chain of any length to form a paraffin. The second is an equilibrium adsorption-desorption step to form an olefin. In both cases, when the active intermediate is "terminated", another initiation site, MH, is created, which can again participate in chain growth by reacting with CO and H_2. The mechanism, therefore, operates with a constant number of active catalyst sites. This is important if the mechanism is expected to reflect a Schulz-Flory distribution of products.

In the development of this mechanism and in the development of the rate expressions which describe the mechanism, some important assumptions were made. These were as follows:

A. Since oxygenated products, excluding H_2O and CO_2, seem to be formed in a manner similar to olefins and since the quantity formed is small for most Fischer-Tropsch catalysts, oxygenates are not considered at this time.

B. Branched olefins and paraffins are considered to be produced from the recoordination of olefins, i.e., the reattachment of olefins to the metal site. Recoordination is part of the proposed mechanism. However, distinction between recoordination of olefins in the branched form versus the unbranched form is not made.

C. Aromatics are considered to be small enough fractions of the total product to be eliminated from consideration at this time.

D. Catalyst deactivation is not considered.

E. The formation of free carbon is not considered, neither is the second route to methane through free carbon suggested by Dry (6).

F. The Schulz-Flory assumption that "All hydrocarbon species on the catalyst surface have an equal probability to add a carbon and form an oligomer one carbon longer," in kinetic terms suggests that the rate

constant for polymerization is a constant function for all carbon numbers. This assumption is adopted not only for the polymerization rate constants but also for the paraffin termination and olefin formation rate constants.

G. The powers on all reactant and product concentration terms in the mechanism are assumed to be unity.

H. The steady state assumption is used on the rates of formation of all metal site complexes.

I. The total number of "active" metal sites is assumed to be constant, i.e.,

$$[CAT] = MH + M(CH_2)H + \sum_{j=2}^{n} M(CH_2)_jH = CONSTANT \qquad (4)$$

Performance data in the literature show clear limitations to some of these assumptions. However, they are adequate for a first test of the mechanism on real data and for evaluation of gross product changes as a function of reactor design and operating conditions.

Based on these assumptions, then, the final product rate expressions (as derived in Appendix A) are:

Methane

$$r_{CH_4} = C\, k_H\, [H_2]\ [MH] \qquad (5)$$

Paraffins $n \geq 2$

$$r_{C_nH_{2n+2}} = \left(A^{n-1}\, C + B \sum_{i=2}^{n} A^{n-i}[C_iH_{2i}]\right) k_H[H_2]\ [MH] \qquad (6)$$

Olefins $n \geq 2$

$$r_{C_nH_{2n}} = \left[k_o \left(A^{n-1} C + B \sum_{i=2}^{n} A^{n-i} [C_iH_{2i}]\right) - \frac{k_o}{K_e} [C_nH_{2n}]\right] [MH] \quad (7)$$

The simplified rate expression adopted for the water-gas shift is as follows:

$$r_{WG} = k_{WG} \left([CO][H_2O] - \frac{1}{K_{e_{WG}}} [CO_2][H_2]\right) [CAT] \quad (8)$$

It is assumed that this reaction proceeds in parallel with the Fischer-Tropsch reaction. Since Fischer-Tropsch catalysts have shift activity, the rate of reaction is assumed to be proportional to the catalyst concentration [CAT]. However, as it is not known whether the shift reaction requires the same active metal site as the Fischer-Tropsch reaction, it was decided that it should not compete for the same catalyst sites. Therefore, in this study the shift reaction is not assumed to be proportional to available Fischer-Tropsch initiation sites [MH], neither does it influence their concentration. The importance of the shift reaction to the understanding of the differences between reactor systems is discussed later in this report.

FIGURE 4.1-1

HYDROCARBON DISTRIBUTION FROM SCHULZ-FLORY POLYMERIZATION

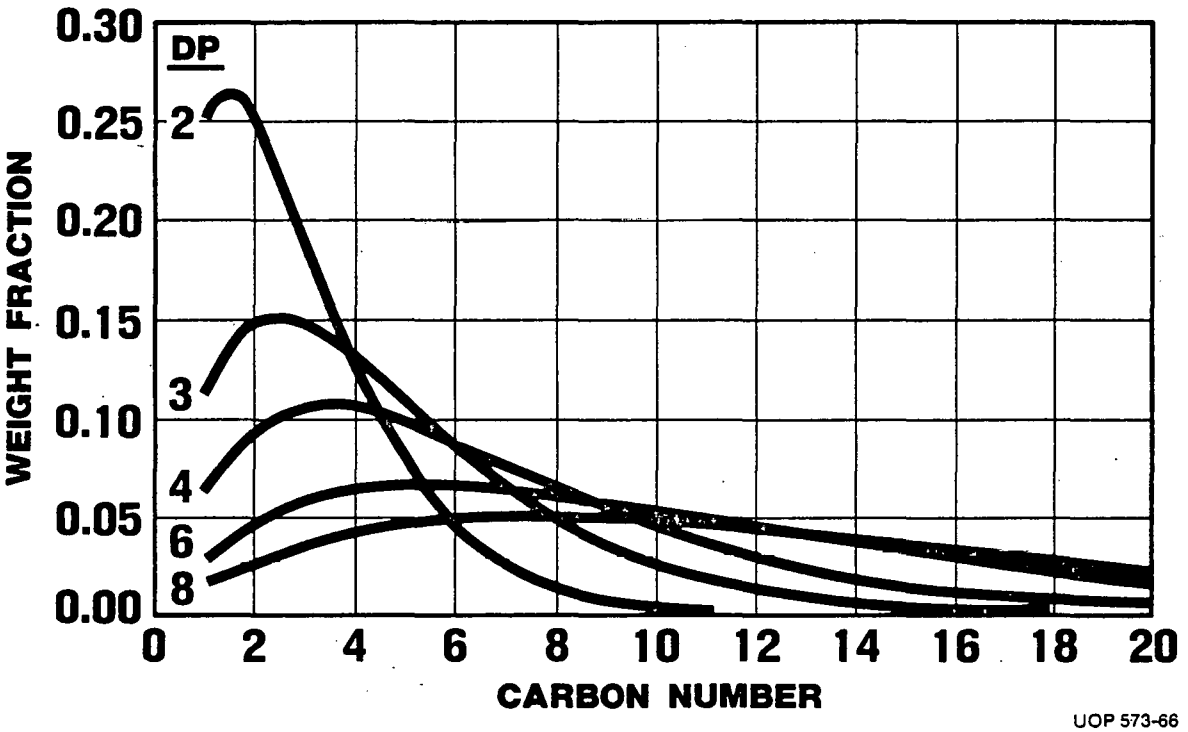

UOP 573-66

FIGURE 4.1-2

MECHANISM

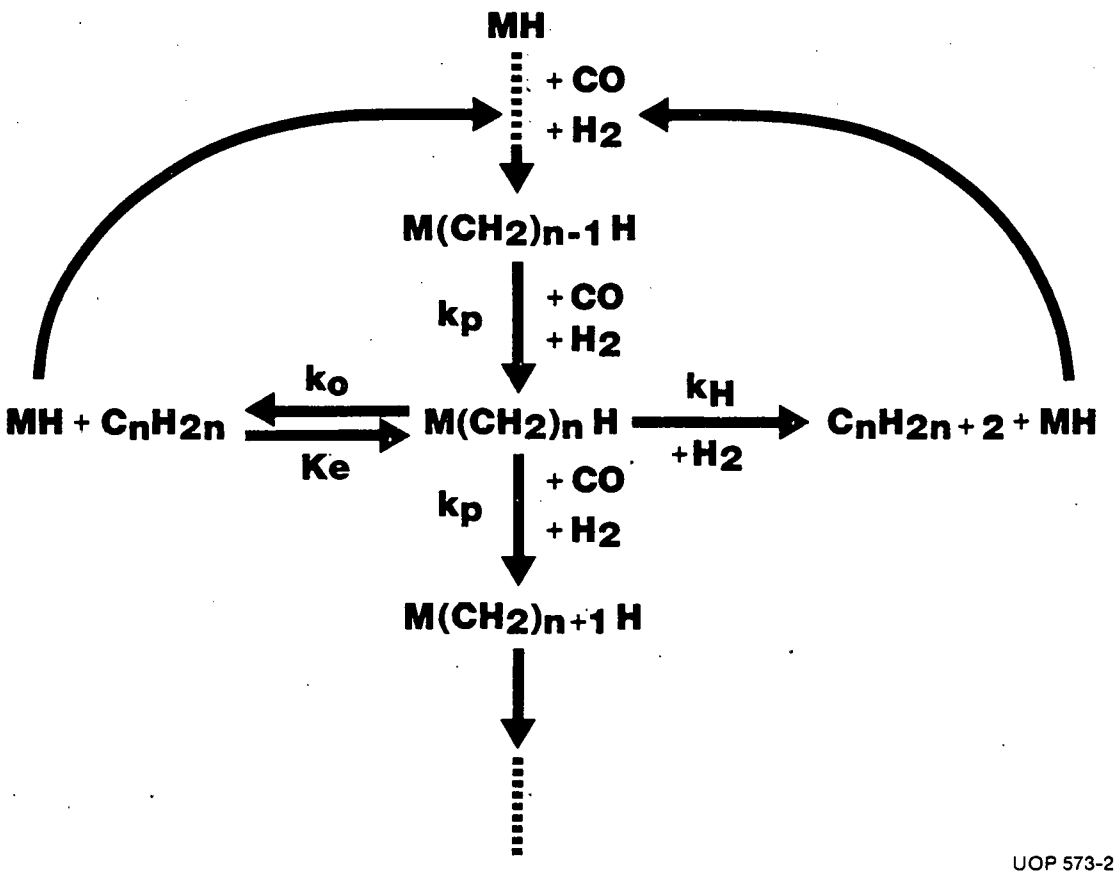

UOP 573-2

4.2 REACTOR MODELING

4.2.1 Modular Approach

It was critical in the development of the mathematical models to distinguish between system differences caused by reactor characteristics and differences caused by computer logic error. It was toward this end that a modular approach to programming was considered.

In the modular system any calculation procedures that are common to all reactor systems are put into a common subroutine which can then be incorporated into each reactor system. The obvious advantage is that the calculations are identical for all systems. In actual practice, however, a complete module is rarely identical for all reactor systems. A modified modular approach was therefore used in which "identical calculations" were supplemented for each reactor system. These modules now perform the same function in each reactor model and have identical core calculation procedures, but are tailored for the individual reactor systems.

A "modular" diagram which represents the basic logic flow of the three reactor models is illustrated in Figure 4.2-1. A few of the modules are unique to a given model as indicated. The basic flow consists of the usual input and output sections with the core of each program being the REACTOR module. This module contains the basic mass and energy balances for each system, and draws on a variety of support modules to provide the necessary information to complete its function. A description of each of the modules follows.

4.2.1.1 Input, Output of Input, and Setup

The INPUT module provides all of the information necessary for the computer models to function. A list of the input parameters for each program is provided in the Appendix B.

The module labeled OUTPUT OF INPUT prints out the input and is merely a convenience, so the programmer can check for errors in the input parameters.

The SETUP module manipulates the input parameters for eventual use in the REACTOR module. For example, if a volumetric flow rate is required in the REACTOR module, but a molar flow rate is used as an input parameter, the SETUP module will convert molar flow to volumetric flow assuming an ideal gas.

4.2.1.2 Physical Properties Linkage, Dew Point and Liquid Properties

These modules are unique to the slurry reactor model. They are used as a link to UOP "in-house" programs which are capable of supplying all component physical properties as well as performing basic thermodynamic operations on any process stream.

4.2.1.3 Hydraulics

Pressure drop in the tube-wall reactor and in the slurry reactor is negligible when compared to the operating pressure. For these models it is, therefore, assumed that the reactor operates at a uniform pressure and hydraulic calculations are not required. However, this is not the case for the entrained bed reactor. Kellogg in its Synthol Feasibility Study (4) reported pressure drops of as much as 80 psi. Not only is this pressure drop significant, but its magnitude can be appreciably altered by operating conditions such as catalyst loading, i.e., pounds of catalyst per cubic foot of gas fed to the reactor. A UOP "in-house" calculation procedure is used as a basis for the HYDRAULICS module incorporated into the entrained bed reactor model, and calculates a pressure profile and catalyst loading through the reactor based on the operating conditions chosen.

4.2.1.4 Heat Balance Information

The function of this module is to supply heat of reaction and heat capacity information to the REACTOR module. The heats of reactions are calculated on a per mole of CO converted basis using heats of formations at 300°C obtained from "Selected Values of Physical and Thermodynamic Properties of Hydrocarbons and Related Compounds" issued by the American

Petroleum Institute Research Project-44. The values and equations used for these calculations can be found in Appendix C.

The heat capacities of the various components were obtained from Smith and Van Ness (42). The values and equations used for these calculations can also be found in Appendix C.

4.2.1.5 Heat Transfer Information

In the tube-wall and entrained bed reactors, heat of reaction is removed by heat exchange within the reactor system. It is, therefore, necessary to calculate an overall heat transfer coefficient.

The tubular reactor model has the capability of operating as two different reactor systems, i.e., a fixed bed tubular reactor and a flame-sprayed tube-wall reactor. The resistances to heat transfer due to the metal wall and due to the coolant film obviously exist in both cases, but the resistance due to the film on the reactant side does not exist in the case of the tube-wall reactor. In this case, the reaction takes place on the flame-sprayed catalyst which is physically part of the tube wall. Because of the potential instability of cocurrent and countercurrent cooling systems described by Degnan and Wei (43), a boiling cooling media (Dowtherm) was selected. The high heat transfer coefficient and constant coolant temperature, combined with the large amount of cooling surface inherent to the tube-wall reactor, results in very little temperature variation along this reactor. The calculation procedure has, therefore, been simplified by ignoring the resistance to heat transfer from the catalyst surface to the gas phase, and the catalyst surface and gas phase are assumed to be at the same temperature. On this basis then, the overall heat transfer coefficients for the fixed-bed and tube-wall reactors are, respectively:

$$U_{\text{fixed bed}} = \frac{1}{\frac{1}{h_o} + \frac{t}{K_t} + \frac{1}{h_s}} \tag{9}$$

$$U_{\text{tube wall}} = \frac{1}{\frac{1}{h_o} + \frac{t}{K_t} + \frac{c}{K_c}} \tag{10}$$

For the fixed-bed system, the overall heat transfer coefficient becomes equal to the reactant side film resistance, i.e., $U_{\text{fixed bed}} = h_s$ because the coolant film resistance and metal resistance are insignificant compared to the reactant side film resistance.

The values used for h_o, K_t, and K_c were assumed constant and were equal to 300 Btu/hr-ft^2-°F, 34.6 Btu/hr-ft-°F, and 34.6 Btu/hr-ft-°F, respectively. The value for h_o was based on Dowtherm as coolant, while the values for K_t and K_c were based on iron. However, h_s is dependent on reactant properties. The equation used to calculate h_s came from McAdams "Heat Transmission" (44), with the modification suggested by Smith to allow for the effect of catalyst in the tubes:

$$h_s = \frac{0.023 \times C_{pb}\, G}{\left(\frac{DG}{\mu_f}\right)^{0.2} \left(\frac{C_p \mu}{k}\right)^{2/3}} \times 6 \tag{11}$$

where:

DG/μ_f = Reynolds Number

$C_p\mu/k$ = Prandtl Number

G = Mass flux

C_{pb} = Heat Capacity

4.2.1.6 Integration

Franks in his book titled "Modeling and Simulation in Chemical Engineering" (45) describes the integration routines exactly as they were used in all three reactor models. Three methods of integration are available within Frank's INT subroutine. These include a first-order method, simple Euler; a second-order method, modified Euler; and a fourth-order method, Runga-Kutta. The fourth-order method was never used.

4.2.2 Reactor Module

More than any other module, the reactor module delineates the differences between reactor systems. This is done in terms of the heat and weight balance equations, and in terms of how the equations are manipulated to arrive at a final solution. Each system will be described separately below.

4.2.2.1 Tube-Wall Reactor

As has already been described, the tube-wall reactor is basically a heat exchanger. It can be schematically represented by Figure 4.2-2. The assumptions made in the development of the model were as follows:

1. Gas flows in ideal plug flow through the reactor.

2. There are no mass transfer limitations in the gas phase.

3. The gas phase and the catalyst are at the same temperature.

The mass balance which resulted from these assumptions and from the rate expressions derived in the Mechanism Sections of this report is as follows:

$$\sum_{i=1}^{N_C} \frac{d M_i}{d X} = \sum_{i=1}^{N_C} \sum_{j=1}^{NR} S_{ij} \cdot r_j \cdot A \qquad (12)$$

The stoichiometric matrix, S_{ij}, controls the stoichiometric relationship between products and reactants. Table 4.2-1 describes the form used for i = 63 components and j = 60 reactions.

The basic heat balance is as follows:

$$\left(\sum_{i=1}^{N_C} M_i \cdot C_{Pi}\right)\frac{d\,T}{d\,X} = N_T\,\pi\,(D)\cdot U(T_W - T) - A\sum_{j=1}^{NR}(r_j \cdot H_{Rj}) \qquad (13)$$

r_j and H_{Rj} are based on one mole of CO.

From left to right in Equation 13, the terms can be characterized as the specific heat term, the heat removal term, and the heat of reaction term, respectively.

The tube-wall reactor model can be used with the reaction occurring on either the shell side or the tube side of the heat exchanger. The diameter in the heat removal term is equal to the inside diameter of the tube, if the reaction is on the tube side. If the reaction is on the shell side, it is equal to the outside diameter, including catalyst thickness.

4.2.2.2 Entrained Bed Reactor

The entrained bed reactor, as described earlier, is a fast fluidized reactor divided into five sections. Three of these sections are open reactors where the only heat removed is through heat loss to the atmosphere. The other two sections remove heat by exchange with either an oil coolant or steam. As a result, part of the entrained bed reactor module is devoted to identifying, during the integration, the section being calculated.

A schematic representation of the reactor can be found in Figure 4.2-3. The assumptions made in the development of the model were as follows:

1. Catalyst and gas move in an ideal plug flow.

2. There is perfect contacting between solids and gas.

3. There are no mass transfer limitations either in the gas phase or within the catalyst particles.

The mass balance resulting from these assumptions is identical to Equation 12. The only clarification required is on the cross sectional area. In the heat removal sections, the total area is calculated by determining the cross-sectional area of a single exchanger tube and multiplying by the number of tubes. In all other sections, the area is determined by using the inside diameter of the reactor.

The heat balance is as follows:

$$\left(\sum_{i=1}^{N_C} (M_i C_{pi}) + W_S C_{ps} \right) \frac{d T}{d X} = N_T \pi (D) \cdot U \cdot (T_W - T) - A \sum_{j=1}^{NR} (r_j \cdot H_{Rj}) \quad (14)$$

The two differences between Equations 13 and 14 are the incorporation of solids in the specific heat term and the manner in which the heat removal term is calculated. In the case of no heat removal, the number of tubes, N_T, is unity and D is equal to the diameter of the reactor. The overall heat transfer coefficient, U, is calculated assuming an insulated wall, and the wall temperature, T_W, is held constant.

In the case of heat removal with an oil coolant, N_T is provided and D is equal to the inside diameter of a tube. U is calculated assuming bare tubes, T_W is set equal to the coolant temperature and is recalculated in each integral interval ΔX. First the total heat removed is calculated for the interval by the equation:

$$Q_L = N_T \pi (D) \cdot U \cdot (T_W - T) \cdot \Delta X \quad (15)$$

The temperature increase of the coolant resulting from absorbing Q_L is calculated by:

$$\Delta T = \frac{Q_L}{M_o C_{Po}} = T_{W_{New}} - T_{W_{Old}} \qquad (16)$$

$T_{W_{New}}$ is then used as the coolant temperature for the next interval ΔX.

When steam is used as a coolant, the wall temperature is assumed constant and dependent on the steam pressure desired.

4.2.2.3 Slurry Reactor

In comparison to the tube-wall and entrained bed reactors, heat transfer is not a problem in the slurry reactor model. The system is assumed isothermal, since cooling coils are immersed in the reaction medium. However, because of the three phase nature of the slurry reactor, fundamental decisions with regard to phase equilibrium, potential mass transfer limitations, and solids distribution are required. The slurry system, as it reflects these decisions, can be schematically represented by Figure 4.2-4. The assumptions involved are as follows:

1. Liquid is completely back-mixed.

2. The system is isothermal.

3. Gas moves in ideal plug flow.

4. All reactions take place in the liquid phase.

5. Solids are evenly dispersed in the liquid phase.

6. Mass transfer limitations only exist in the liquid phase from the gas-bubble interface to the bulk liquid.

7. Gas and liquid are at equilibrium at the gas-liquid interface.

The overall rate of reaction, as implied by these assumptions, is predominately limited by mass transfer from gas bubbles to bulk liquid and by intrinsic kinetics. The mass transfer limiting portion of the mass balance equation has been described by Satterfield and Huff (46) for H_2 as follows:

$$-U_G \frac{dC_{H,G}}{dZ} = k_{L,H}\, a\, (C_{H,L}^* - C_{H,L}) \qquad (17)$$

where:

U_G = superficial gas velocity (cm^3/cm^2 - sec)

$C_{H,G}$ = concentration of hydrogen in gas phase (g moles/cm^3 gas)

Z = vertical distance measured from reactor entrance (cm)

$k_{L,H}$ = liquid film mass transfer coefficient for hydrogen (cm^3 liquid/cm^2 gas-bubble surface area - sec)

a = interfacial area of gas bubbles (cm^2 bubble surface area/cm^3 expanding liquid)

$C_{H,L}^*$ = concentration at equilibrium with the gas

$C_{H,L}$ = concentration in the liquid phase (g moles/cm^3 liquid)

This equation implies that the gas superficial velocity is constant through the reactor system. Although this was a necessary simplification for the analysis performed by Satterfield and Huff, it is not a rigorous solution to the problem. Indeed, the gas volume can contract as much as 50% through the system. Correcting Equation 17 and slightly changing nomenclature leads to the following equation:

$$\frac{-1}{A}\frac{d(V_G Y_i)}{dZ} = k_{L,i}\, a\, C_L\left(\frac{Y_i}{K_i} - X_{bi}\right) \qquad (18)$$

This equation can be further simplified by taking advantage of the fact that:

1. $$\frac{d(V_G Y_i)}{dZ} = V_G\frac{dY_i}{dZ} + Y_i\frac{dV_G}{dZ}$$

2. $$\sum_{i=1}^{n}\frac{dY_i}{dZ} = 0$$

3. $$\sum_{i=1}^{n} Y_i = 1$$

Equation 18 can now be separated into the following two differential equations (Derivation in Appendix D):

$$\frac{dV_G}{dZ} = -A\, C_L \sum_{i=1}^{n} k_{L,i}\, a\left(\frac{Y_i}{K_i} - X_{bi}\right) \qquad (19)$$

$$\frac{dY_i}{dZ} = \frac{AC_L Y_i}{V_G}\sum_{i=1}^{n}\left[k_{L,i}\, a\left(\frac{Y_i}{K_i} - X_{bi}\right)\right] - \frac{AC_L}{V_G}\, k_{Li,a}\left(\frac{Y_i}{K_i} - X_{bi}\right) \qquad (20)$$

If the values of A, C_L, $k_{L,i}$, a, K_i, and X_{bi} are known, these equations can be integrated through the reactor, and a product rate and composition determined. Values of K_i and A are known when reactor operating conditions and design are set. Zaidi, et al. (47) and Koelbel (48) have reported a value for the interfacial surface area, a, of 305 ft^2/ft^3.

Zaidi, et al. have also reported values for the liquid film mass transfer coefficient, $k_{L,i}$, for CO in molten paraffin on the order of 2.36 ft/hr. The values of $k_{L,i}$ for other components were developed as follows.

Calderbank and Moo-Young (49) have developed an equation which describes the value of k_L as:

$$k_L = 0.31\left(\frac{D_L}{\nu_L}\right)^{2/3} \frac{U_L \Delta \rho_L g^{1/3}}{\rho_L{}^2} \qquad (21)$$

where:

D_L = diffusivity in the continuous phase

ν_L = kinematic viscosity of the continuous phase

U_L = continuous phase viscosity

$\Delta \rho_L$ = difference in density between dispersed and continuous phases

ρ_L = continuous phase density

g = acceleration due to gravity

If the slurry reactor is at steady state, the values for ν_L, U_L, $\Delta \rho_L$, ρ_L, and g will be roughly constant. The equation can then be rewritten as:

$$k_L = \text{Constant} \times D_L{}^{2/3} \qquad (22)$$

Wilke and Chang (50) have described the diffusivity of solute A in solvent B as:

$$D_{AB} = 7.4 \times 10^{-8} \frac{T_a(\psi_B M_B)^{1/2}}{\mu\, V_A{}^{0.6}} \qquad (23)$$

where:

$\psi_B \cong 1.0$ for hyrocarbons

M_B = molecular weight

T_a = absolute temperature

μ = viscosity of solution

V_A = molar volume of solute as liquid at its normal boiling point

Since ψ_B, M_B, T_a, and μ are constant for a given solvent, the diffusivity can be rewritten as:

$$D_{AB} = \text{Constant} \frac{1}{V_A{}^{0.6}} \tag{24}$$

If Equations 22 and 24 are combined, the resulting equation is:

$$k_{L_A} = \text{Constant} \frac{1}{V_A{}^{0.4}} \tag{25}$$

This relation suggests that if the value for the mass transfer coefficient for one component in a given liquid is known, e.g., CO, the mass transfer coefficient of a second component can be estimated by knowing the ratio of the liquid molar volumes of these two components. It is recognized that this is a gross approximation. However, due to a lack of data on k_L values for hydrocarbons and due to a desire for internal consistency, the above method was used for determining k_L values for all components relative to CO.

X_b is the only parameter remaining to be known before integration of the mass transfer mass balance equation can be performed. X_b, however, is also intimately tied to the intrinsic kinetics of the slurry system as described by the mass balance equation:

$$\sum_{i=1}^{NC} \frac{1}{A}\frac{dM_i}{dZ} = \sum_{i=1}^{NC}\sum_{j=1}^{NR} S_{ij} \cdot r_j\,(X_{b_i}) \qquad (26)$$

or for a completely back-mixed system:

$$\sum_{i=1}^{NC} \frac{1}{A}\frac{(M_{i_f} - M_{i_o})}{L} = \sum_{i=1}^{NC}\sum_{j=1}^{NR} S_{ij} \cdot r_j(X_{b_i}) \qquad (27)$$

Since the rate of mass transfer must equal the rate of reaction, the following relationship must be true from Equations 18 and 27:

$$M_{i_f} - M_{i_o} = k_{L_i} \cdot a\, C_L A \int_o^L \left(\frac{Y_i}{K_i} - X_{b_i}\right) dZ = A \cdot L \sum_{i=1}^{NC}\sum_{j=1}^{NR} S_{ij} \cdot r_j(X_{bi})$$

The key to the solution of the slurry mass balance equations is in choosing values of X_b such that the above equalities are fulfilled.

The heat balance equation for the slurry system is very straightforward. In order for the reactor to be isothermal, any heat generated by reaction must be removed by heat removal. Therefore:

$$Q_L = A \cdot L \cdot \sum_{j=1}^{NR} (r_j \cdot H_{R_j}) \qquad (28)$$

4.2.3 Program Capabilities

The program capabilities are best described in outline form below:

I. Tubular Reactor Model

A. Reactor Configuration

1. Fixed Bed

The catalyst and reaction are on the tube side of the exchanger with the coolant on the shell side.

2. Tube-Wall -- Tube Side

The catalyst is flame-sprayed to the inside of the tubes with the reaction taking place in the tubes. The coolant is in the shell.

3. Tube-Wall -- Shell Side

The catalyst is flame-sprayed to the outside of the tubes and reaction is on the shell side of the exchanger. The coolant is in the tubes.

B. Temperature Control

1. Isothermal

The temperature is fixed and the heat removed is assumed to exactly balance the heat generated by reaction.

2. Adiabatic

No heat is removed and the temperature is allowed to rise with the heat generated by reaction.

3. Non-adiabatic

The temperature is calculated by balancing the heat removed via coolant against the heat generated by reaction.

C. Coolant Type

1. Boiling Dowtherm

2. Boiling Water

In both these cases, "boiling" implies an excess of coolant at constant temperature.

II. Entrained Bed Reactor Model

A. Reactor Configuration

1. Fast Fluidized

One requirement of a fast fluidized bed is that gas move in plug flow. A dense fluidized bed is characterized by back-mixed gas and the model is, therefore, not applicable to this case.

B. Temperature Control

1. Isothermal

2. Non-adiabatic

C. Heat Removal

1. Coolant Type

A. Boiling Water

B. Oil

The oil is not boiling. The increase in oil temperature is calculated based on heat removed from the reaction system.

2. Exchanger Length

In the entrained bed reactor, heat removal does not occur through the entire length of the reactor. Two separate exchanger sections are provided, the lengths of which are variable.

III. Slurry Reactor Model

A. Reactor Configuration

The slurry model uses as basic assumptions back-mixed liquid and plug flow gas. It is not applicable to any other configuration.

B. Temperature Control

1. Isothermal only.

C. Mass Transfer

Mass transfer limitations are only considered from the liquid interface to the bulk liquid. No other mass transfer limitations are considered. Mass transfer coefficients are easily changed.

IV. Capabilities Common to All Reactor Systems

A. Changes can be conveniently made in:

1. Reactor Dimensions
2. Catalyst Concentration
3. Catalyst Rate Constants
4. Operating Conditions

B. Fit versus Predict

The programs can input operating conditions and yield data, and calculate kinetic rate constants which best "fit" the data. Or, the program can input feed composition, operating conditions and kinetic rate constants and "predict" product yields.

C. Kinetic Mechanism

Because of the modular approach used for modeling, new kinetic mechanisms can be easily incorporated into the programs.

FIGURE 4.2-1

REACTOR MODELING MODULAR DIAGRAM

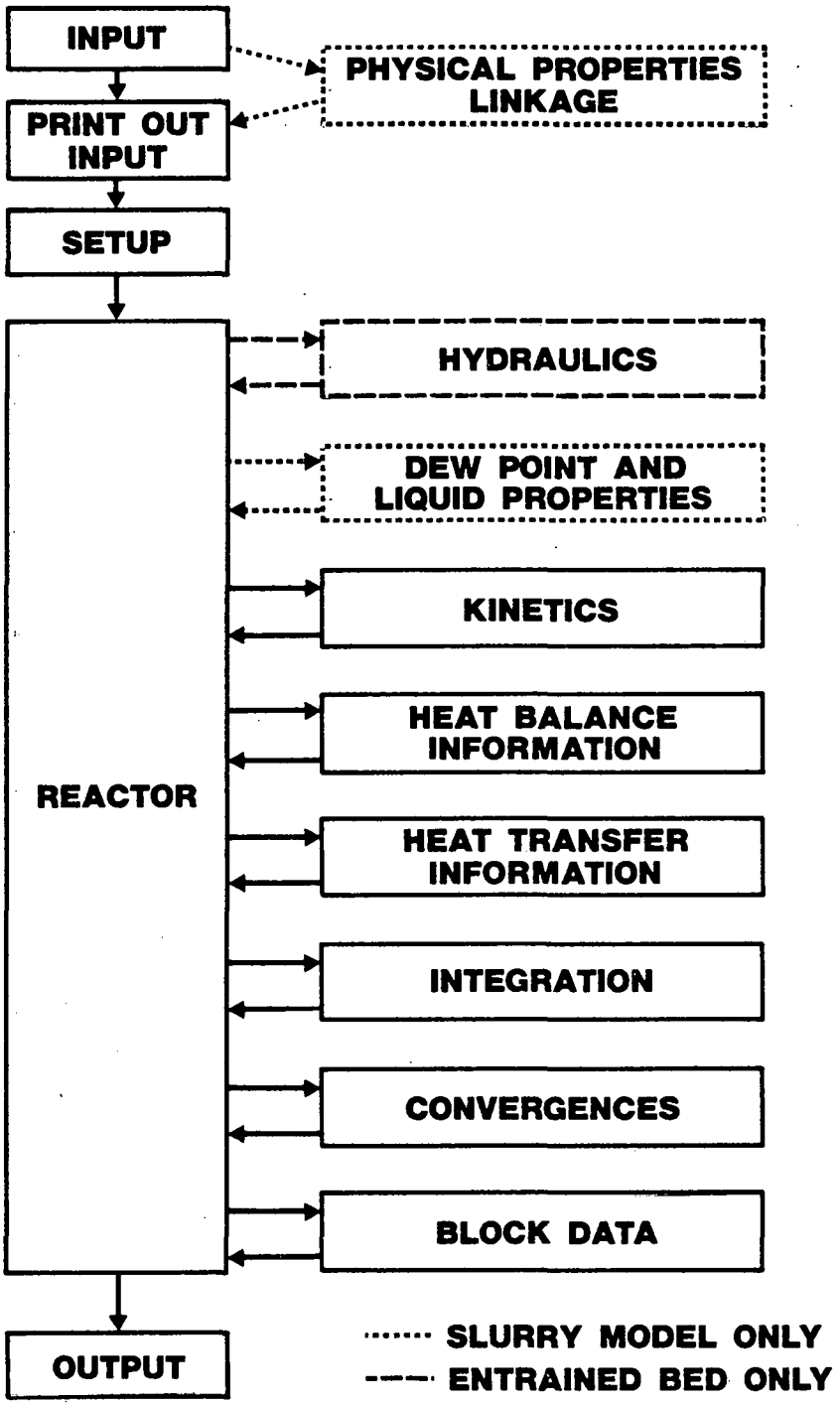

UOP 573-52

FIGURE 4.2-2

SCHEMATIC OF TUBE WALL REACTOR

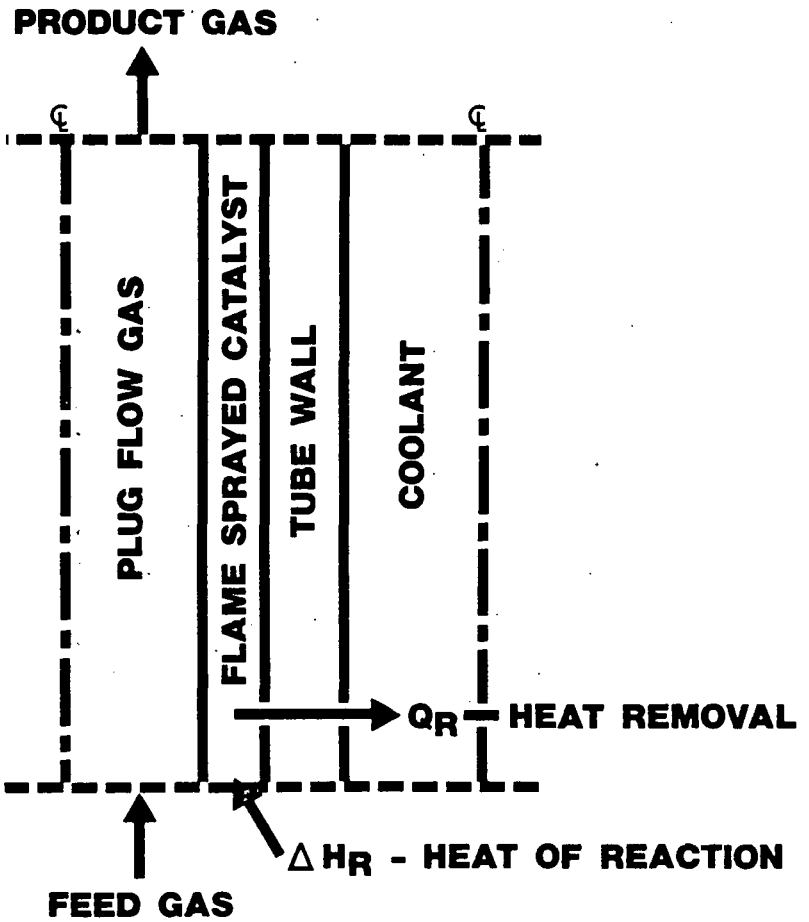

UOP 573-54

FIGURE 4.2-3

SCHEMATIC OF ENTRAINED BED REACTOR

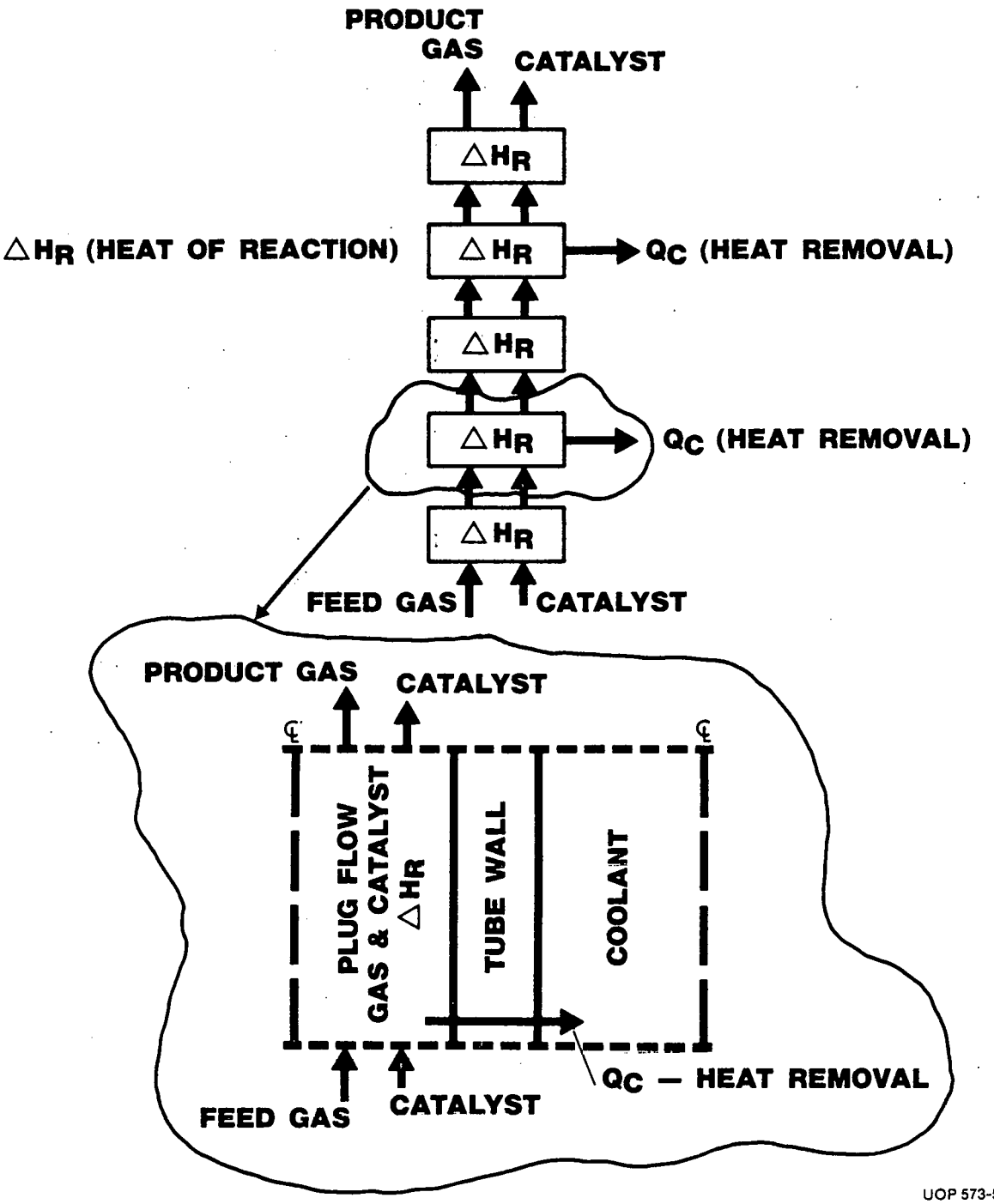

UOP 573-53

FIGURE 4.2-4

SCHEMATIC OF SLURRY REACTOR

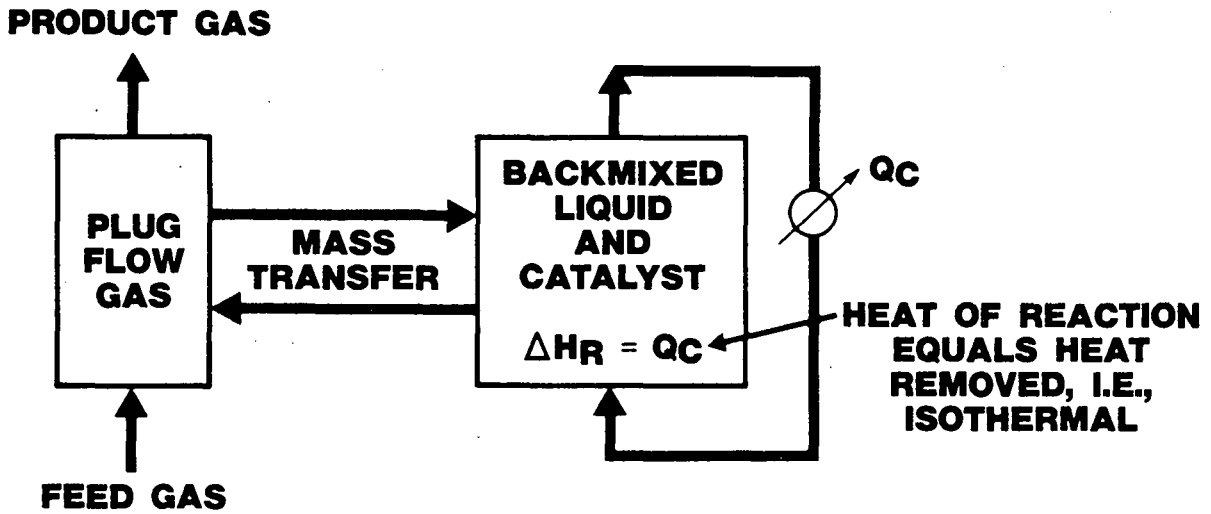

MASS TRANSFER

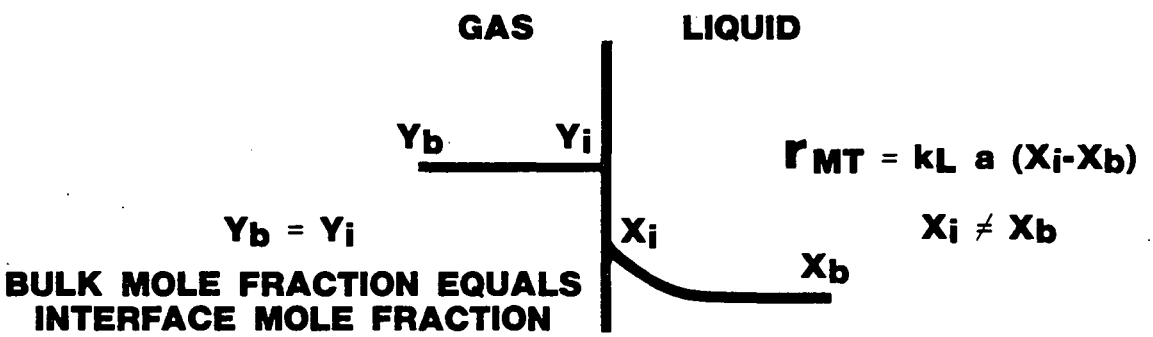

$$Y_i = K_i x_i$$

VAPOR AND LIQUID ARE AT EQUILIBRIUM AT THE INTERFACE

UOP 573-55

TABLE 4.2-1

STOICHIOMETRIC MATRIX

Reaction	i = Component j =	1 H_2O	2 H_2	3 CO	4 CO_2	5 CH_4	6 C_2H_6	7 . . . 34 C_3H_8 . . . $C_{30}H_{62}$	35 C_2H_4	36 C_3H_6	37 . . . 63 C_4H_8 . . . $C_{30}H_{60}$
CH_4	1	+1	-3	-1	0	+1	0	0	0	0	0
C_2H_5	2	+2	-5	-2	0	0	+1	0	0	0	0
C_3H_3	3	+3	-7	-3	0	0	0	+1	0	0	0
$C_{30}H_{62}$	30	+30	-61	-30	0	0	0	0	0	0	0
C_2H_4	31	+2	-4	-2	0	0	0	0	+1	0	0
C_3H_6	32	+3	-6	-3	0	0	0	0	0	+1	0
C_4H_8	33	+4	-8	-4	0	0	0	0	0	0	+1
$C_{30}H_{60}$	59	+30	-60	-30	0	0	0	0	0	0	+1
Water Gas	60	-1	+1	-1	+1	0	0	0	0	0	0

4.3 DISCUSSION OF RESULTS

4.3.1 Data Fitting

4.3.1.1 Data Fitting Procedures

The reliability of the mechanism was tested by fitting rate constants to data from all three reactors.

The first step in the data fitting procedure was to identify the variables to be fit. The assumption in the mechanism that each of the rate constants is a constant function for all carbon numbers results in the product distribution being dependent on three rate constants and an equilibrium constant. These are the polymerization rate constant, k_p, the hydrogenation rate constant, k_H, the forward rate constant for the olefin formation, k_o, and its corresponding equilibrium constant, K_e. These are the independent variables in the kinetic mechanism.

The next step was to characterize the product distribution using four corresponding dependent variables. Three of the four became obvious choices. An overall carbon balance of the system could be represented by CO conversion. The distribution of these carbons in the product could be approximated by the degree of polymerization as calculated from a plot of $\ln X_n$ vs. n. (The slope was determined from the gasoline fraction, i.e., between carbon numbers 5 and 11.) The hydrogen balance could be represented either by hydrogen conversion or, since only olefins and paraffins are produced as products, by olefin-to-paraffin ratio. Unless one is willing to consider variations in rate constant or olefin-to-paraffin ratio with carbon number, the three variables mentioned above describe the product in its entirety. From considerations of availability of consistent experimental data, and the desire to use the simplest possible approach in this first modeling attempt, the number of dependent variables has been limited to these three. Unfortunately, trying to fit four independent variables with three dependent variables leads to an infinite number of solutions.

A variable study was, therefore, undertaken to determine if the product distribution was sufficiently insensitive to one of the independent variables to be set equal to a constant. This would reduce the problem to an equal number of independent and dependent variables, thus leading to a unique solution. This study was done in an ideal plug flow reactor under isothermal conditions. A typical result for a given set of rate constants is represented in Figure 4.3-1. Two results of the constraints imposed on the mechanism are reflected in this plot. The first is in the methane production. Both the olefins and the paraffins, individually, are represented as straight lines and, therefore, follow a Schulz-Flory relationship. However, since there is no olefin of carbon number unity, methane can not follow a Schulz-Flory relationship relative to the total carbon number distribution, i.e., sum of the olefins and paraffins.

The second result is the olefin-to-paraffin ratio. Weitkamp, et al. (51), have shown that, for an iron catalyst operating in a fluidized bed, the olefin-to-paraffin ratio remains approximately constant beyond carbon number five. This implies that the olefin and paraffin lines in Figure 4.3-1 are parallel. Although this appears to be the case, in fact, the lines are gradually converging and the olefin-to-paraffin ratio is continually decreasing with carbon number. Later runs with back-mixed reactors did show a constant olefin-to-paraffin ratio above a carbon number of 10 and only a small decrease above a carbon number of 5. At the present time it is not certain whether predictions of olefin-to-paraffin ratio with the proposed mechanism are meaningful, or whether some variation of rate constants with carbon number will be necessary.

Figure 4.3-2 represents the results when, for a given set of k_p, k_H, and k_O values, the value of K_e was changed from low to high. The curvature of the olefin line is caused by the light olefins approaching their respective equilibrium values. This variance from the idealized Schulz-Flory distribution was not the original objective of the mechanism. Although the intent is not to minimize the importance of this approach to equilibrium, as a first approach to the problem the value of K_e has been arbitrarily fixed at a low value for the remainder of our work, so as to more closely approximate the Schulz-Flory distribution of products. After

a value for K_e is imposed, the overall problem of fitting is reduced to three dependent variables and three independent variables and can be readily solved.

In addition to limiting the number of independent variables, the variable study provided information regarding the relative sensitivity of CO conversion, degree of polymerization, and olefin-to-paraffin ratio to the three remaining independent variables, k_p, k_O, and k_H (Table 4.3-1). CO conversion is obviously most influenced by k_p and was, therefore, chosen as its fitting parameter. The degree of polymerization and olefin-to-paraffin ratio were affected equally by k_H and k_O. An arbitrary decision was taken to fit k_H to the degree of polymerization and k_O to the olefin-to-paraffin ratio. However, the same results were achieved when the fitting parameters for k_O and k_H were reversed.

The preceding discussion has revolved around three unknown rate constants. Actually each rate constant contains two unknown parameters, i.e., the Arrhenius frequency factor and the activation energy. The Arrhenius equation can be written as:

$$k_T = k_O{}^o e^{-\Delta E/RT_a} \tag{29}$$

For a given catalyst, the frequency factor and the activation energy are fixed and the rate constant varies only as a function of temperature. The values of $k_O{}^o$ and ΔE were determined from the standard Arrhenius plot of ln k_O versus $1/T_a$.

The rate expression for the water-gas shift reaction was given by Equation 8. Since the equilibrium constant is well known, the only variable that needs to be fit is the forward rate constant, k_{WG}. The CO_2 concentration was chosen as the fitting parameter, since for the reaction included in the models the production of CO_2 is unique to the shift reaction.

4.3.1.2 Data Fitting Results

As mentioned in Section 4.3.1.1 of this report, the Arrhenius activation energies were determined by fitting the frequency factors to data at different temperatures. The fitting parameters were CO conversion, degree of polymerization and olefin-to-paraffin ratio.

The tube-wall reactor system was chosen for this work; first, because the simplicity of the plug flow system made results easy to interpret, and, second, because consistent results at different temperatures were not available for the other reactor systems. Table 4.3-2 represents temperature data collected by Haynes, et al., of PETC (11) for the tube-wall reactor operating with flame-sprayed taconite catalyst at 650 psig. The degree of polymerization for each of these sets of data was determined in the following manner:

1. The product was divided into the following components:

   a) C_1-C_4 (gas)
   b) C_5-C_{11} (gasoline)
   c) C_{12}-C_{25} (diesel)
   d) C_{26}+ (heavy)

2. The Schulz-Flory plot of degree of polymerization versus weight fraction shown in Figure 4.3-3 was used to determine which degree of polymerization most nearly approximated the actual data.

The olefin-to-paraffin ratio required special consideration. As mentioned earlier, it remains to be determined whether the mechanism can predict olefin-to-paraffin ratio as a function of carbon number. In order to avoid this problem, an artificial ratio of unity was used in each of the data fitting runs. This in effect reduced the number of independent variables to two, CO conversion and degree of polymerization. However, despite the deficiencies of this first, deliberately simplified approach,

useful insight into the strengths and weaknesses of the various reactor systems was gained. The final information used as input for the tube-wall fitting is given in Table 4.3-3.

The frequency factor results versus temperature as well as the corresponding activation energies are given in Table 4.3-4. The values are based on a reference temperature of 1100°R. As can be seen, excellent agreement in frequency factors was achieved. The largest variance (15.3%) is for the water-gas shift reaction. The smallest variance (2.5%) is for the polymerization rate constant. The activation energies are typical of those for catalyzed reactions.

Because of the limited temperature data available, the above procedure for determining activation energies could not be used for each reactor system. Consequently, the activation energies given in Table 4.3-4 were used without modification for the gas phase reactor systems. In the case of the slurry reactor, Satterfield and Way (52) have shown that for a system where the carrier liquid is completely inert to reaction and/or adsorption on the catalyst site, the liquid phase reaction rate constant can be related to the gas phase reaction rate constant by the following equation:

$$k_L = K \frac{V_G}{V_L} \quad k_G \tag{30}$$

where:

k_L = liquid phase reaction rate constant

K = vapor-liquid equilibrium constant, $K = \frac{y}{x}$

- y = mole fraction in gas
- x = mole fraction in liquid

V_G = molar volume of gas at reactor conditions

V_L = molar volume of liquid at reactor conditions

k_G = gas phase reaction rate constant

Equations of this form were incorporated into the slurry mathematical model allowing k_G and the activation energies given in Table 4.3-4 to be used for the slurry system. The relatively good agreement obtained in fitting data for other reactor systems confirms that this is a reasonable assumption.

While the fixed-bed tubular reactor is not one of the reactors to be compared in this study, an abundance of data is available for a reactor of this type developed by the Pittsburgh Energy Technology Center (53, 54), in which lathe turnings were used as catalysts. Since the tube-wall reactor model can also be used for a fixed-bed reactor, a comparison of the catalyst used in these two systems was made. The frequency factor fit for the lathe turning reactor was made on the basis of Experiment 26C of the PETC work (54). (See Table 4.3-5). The comparison is presented in Table 4.3-6.

At first glance, the lathe turnings results look quite different from the tube-wall results. However, upon closer analysis, two explanations emerge. The first is related to catalyst activity. The computer model performs its calculations using weight as its basis for catalyst concentration. Actually, for this catalyst which has very little pore volume, the catalyst activity is more closely related to the external surface area than to the weight. The surface area per unit weight of the lathe turning catalyst was compared to that of the tube-wall catalyst, and was found to be very close to the ratio of the frequency factors for the polymerization and for the water-gas shift rate constants. In other words, the high apparent activity of the lathe turning catalyst could be easily explained by its higher surface area. The polymerization rate constant was, therefore, used as a basis to adjust the frequency factors derived for the lathe turning catalyst to the catalyst surface area in the tube-wall reactor. The adjusted numbers are also shown in Table 4.3-6.

In spite of this adjustment, the agreements between catalysts for the hydrogenation and for the olefin formation frequency factors are still poor. This led to the second explanation. The lathe turning catalyst used for fitting purposes was potassium promoted while the tube-wall

catalyst was not. There is much evidence in the literature (30, 55) that suggests that potassium promotion increases the degree of polymerization of the product. Based on a comparison of frequency factors, this phenomenon might be explained by a reduction in the hydrogenation/termination rate, thereby producing a heavier product via additional polymerization. Weitkamp, et al. (51), have provided support to this theory by showing a significant shift from a paraffinic to olefinic product with the addition of potassium.

Additional support for these explanations is provided when similar comparisons are made for the slurry and entrained bed systems. Koelbel's (7) yields and operating conditions, shown in Table 4.3-7, were used for fitting the slurry system. The Kellogg Feasibility Study (4) was used as a basis for yields and some of the operating conditions for the entrained bed system. In the latter case, however, Sasol literature, as well as engineering judgment, was required to supplement some deficiencies in the available data. The final information used for fitting is given in Table 4.3-8.

Frequency factor derivations are given at the top of Table 4.3-9. Here again the magnitudes of the frequency factors for the polymerization rate constant were found to be roughly in proportion to the catalyst surface areas. For example, the difference between the frequency factors for the slurry and entrained bed reactors could be explained by the average particle size of the catalyst being 30 and 40 microns, respectively. In addition, the surface area per unit weight of catalyst is very high for both these systems, and is reflected in the high frequency factors relative to the tube-wall system.

The bottom of Table 4.3-9 shows the values of frequency factors after adjustment for surface area relative to the tube-wall catalyst. The similarity of values for the lathe turning catalyst and for the slurry catalyst is significant. Both catalysts are potassium promoted and this is reflected in the values for k_H^o and k_o^o. While the entrained bed values are not as close, they are still in reasonable agreement, considering the lack of a consistent set of operating data for fitting. The only

frequency factor that is completely out of line is for the water-gas shift in the entrained bed system. A closer scrutiny of the data revealed a high concentration of CO_2 in the combined feed. As a result, water-gas shift was found to be at equilibrium throughout the entire reactor. It is obviously impossible to determine a forward rate of reaction when that reaction is at equilibrium. This value must, therefore, be disregarded.

The frequency factors used in the entrained bed and slurry variable studies are those listed at the top of Table 4.3-9. These produced the most favorable yield structures for their respective reactor systems. The tube-wall frequency factors, however, produced yield structures that were much too high in methane yield and much too low in gasoline yield. Conversely, the lathe turning values, although better, produced a product structure that was too heavy. A compromise led to the final selection of the lathe turning values modified for slightly less potassium promotion. This was accomplished by increasing the hydrogenation frequency factor from 0.07 to 0.1. The values used were: $k_p^o = 73.0$; $k_H^o = 0.1$; $k_o^o = 0.0129$; and $k_{WG}^o = 205.0$.

A very important overall conclusion was drawn from reflecting on the data fitting results. That is, a <u>single</u> mathematical mechanism has been developed that, when incorporated into models of three completely different reactor systems operating at completely different operating conditions, gave reasonable agreement on the rate constants associated with Fischer-Tropsch catalysts manufactured by several independent investigators. Also, the data with and without potassium promotion of the catalyst show that the mechanism will allow interpretation of yield differences resulting from different catalyst formulations. The reactor comparisons, therefore, proceeded with some confidence that the models also can be used to predict with reasonable accuracy the gross product distributions for each system.

4.3.2 Parsons Comparison

Under DOE Contract No. E(49-18)-1775, Ralph M. Parsons Company (16) prepared a report which describes "The results of a conceptual design and

economic evaluation for a conceptual Fischer-Tropsch plant responsive to U.S. demands and economic requirements." The Fischer-Tropsch synthesis reactor chosen for this study was the tube-wall system. The yield structure was based on Experiment 26C (Table 4.3-5) with the lathe turning catalyst mentioned earlier. The activity of the catalyst was determined from Experiment HGR-34 (Table 4.3-10) which studied flame-sprayed magnetite. The final design selected by Parsons is given in Table 4.3-11. A comparison of this conceptual design with the PETC experimental data is given in Table 4.3-12. A critical analysis suggests that the activity selected for the conceptual design was very optimistic. The fit results presented in Table 4.3-6 earlier suggested that the polymerization activity, k_p^o, of lathe catalyst is very nearly the same as that for flame-sprayed taconite catalyst. Haynes, et al. (1), have shown that taconite catalyst is significantly less active than magnetite catalyst and yields a higher molecular weight product. Closer examination of Experiments 26C and HGR-34 shows that potassium-promoted magnetite has a much lighter product structure than potassium-promoted lathe turnings. Potassium-promoted taconite must, therefore, be used as catalyst if the lathe turning yield structure represented in the Parsons study is desired.

A study was undertaken to compare the Parsons reactor design and operating conditions, which were based on flame-sprayed magnetite, to that which would result from a flame-sprayed, potassium-promoted taconite (or lathe turning equivalent). The results are given in Table 4.3-13. Case 1 used the Parsons reactor design. (The GHSV is not quite the same, but this is the result of using bare tubes in the model while Parsons used finned tubes.) The lower activity and heavy product distribution of the taconite catalyst is reflected in a low CO conversion and a high degree of polymerization. In Case 2, the temperature was increased to 640°F and the size of the reactor was increased until a CO conversion on the fresh feed of 90% was achieved. The predicted yields are then close to what was used in the Parsons study, but the total syngas conversion ($CO + H_2$) remains lower than that used by Parsons, and the reactor is roughly twice the size with an operating temperature considerably higher.

This study is presented as an example of how the reactor models can be used to interpret experimental data and predict the results of using commercial-scale equipment. The design shown in Table 4.3-13 is not represented as an optimized design for a tube-wall reactor. In fact, it is doubtful that this reactor could operate at 640°F and the H_2/CO ratio indicated without significant problems of free carbon formation.

4.3.3 Variable Studies

4.3.3.1 Tube-Wall Reactor

The base case operating conditions chosen for the tube-wall reactor variable studies were as follows:

Gas	:	Once-through
Temperature	:	310°C (589°F)
Pressure	:	415 psia
J Factor	:	5 SCFH FF/ft^2 catalyst
H_2/CO Ratio	:	2.0
Catalyst Density	:	11.85 lb/ft^3 of reactor.

These are not necessarily the optimum operating conditions for this reactor system. They were chosen so the sensitivity to CO conversion and degree of polymerization could be properly shown as a function of various parameter changes.

Figures 4.3-4 through 4.3-6 show CO conversion versus reactor temperature as functions of pressure, J factor, and inlet H_2/CO ratio, respectively. In general, conversion is found to increase almost linearly with increasing temperature until high conversions (> 90%) are reached. At this point there is an exponential approach to 100% conversion. At a given temperature, conversion is found to increase with increasing pressure, decreasing J factor, and increasing H_2/CO ratio.

Figures 4.3-7 through 4.3-9 give degree of polymerization versus reactor temperature as functions of pressure, J factor, and H_2/CO ratio,

respectively. In agreement with the literature, DP decreases with increasing temperature. At a fixed temperature, DP increases with increasing pressure, increasing J factor, and decreasing H_2/CO ratio.

The H_2/CO ratio information presented in Figure 4.3-9 is represented in another form in Figure 4.3-10. Here, degree of polymerization is plotted versus CO conversion at varying inlet H_2/CO ratios. Notice that with a single reactor configuration and at a fixed conversion there is a maximum degree of polymerization at a H_2/CO ratio near unity. This is explained as follows. As H_2/CO ratio decreases, conversion decreases with a corresponding increase in the degree of polymerization. To return the conversion to its original value, it is necessary to increase temperature which decreases DP. At a H_2/CO ratio of 0.7, the temperature effect on degree of polymerization dominates the H_2/CO ratio effect, while the opposite is true at a H_2/CO ratio of 2.0.

A second influence of H_2/CO ratio on degree of polymerization can be seen in the plot of DP versus temperature at varying recycle-to-feed ratios (Figure 4.3-11). Initially it was felt that increasing the recycle ratio would increase olefin concentration in the combined feed and, therefore, encourage propagation to heavier products (higher DP). Inspection of Table 4.3-14 shows that the olefin concentration does increase modestly, but the hydrogen and carbon monoxide concentrations remain an order of magnitude higher and, therefore, continue to be the dominant factors in determining the degree of polymerization.

This dominance can be seen more clearly when one understands the severe effects of recycle ratio on degree of polymerization at low temperature versus at high temperature (Figure 4.3-11). Two temperatures, i.e., 539 and 615°F, were chosen for monitoring, at different recycle ratios, the H_2 and CO concentrations and the degree of polymerization as a function of reactor length. Figures 4.3-12 and 4.3-13 represent the concentration changes while Figures 4.3-14 and 4.3-15 represent the degree of polymerization changes.

At 539°F, the CO conversion is rather low. The concentrations of both H_2 and CO, therefore, remain relatively high throughout the reactor length. The influence of these concentrations on both termination and polymerization is such that the degree of polymerization decreases almost linearly with reactor length. As the recycle ratio is lowered, the change in H_2/CO ratio becomes higher, thus accelerating the decline in degree of polymerization. Near the end of the reactor, the lines cross and a lower degree of polymerization is seen for the lowest recycle ratio.

At 615°F, the CO conversion is rather high. Although the concentration of H_2 remains relatively high, the concentration of CO begins to level off at a low value, particularly for R/F = 0. As a result, the influence of CO on the rate of polymerization ($r_p \cong k_p[CO][H_2]$) becomes minor, and the rates of termination ($r_t \cong k_H [H_2]$) and polymerization become dependent on the hydrogen concentration alone. As can be seen in Figure 4.3-15, the net effect is a leveling out of degree of polymerization with reactor length. The recycle ratio lines never cross, and the degree of polymerization for R/F = 0 remains the highest throughout the reactor.

4.3.3.2 Entrained Bed Reactor

Because of the complexity of the entrained bed system, the effect of a single variable change is difficult to study. For example, the definition of reactor temperature is a problem due to the nature of the heat removal system. Given a fixed inlet temperature, the outlet temperature, and consequently the average reactor temperature, could be changed by adjusting the cooling oil rate to the heat removal coils. An illustration of the models prediction of this effect on CO conversion and degree of polymerization can be seen in Figures 4.3-16 and 4.3-17. As cooling oil rate is reduced, reactor ΔT increases, resulting in an increased conversion and decreased degree of polymerization.

The limited flexibility inherent to the entrained bed reactor system created another example of the difficulty in changing a single variable. An attempt was made to reduce the recycle ratio to below one. When this

was done, the partial pressures of both hydrogen and carbon monoxide in the combined feed increased. In addition, the superficial velocity in the reactor was reduced resulting in increased residence time and higher catalyst concentrations. The net result was a temperature runaway before the first set of exchangers was reached.

These types of complexities led to two guidelines for conducting variable studies on the Kellogg design:

1. A constant ΔT across the reactor was maintained by adjusting cooling oil rate equally between the two heat removal sections, and

2. The rate and composition of hydrocarbons in the recycle gas were held constant and equal to that shown by Kellogg.

With these guidelines, CO conversion and degree of polymerization were investigated as functions of inlet temperature, inlet pressure, β (defined as standard cubic feet of fresh feed per hour per pound of catalyst), catalyst circulation rate, and H_2/CO ratio in the combined feed. Figures 4.3-18 to 4.3-22 represent the results.

As expected, increasing temperature and H_2/CO ratio leads to increasing conversion and decreasing degree of polymerization. Increasing pressure increases both CO conversion and the degree of polymerization.

The influence of catalyst circulation rate is unique to the entrained bed system. Yerushami, et al. (56), have shown that for a fixed gas rate, if the catalyst circulation rate is increased, i.e., the catalyst loading is increased (lbs catalyst per ft^3 of gas), additional slippage will occur resulting in higher catalyst density in the reactor. This effect can be seen in Figure 4.3-23 for the base case. The increased catalyst density leads to higher conversions (Figure 4.3-21), but apparently has little effect on the degree of polymerization.

The influence of solids loading on catalyst density led to the term β, defined above, being chosen as a correlating factor rather than gas

hourly space velocity (GHSV). Although GHSV may be a measure of space utilization efficiency, it is not an accurate measure of catalyst utilization efficiency for the entrained bed reactor. CO conversion decreases dramatically with increasing β (Figure 4.3-20), while degree of polymerization increases only slightly.

The final variable to be studied was recycle to feed ratio. In this case the ΔT guideline was adhered to, but steady state continuous recycle was simulated by continually adjusting recycle gas composition until it matched the gas composition produced from a flash of reactor effluent. The results are presented in Figures 4.3-24 and 4.3-25. As expected, increased recycle to feed ratio results in lower overall CO conversion. The influence of this lower conversion on degree of polymerization can be seen in Figure 4.3-25. From the tube-wall recycle studies (Section 4.1) at low temperatures, it was shown that large changes in CO concentrations relative to H_2 concentrations, characteristic of low conversions, significantly reduce the rate of polymerization relative to the rate of termination. The net result is a lower degree of polymerization at lower recycle-to-feed ratios. At higher temperatures and higher conversions, the final CO concentrations for both recycle cases are low enough that their influence on polymerization relative to each other is insignificant. The corresponding degrees of polymerization are, therefore, approximately equal.

4.3.3.3 Slurry Reactor

In choosing operating conditions for the slurry reactor variable study, sensitivity to parameter changes for both upward and downward directions of perturbation was desired. Koelbel's choice of operating conditions, i.e., low temperature, low pressure, low H_2/CO ratio, and high conversion (Table 4.3-15), limited the sensitivity to CO conversion at elevated pressures. Space velocity was, therefore, increased to reduce CO conversion to roughly 90%. The results of the present study are shown in Figures 4.3-26 and 4.3-27. The effect of a 126 psi increase in pressure on CO conversion is roughly 4% at low temperatures while decreasing to 1.5% at high temperatures. The effect on degree of polymerization, on the other hand, was almost negligible at all temperatures.

GHSV studies were performed at Koelbel's operating pressure, i.e., 174 psia, and can be seen in Figures 4.3-28 and 4.3-29. As expected, CO conversion decreases with increasing space velocity. The degree of polymerization on the other hand increases with increasing space velocity. This is clearly a result of the relative concentrations of CO and H_2 in the reactor at different conversion levels. The influence of CO and H_2 concentrations on degree of polymerization have been discussed in the tube-wall reactor section (Section 4.3.3.1) and will be discussed further in Section 4.3.4. The same arguments apply here.

Figures 4.3-30 and 4.3-31 represent the effects of H_2/CO ratio. H_2/CO ratio has a large influence on the degree of polymerization, while having a smaller effect on CO conversion. Here again, the effect of relative H_2 and CO concentrations on the competition between termination reactions and polymerization reactions is clearly demonstrated.

The question of mass transfer limitations in the slurry reactor has received significant attention in the literature but, to date, has not been answered conclusively. A set of conditions suggested by Koelbel (7) was used to determine the sensitivity of two mass transfer parameters on CO conversion and degree of polymerization. The first parameter, the specific interfacial area, is a measure of the bubble surface area available per volume of reactor space. The second parameter, the mass transfer rate constant, fixes the rate of mass transfer for a given component.

Although some work has been done on determining specific interfacial areas in slurry systems, values reported are at best approximations. The value chosen for the majority of these studies, 305 ft^2/ft^3, is consistent with those reported by Koelbel (2) and Deckwer (57). A study was made to determine the influence of a 20% lower interfacial area. Figures 4.3-32 and 4.3-33 represent results with interfacial surface area of 244 and 305 ft^2/ft^3. A lower interfacial surface area reduces the CO conversion roughly 0.2-0.8%, but does not affect the degree of polymerization. The latter result is not surprising since the interfacial area should influence the rate of mass transfer of all components equally.

In order to study the influence of mass transfer rate on CO conversion and degree of polymerization, the values of the mass transfer rate constant, k_L, for hydrogen and CO were individually adjusted 20% above and below their respective base values. The results are presented in Figure 4.3-34. As can be seen, neither the mass transfer rate constant for H_2 nor the constant for CO has a dramatic effect on either CO conversion or degree of polymerization.

These results do not support the conclusion that the slurry reactor operating at Koelbel's conditions is mass transfer limited.

4.3.3.4 Ebullating Bed Reactor

The ebullating bed reactor is believed to differ from the slurry reactor in two respects, i.e., catalyst particle size and liquid flow characteristics.

Since heat removal is accomplished by a circulating liquid stream, larger particles are used to prevent the catalyst carryover which would normally occur if slurried catalyst was used. However, this size difference also introduces the question of possible mass transfer limitations within the pore structure of the larger particles. Although many similarities exist between an ebullating bed reactor and a slurry reactor, this added complexity prevented the development of an ebullating bed model. However, if one speculates on the influence of pore diffusion, the following results might be drawn:

1. Since, by definition, mass transfer limitations result in lower concentrations of reactants at the catalytic site, conversion per site will be lower for the ebullating bed system than for the slurry system.

2. Throughout Section 4.3, the dependence of product yields on the relative concentrations of H_2 and CO has been illustrated. Since the diffusivity of hydrogen in molten wax is higher than that of CO [Zaidi, Louisi, Ralek, Deckwer, (47)], pore diffusion

limitations will result in a higher H_2/CO ratio at the catalytic site and consequently a lower degree of polymerization could be expected.

Liquid flow characteristics in the ebullating bed reactor are also believed to differ from the slurry reactor. Larger particles not only create concerns about pore diffusion, but large particles also maintain a much more structured order in a flowing environment than do fine particles, thereby restricting back-mixing of the liquid. To observe the influence of restricted back-mixing, the slurry model was run as a two-stage system using the Koelbel reactor as a basis. As one can see from Table 4.3-16, the total CO conversion for the two-stage system is 97% compared to 91% for the single-stage system, and the degrees of polymerization are 5.1 and 4.0, respectively. The first stage in the two-stage system is the primary cause for these differences. In the case of conversion, the H_2 and CO concentrations in the first stage are higher than those in the single stage system. This higher driving force results in a 85% conversion. If a driving force equivalent to the single stage system was used, the conversion would be roughly 53%. The net result is a higher total CO conversion in the two-stage system. In the case of degree of polymerization, the H_2/CO ratio in the first stage is 1.4 compared to 1.8 for the single stage system. Here again the driving force to a higher degree of polymerization is much greater than the equivalent driving force in the single stage system, and the net result reflects this.

4.3.4 Response of Degree of Polymerization to Space Velocity

One puzzling result of the modeling work was the prediction that the degree of polymerization would decrease as the residence time increased. This was true regardless of reactor type and occurred within the entire range of Fischer-Tropsch operating conditions. A polymerization product intuitively becomes heavier the lower the reactor gas hourly space velocity.

The key to understanding this result lies in the competition between polymerization and termination. The longer the growing chain remains at a

catalyst site before being hydrogenated to a paraffin, or leaves the catalyst site as an olefin, the higher the degree of polymerization and the molecular weight of the product. This, therefore, will be a function of the relative rates of these processes.

The polymerization term ($D = k_p [CO] [H_2]$) is a function of the partial pressure of both CO and H_2. The irreversible hydrogenation to paraffins term ($E = k_H [H_2]$) is only a function of hydrogen partial pressure. Because of the water-gas shift reaction, the CO conversion through a reactor is much higher than the hydrogen conversion, resulting in the partial pressure of CO dropping much more across the reactor than that of hydrogen. For example, the volumetric percentage of CO may go from 35% at the inlet to 5% at the outlet, while the hydrogen goes from 65% to 45%. This will result in the polymerization term falling to 10% of that at the inlet while the hydrogenation term is still 70% of that at the inlet. The ratio has, therefore, changed by a factor of 7, and this will cause a falling molecular weight of product and a lower degree of polymerization with increasing conversion.

The other factor that can influence the molecular weight of the product is related to the reversible termination reaction to form olefins. The effect of this reaction is to influence the proportion of CO reacting to initiate new chains compared to that elongating existing chains. As the concentration of olefins in the vapor phase increases, the reverse reaction will slow down the rate of release of olefins to the vapor phase. However, in the investigations carried out to date with the reactor models, two factors combine to make this effect insignificant. First, the concentration of olefins is still quite low at the outlet of the reactor in all cases, because of the high concentrations of H_2, CO_2 and H_2O, which are inherent to the reaction system. (The slurry system has the highest olefin concentration at the outlet, but it is still less than 5 mol-%.) The rate of the reverse reaction, therefore, will be low because of the low olefin concentrations. Second, the value of K_e used in these studies was not determined from experimental data. (The selected value is discussed in Section 4.3.1.) If experimental data support a lower value of K_e (i.e., a higher rate constant for the reverse reaction), this can

increase the influence of this effect. An investigation of the effect of olefin concentration on the degree of polymerization of the product will have to wait for further experimental data.

Table 4.3-17 provides an overall view of what happens with increasing CO conversion. Here the conversion at the reactor outlet is 98.3%. The hydrogen content remains high while the olefins only reach 3 mol-%. The CO concentration decreases from 32 to 1 mol-%.

Another way of understanding this phenomenon is from a purely mathematical point of view. A decreasing degree of polymerization fundamentally means that the rate of formation of a heavy component is less than that of a light component. Or, the rate of formation of a light component divided by that of a heavy component is greater than unity. As an example:

$$\frac{r_{C_2H_6}}{r_{C_3H_8}} > 1 \qquad (31)$$

Using the mathematical expressions derived for these rates, one obtains:

$$\frac{r_{C_2H_6}}{r_{C_3H_8}} = \frac{AC + B[C_2H_4]}{A^2C + B \cdot A\,[C_2H_4] + B\,[C_3H_6]} \qquad (32)$$

If Equation 32 is rearranged, one obtains:

$$\frac{r_{C_2H_6}}{r_{C_3H_8}} = \frac{1}{A + \dfrac{[C_3H_6]}{\dfrac{AC}{B} + [C_2H_4]}} \qquad (33)$$

For this ratio to be greater than unity, the denominator must be less than unity, or:

$$\frac{[C_3H_6]}{\frac{AC}{B} + [C_2H_4]} < 1 - A \qquad (34)$$

Typical magnitudes (Tube Wall Reactor R-29T) of these numbers are as follows:

$$A = 0.504$$

$$\frac{AC}{B} = 8.97 \times 10^{-3}$$

$$[C_3H_6] = 1.0 \times 10^{-6}$$

$$[C_2H_4] = 1.15 \times 10^{-6}$$

Considering the relative magnitude of the olefin concentration terms compared to the value of AC/B, it is apparent that the left side of Equation 34 is less than the right side and, therefore, the degree of polymerization is decreasing through the reactor.

What are the factors required to reverse the trend causing the degree of polymerization to decrease through the reactor? In other words, what is required for the following equation to hold:

$$\frac{[C_3H_6]}{\frac{AC}{B} + [C_2H_4]} > 1 - A \qquad (35)$$

The most obvious factor is for the concentrations of the olefins to increase to an order of magnitude equivalent to, or greater than the value of AC/B. As mentioned earlier, this is unlikely since olefin concentrations always remain extremely low throughout the reactor.

Another possibility lies in the value of A. One notices that as A approaches unity, the right side of Equation 35 approaches zero and at some point will be less than the left side. The definition of A is:

$$A = \frac{k_p[CO][H_2]}{k_p[CO][H_2] + k_H[H_2] + k_o} \quad (36)$$

where terms are defined in Section 4.1. For A to approach unity,

$$k_H\,[H_2] + k_o << k_p\,[CO][H_2] \quad (37)$$

The right and left sides of this equation represent the polymerization rate term and the termination rate terms, respectively. Therefore, as one might expect, polymerization must completely dominate termination in order to have an increasing degree of polymerization through the reactor.

A third possibility lies in the value of B. If B is very large, the value of AC/B will eventually become the same order of magnitude as the olefin concentration terms. B is defined as:

$$B = \frac{k_o}{K_e\,(k_o + k_p[CO][H_2] + k_H\,[H_2])} \quad (38)$$

Since $k_o/(k_p + RI + RT)$ is always less than unity, the only way to make B large is to have K_e very small. This is precisely the conclusion at the beginning of this section.

To this point, the entire discussion has revolved around the mechanism as it was originally derived. It should be pointed out that there were three assumptions made during the derivation that may be influencing the results. The first is the assumption of steady state. In a non-steady state system, it is obviously impossible in a polymerization reaction to make a C_{20} component before a C_{19} component is available. The steady state assumption, on the other hand, suggests that all components are available immediately upon entering the reactor. The rate of production of any given component, therefore, can not be inhibited by the lack of availability of another.

The second is the assumption of fixed rate constants and equilibrium constants for all carbon numbers. Since degree of polymerization is influenced by the rates of formation of components relative to each other, it is apparent how fixed rate constants could restrict this particular yield characteristic.

The third is the assumption with regard to order of the reactions. The polymerization term was assumed to be first order with respect to both hydrogen and carbon monoxide. The paraffin termination term was assumed to be first order with respect to hydrogen only. The olefin termination was assumed to be zero order. If polymerization was found to be zero order with respect to CO, for example, the entire analysis with regard to relative CO and hydrogen concentrations would no longer hold, and the influence on degree of polymerization would be quite different.

In summary:

1. Given the existing mechanism, increasing H_2/CO ratio through the reactor has influenced the competition between polymerization rates and termination rates in such a way as to result in a decreasing degree of polymerization with reactor length.

2. Resolution of some of the assumptions incorporated into the existing mechanism may influence this result.

4.3.5 Reactor Comparisons

Since a model was not developed for the ebullating bed system, comparisons were limited to the tube-wall, slurry, and entrained bed reactors. The three areas concentrated on were as follows:

1. The base operating conditions chosen for each reactor system.

2. At the base conditions, the efficiency of utilization of CO and H_2 as well as the quantities of H_2O, CO_2 and hydrocarbon produced.

3. The sensitivity of CO conversion and degree of polymerization to operating condition changes.

The first of these comparisons is presented in Table 4.3-18. The slurry operating conditions and yields represent those given by Koelbel for a demonstration unit of 10,000 liter capacity (20). The entrained bed operating conditions and yields are taken from the Standard Oil of Indiana Feasibility Study performed by Kellogg (4). The tube-wall conditions were originally going to be taken from the Ralph M. Parsons study (16); however, as mentioned in Section 4.3.2, these conditions appeared to be overly optimistic. Two sets of conditions are shown for the tube-wall and are those that bracket the final operating conditions selected for the engineering evaluation. For each reactor type, the final selection appears to represent the most optimistic set of operating conditions, assuming present day catalysts.

There are three representations of reactor efficiency in Table 4.3-18, i.e., J factor, gas hourly space velocity, and β. Respectively, they represent the utilization efficiencies of catalyst surface, reactor space, and catalyst weight.

A comparison of GHSV's suggests that the entrained bed reactor utilizes reactor space roughly 3-1/2 times more efficiently than either the slurry or tube-wall reactor. The reason is the higher catalyst density per unit volume in the entrained bed reactor. However, this can be misleading, since the entrained bed reactor has an additional vessel which acts solely as a temporary holding tank for circulating catalyst. If one were to recalculate the GHSV using the volume of reactor plus holding tank, the value would decrease to roughly 350 hr^{-1}, and would not look nearly as attractive.

From a catalyst perspective, a comparison of β's suggests that the slurry and entrained bed reactors utilize a pound of catalyst roughly 4-1/2 and 2-1/2 times, respectively, as efficiently as the tube-wall reactor. At the same time, the J factor indicates that the catalyst

surface available for that pound of catalyst is roughly between 5 and 8 times as great for the slurry and entrained bed as for the tube-wall system.

It is apparent that the tube-wall reactor design is least efficient with regard to both reactor space and catalyst utilization. Regarding the remaining two systems, the entrained bed system seems to have a slight edge in the utilization of reactor space while the slurry system is clearly the most catalyst efficient.

One of the most important questions asked during the evaluation of these reactor systems was -- How efficiently does each reactor system convert CO and H_2 to usable product? To answer this question, a comparison was made at "base case" conditions for each reactor system. In the case of the entrained bed and slurry reactors, the base case was the Kellogg (4) and Koelbel (7) designs, respectively. In the case of the tube-wall reactor, the base case consisted of feed and product yields from the Parsons design (16) modified to represent potassium-promoted taconite as catalyst.

Table 4.3-19 represents reactant conversion and product yields per mole of fresh feed and per mole of CO plus H_2 converted. A comparison of total weight of hydrocarbon produced per mole of fresh feed suggests that the entrained bed reactor makes more product than the slurry reactor, which makes more product than the tube-wall reactor. Although these numbers may represent the performance of each specific reactor, they do not reflect the performance of the overall reactor systems for conversion of synthesis gas. For example, the entrained bed reactor uses a large amount of recycle gas and conversion is therefore higher on a fresh feed basis than for the other two reactors. The tube-wall reactor has a high feed gas H_2/CO ratio and this results in a lower synthesis gas conversion than in the slurry reactor. Variations in feed compositions also affect the figures in Table 4.3-19.

If moles of CO plus H_2 converted is used as a basis, the influences of feed compositions and water-gas shift can be eliminated. For every

mole of CO converted via water-gas shift, for example, a mole of H_2 is produced and, therefore, the sum of H_2 plus CO remains unchanged. A comparison of total weight of hydrocarbon produced on this basis shows only minor differences between reactor systems. However, the efficiency with which the shift reaction is being used is clearly shown by the relative consumptions or productions of H_2, CO, H_2O, and CO_2.

In the case of the entrained bed system, the CO_2 level in the combined feed, caused by high concentrations in the recycle gas, is so high that the shift reaction is at equilibrium, i.e., no CO_2 produced. Virtually every mole of CO entering the reactor is converted to hydrocarbon product. On the other hand, not one mole of H_2 is being produced within the reactor. The net result is that a large water-gas shift system is required upstream of the entrained bed reactor in order to supply the necessary hydrogen for feed.

In contrast, the shift reaction in the slurry reactor is far from equilibrium as reflected by the CO_2 produced. A significant portion of the CO is being converted to CO_2 in order to produce the necessary hydrogen, but the weight of hydrocarbon produced is equivalent or perhaps slightly greater than the other systems. Also the shift reaction is taking place in the same vessel as the Fischer-Tropsch reaction. Auxiliary equipment for adjustment of H_2/CO ratio is, therefore, not necessary, and as steam for the shift system does not have to be produced, an overall advantage in thermal efficiency will result.

The tube-wall reactor falls in between. This reactor requires a high H_2/CO ratio in the feed and, therefore, requires auxiliary shift reaction equipment. At the same time, the CO_2 content of the feed is not high enough to prevent the production of unneeded H_2 at the expense of CO. The combination of these two effects causes the tube-wall system to produce significantly less hydrocarbon per mole of fresh feed than the other systems.

The third set of comparisons, i.e., sensitivity of CO conversion and degree of polymerization to operating conditions, is represented in

Figures 4.3-35 through 4.3-41. The study was performed by adjusting either pressure, temperature, or H_2/CO ratio while maintaining all other base conditions constant.

Pressure can be seen to have a dramatic effect on CO conversion for both the entrained bed and tube-wall systems. The slurry system, however, is only modestly influenced. The insensitivity of the slurry system is caused by: a) back-mixing of the liquid phase which causes the concentration driving force for reaction to be constant and equal to the outlet conditions, and b) solubilities in the liquid phase. At 300 psig, the CO conversion in the slurry system is 94.5%. The liquid phase CO and H_2 concentrations are 6.5×10^{-4} and 8.5×10^{-4} moles/ft^3 liquid, respectively. At 174 psig, the conversion is 85% and the CO and H_2 concentrations are 8.4×10^{-4} and 5.23×10^{-4}, respectively. The rate of conversion is proportional to the product of these concentrations. At 300 psig this is 5.52×10^{-7}, while at 174 psig this is 4.39×10^{-7}. The ratio of these numbers is 1.26 and is a measure of the relative increase in driving force for CO conversion due to increased pressure. In the gas phase, this same ratio would be equal to the ratio of the pressures or 1.67. Clearly the liquid phase response to pressure is less dramatic than for the gas phase.

The decrease in the degree of polymerization with pressure in the slurry system (Figure 4.3-36) can be explained in a similar manner. As mentioned earlier, the degree of polymerization is determined by competition between rates of termination and polymerization. The rate of polymerization is generally described as being proportional to the product of H_2 and CO concentrations, i.e., $r_p \propto [CO]\,[H_2]$, while the rate of termination is proportional to just the H_2 concentration, i.e., $r_t \propto [H_2]$. For a gas phase system, when the pressure is increased from 174 psig to 300 psig, these concentrations at the reactor inlet increase in direct proportion to the absolute pressure by a factor of 1.67. The competition between polymerization and termination is, therefore, changed by a factor of 1.67 consistent with the ratio of r_p to r_t. In the slurry system, the solubility changes with respect to pressure coupled with the relative conversion levels determine the liquid phase concentrations and, therefore, the

relative rates. Solubility alone is roughly proportional to pressure, and one would, therefore, expect to see an increase in concentrations similar to the gas phase systems. However, the increased pressure also increases conversion thereby lowering the outlet concentrations. From 174 to 300 psig, the net result is a decrease in CO concentration from 8.4×10^{-4} to 6.5×10^{-4} moles/ft^3 liquid and an increase in H_2 concentration from 5.23×10^{-4} to 8.5×10^{-4} moles/ft^3 liquid. This corresponds to factors of 0.77 and 1.63 for changes in the CO and H_2 concentrations, respectively. The ratio of r_p to r_t, i.e. 0.77 x 1.63/1.63 = 0.77, reflects an increase in the role of termination relative to polymerization and is consistent with a decreasing degree of polymerization.

The influence of temperature on CO conversion and degree of polymerization is presented in Figures 4.3-37 and 4.3-38. As in the case of pressure, CO conversion in the slurry reactor is less sensitive to temperature than in the other two systems. The back-mixed nature of the slurry system results in reaction rates being dependent on outlet concentrations of reactants. Because these concentrations are low, the rates are much slower than in the other systems. Conversion is attained by using longer residence time, rather than by having the higher concentration driving forces of the plug flow reactors. This lethargic nature of the slurry reaction rates is reflected in the response of CO conversion to temperature.

There are few operating variables that have a more dramatic effect on degree of polymerization than temperature (Figure 4.3-38). The reason lies in understanding the competition between rates of polymerization and hydrogenation as they relate to the rate constants. The rates of polymerization and hydrogenation are proportional to Arrhenius rate constants with activation energies of 26,430 and 28,825 Btu/lb mole, respectively. An increase in temperature from 500°F to 600°F increases the polymerization and hydrogenation rate constants by factors of 3.71 and 4.17, respectively. Thus, the ratio of polymerization to rate of termination decreases to 0.89 of its original value, which causes the degree of polymerization to decrease with increasing temperature.

Although the above discussion satisfactorily explains the direction of change, it does not explain the insensitivity of the entrained bed reactor system relative to the slurry or tube-wall systems. The slurry reactor was defined as being isothermal. Although the tube-wall reactor was not defined in this manner, the heat transfer coefficient for heat removal was such that nearly isothermal conditions were attained. The entrained bed system was the only system which had three areas of increasing temperature through the reactor. But why would this cause the entrained bed yield structure to be less sensitive to temperature? Figure 4.3-42 illustrates the reason. Line I represents the degree of polymerization versus temperature line which would exist under isothermal conditions. Earlier it was mentioned that increasing the temperature from 500 to 600°F increases the termination rate constant by a factor of 4.17. When the same ΔT is applied from 600 to 700°F, the termination rate constant only increases by a factor of 3.28. In other words, the influence of increasing temperature at low temperatures is greater than at high temperatures. The entrained bed system was operated with a constant 36°F ΔT across the reactor at each inlet temperature. At T_1 on Figure 4.3-42, this 36°F ΔT will have the effect of dropping the degree of polymerization from point a to point b. At T_2, the same 36°F will have less effect and will only drop the degree of polymerization from point c to point d. The same applies for T_3. The net result is Line II which has a slope much less steep than the isothermal line.

The influence of combined feed H_2/CO ratios on CO conversion and degree of polymerization is presented in Figures 4.3-39 and 4.3-41. Not surprisingly, an increase in H_2/CO ratio results in an increase in CO conversion. Both the rates of polymerization and termination are proportional to H_2 concentration, and although the concentration of CO does drop with increasing H_2/CO ratio, its influence is surpassed by that of increasing H_2 concentration. It is interesting, however, that the increase in CO conversion between 1.0 and 2.0 H_2/CO ratios is significantly less than between 0.7 and 1.0 H_2/CO ratios, particularly in the tube-wall and slurry reactors. A closer look at the water-gas shift reaction explains this phenomenon. The CO conversion in Figure 4.3-39 is a combination of that converted to hydrocarbon and to CO_2 via the shift reaction. As the H_2/CO

ratio is increased, the reaction of CO and H_2O to form H_2 and CO_2 is inhibited. Obviously, this influence is greater from 1.0 to 2.0 H_2/CO ratio than from 0.7 to 1.0 H_2/CO ratio. In Figure 4.3-40 the shift reaction has been normalized out of the results, and only CO conversion to hydrocarbons is reported. It can be seen that, now, the influence of H_2/CO ratio is equivalent for the entrained bed and tube-wall reactors. The slurry reactor, however, is less sensitive. Here, as in the case of temperature, the back-mixed nature of the slurry system has resulted in slower rates causing less severe response to operating changes.

Although slurry back-mixing is responsible for slower rates, it is also responsible for the large influence of combined feed H_2/CO ratio on degree of polymerization. While in large part the plug flow reactor products distribution are being determined by near inlet H_2/CO ratios, i.e., 0.7, 1.0, and 2.0, the back-mixed reactor product distribution is being determined by outlet H_2/CO ratios, i.e., 1.15, 2.33, and 6.17. Figure 4.3-41 clearly reflects these results.

FIGURE 4.3-1

LOG OF MOLE FRACTION vs. CARBON NUMBER

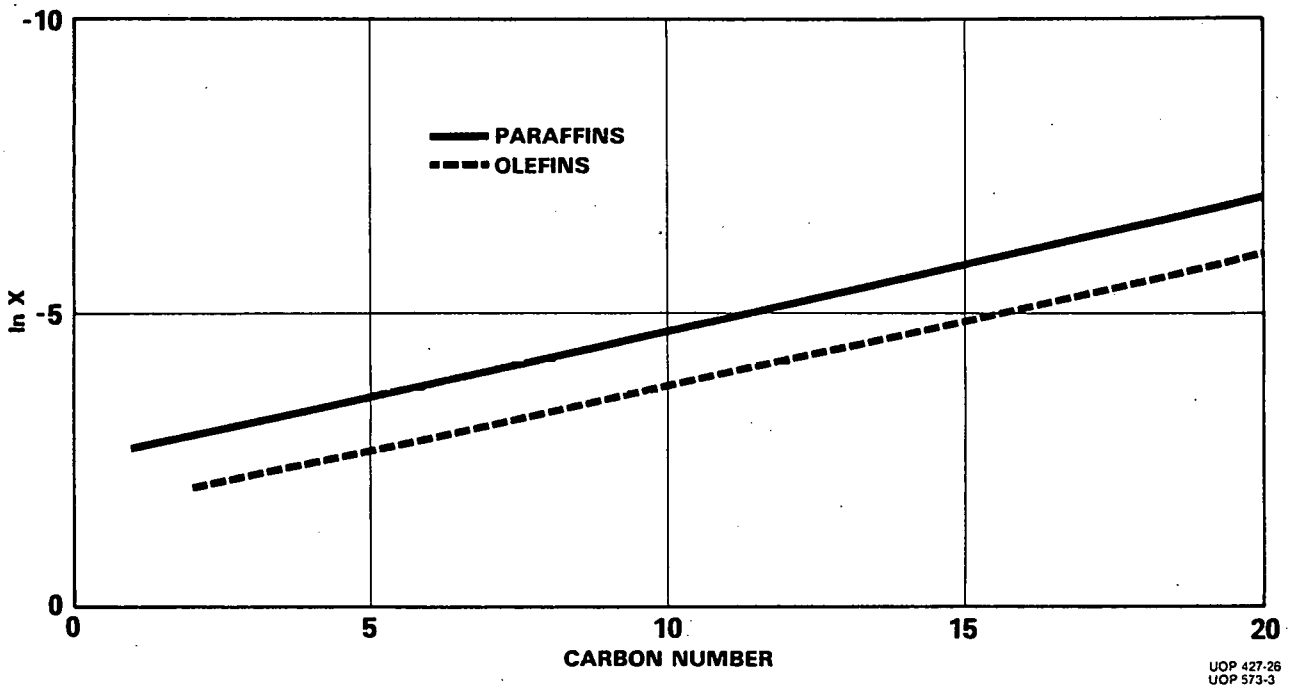

FIGURE 4.3-2

LOG OF MOLE FRACTION vs. CARBON NUMBER

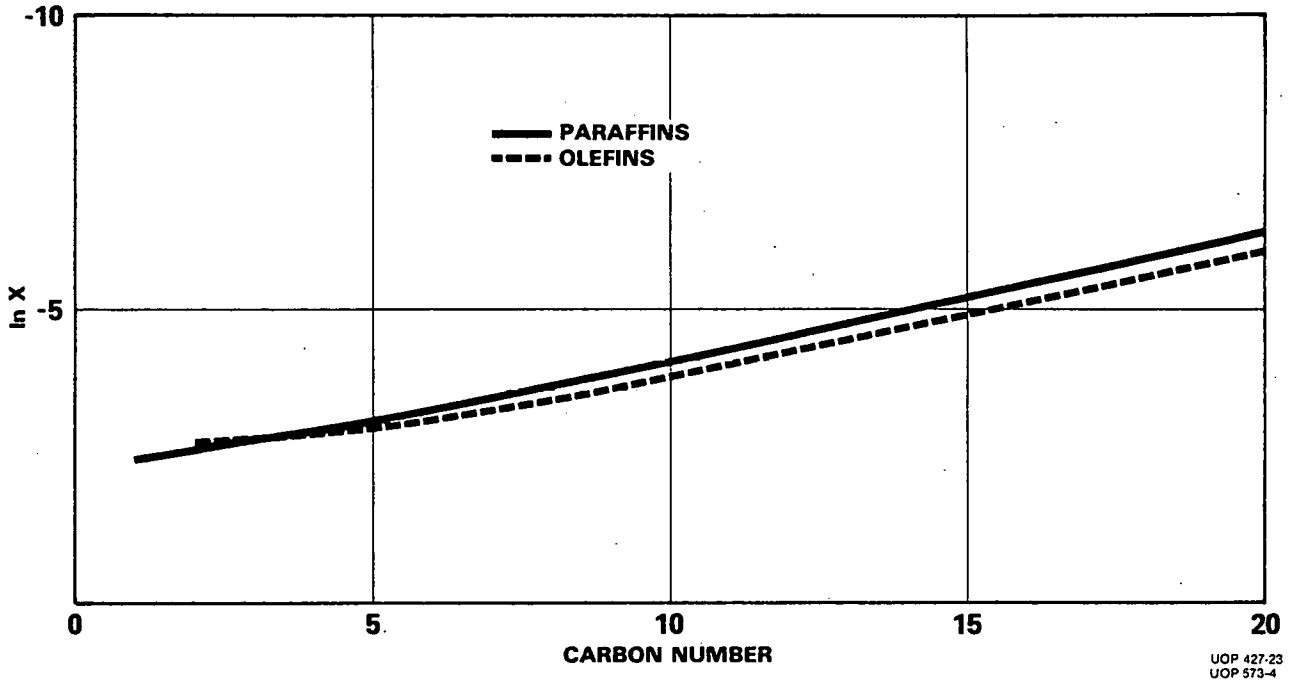

FIGURE 4.3-3

VARIATION OF TYPICAL PRODUCT SPLIT WITH DEGREE OF POLYMERIZATION

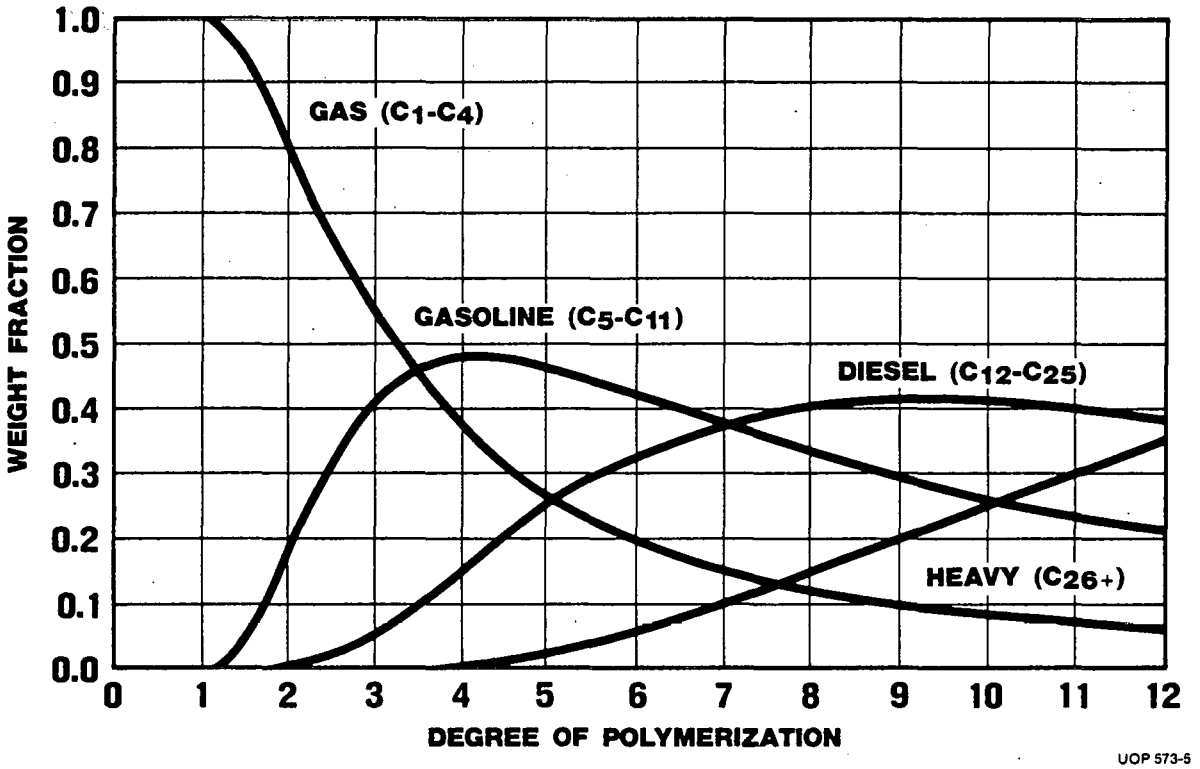

FIGURE 4.3-4

FISCHER TROPSCH

TUBE WALL REACTOR
CO CONVERSION vs. TEMPERATURE
VARIABLE PRESSURE

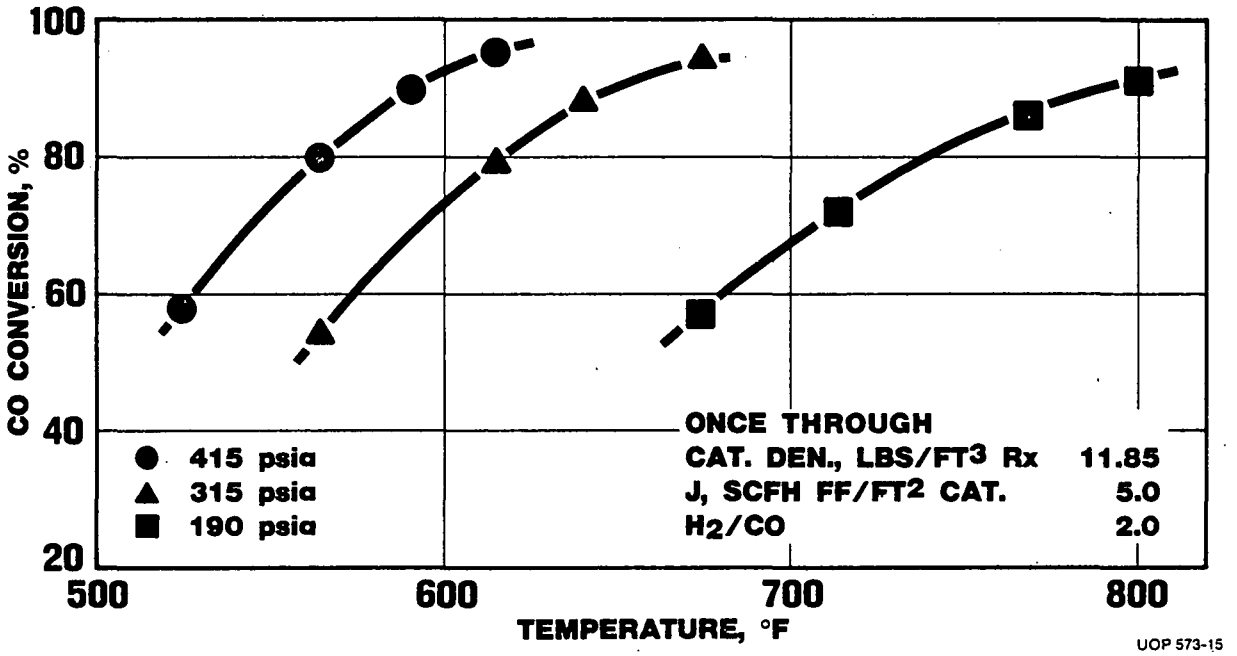

FIGURE 4.3-5

FISCHER TROPSCH

TUBE WALL REACTOR
CO CONVERSION vs. TEMPERATURE
VARIABLE J FACTOR

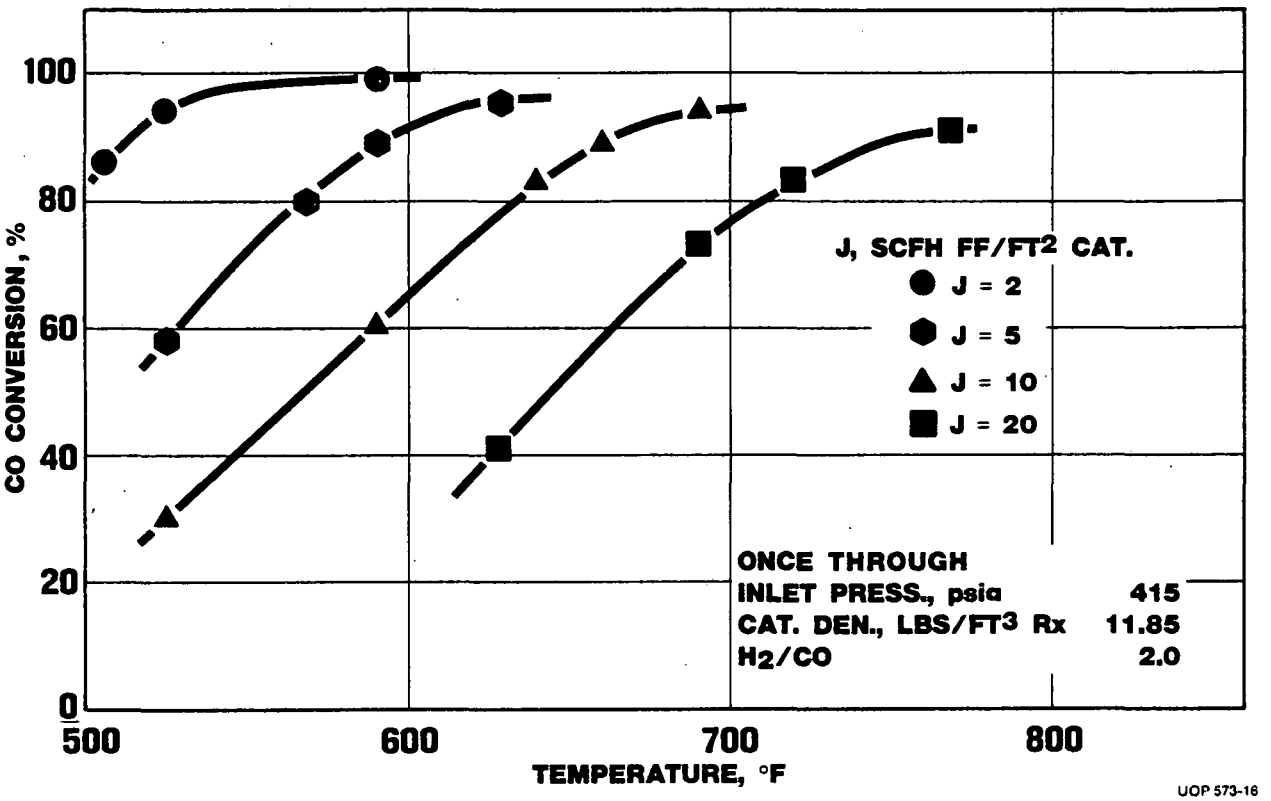

FIGURE 4.3-6

FISCHER TROPSCH

TUBE WALL REACTOR
CO CONVERSION vs. TEMPERATURE
VARIABLE H_2/CO RATIO

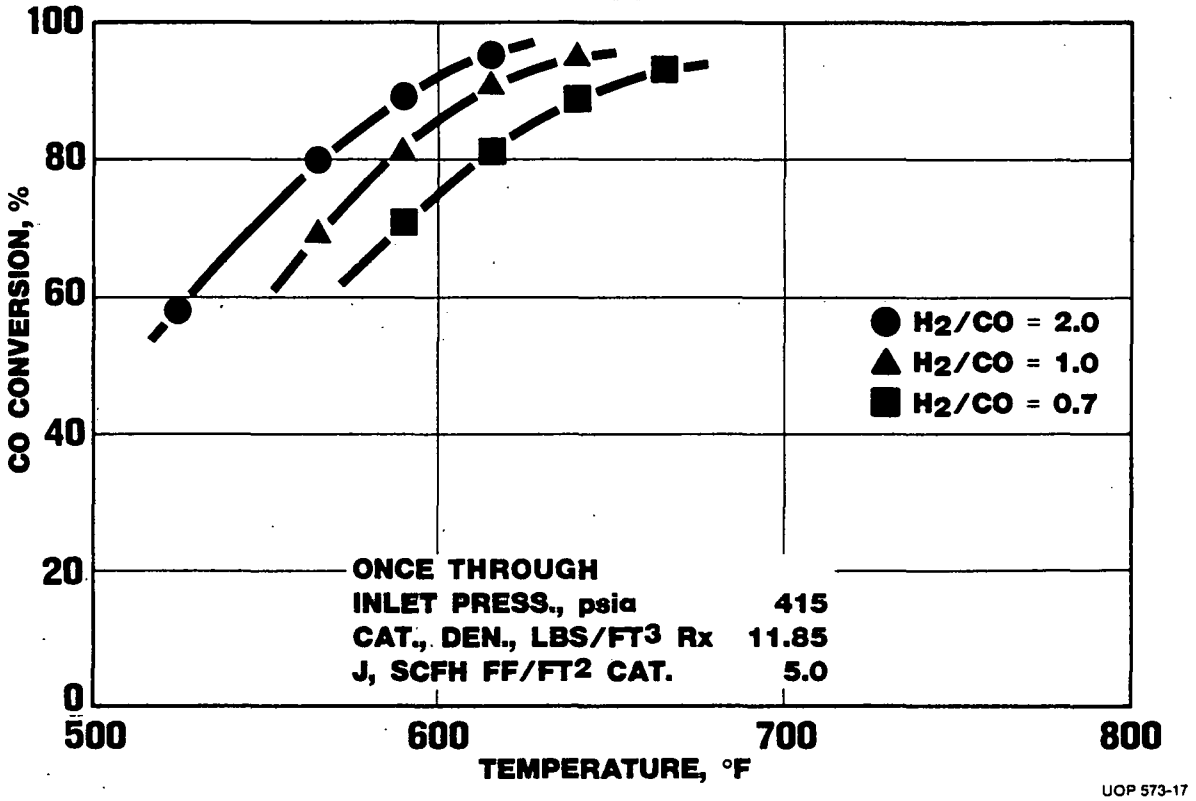

UOP 573-17

FIGURE 4.3-7

FISCHER TROPSCH

TUBE WALL REACTOR
DEGREE OF POLYMERIZATION vs. TEMPERATURE
VARIABLE PRESSURE

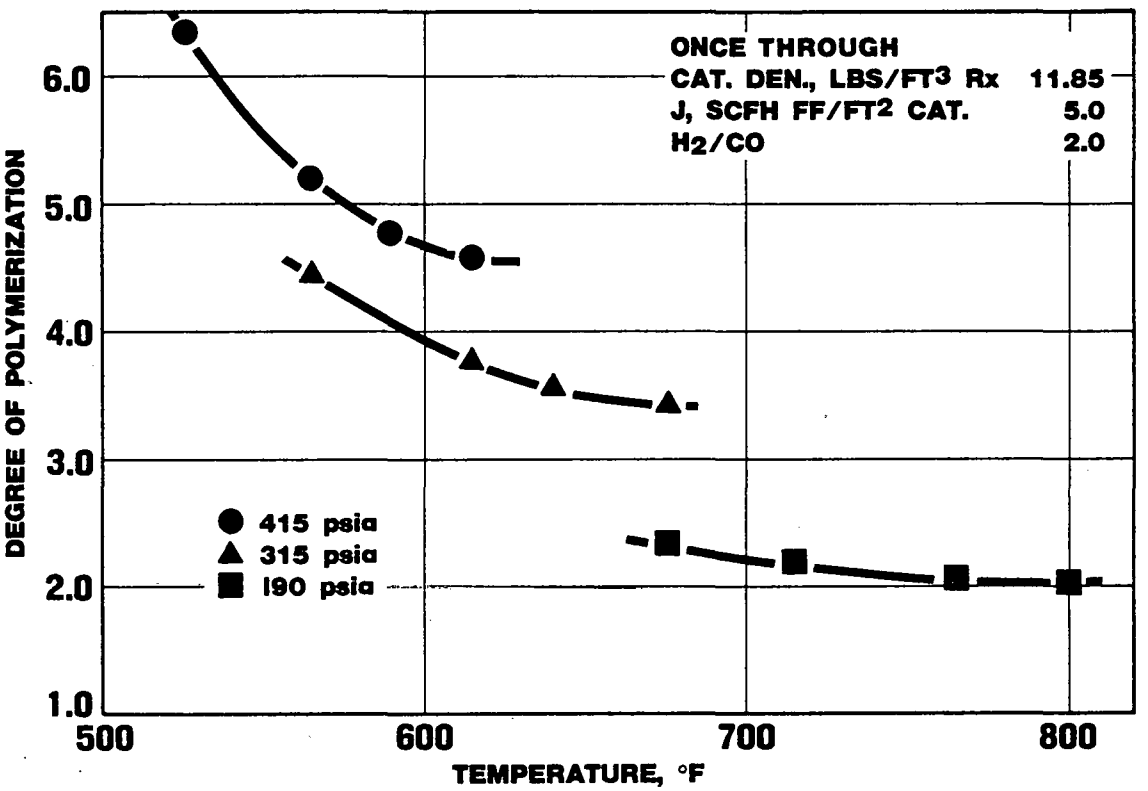

UOP 573-18

FIGURE 4.3-8

FISCHER TROPSCH

TUBE WALL REACTOR
DEGREE OF POLYMERIZATION vs. TEMPERATURE
VARIABLE J FACTOR

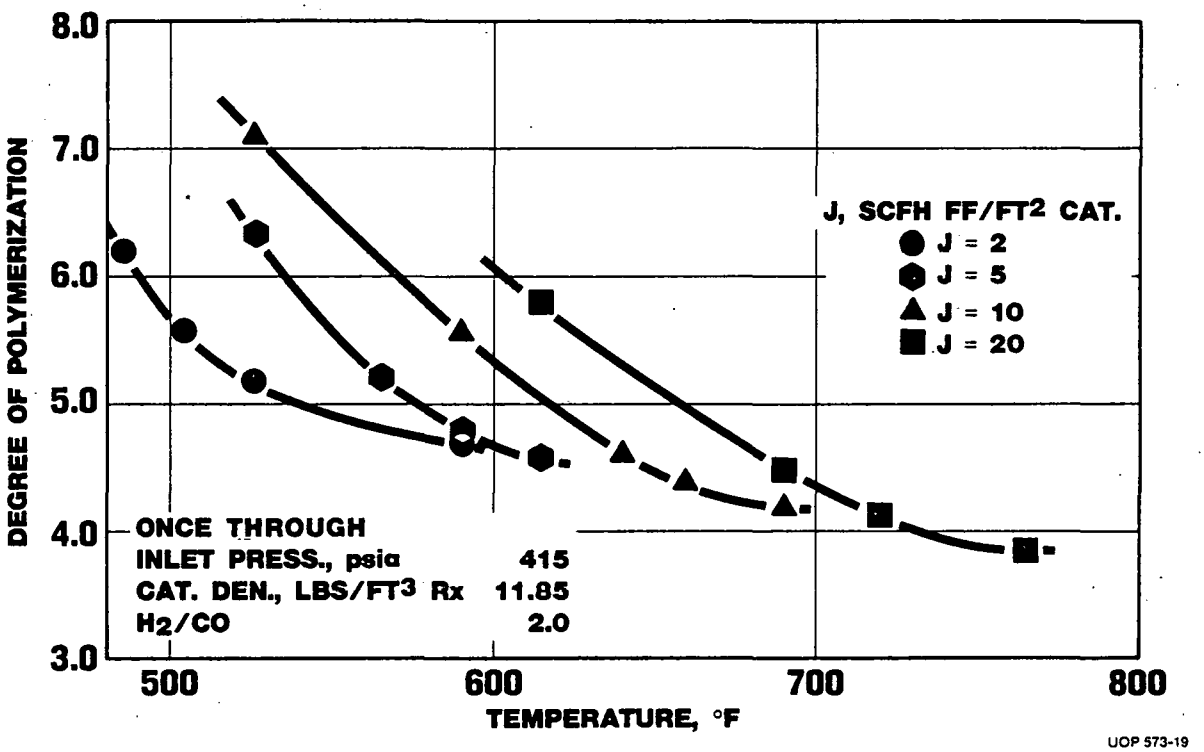

FIGURE 4.3-9

FISCHER TROPSCH

TUBE WALL REACTOR
DEGREE OF POLYMERIZATION vs. TEMPERATURE
VARIABLE H_2/CO RATIO

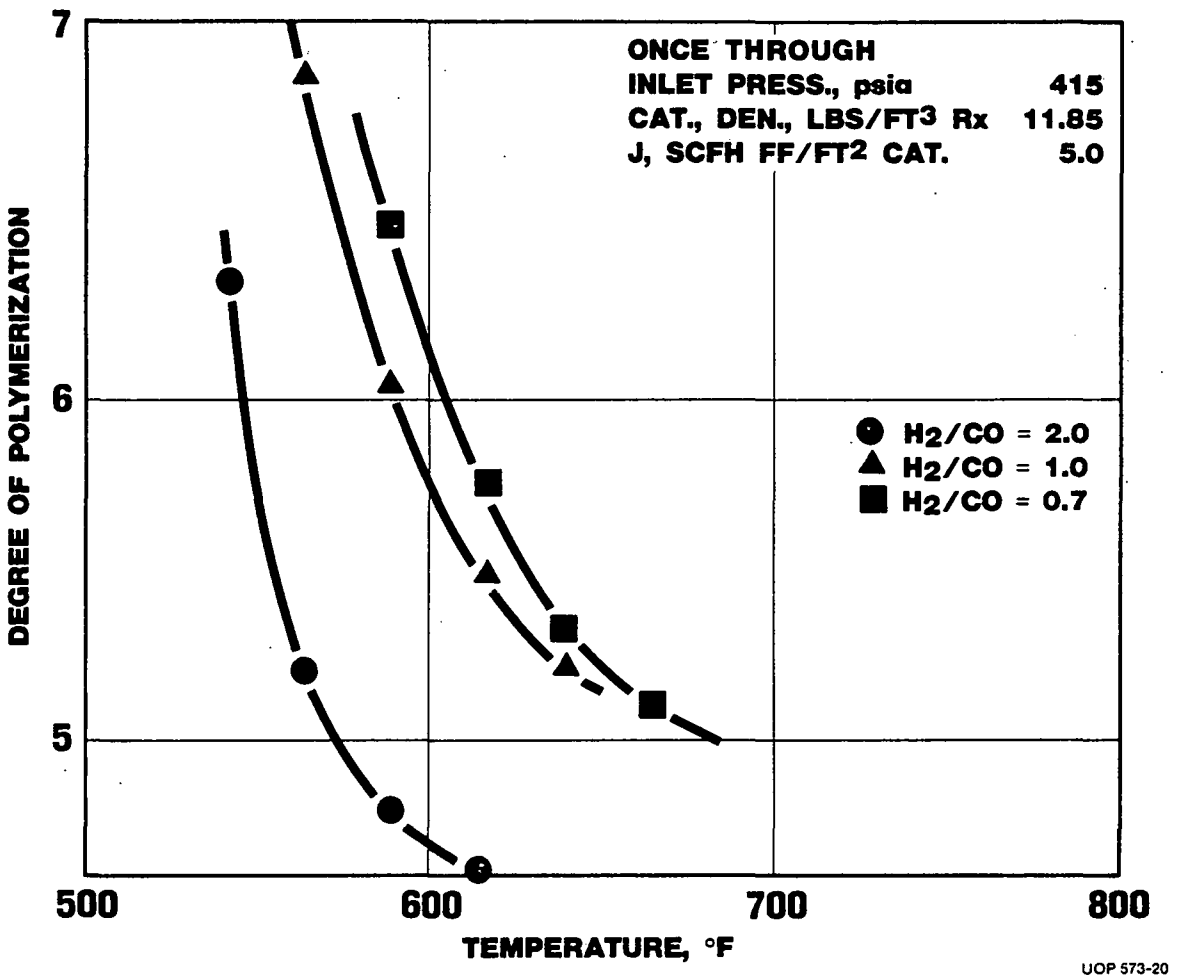

FIGURE 4.3-10

FISCHER TROPSCH

TUBE WALL REACTOR
DEGREE OF POLYMERIZATION vs. CO CONVERSION
VARIABLE H_2/CO

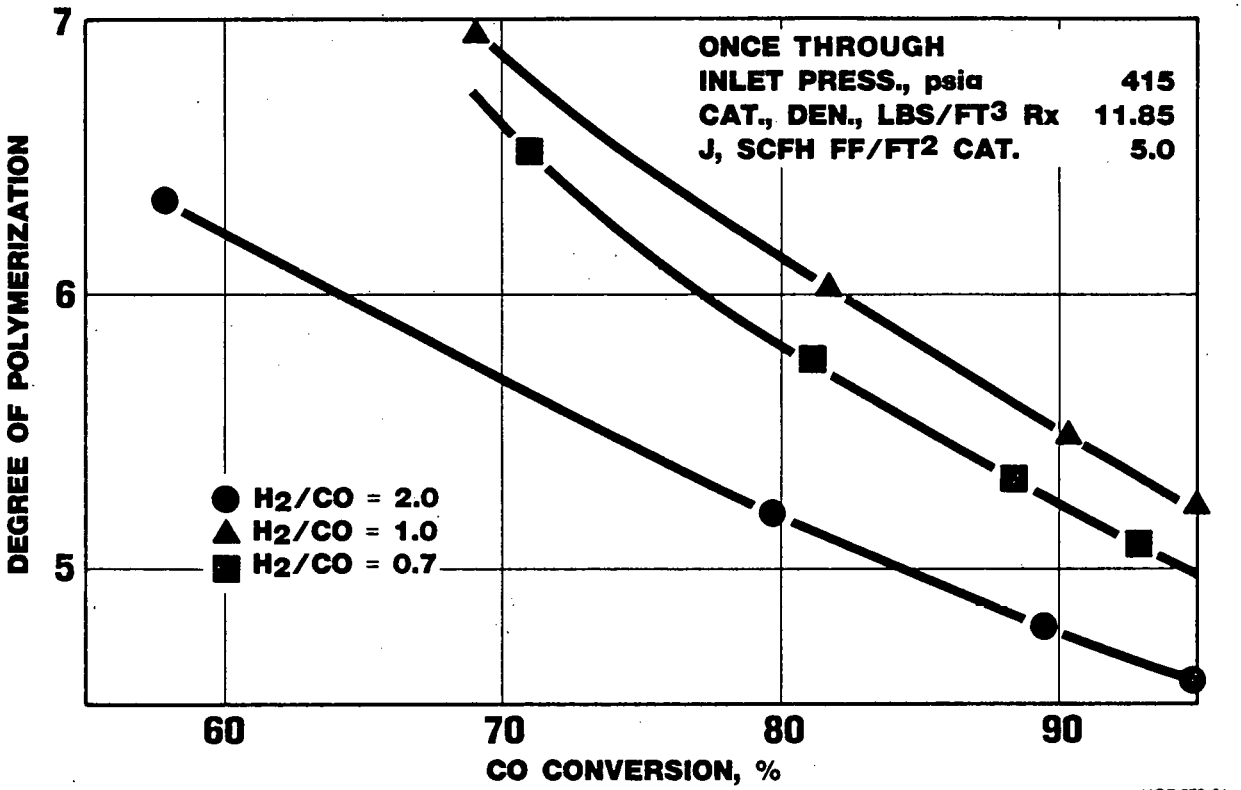

UOP 573-21

FIGURE 4.3-11

FISCHER TROPSCH

TUBE WALL REACTOR
DEGREE OF POLYMERIZATION vs. TEMPERATURE
VARIABLE RECYCLE TO FEED RATIO

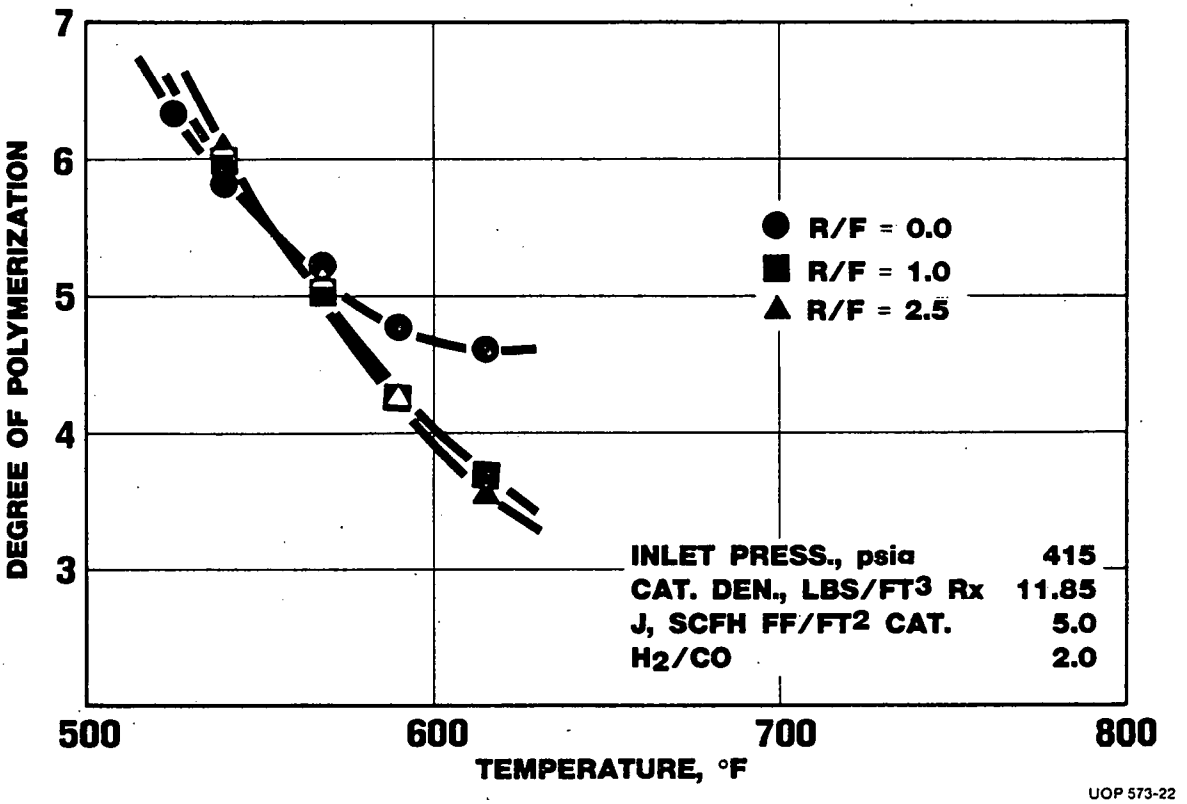

FIGURE 4.3-12

FISCHER TROPSCH

TUBE WALL REACTOR
H_2 AND CO MOLE FRACTIONS vs. REACTOR LENGTH (T = 539°F)

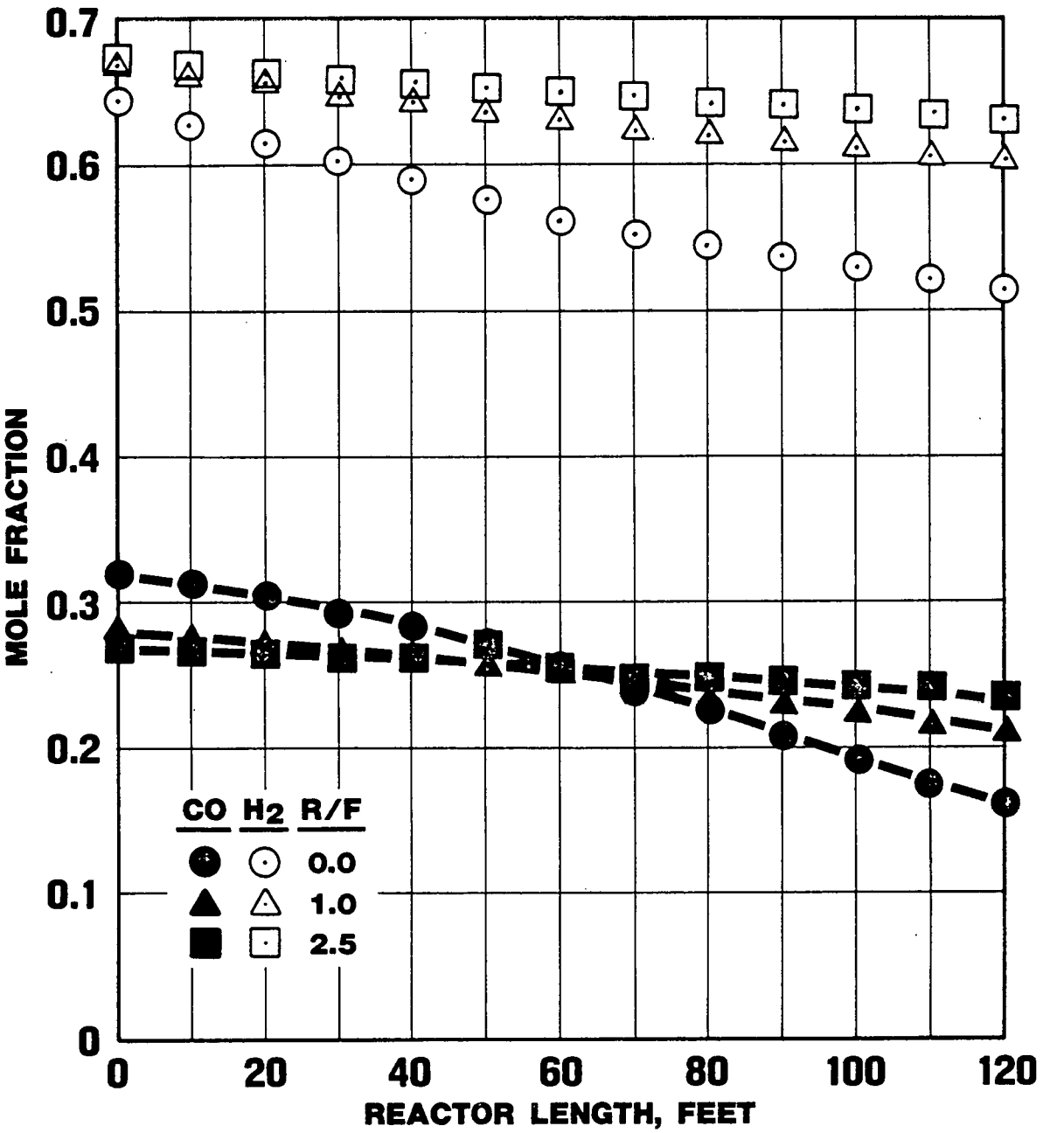

UOP 573-23

FIGURE 4.3-13

FISCHER TROPSCH

TUBE WALL REACTOR
H_2 AND CO MOLE FRACTIONS vs. REACTOR LENGTH (T = 615°F)

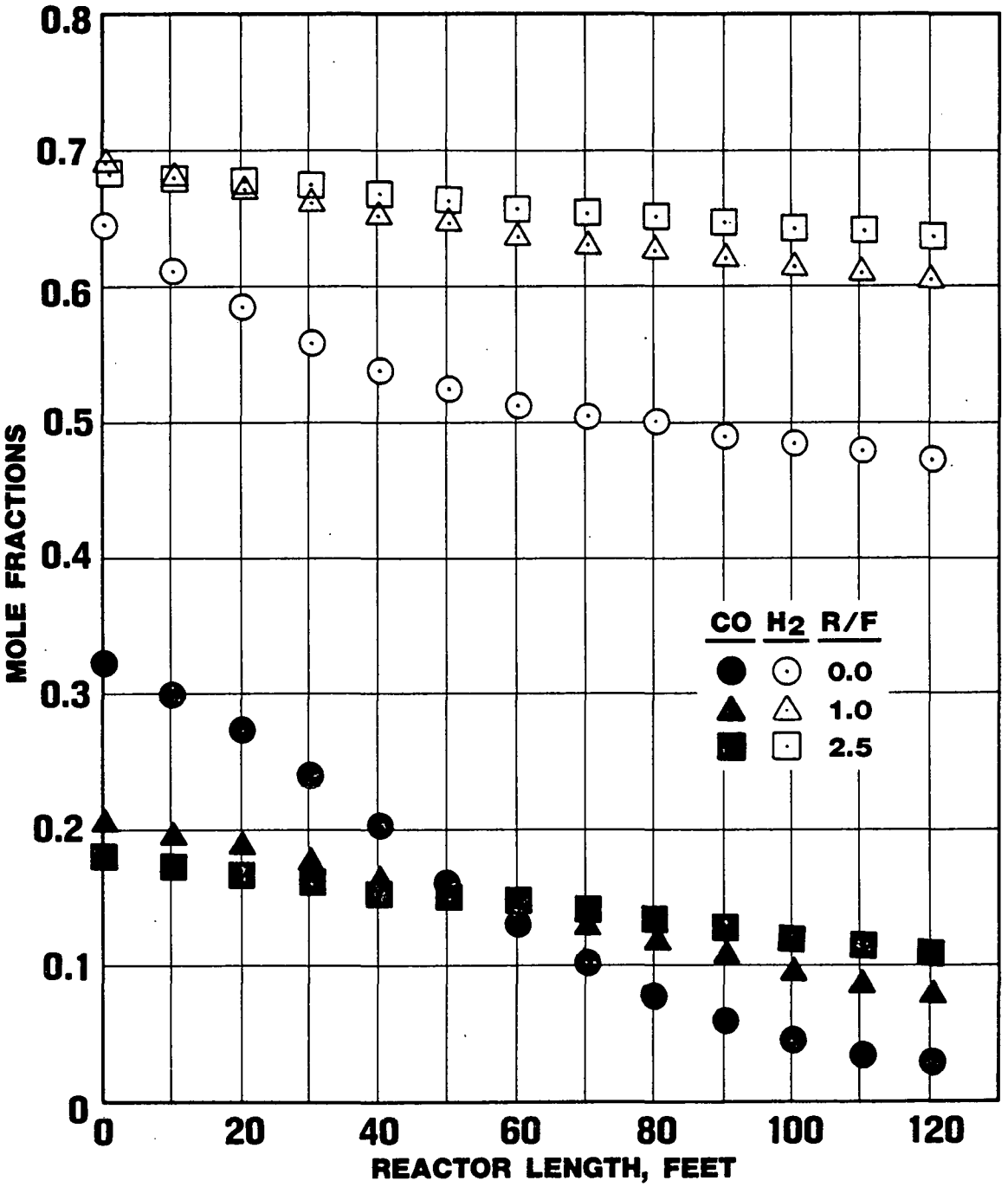

UOP 573-47

FIGURE 4.3-14

FISCHER TROPSCH

TUBE WALL REACTOR
DEGREE OF POLYMERIZATION vs.
REACTOR LENGTH (T = 539°F)

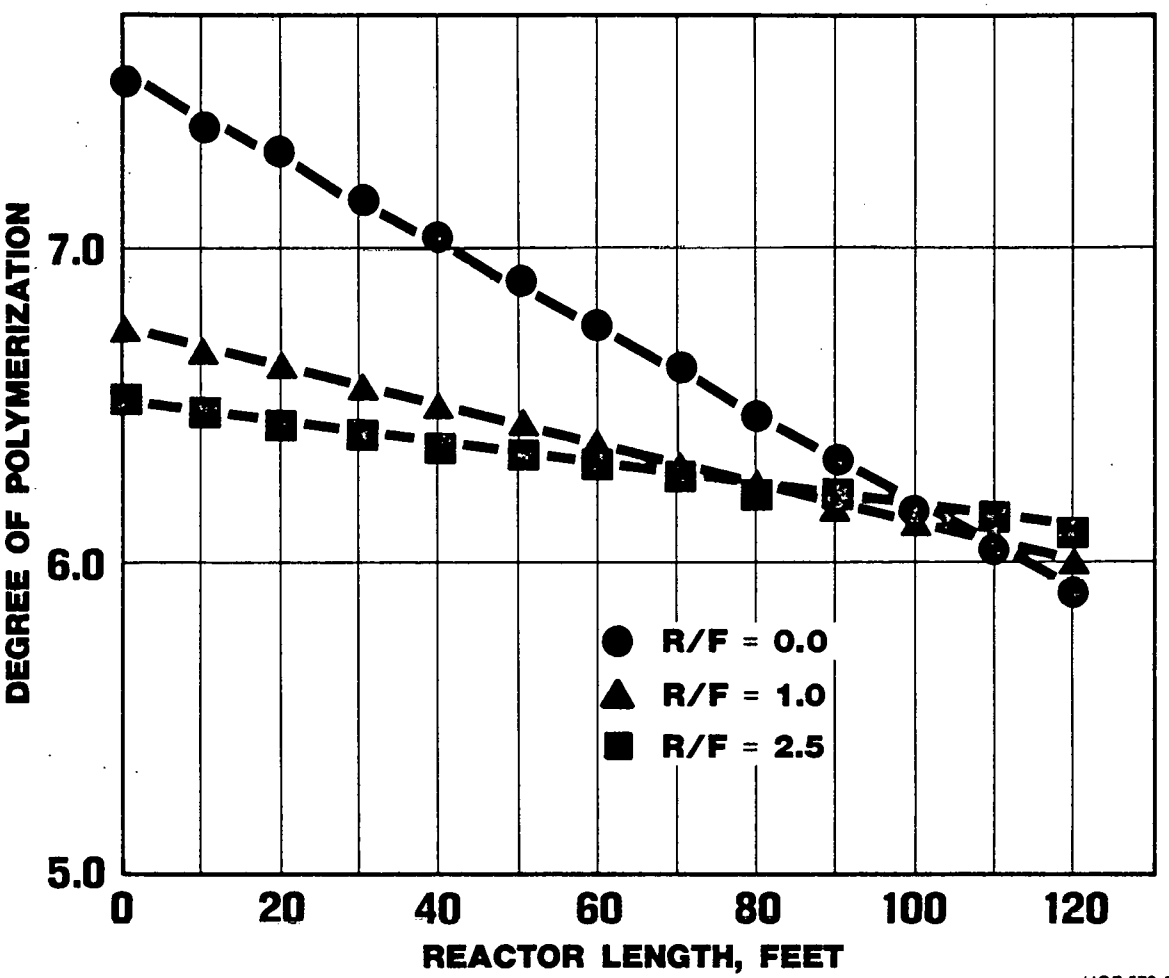

UOP 573-24

FIGURE 4.3-15

FISCHER TROPSCH

TUBE WALL REACTOR
DEGREE OF POLYMERIZATION vs. REACTOR LENGTH (T = 615°F)

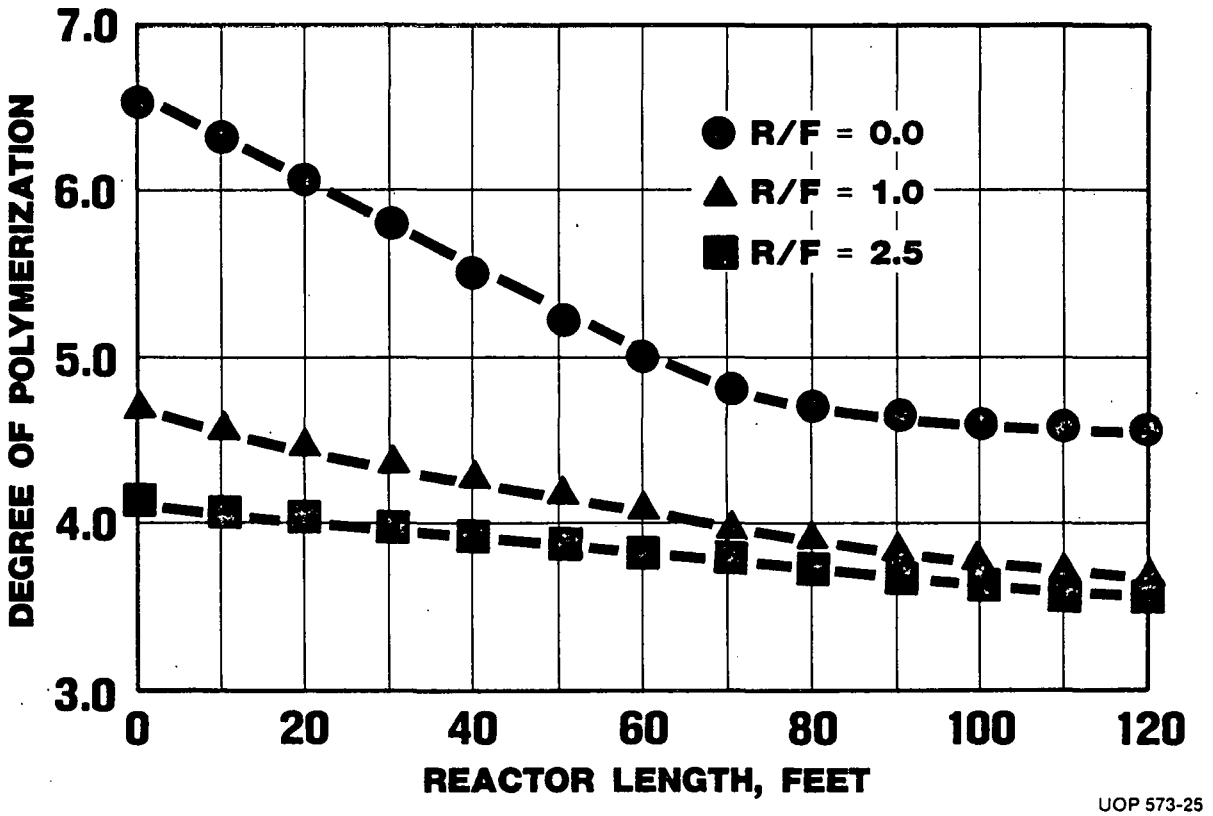

UOP 573-25

FIGURE 4.3-16

FISCHER-TROPSCH
ENTRAINED BED REACTOR
CO CONVERSION vs. REACTOR △T

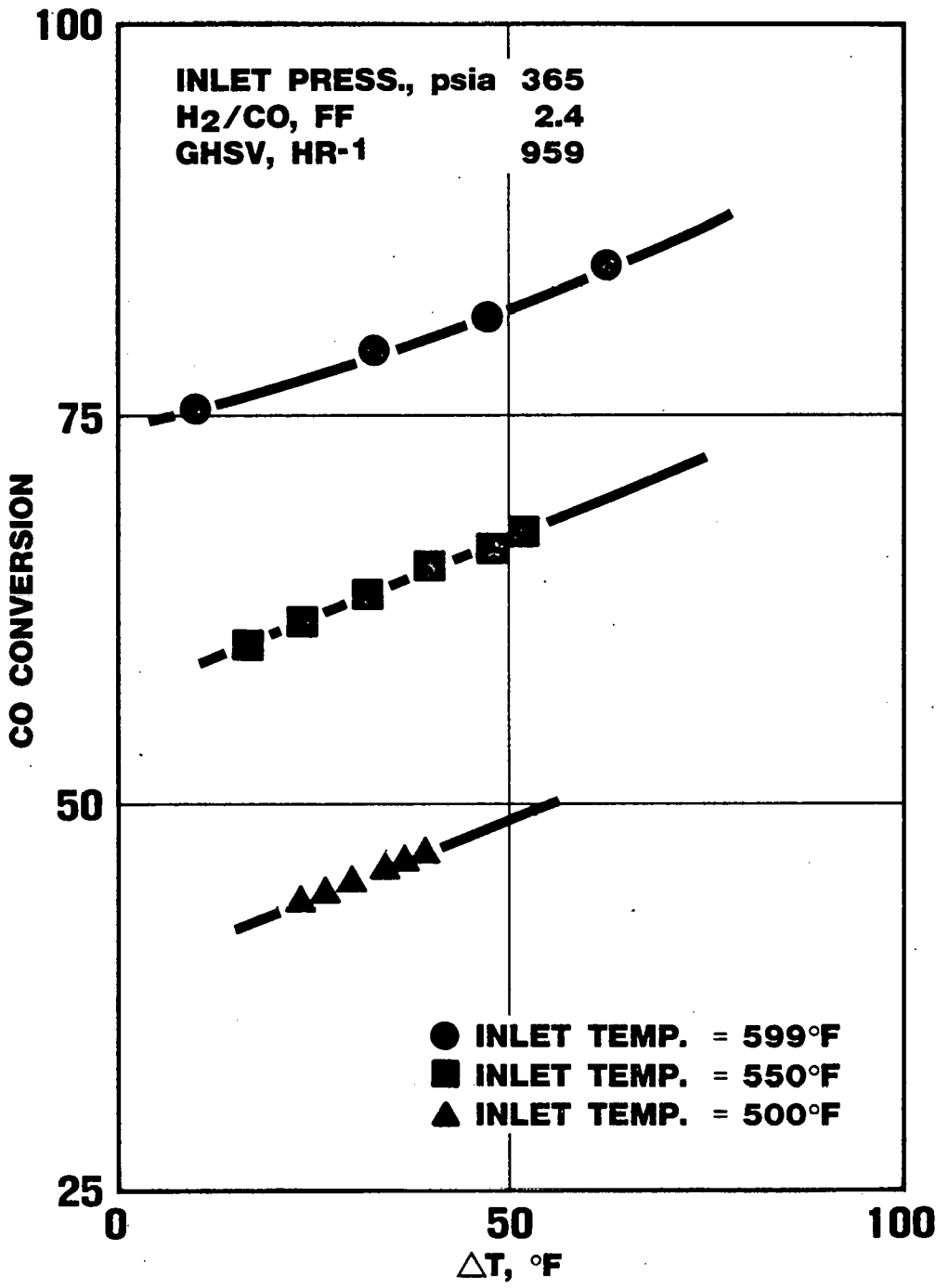

UOP 573-6

FIGURE 4.3-17

FISCHER-TROPSCH

ENTRAINED BED REACTOR
DEGREE OF POLYMERIZATION vs. REACTOR ΔT

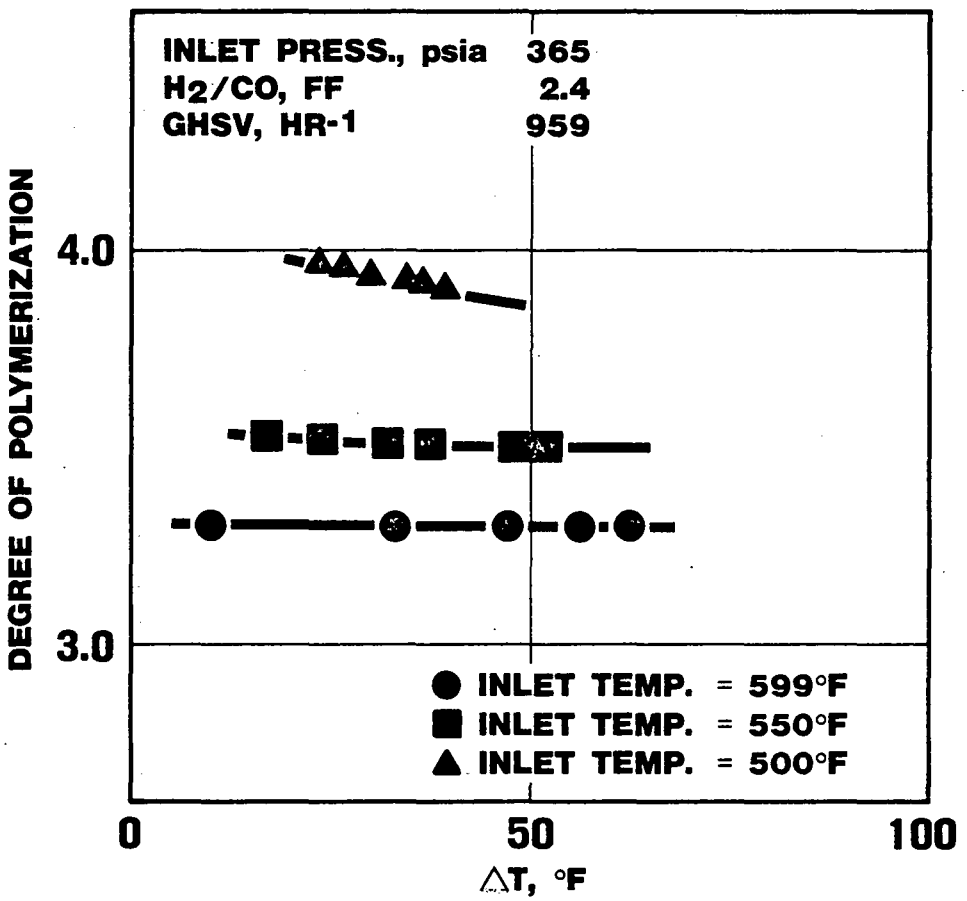

FIGURE 4.3-18

FISCHER TROPSCH

ENTRAINED BED REACTOR
CO CONVERSION vs. TEMPERATURE
DEGREE OF POLYMERIZATION vs. TEMPERATURE

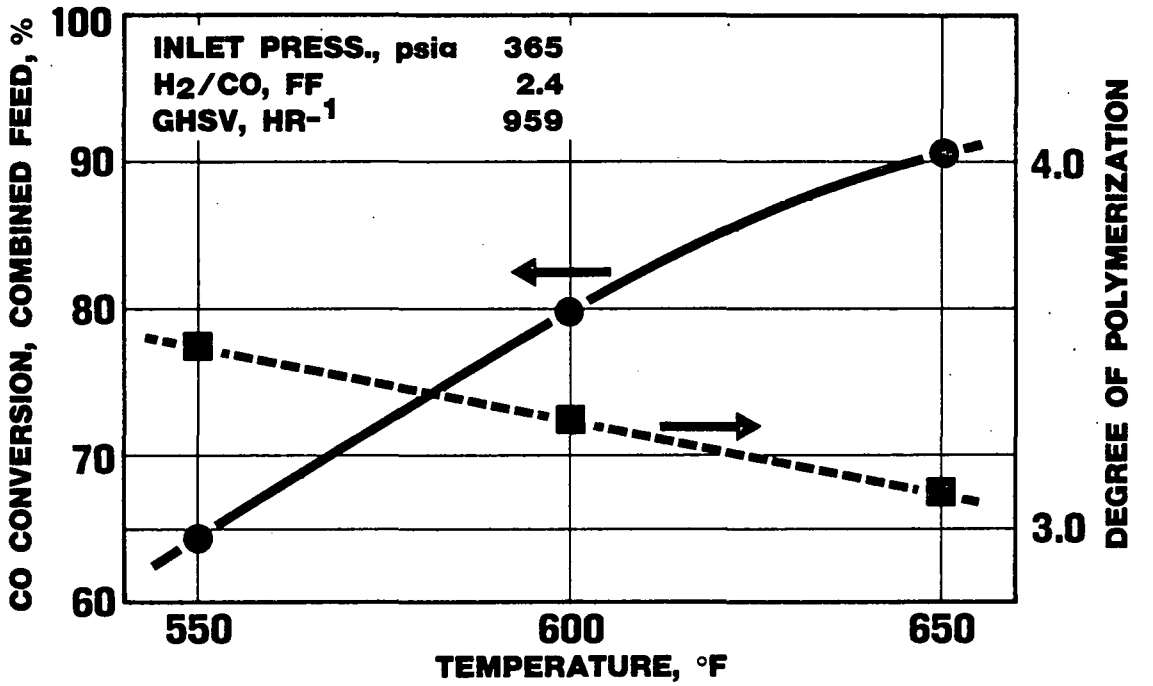

UOP 573-26

FIGURE 4.3-19

FISCHER TROPSCH

ENTRAINED BED REACTOR
CO CONVERSION vs. PRESSURE
DEGREE OF POLYMERIZATION vs. PRESSURE

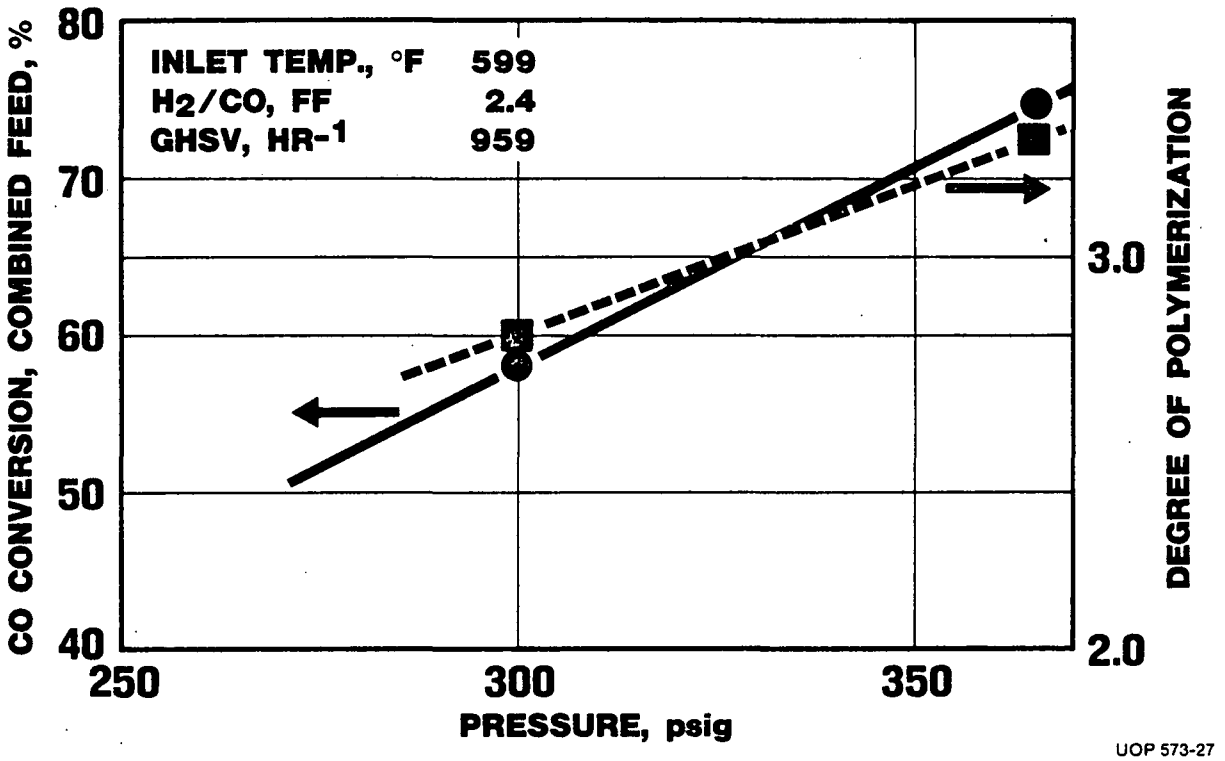

UOP 573-27

FIGURE 4.3-20

FISCHER-TROPSCH

ENTRAINED BED REACTOR
CO CONVERSION vs. β
DEGREE OF POLYMERIZATION vs. β

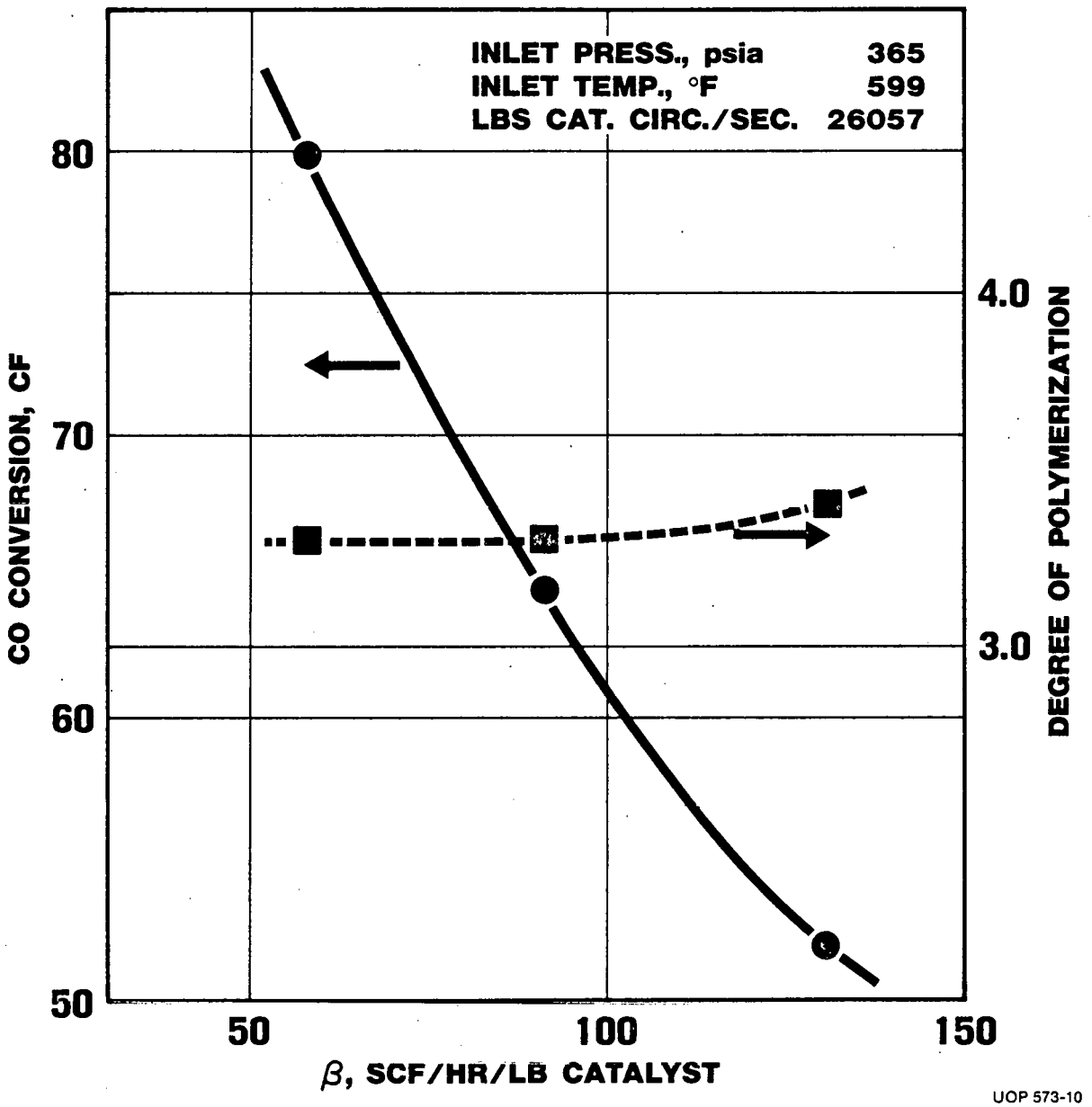

UOP 573-10

FIGURE 4.3-21

FISCHER-TROPSCH

ENTRAINED BED REACTOR
CO CONVERSION vs. CATALYST CIRCULATION
DEGREE OF POLYMERIZATION vs. CATALYST CIRCULATION

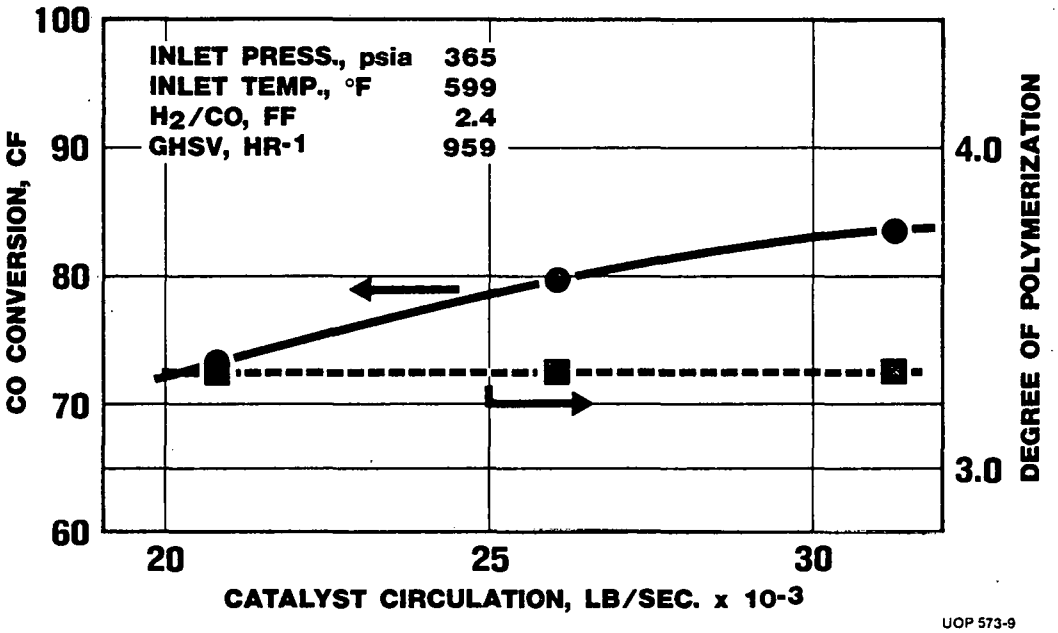

FIGURE 4.3-22

FISCHER TROPSCH

ENTRAINED BED REACTOR
CO CONVERSION vs. H_2/CO RATIO
DEGREE OF POLYMERIZATION vs. H_2/CO

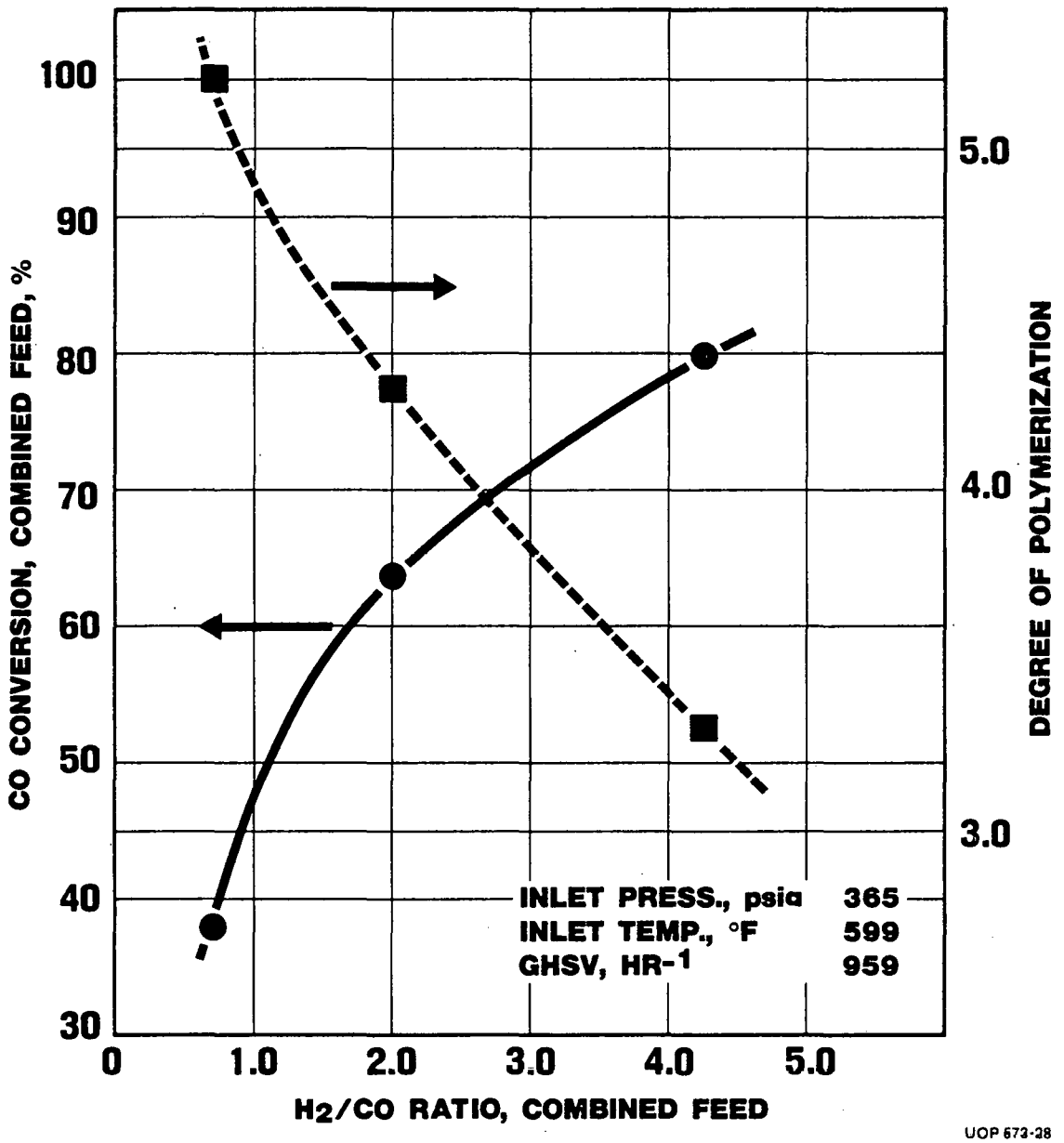

UOP 673-28

FIGURE 4.3-23

FISCHER-TROPSCH

ENTRAINED BED REACTOR AVERAGE CATALYST DENSITY vs. CATALYST CIRCULATION RATE

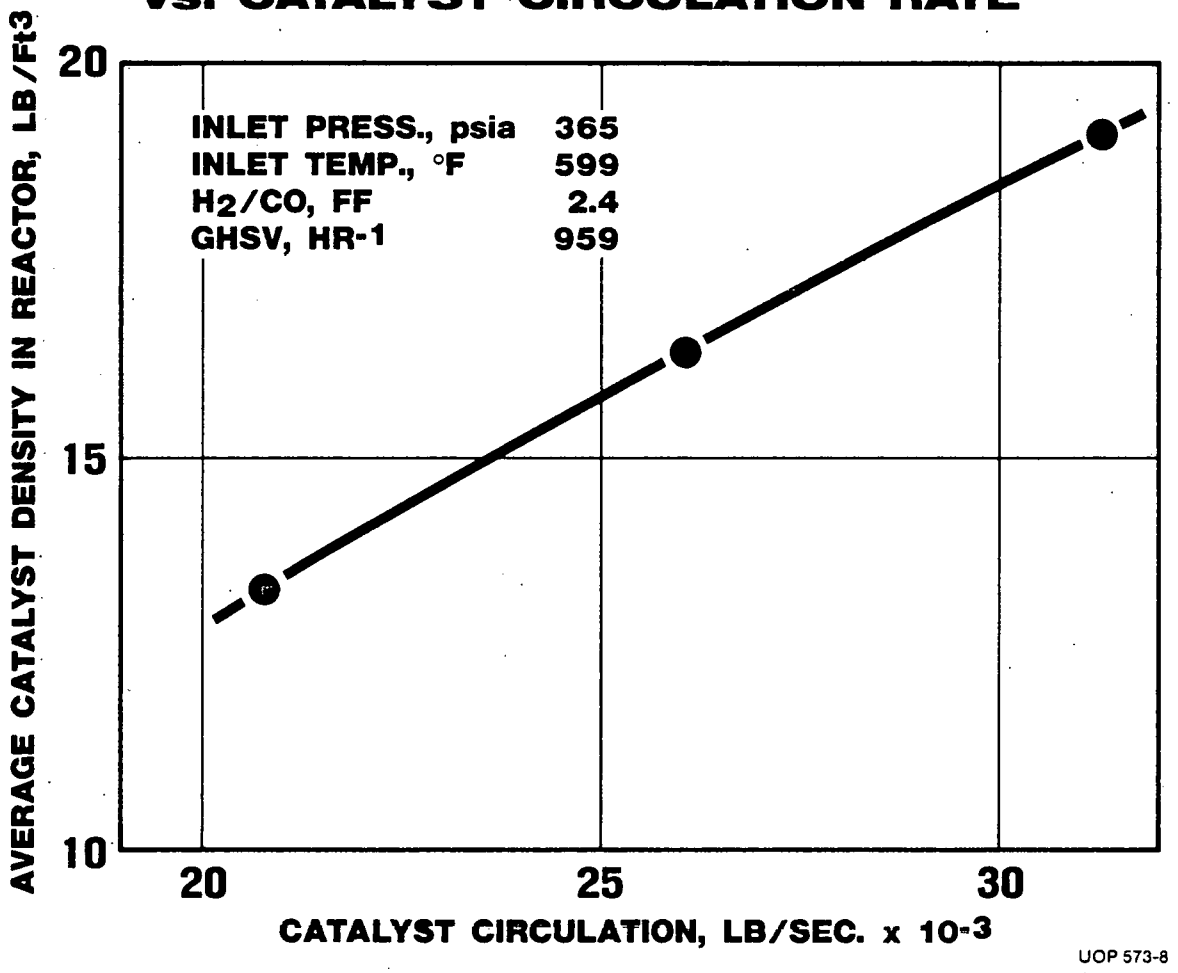

UOP 573-8

FIGURE 4.3-24

FISCHER TROPSCH

ENTRAINED BED REACTOR
CO CONVERSION vs. TEMPERATURE

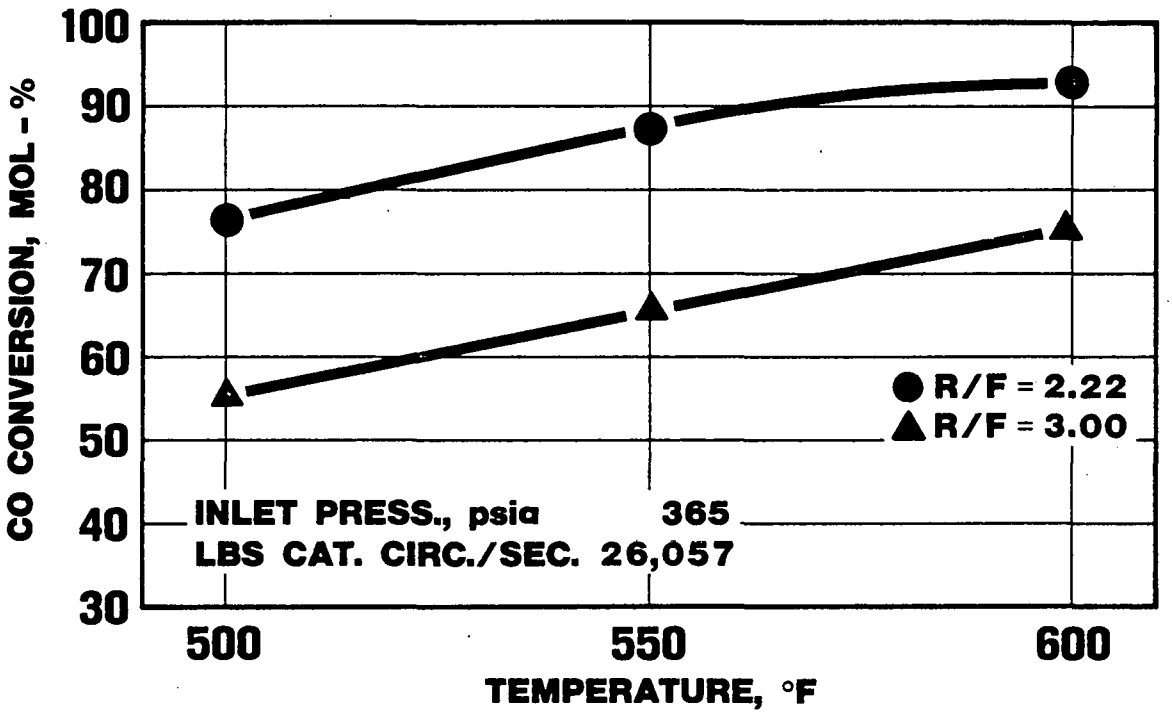

UOP 573-29

FIGURE 4.3-25

FISCHER TROPSCH

ENTRAINED BED REACTOR

DEGREE OF POLYMERIZATION vs. TEMPERATURE

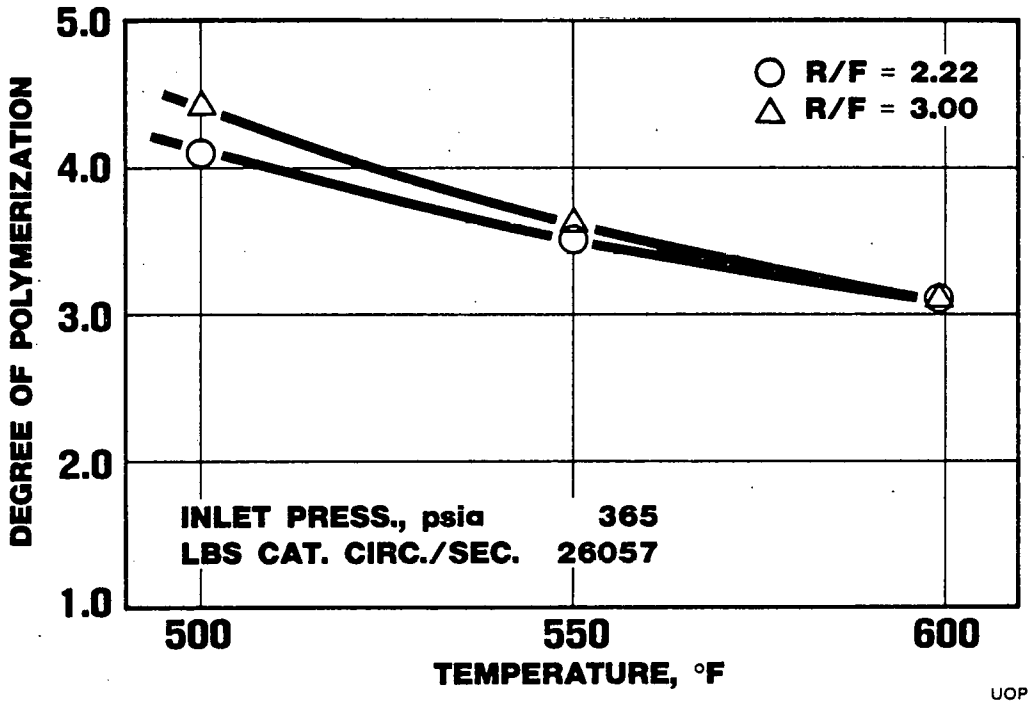

UOP 573-30

FIGURE 4.3-26

FISCHER TROPSCH

SLURRY REACTOR
CO CONVERSION vs. TEMPERATURE

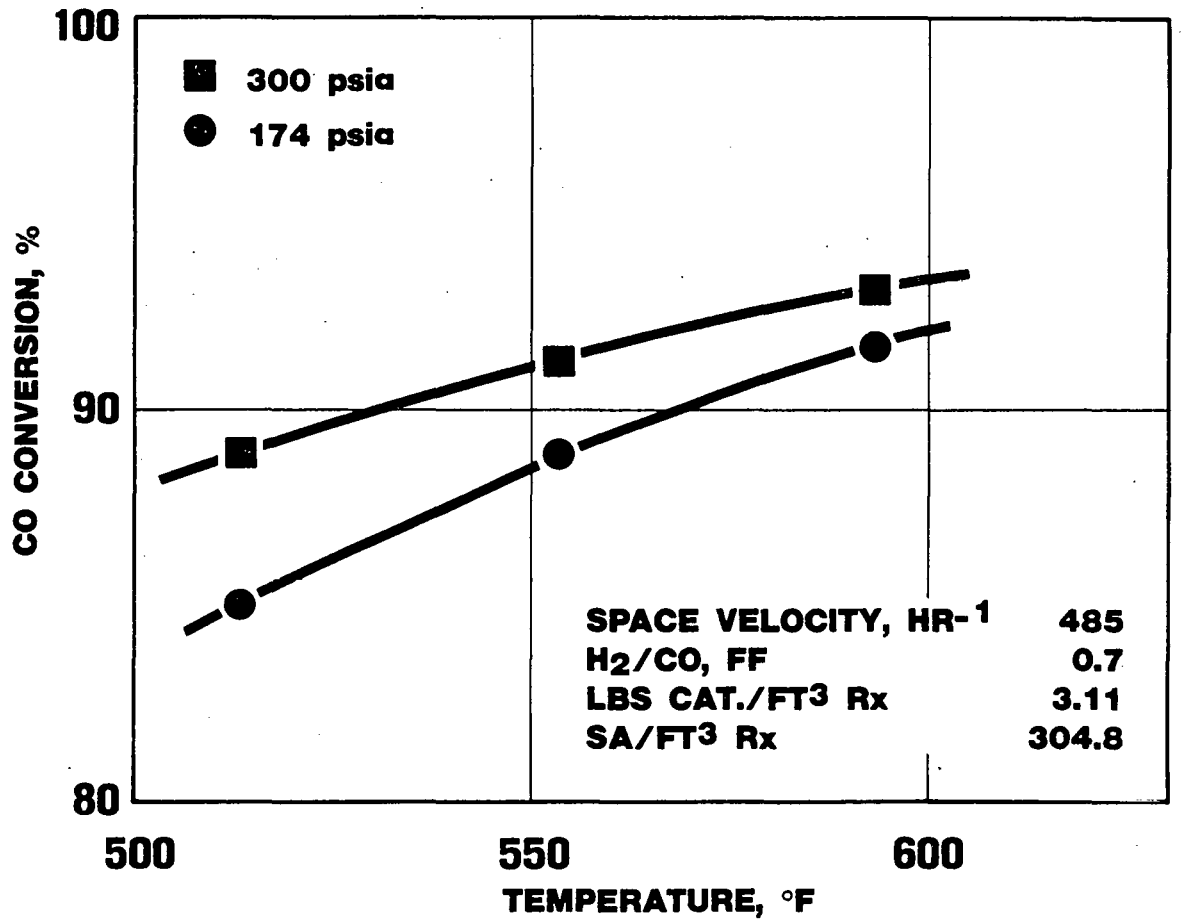

UOP 573-31

FIGURE 4.3-27

FISCHER TROPSCH

SLURRY REACTOR

DEGREE OF POLYMERIZATION vs. TEMPERATURE

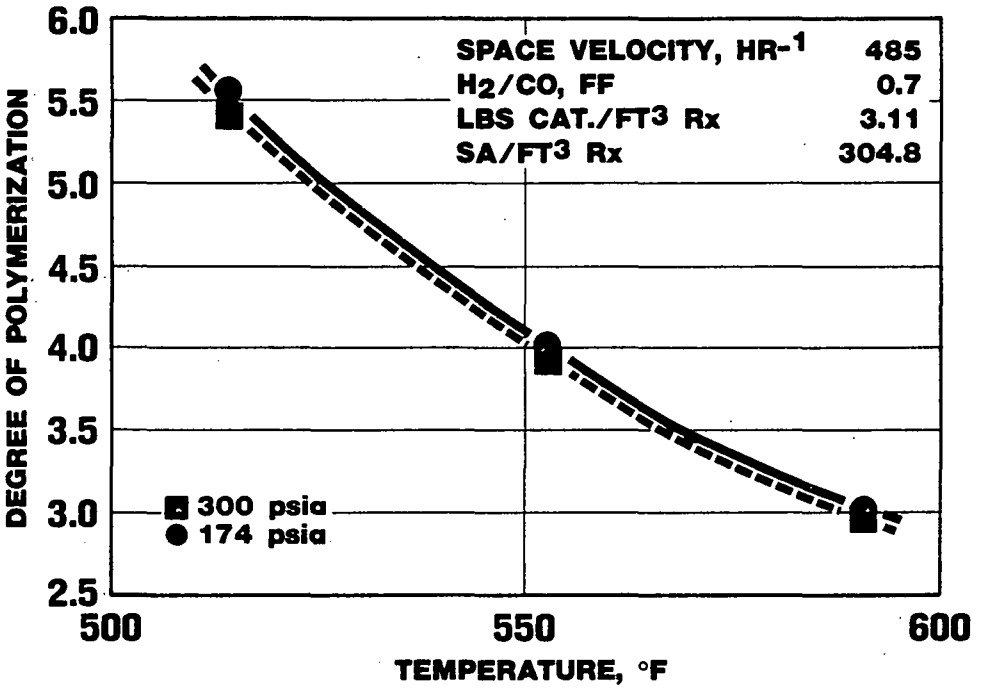

UOP 573-32

FIGURE 4.3-28

FISCHER TROPSCH

SLURRY REACTOR
CO CONVERSION vs. TEMPERATURE

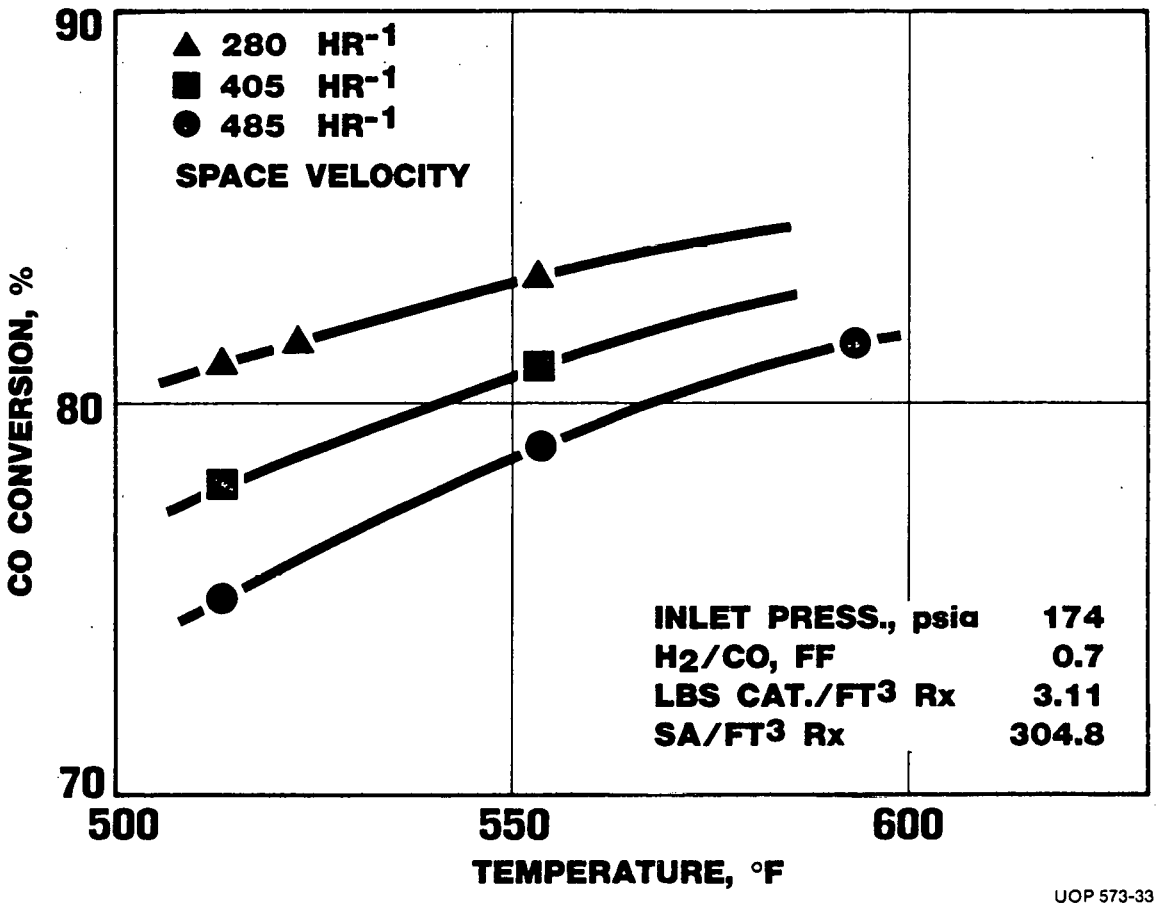

UOP 573-33

FIGURE 4.3-29

FISCHER TROPSCH

SLURRY REACTOR

DEGREE OF POLYMERIZATION vs. TEMPERATURE

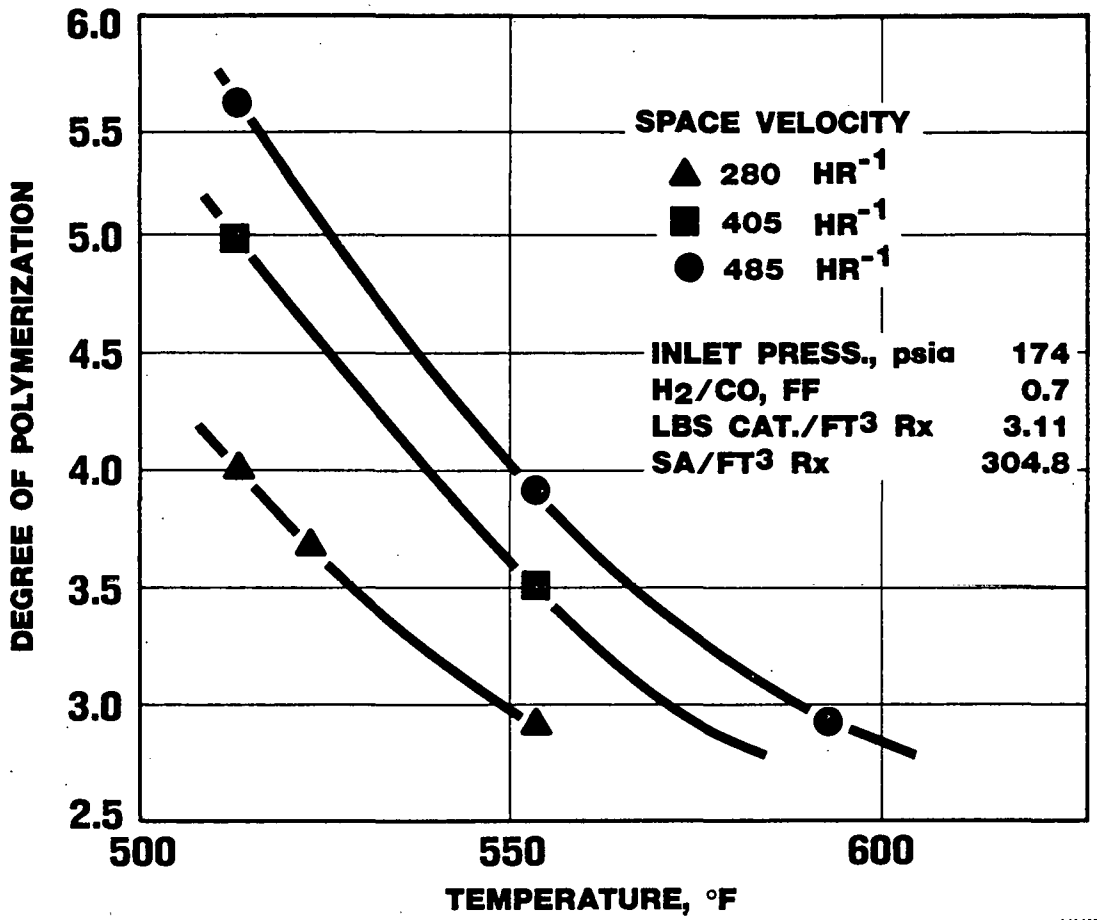

UOP 573-34

FIGURE 4.3-30

FISCHER TROPSCH

SLURRY REACTOR
CO CONVERSION vs. TEMPERATURE

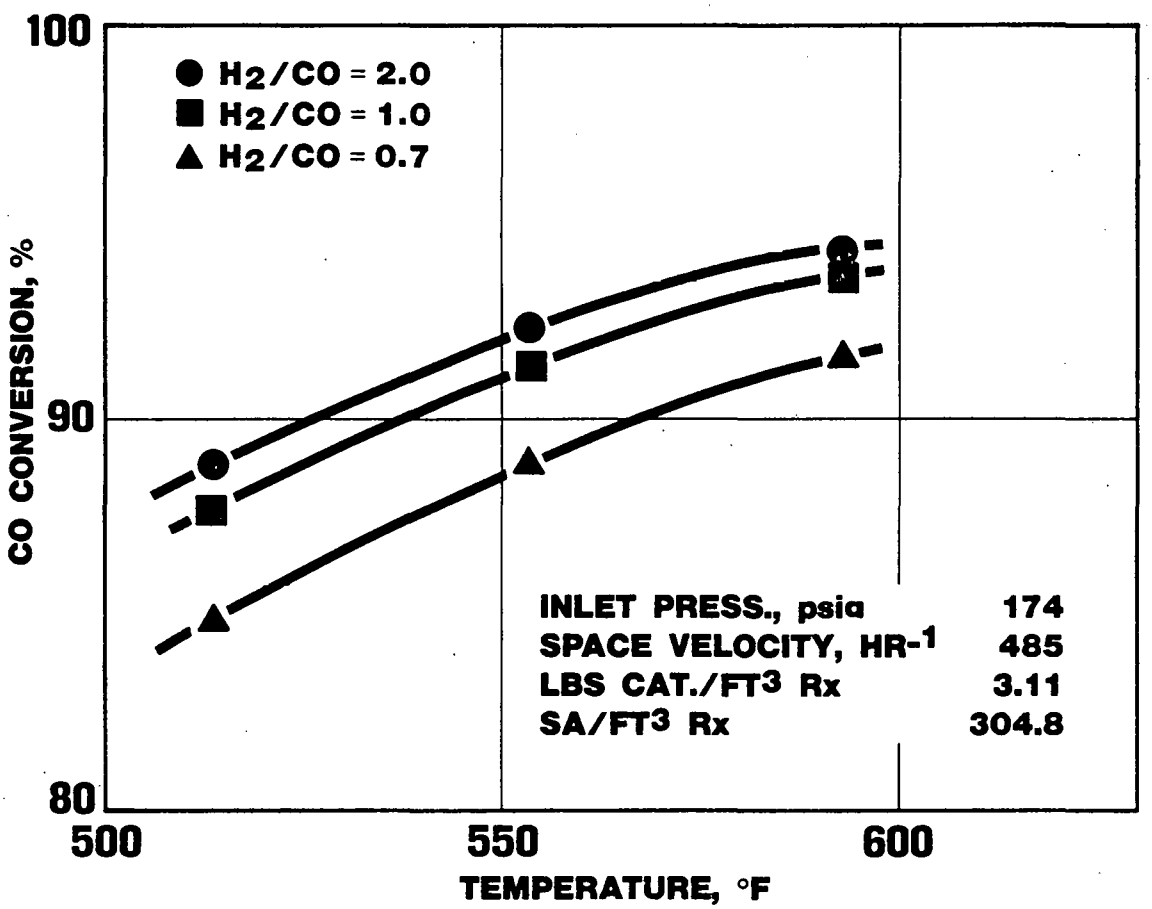

UOP 573-35

FIGURE 4.3-31

FISCHER TROPSCH

SLURRY REACTOR

DEGREE OF POLYMERIZATION vs. TEMPERATURE

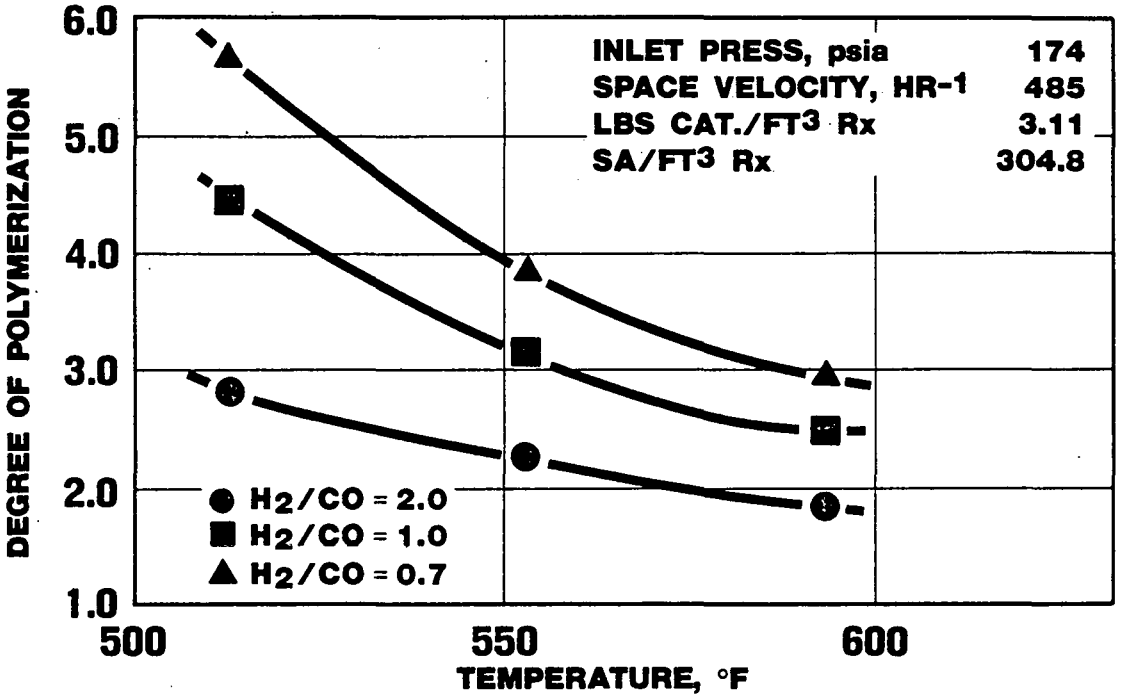

UOP 573-36

FIGURE 4.3-32

FISCHER-TROPSCH

SLURRY REACTOR
CO CONVERSION vs. TEMPERATURE

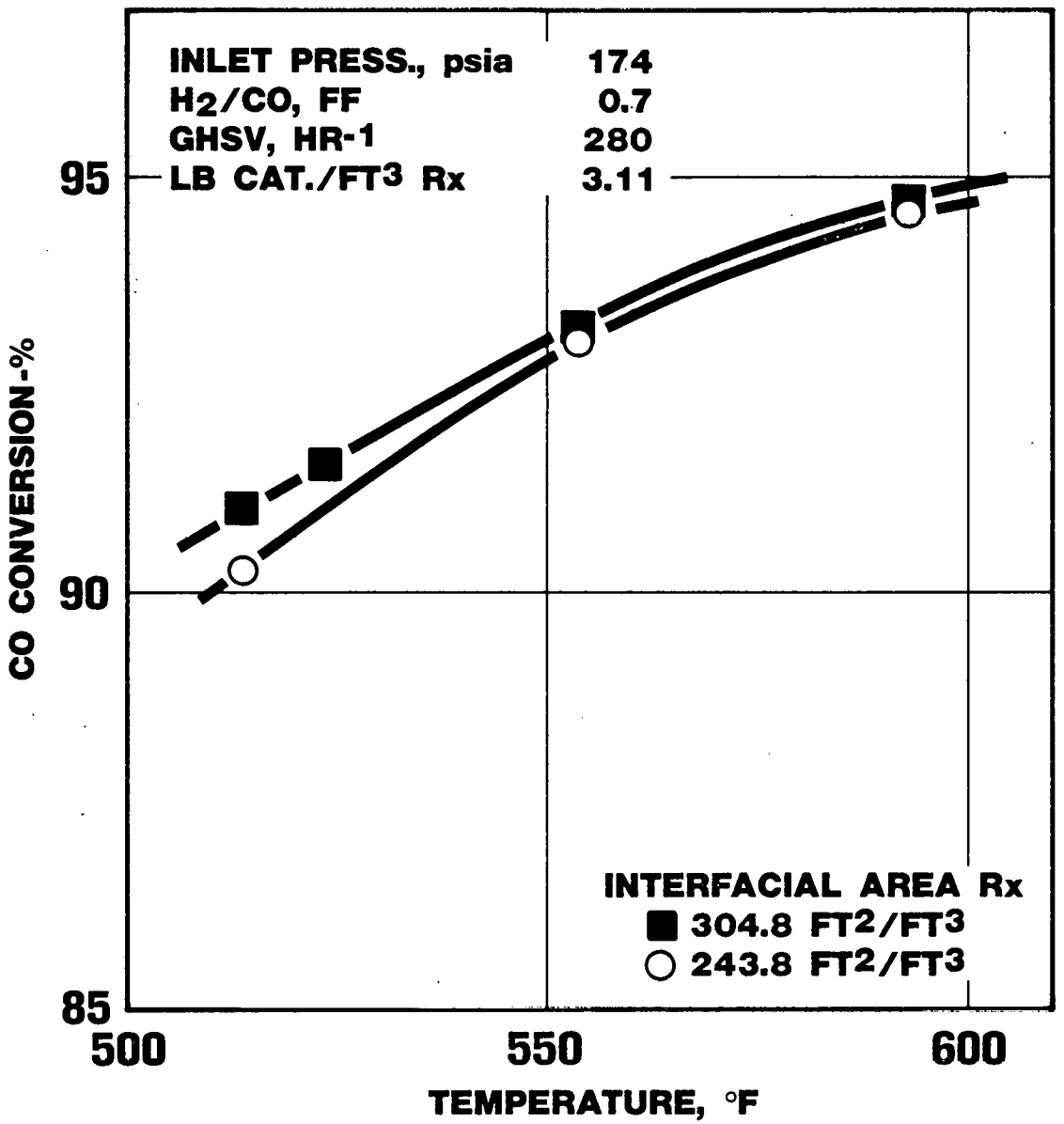

UOP 573-11

FIGURE 4.3-33

FISCHER-TROPSCH

SLURRY REACTOR
DEGREE OF POLYMERIZATION
vs. TEMPERATURE

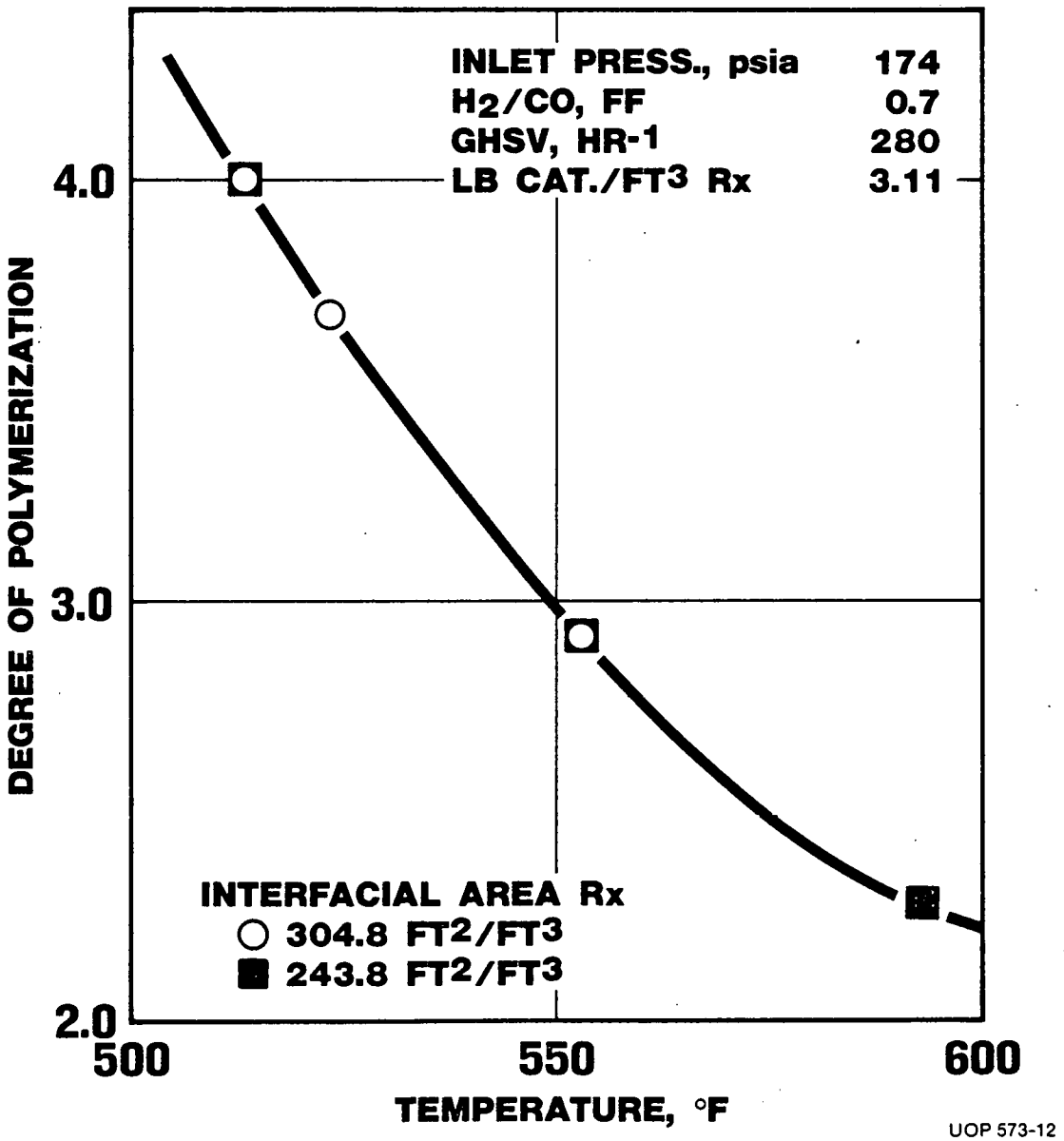

UOP 573-12

FIGURE 4.3-34

FISCHER-TROPSCH

SLURRY REACTOR SYSTEM
CO CONVERSION AND DEGREE OF POLYMERIZATION vs. RELATIVE MASS TRANSFER RATE CONSTANTS

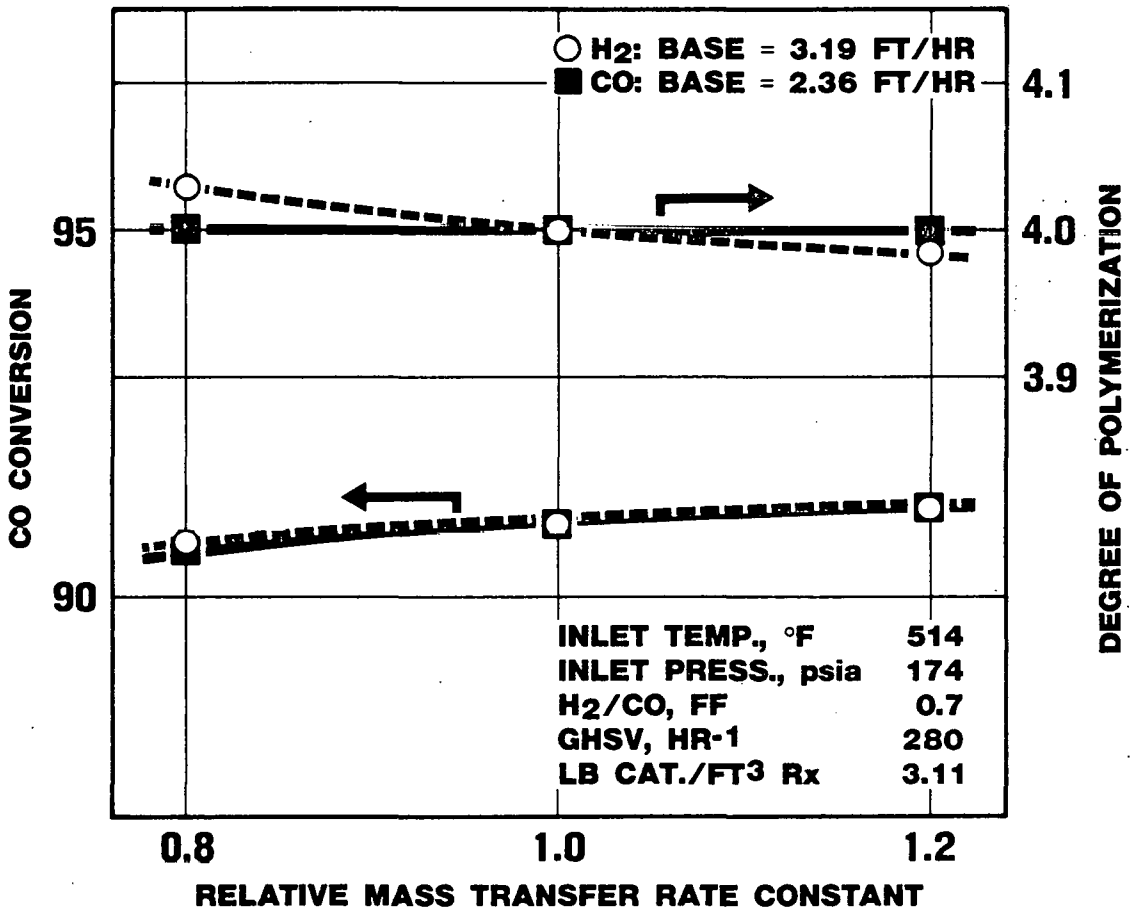

UOP 573-13

FIGURE 4.3-35

FISCHER TROPSCH

REACTOR COMPARISON
CO CONVERSION vs. PRESSURE

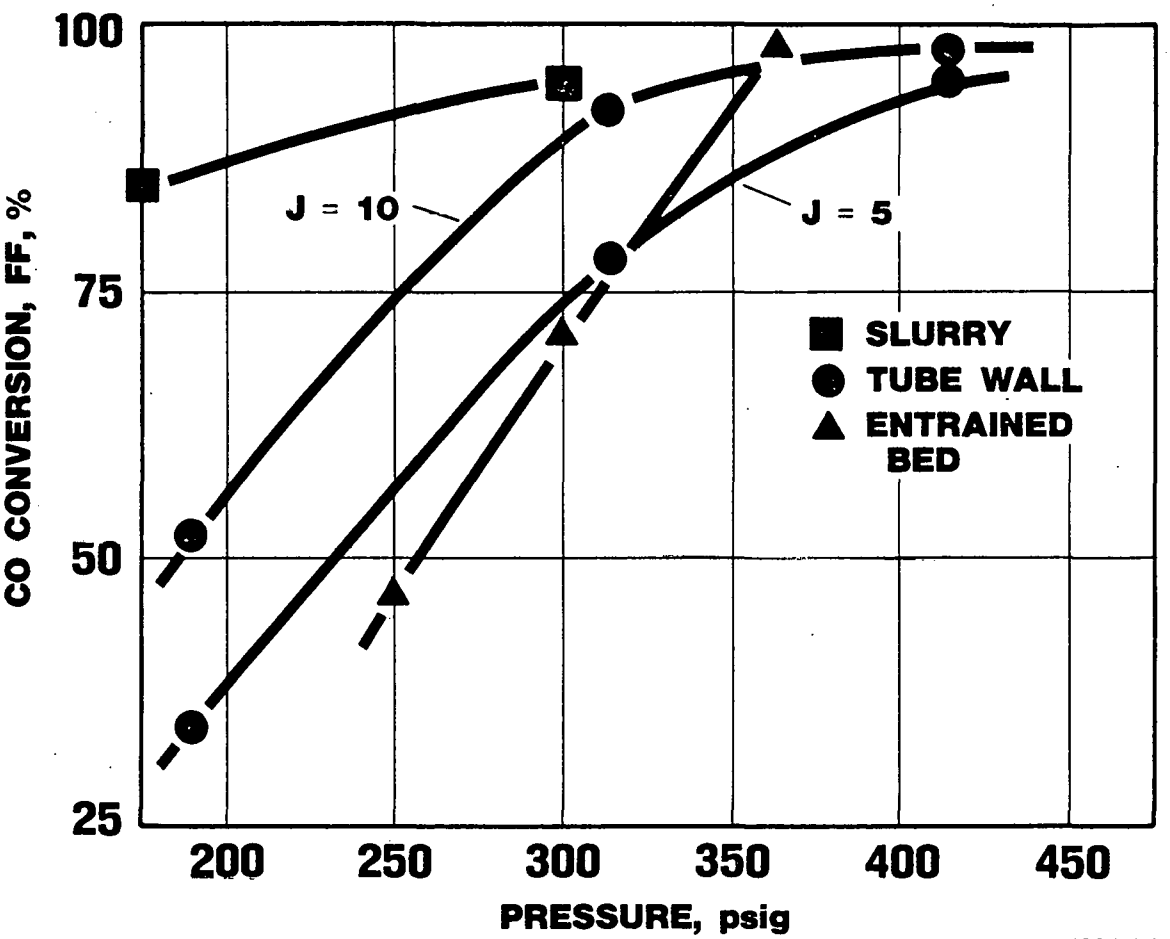

UOP 573-37

FIGURE 4.3-36

FISCHER TROPSCH

REACTOR COMPARISON

DEGREE OF POLYMERIZATION vs. PRESSURE

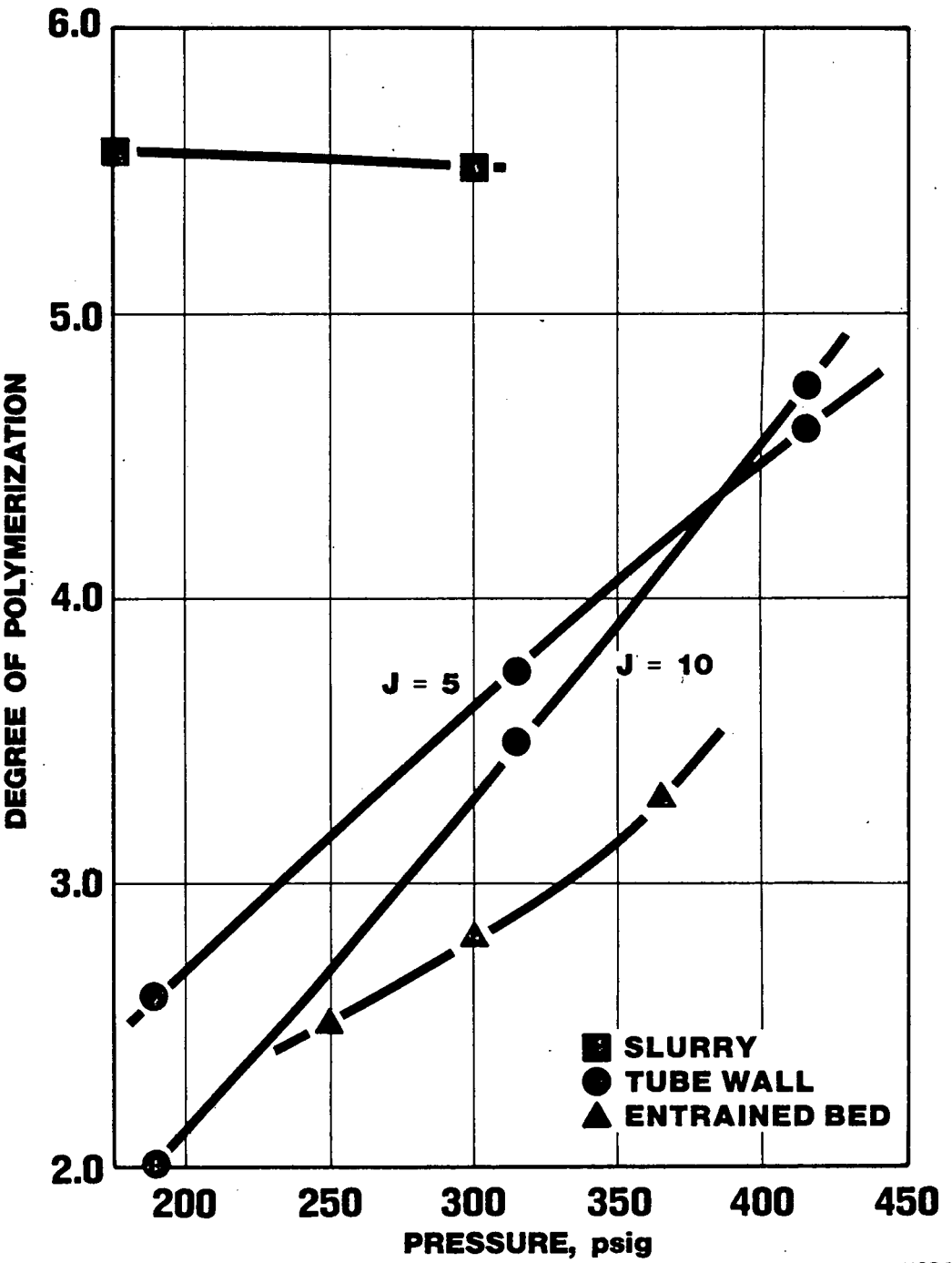

UOP 573-38

FIGURE 4.3-37

FISCHER TROPSCH

REACTOR COMPARISON
CO CONVERSION vs. TEMPERATURE

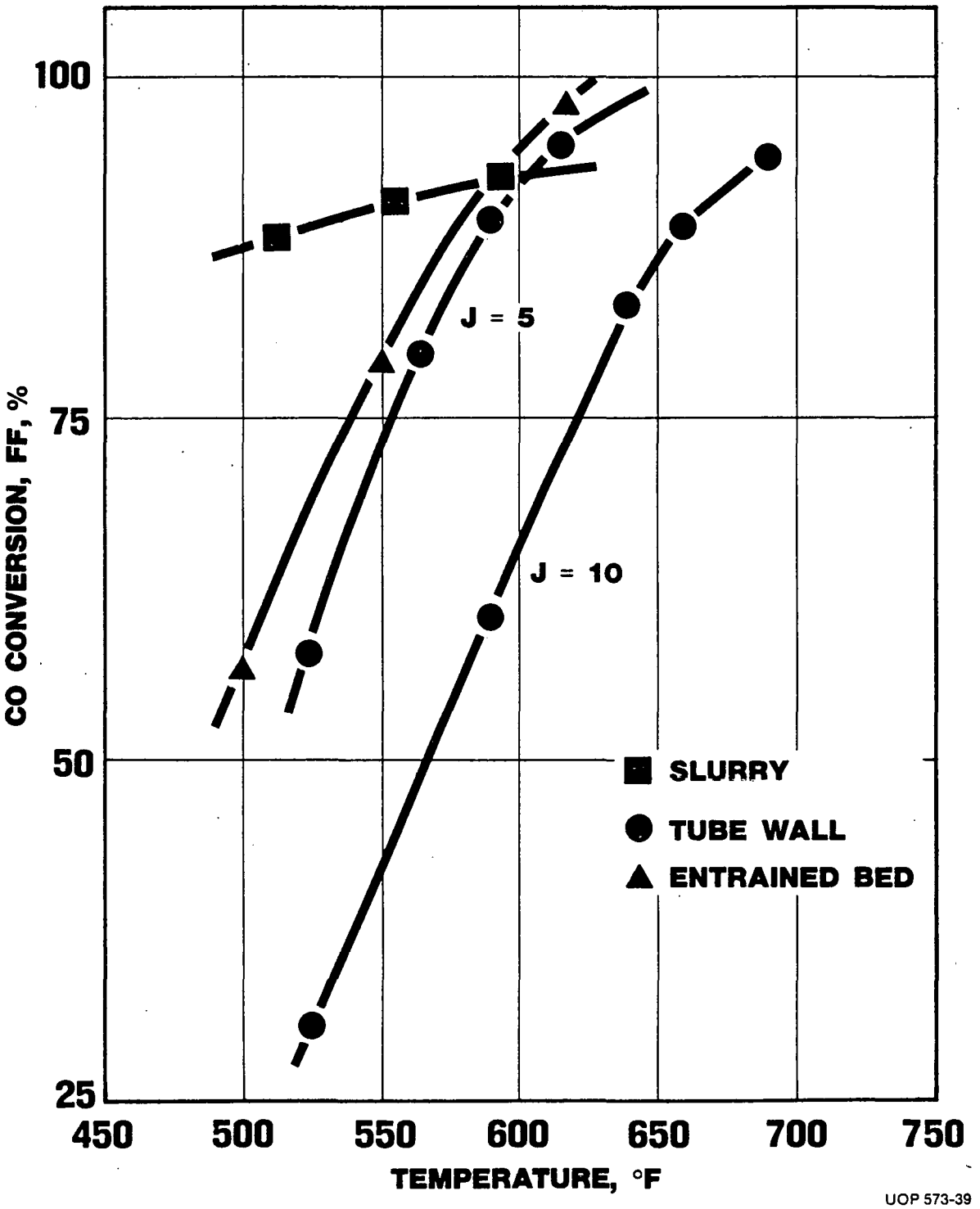

UOP 573-39

FIGURE 4.3-38

FISCHER-TROPSCH

REACTOR COMPARISON
DEGREE OF POLYMERIZATION vs. TEMPERATURE

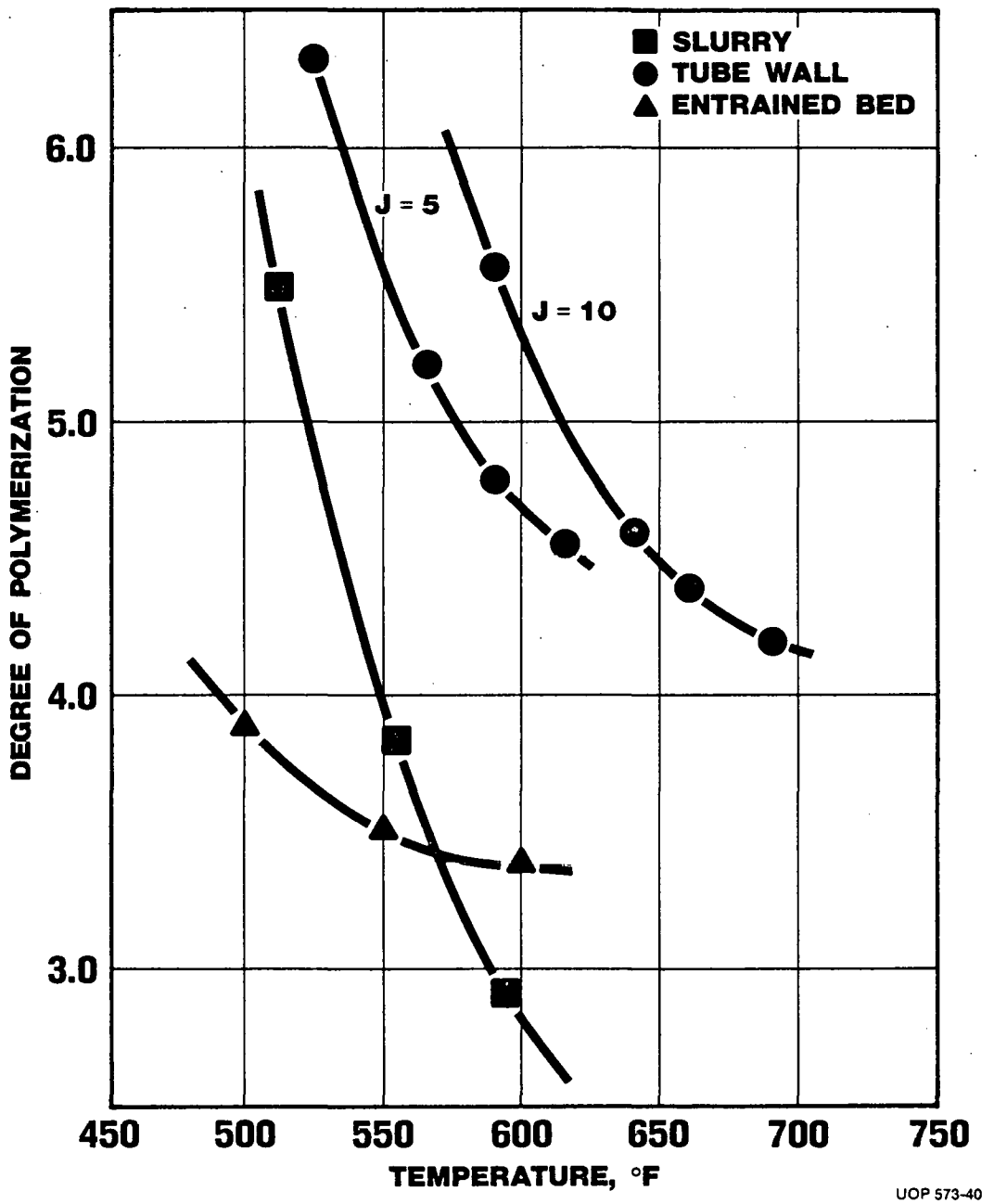

FIGURE 4.3-39

FISCHER TROPSCH

REACTOR COMPARISON
CO CONVERSION vs. H_2/CO

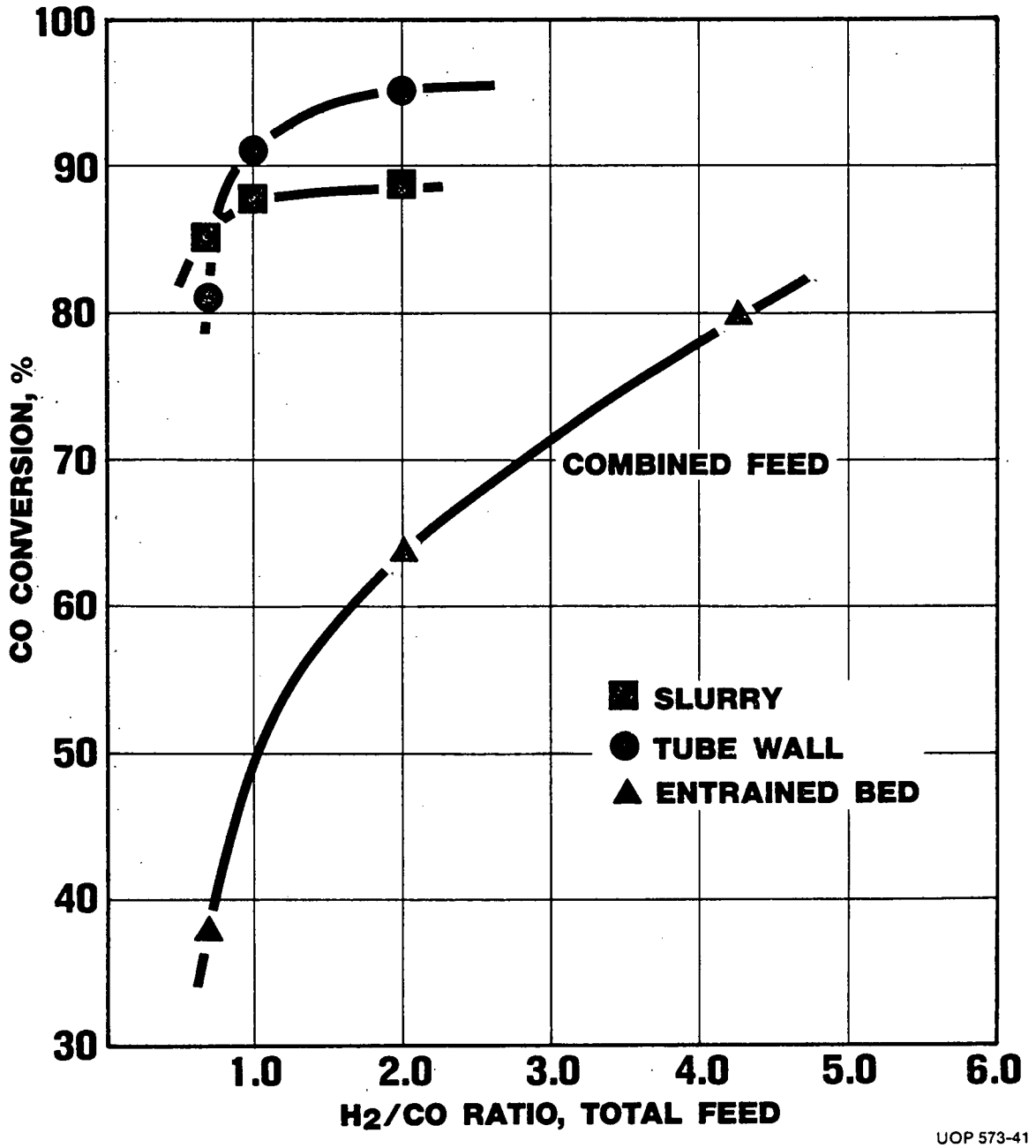

FIGURE 4.3-40

FISCHER TROPSCH

REACTOR COMPARISON
CO CONVERSION TO HYDROCARBONS
vs. H_2/CO RATIO, COMBINED FEED

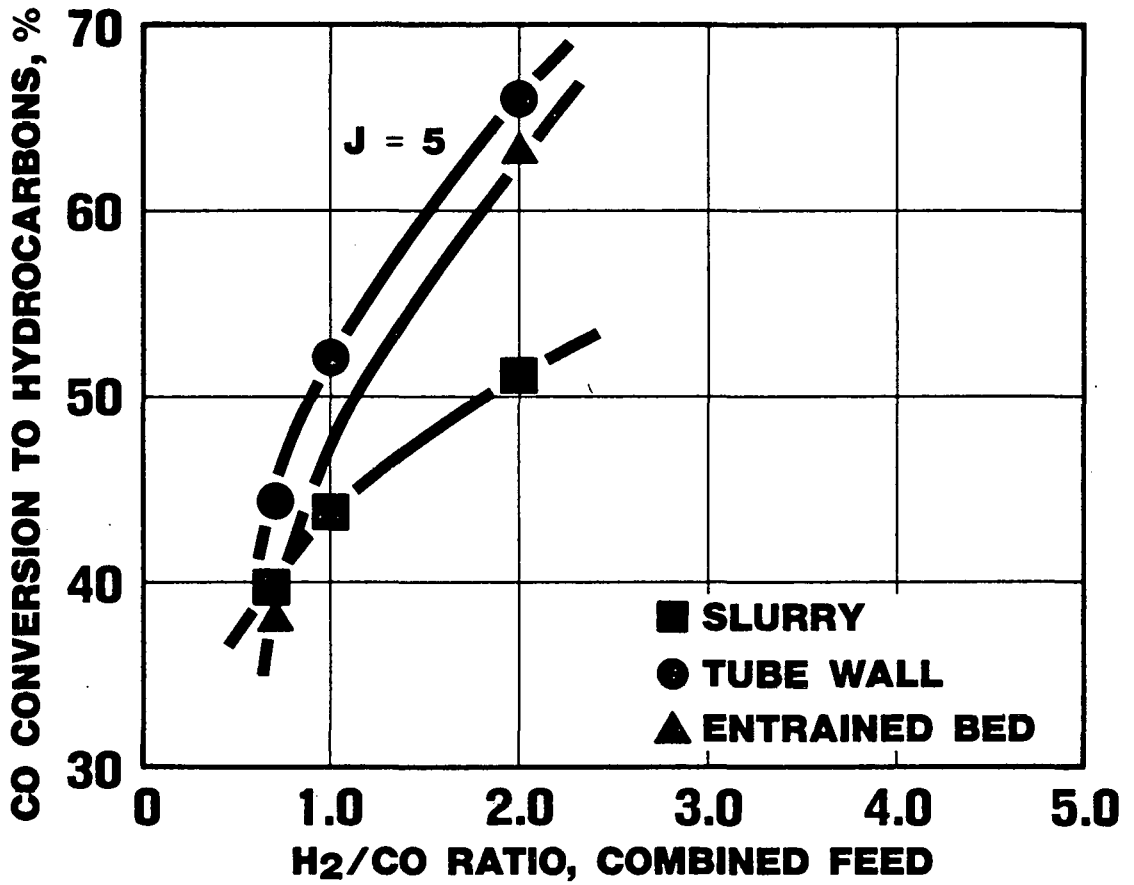

UOP 573-42

FIGURE 4.3-41

FISCHER TROPSCH

REACTOR COMPARISON

DEGREE OF POLYMERIZATION vs. H_2/CO

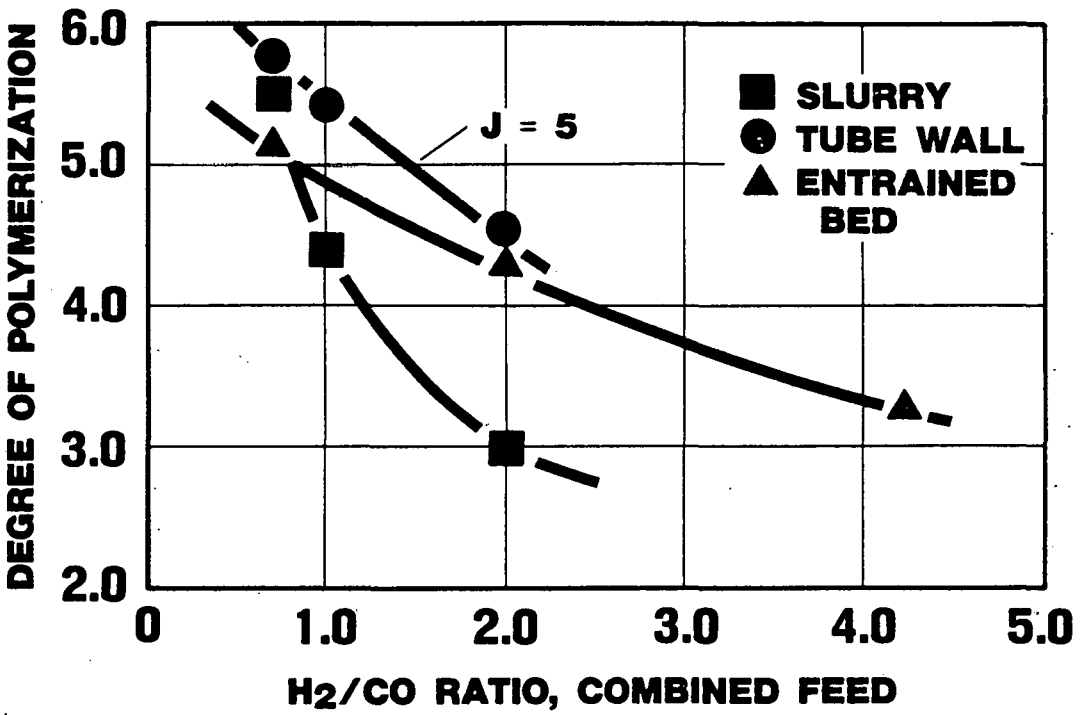

UOP 573-43

FIGURE 4.3-42

FISCHER TROPSCH

ENTRAINED BED REACTOR
INFLUENCE OF ΔT
ON DEGREE OF POLYMERIZATION

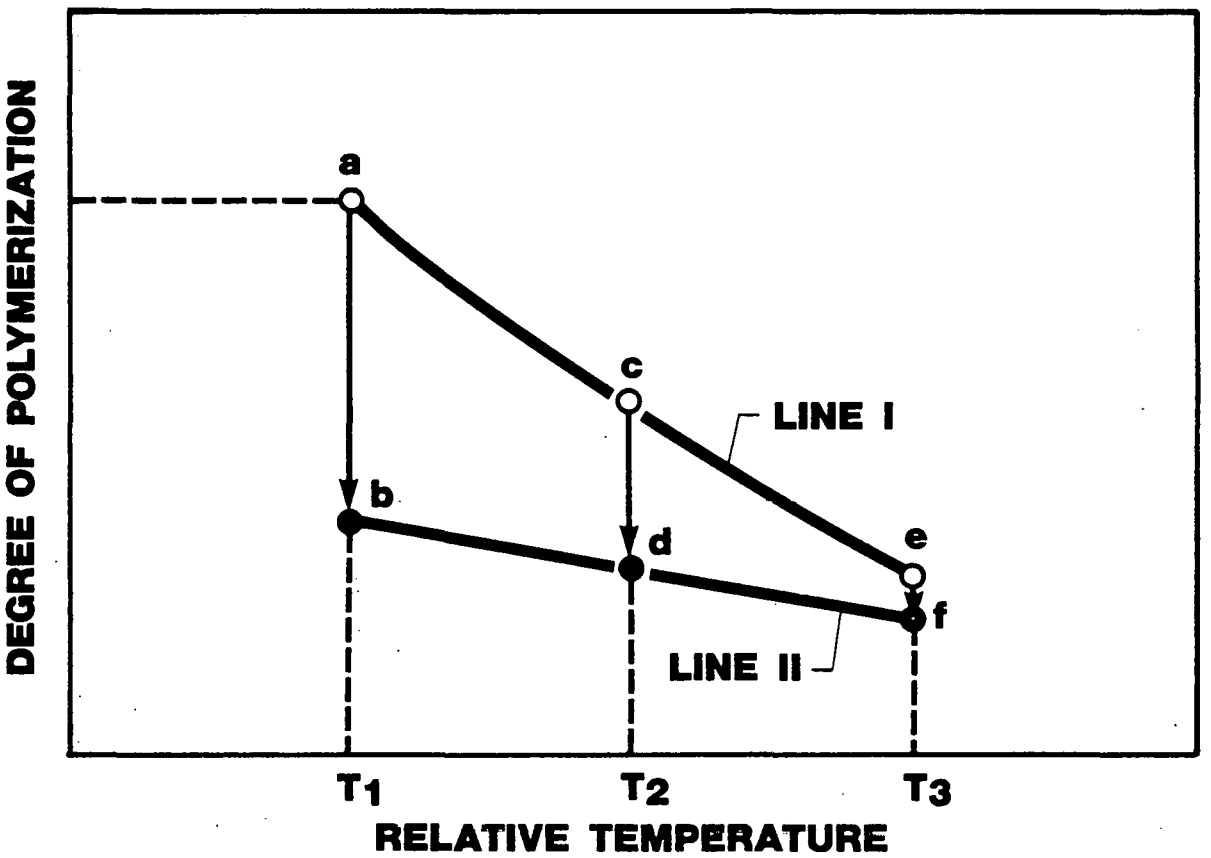

UOP 573-44

TABLE 4.3-1

FISCHER TROPSCH

MAGNITUDE OF VARIABLE DEPENDENCE

DEPENDENT INDEPENDENT	CO CONVERSION	DEGREE OF POLYMERIZATION	OLEFIN TO PARAFFIN RATIO
K_P ⇑	⇑	↑	—
K_H ⇑	—	⇓	⇓
K_O ⇑	—	⇓	⇑

UOP 573-46

TABLE 4.3-2

EFFECT OF TEMPERATURE,
P = 650 psig, H_2/CO = 2.11

PETC Tube-Wall Data

T, °C (°F)	275 (526)	310 (589)	335 (634)
% CO Conversion	30.7	54.8	77.2
Product Distribution, Wt-%:			
$C_1 + C_2$	60.0	67.0	69.7
C_3	9.9	10.3	10.5
Gasoline ($C_3^=$ - 204°C)	24.1	20.6	14.2
Diesel (204 - 316°C)	4.3	1.1	3.4
Fuel Oil (316 - 450°C)	1.7	1.0	2.2
Wax (> 450°C)	0	0	0
Gross Molar Flow Rate, (moles/hr x 10^4)	1.51	3.53	6.62

Values Used for Data Fitting

Degree of Polymerization	2.7	2.2	2.1
Olefin-to-Paraffin Ratio	1.0	1.0	1.0

TABLE 4.3-3

TUBE-WALL REACTOR FITTING

Fresh Feed Rate, moles/hr	0.009608
Composition, mol-%	
H_2O	0.5
H_2	66.2
CO	31.0
CO_2	0.5
CH_4	1.9
J Factor (SCFH FF/ft^2 Cat Surface Area)	23.87
Reactor Dimensions	
Inside Diameter of Tube, ft	0.0402
Outside Diameter of Tube, ft	0.0875
Shell Diameter, ft	0.175
Length, ft	0.5
Catalyst Thickness, ft	0.00208

TABLE 4.3-4

TUBE-WALL FREQUENCY FACTORS

Temp, °C (°F)	275 (526)	310 (589)	335 (634)	Derived Activation Energies (Btu/lb mole)
Frequency Factors				
k_p^o [$(ft^3_{Rx})^2$/lb Cat-hr-mole]	73.3	71.5	73.0	26,400
k_H^o (ft^3_{Rx}/lb Cat-hr)	0.436	0.494	0.465	28,800
k_o^o (ft^3_{Rx}/lb Cat-hr)	0.0180	0.0203	0.0193	27,000
k_{WG}^o [$(ft^3_{Rx})^2$/lb Cat-hr-mole]	169.58	144.38	170.5	33,000

I = Input C = Calculated

	I	C	I	C	I	C
% CO Conversion	30.7	30.7	54.8	54.9	77.2	77.2
Degree of Poly.	2.70	2.71	2.20	2.19	2.10	2.10
Olefin/Paraffin	1.00	1.00	1.00	0.988	1.00	0.981
CO + H_2 Conversion	28.4	27.3	51.1	46.0	66.1	59.2
CO_2 Molar Flow	1.51×10^{-4}	1.50×10^{-4}	3.53×10^{-4}	3.53×10^{-4}	6.62×10^{-4}	6.61×10^{-4}

Note: All frequency factors are based on a reference temperature of 1100°R.

TABLE 4.3-5

EXAMPLE EXPERIMENTAL RESULTS
STEEL LATHE TURNINGS CATALYST (SLTC) FISCHER-TROPSCH RUNS

Item	Experiment 26 Period C
Catalyst Type	SLTC
Synthesis, hours	416 - 488
Reactor Conditions	
Fresh Feed Rate, scfh	1,214
Space Velocity, vol/vol/hr	607
Reactor Pressure, psig	405
Recycle to Fresh Feed:	
Total	27
Hot	25.5
Cold	1.5
CO_2 scrubbed	1.5
Reactor Temperature, °F	
In Gas	552
Out Gas	610
Increment	58
Average Catalyst Temperature, °F	586
Maximum Catalyst Temperature, °F	622
H_2:CO Ratio, Fresh Gas	1.45
Results	
CO_2 Free Contraction, %	74.6
H_2 Conversion, %	73.7
CO Conversion, %	88.7
H_2 + CO Conversion, %	79.8
H_2:CO Ratio:	
Recycle Gas	3.35
Usage	1.21
Water Vapor in Recycle Gas, vol-%	7.0
Tail Gas Composition, vol-%(a)	
H_2	55.2
CO	16.5
N_2	1.2
CO_2	9.6

Continued on Next Page

TABLE 4.3-5 (Continued)

Item	Experiment 26 Period C
Tail Gas Composition, vol-%[a]	
C_1	9.8
$C_2^=$	0.7
C_2	2.3
$C_3^=$	0.3
C_3	1.0
$C_4^=$	0.6
C_4	1.8
$C_5^=$	0.2
C_5	0.8
$C_6^=$	0
C_6	0
Yield, g/m^3 (H_2 + CO) Converted	
C_1	24
$C_2^=$	3
C_2	12
$C_3^=$	2
C_3	7
$C_4^=$	6
C_4	18
$C_5^=$	2
C_5	9
$C_6^=$	0
C_6	0
Oil	0.97
Aqueous	130
C_1 - C_3OH[b]	8
Other Oxygenates[b]	3
Water	119
CO_2 307	
Hydrocarbon Recovery, g/m^3	191
Theoretical Recovery, g/m^3	201
Hydrocarbon Recovery, wt-%	
C_1 + C_2	19.4
C_3	3.5
Gasoline (C_3 = < 400°F)	59.0
Diesel Oil (400 to 600°F)	9.1
Fuel Oil (600 to 842°F)	6.2
Wax (< 842°F)	2.8

(a) Dry basis.
(b) Calculated as hydrocarbons.

TABLE 4.3-6

TUBE-WALL vs. LATHE TURNINGS
FREQUENCY FACTORS

	Tube-Wall	Lathe Turning	Adjusted Lathe Turning
k_p^o [$(ft^3_{Rx})^2$/lb Cat-hr-mole]	73.0	113.0	73.0
k_H^o (ft^3_{Rx}/lb Cat-hr)	0.465	0.108	0.070
k_o^o (ft^3_{Rx}/lb Cat-hr)	0.0193	0.002	0.0013
k_{WG}^o [$(ft^3_{Rx})^2$/lb Cat-hr-mole]	170.0	318.0	205.0

Note: All frequency factors are based on a reference temperature of 1100°R.

TABLE 4.3-7

OPERATING DATA AND RESULTS OF LIQUID-PHASE SYNTHESIS FOR ONE-STEP OPERATION WITH A SINGLE PASSAGE OF THE GAS OVER IRON CATALYSTS

Effective Reaction Space, volume suspension including dispersed gas, (λ)	10,000
Catalyst, kg Fe	800
Synthesis Gas Pressure, bar	12
Synthesis Gas, (volume ratio, $CO:H_2$)	1.5
Quantity of Synthesis Gas, Nm^3/h	2700
Linear Velocity of the Compressed Gases at Operating Temperature Referred to the Free Reactor Cross Section, cm/s	9.5
Total $CO + H_2$ used, Nm^3/h	2300
per m^3 of Reaction Chamber	230
per kg of Fe	2.6
Average Synthesis Temperature, °C	268
CO Conversion, %	91
$CO + H_2$ Conversion, %	89
Synthesis Products Referred to $CO + H_2$ used, g/Nm^3	
Hydrocarbons	
C_1+	178
$C_1 + C_3$	12
C^{3+}	166
O-containing Products in the Synthesis Water, g/Nm^3	3
Space-time Yield of C_3+ Products incl. O-products in 24 hours (kg/m^3 of reaction chamber)	930

Continued on Next Page

TABLE 4.3-7 (Continued)

Composition of a Product from the Demonstration Plant
(Mode of Operation Adjusted for Gasoline Production)

	$CO + H_2$, g/Nm^3	Wt-% of Total Product C_1+	Olefin, %
Methane + Ethane	5.7	3.2	0
Ethylene	613	3.6	100
C_3	40.3	22.6	75-85
C_4	9.1	5.1	70-80
40-180°C Fraction	95.5	53.6	70
180-220°C	7.1	4.0	48
220-320°C	10.7	6.0	37
> 320°C	3.3	1.9	7
Total	178.0	100.0	

TABLE 4.3-8

SLURRY AND ENTRAINED BED INPUT FOR FITTING PURPOSES

	Slurry	Entrained Bed
Fresh Feed Rate, moles/hr	251.6	86,585.9
Composition, %		
H_2O	3.0	0.01
H_2	38.0	66.51
CO	54.0	27.71
CO_2	5.0	5.77
Recycle Rate, moles/hr	-	192,500.00
Composition		
H_2O		0.37
H_2		4.78
CO		2.83
CO_2		26.82
Cl		16.92
$\underline{n}$-C_2		3.90
$\underline{n}$-C_3		1.19
$\underline{n}$-C_4		0.52
$\underline{n}$-C_5		0.15
$\underline{n}$-C_6		0.03
$\underline{n}$-C_7		0.0081
$\underline{n}$-C_8		0.0017
$\underline{n}$-C_9		0.0005
$\underline{n}$-C_{10}		0.0002
$=C_2$		3.72
$=C_3$		4.50
$=C_4$		2.72
$=C_5$		1.05
$=C_6$		0.33
$=C_7$		0.115
$=C_8$		0.034
$=C_9$		0.0115
$=C_{10}$		0.0038
Pressure, psia	174	380 (inlet)
Temperature, °F	514	599 (inlet)
Space Velocity, $\frac{SCF_{FF}}{hr\text{-}ft^3 \text{ reactor}}$	280	959
Catalyst Concentration (lbs cat/ft^3 slurry)	4.44	-
$\frac{\text{lbs cat circulated}}{\text{sec.}}$	-	26,057

Continued on Next Page

TABLE 4.3-8 (Continued)

Total Reactor Δ T, °F	-	36
% CO Conversion, FF	91	97.8
Degree of Polymerization	4.0	3.3
Olefin-to-Paraffin Ratio	1.0	1.0
Gross CO_2 Molar Flow, moles/hr	73.4	5,133.6

TABLE 4.3-9

FREQUENCY FACTOR COMPARISON

Frequency Factor	Tube-Wall	Lathe Turning	Slurry	Entrained Bed
k_p^o [$(ft^3_{Rx})^2$/lb Cat-hr-mole]	73.0	113.0	2604.0	1821.0
k_H^o (ft^3_{Rx}/lb Cat-hr)	0.465	0.106	3.94	1.11
k_o^o(ft^3_{Rx}/lb Cat-hr)	0.0193	0.002	0.06	0.015
k_{WG}^o [$(ft^3_{Rx})^2$/lb Cat-hr-mole]	170.0	318.0	10,699.0	228.8

NORMALIZED FOR SURFACE AREA PER POUND OF CATALYST DIFFERENCES USING TUBE-WALL AS BASE

Frequency Factor	Tube-Wall	Lathe Turning	Slurry	Entrained Bed
k_p^o [$(ft^3_{Rx})^2$/lb Cat-hr-mole]	73.0	73.0	73.0	73.0
k_H^o (ft^3_{Rx}/lb Cat-hr)	0.465	0.070	0.110	0.045
k_o^o (ft^3_{Rx}/lb Cat-hr)	0.0193	0.00129	0.0016	0.0006
k_{WG}^o [$(ft^3_{Rx})^2$/lb Cat-hr-mole]	170.0	205.0	300.0	9.2

Note: All frequency factors are based on a reference temperature of 1100°R.

TABLE 4.3-10

EXAMPLE EXPERIMENTAL RESULTS
FLAME SPRAYED CATALYST (FSC) FISCHER-TROPSCH RUNS

Item	Experiment No. HGR 33		Experiment No. HGR 34	
Catalyst Type	Coated Plates	Coated Plates	Coated Plates	Coated Plates
Fresh Gas Velocity, vol/vol/hr	600	1000	1000	2000
Fresh Feed Rate, scfh	165	275	275	550
Recycle Ratio Total Recycle:Fresh Feed, vol/vol	51	15.9	20.4	14.4
Reactor Pressure, psig	400	400	400	400
Catalyst Temperature, °F				
Average	516	617	608	617
Differential	36	90	72	90
H_2 Conversion, %	73.4	90.9	90.1	83
CO Conversion, %	80.6	98.8	98.2	94.4
H_2 + CO Conversion, %	76.4	94.4	93.4	87.5
Overall Weight Balance, %	93.6	90.8	87.8	96.6
Hydrocarbons Recovered lb/1,000 scf fresh gas	7.4	9.5	10.3	11.6
Hydrocarbons Recovered, wt-%				
$C_1 + C_2$	59.7	36.5	33.9	29.5
C_3	6.6	14.1	13.3	12.8
Gasoline (C_3= < 400°F)	31.8	43.7	48.5	53.0
Diesel Fuel (400 to 600°F)	1.9	5.0	4.0	3.8
Fuel Oil (600 to 842°F)	0	0.4	0.2	0.5
Wax (> 842°F)	0	0.3	0.1	0.4

TABLE 4.3-11

KEY REACTOR DESIGN BASIS ELEMENTS

Capacity, Btu/day Total Products HHV, billion	500
Pressure, psig	400
Temperature (average), °F	606
Space Velocity Factors	
J, scf/hr/sq ft of catalyst area	10
S_V, scf/hr/cu ft of reaction zone volume	1,330
Catalyst Activity	1.33
Syngas Composition	
Fresh Feed H_2:CO Ratio	1.45
CO + H_2 Conversion, %	80
Reactor Recycle Ratio	
Volume Recycle Gas : Volume (CO + H_2) in Fresh Syngas Feed	1.5
Heat of Reaction at Reactor Conditions	
Btu/scf of (CO + H_2) Converted	72.8

REACTOR PRODUCT COMPOSITION

	Weight Percent
C_1, C_2, C_2^-	19.3
C_3, $C_3^=$	4.5
C_4, C_4^-	11.9
C_5, C_5^-, C_6	13.6
C_7, C_8, C_9	19.2
C_{10}, C_{11} to 640°F BP	18.8
640 to 940°F BP	7.3
Alcohols and Ketones	4.9
Acids	0.5
Total	100.00

TABLE 4.3-12

CONCEPTUAL FISCHER-TROPSCH REACTOR DESIGN
COMPARED WITH PETC EXPERIMENTAL DATA

Item	Experiment HGR 34		SLTC Experiment 26C	TWR Experiment FT-TW-1	Conceptual Design Basis
"J", scfh/sf Catalyst Surface	8.85	17.7	1.5	30	10.0
H_2:CO Ratio in Feed	1.41	1.41	1.45	3	1.45
Recycle Ratio	20.4	14.4	27.0	-	1.5
(CO + H_2) Conversion, %	93.4	87.5	80.0	52.0	80.0
Total Reaction Heat Calculated, Btu/sf/hr	583.0	1092.0	84.0	1100.0	563.0

TABLE 4.3-13

TUBE-WALL REACTOR DESIGN COMPARISON

OPERATING CONDITIONS	Parsons	UOP Model Prediction	
Case	Study	1	2
Inlet Temperature, °F	571	571	606
Coolant Temperature, °F	606	606	640
Pressure, psia	415	415	415
J Factor (FF), $ft^3/hr\text{-}ft^2$	10.0	10.0	5.38
GHSV (FF), hr^{-1}	1330	1331	716.2
Recycle Ratio	1.5	1.5	1.5
H_2/CO Ratio			
Fresh Feed	1.45	1.45	1.45
Combined Feed	2.17	2.17	2.03
Catalyst	Flame sprayed magnetite	K promoted, flame sprayed taconite	
YIELD INFORMATION			
CO Conversion, mol-%			
Fresh Feed	88.7	34.9	90.0
Combined Feed	55.6	21.9	54.4
Degree of Polymerization	4.30	5.92	4.30
CO + H_2 Conversion, mol-%	53.3	18.8	41.1

TABLE 4.3-14

INFLUENCE OF RECYCLE TO FEED RATIO ON COMPONENT CONCENTRATIONS IN COMBINED FEED

RUN	1-T	5	32
Recycle/Feed	0	1.0	2.5
Mole Fraction in Combined Feed			
H_2	0.645	0.69	0.69
CO	0.323	0.23	0.21
Total Olefins	0	0.008	0.016
% CO Conversion (on Fresh Feed)	89.5	86.7	86.2
Degree of Polymerization	4.78	4.23	4.24

TABLE 4.3-15

SLURRY OPERATING CONDITIONS

	Koelbel	Base Case
GHSV (Hr^{-1})	262	453
Pressure (psia)	174	300
H_2/CO Ratio	0.7	0.7
Temperature (°F)	514	514
CO Conversion (%)	91	91

TABLE 4.3-16

COMPARISON OF SINGLE-STAGE
AND TWO-STAGE SLURRY REACTOR

	Single-Stage	Two-Stage 1st Length	Two-Stage Total
Reactor Length (Ft)	26.0	15.0	26.0
Reactor Diameter (Ft)	4.22	4.22	4.22
GHSV (Hr^{-1}) (FF)	262.4	453.2	262.4
Temperature (°F)	514	514	514
Pressure (psia)	174	174	174
H_2/CO (Product)	1.8	1.20	2.92
CO Conversion (%)	91	78	95
Degree of Polymerization	4.0	5.4	4.7

TABLE 4.3-17

YIELDS VERSUS REACTOR LENGTH

Tube-Wall Reactor		H_2/CO, FF = 2.0		
Once Through		Temperature, °F = 640		
CO Conversion = 98.3%		Pressure, psig = 415		
Relative Reactor Position	0	0.2	0.8	1.0
Yields				
H_2 (Mole Fraction)	0.645	0.522	0.406	0.374
CO (Mole Fraction)	0.323	0.133	0.012	0.010
Total Olefins	0	0.017	0.029	0.030
Degree of Polymerization	6.01	4.70	4.32	4.32

TABLE 4.3-18

REACTOR BASE COMPARISON

	Tube-Wall		Slurry	Entrained Bed
J Factor	5	10	1.9	1.2
GHSV (hr^{-1})	103	241	280	959
β (SCF/lb Cat/Hr)	10	20	90	58
Temp (°F)	590	660	514	616*
Pressure (psig)	400	400	159	365**
H_2/CO mol ratio (FF)	2.0	2.0	0.7	2.4
H_2/CO mol ratio (CF)	-	-	-	4.23
Recycle Ratio	-	-	-	2.36
% CO Conv (FF)	89.5	89	91	97.8
% CO Conv (CF)	-	-	-	79.7
DP	4.78	4.4	4.0	3.3

* Mean Temperature [(Inlet + Outlet)/2]

** Inlet Pressure

TABLE 4.3-19

REACTOR COMPARISON

	Base			Per Mole CO + H_2 Used			
	Tube-Wall	Entrained Bed	Slurry		Tube-Wall	Entrained Bed	Slurry
$\frac{\text{Moles } H_2 \text{ Converted}}{\text{Mole FF}}$	0.35	0.60	0.29	$\frac{\text{Moles } H_2}{\text{Mole CO + } H_2 \text{ Used}}$	0.55	0.69	0.37
$\frac{\text{Moles CO Converted}}{\text{Moles FF}}$	0.29	0.27	0.49	$\frac{\text{Moles CO}}{\text{Mole CO + } H_2 \text{ Used}}$	0.45	0.31	0.63
$\frac{\text{Mole } H_2O \text{ Produced}}{\text{Mole FF}}$	0.12	0.27	0.0084	$\frac{\text{Moles } H_2O}{\text{Mole CO + } H_2 \text{ Used}}$	0.19	0.31	0.011
$\frac{\text{Moles } CO_2 \text{ Produced}}{\text{Mole FF}}$	0.09	0.0	0.24	$\frac{\text{Moles } CO_2}{\text{Mole CO + } H_2 \text{ Used}}$	0.14	0.0	0.31
$\frac{\text{Lbs HC Produced}}{\text{Mole FF}}$	2.90	3.92	3.56	$\frac{\text{Lbs HC}}{\text{Mole CO + } H_2 \text{ Used}}$	4.53	4.51	4.56

4.4 CONCLUSIONS

4.4.1 General

- A mathematical mechanism has been developed which, when incorporated into models of three completely different reactor systems operating at completely different operating conditions with Fischer-Tropsch catalysts of different manufacture, gives reasonably good agreement on correlating rate constants derived from the experimental data published for these systems.

- The mechanism, as demonstrated for potassium-promoted catalyst, allows interpretation of yield differences resulting from different catalyst formulations.

- As demonstrated for the tube-wall reactor study of the Parsons design, the reactor models can be used to evaluate existing conceptual designs not only in terms of gross product yield but also in terms of reactor design and operating conditions.

- Because of the success of this mechanism in describing inherent strengths and weaknesses in a variety of Fischer-Tropsch reactor systems, work is proceeding on eliminating some of the mechanism deficiencies, thereby providing additional support to conclusions already drawn and providing additional insight into product yields.

- The largest influence on product yield is the relative concentration of H_2 and CO. The latter concentration is of particular importance when the order of reaction with respect to each component is assumed to be unity, since hydrogen's influence on the competition between the rate of polymerization and the rates of termination is minimal under these circumstances.

- Of all operating parameters (excluding catalyst), temperature has the strongest influence on gross product yields. An increase in reactor temperature results in an increase in CO conversion and a decrease in degree of polymerization.

- An increase in pressure results in an increase in CO conversion. If pressure is increased and the CO conversion is maintained constant by a corresponding increase in space velocity, the degree of polymerization will increase.

4.4.2 Tube-Wall Reactor

- The plug flow nature of the tube-wall reactor results in significant changes in the concentration of CO as a function of reactor length. This concentration profile has a marked effect on the degree of polymerization at any point in the reactor.

4.4.3 Entrained Bed Reactor

- As in the case of the tube-wall reactor, the entrained bed reactor is plug flow and, therefore, has a varying degree of polymerization as a function of reactor length. However, because of the large gas recycle rate, the conversion per pass is lower resulting in changes which are less dramatic.

- The high CO_2 concentration in the recycle gas results in a water-gas shift reaction which is near equilibrium throughout the entrained bed reactor.

- In the entrained bed reactor, catalyst circulation rate can be used as an operating parameter to adjust catalyst density within the reactor. Increased catalyst density increases CO conversion without significantly influencing the gross product yields.

4.4.4 Slurry Reactor

- Unlike the tube-wall and entrained bed reactors, the slurry reactor is back-mixed, and the CO and H_2 concentrations are uniform throughout the reactor. Consequently, the degree of polymerization is uniform and is set by CO and H_2 conversion.

- The water-gas shift is far from equilibrium in the slurry reactor and supplies a significant portion of the hydrogen required for conversion to hydrocarbon.

- The influence of mass transfer on the CO conversion and degree of polymerization at the operating conditions of Koelbel's slurry reactor is small.

4.4.5 Reactor Comparisons

- At the operating conditions proposed in the literature for these systems, the slurry reactor will inherently have a higher thermal efficiency than the entrained bed or tube-wall reactors because of the more efficient use of the water-gas shift reaction.

- The sensitivity of slurry reactor product yields to changes in temperature and CO conversion is superior to that in the entrained bed and tube-wall reactors.

- The entrained bed reactor lacks the operating flexibility of the tube-wall and slurry reactor systems.

4.5 MECHANISM IMPROVEMENTS

The mechanism as presented in Section 4.1 reasonably describes the gross product yields for three different reactor systems, and is adequate for comparing inherent strengths and weaknesses of these systems. The success of this approach, coupled with a desire to improve Fischer-Tropsch technology through its application to other reactor systems, has created a

need for expansion of the existing mechanism. A schematic of the proposed expansion is presented in Figure 4.5-1 with the original mechanism shown as black lines.

4.5.1 Free Carbon and Methane

Two undesirable components which require special treatment are free carbon and methane. Catalyst deactivation as well as reactor operational problems have been attributed to the formation of free carbon. In addition, methane is typically found in quantities significantly higher than predicted by simple Schulz-Flory kinetics and, therefore, lowers the production of gasoline and other more desirable products. Dry (6) has proposed a mechanism that not only accounts for the production of free carbon but also suggests a method for methane formation parallel to the hydrogenation of the active intermediate, $M(CH_2)_nH$, described in the original mechanism. Activated carbon and oxygen species are formed by the dissociation of an absorbed CO molecule. The activated oxygen can react with either H_2 or CO to form H_2O and CO_2, respectively. The activated carbon can either react with H_2 to form methane or it can form free carbon. These improvements can be incorporated into the original mechanism as indicated in red in Figure 4.5-1.

4.5.2 Alcohols

Oxygenates, primarily in the form of alcohols, frequently make up a measurable portion of the Fischer-Tropsch product. Normally these are undesirable products, and in the case of nitrided catalysts, which generally are more stable than standard F-T catalysts, they can make up more than 8 wt-% of the total product (58). In addition, F-T alcohols as feed to the Mobil's ZSM-5 catalyst have been shown to give a very selective product. For these reasons, consideration has been given to the incorporation of alcohols into the original mechanism shown in blue in Figure 4.5-1. The similarity of the mechanisms for the production of alcohols and olefins is apparent and is based on the work of Pichler and Schulz (37). Evidence suggests that alcohols, just as olefins, can initiate chains by readsorption on the catalyst sites, thus creating an equilibrium adsorption-desorption between product and catalyst.

4.5.3 Aromatics via Zeolites

The most significant problem in converting synthesis gas to gasoline using standard Fischer-Tropsch catalysts has been the lack of hydrocarbon selectivity. Recently, Mobil discovered a way to circumvent this problem by introducing the concept of a "shape selective" zeolite catalyst. Early approaches combined the Fischer-Tropsch and zeolite functions into a single "bifunctional" catalyst. This approach improves the normal F-T yield structure, away from a typical Schulz-Flory type distribution, by increasing total aromatic yield, reducing olefinic and paraffinic hydrocarbons and decreasing the average carbon number of the product. In addition, compounds above carbon number 11 were significantly reduced to less than 3 wt-% of the total yield.

The "non-trivial polystep" reaction characteristic of bifunctional catalyst and described by Weisz and others (59) is not simply a succession of consecutive reaction steps. Rather it is two discrete sets of reaction steps, each corresponding to a particular catalyst function. These discrete sets are then linked by a stable intermediate component. Catalytica (32) has suggested that alcohols and olefins can be easily transformed into aromatic products over a ZSM-5 type zeolite catalyst. Since these components are generated from a Fischer-Tropsch catalyst, they are likely candidates for the intermediates required to link the F-T and zeolite catalyst functions.

The mechanism that is suggested and which integrates these facts is shown in green in Figure 4.5-1. As before, M represents the metal site associated with the Fischer-Tropsch function, while Z represents the zeolite function. The olefin intermediate, represented by $[C_nH_{2n}]$, is shown interacting as a reversible reaction with the zeolite. In contrast, Catalytica (32) has suggested that alcohols, here represented as $[C_nH_{2n+1}OH]$, react with each other irreversibly in conjunction with the zeolite to form ketone intermediates which then can decompose to olefins. In both cases above, the olefins act as building blocks for the polymerization and cyclization reactions necessary to form aromatics on the zeolite.

The mechanism as described in Figure 4.5-1 should characterize the product structure of the bifunctional, F-T and zeolite, catalyst. The key lies in the ability of the zeolite function to intercept the components associated with the Fischer-Tropsch polymerization reaction and to convert them into aromatics.

FIGURE 4.5-1

FISCHER TROPSCH
MECHANISM IMPROVEMENTS

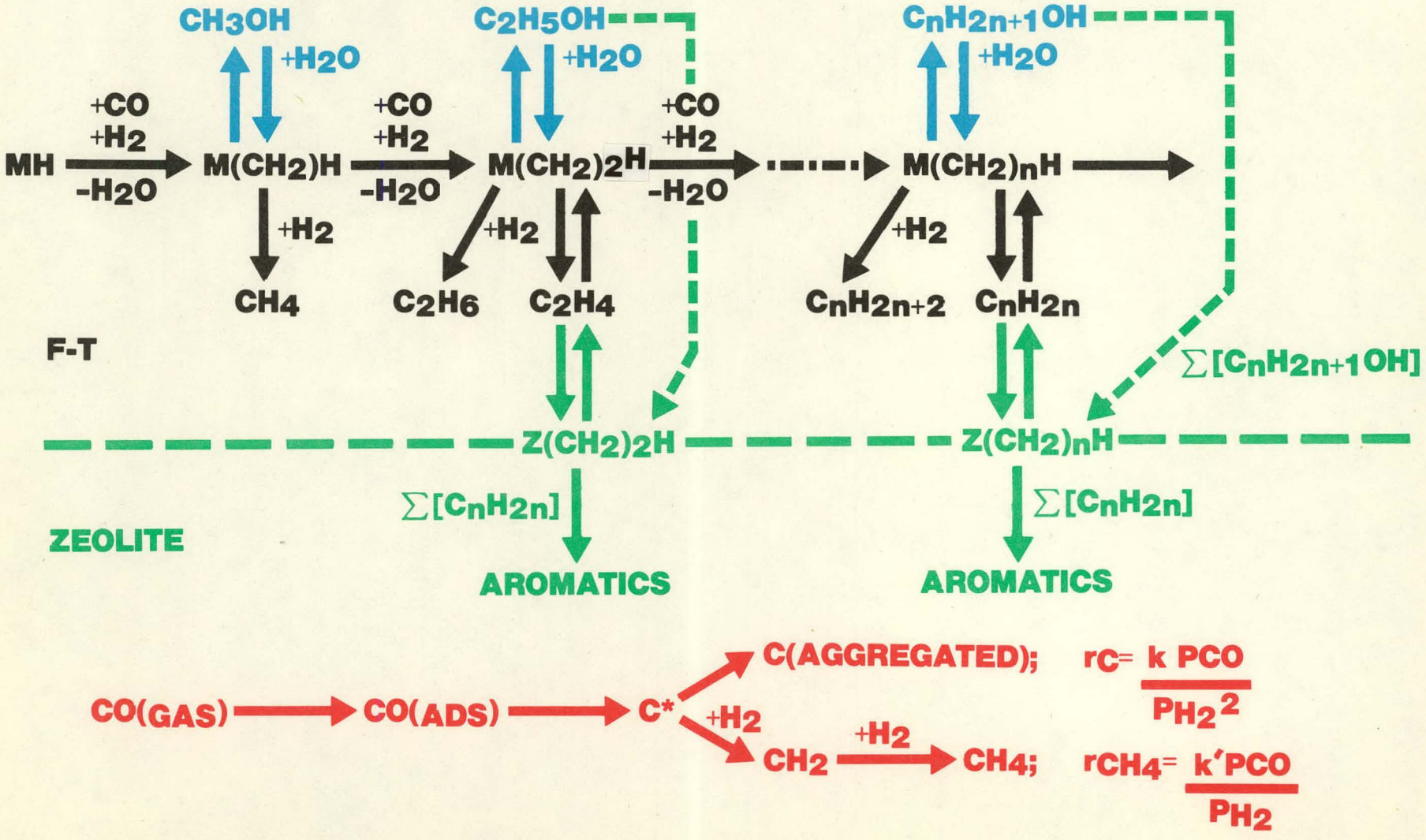

UOP 573-45

SECTION 5 - PHYSICAL COMPARISON OF REACTORS

5.1 CRITICAL DESIGN REVIEW

5.1.1 Introduction

The physical comparison of the reactor systems consists of a general review of each system and a side-by-side comparison of the four systems on specific common points. In Section 5.1 each system is critically reviewed and unique features are discussed.

Section 5.2 is divided into five parts:

- 5.2.1 Basis of Comparison
- 5.2.2 Product Yield Comparison
- 5.2.3 Size and Cost Comparison
- 5.2.4 Thermal Efficiencies
- 5.2.5 Upstream/Downstream Considerations

Conceptual designs were prepared for each of the four reactor systems, with each system being sized to convert the same quantity of $CO + H_2$. This provides a fair basis for comparison of product yields, investment costs and thermal efficiencies.

5.1.2 Entrained Bed Reactor

For the purpose of this reactor comparison, the Pullman Kellogg (4) Synthol reactor has been used as representative of the entrained bed reactor system. The only substantial change made to the flow scheme is to use steam generation for reactor cooling rather than hot oil circulation. This was not done for the reactor modeling work described in Section 4, but was changed for the physical comparison of reactors because it is believed to be a practical change that would result in considerable investment cost savings. This system will be somewhat less flexible with regard to reactor temperature control, because heat removal can not be adjusted

by changing the heat exchange fluid circulation rate; however, other variables, such as feed temperature, catalyst circulation rate, and the H_2 and CO concentrations in the combined feed gas stream should provide acceptable temperature control. The use of direct steam generation may result in a lower skin temperature in the coolers. Whether this can be used will depend on the product yield structure as discussed below.

The Synthol reactor consists of three reactors in series, with intercoolers between reactors. For the purpose of this study, all of the reactor systems were compared at 400 psia nominal operating pressure, which is about 100 psi higher than that used by Kellogg. Further details of the plant basis are presented in Section 5.2.3. The reactors were sized to give the same superficial velocity as the 300 psig design. The kinetic model indicates this increase in space velocity is justified by the increased reaction rate at higher pressure.

This reactor is the only one of the four reactors under consideration that has had commercial demonstration. (The other commercially proven system, the tubular packed bed Arge reactor, was not included in this study.) The Synthol plant designed by Kellogg has been operated by Sasol since 1955. From a design standpoint, the principal advantages of this reactor are:

- It is a commercially proven design
- It allows very high capacity from a single reactor train. (For the 28.05 MM SCFH of CO + H_2 conversion which has been set as the basis for this comparison, only two reactors are required.)

The configuration of this reactor does restrict the choice of operating conditions and this results in several disadvantages. It is a vapor phase reactor, and careful attention must be paid to the hydrocarbon dew point of the vapor flowing through the reactor. The vapor must not come into contact with surfaces below its dew point. The coldest surface in the reactor is the heat exchange surface in the heat removal sections. With direct generation of 600 psig steam, the tube skin temperature will be about 500°F. If oil circulation is used, the lowest skin temperature

will depend on the oil inlet temperature, but with the 472°F inlet temperature suggested by Kellogg, the skin temperature will be very similar to the steam case at around 510°F. If the yield structure at the outlet of the reactor given by Kellogg is used as a basis for calculation, the dew point of the outlet vapor from the reactor is between 565 and 580°F, depending on the operating pressure selected. The dew point of the gas leaving the last heat exchanger will be lower, as about 15% of the overall conversion takes place in the last reactor. However, on the basis of this yield structure, it would appear that this design would result in liquid condensation on the cooling tubes, which would create operating problems for a fluidized catalyst system. The calculation of dew point is, however, very sensitive to the concentration of high molecular weight components. As discussed in section 5.2.2, the Kellogg yield structure does not fall on a Schulz-Flory distribution, and a yield structure was estimated for a product with C_5+ components falling on a Schulz-Flory distribution with a degree of polymerization corresponding to 3.3 (see Table 5.2-3). If the dew point of the reactor effluent is calculated with this net product composition, the dew point of the product is reduced to the range of 445 to 455°F, depending on whether the operation is at the 300 psig nominal pressure used by Kellogg, or the 400 psia used for this study. The dew point of this product is safely below the skin temperature of the heat exchanger tubes.

The yield structure published by Sasol also shows a larger amount of $C_{26}+$ than would correspond to a Schulz-Flory distribution. Kellogg has confirmed that this is the yield structure that they expect to achieve, and indicates that the departure from the Schulz-Flory distribution is due to a number of factors including "the nature of the catalyst" and "polymerization of light components in the recycle". Kellogg also offers the explanation that any liquid film produced at the heat exchanger surface will be removed by the very large flow of catalyst, and that this deposition of product on the catalyst contributes to the need for catalyst replacement.

Any vapor phase fluidized reactor must, therefore, be operated to ensure that no operating problems result from liquid deposition on the

heat removal surface. This will impose many restrictions on the operating conditions chosen and the yield structure that can be tolerated. For example, the degree of polymerization of the product must be lower than would be required for the other systems under consideration in this study. The liquid phase systems can tolerate cooling surfaces below the product dew point, and the tube-wall design selected for this study has a much higher tube-wall temperature (640°F nominal) because it is virtually equal to the vapor temperature. The actual degree of polymerization that can be tolerated by the entrained bed system is unlikely to be any higher than indicated by the yield structure published by Kellogg and Sasol, falling in the range of 3 to 3.5, which is significantly below that required to give the maximum gasoline yield.

While inherently lower gasoline yield is in itself a significant disadvantage of this reactor for the U.S. market, the operating conditions used to hold down the degree of polymerization cause further problems. The degree of polymerization is held down by two principal factors, high temperature and low CO concentration. High temperature causes a very large and undesirable increase in methane production, by a mechanism that appears to be related to free carbon formation at the selected high operating temperature [Dry (6)]. The free carbon also causes rapid catalyst deterioration. Holding down the free carbon formation requires high hydrogen partial pressure, and the combination of high hydrogen partial pressure and low CO concentration results in the process requiring a feed gas with a high H_2/CO ratio.

Dry (15) has shown that high CO_2 partial pressure and high catalyst basicity will hold down methane formation to some degree. Unfortunately, the presence of significant quantities of CO_2 shuts off the shift reaction, requiring all of the hydrogen to be produced in external shift, and high basicity of the catalyst will tend to increase the degree of polymerization.

The required hydrogen partial pressure is obtained by a combination of syngas feed with a high H_2/CO ratio, and a high recycle gas to fresh feed ratio, requiring a low conversion of $CO + H_2$ per pass. The high

recycle gas ratio is beneficial in reducing the temperature rise across the reactor, as the recycle gas is a significant heat sink. Operation with a reduced recycle gas ratio would, therefore, require more, smaller reactors in series. A reduced recycle gas ratio would also tend to increase the dew point temperature of the reactor effluent and thus reduce the tolerable degree of polymerization for the process. Fluidization characteristics of the entrained bed reactor are also very sensitive to changes in recycle gas ratio. A reduction in recycle gas ratio causes a lower velocity in the reactor that results in a higher catalyst concentration. A relatively small reduction in recycle gas rate can cause a significant change across a reactor because by simultaneously increasing CO and catalyst concentration, and reducing the amount of heat sink, it allows a larger temperature rise. This is a very complex system and it is difficult to take into account all of these simultaneous changes when searching for operating conditions that could give an improved yield structure. The kinetic model used in this study could be used for this purpose, but this was not included within the scope of the present study.

If we define the following as criteria for an idealized Fischer-Tropsch reactor:

- It should operate with a degree of polymerization of about 4, in order to maximize the gasoline yield
- It should operate at a low enough temperature to eliminate free carbon formation and give low methane yield
- It should preferably operate on low H_2/CO ratio syngas feed
- It should have a high conversion per pass,

it is apparent that the present design proposed for the entrained bed Fischer-Tropsch reactor cannot satisfy any of these criteria.

If the dew point problem can be eliminated, it seems likely that many of the other faults of this system could be solved. The temperature could be lowered, high conversion could be achieved by increasing the CO partial pressure, and the catalyst basicity could be adjusted to give the desired degree of polymerization. The use of multifunctional catalysts (36, 60)

could provide the answer to this problem, as it would cut off the high boiling point "tail" in the Fischer-Tropsch product. However, such a catalyst is not presently available. There is also some reason to doubt whether such a catalyst could be used in the entrained bed system. This system has high velocity transport heat exchangers. The present iron catalyst is not very erosive and this probably accounts for the successful operation of this type of heat exchanger. A supported iron multifunctional catalyst would probably be much more erosive and dilute phase heat exchangers are unlikely to be practical. A dense bed fluidized reactor with cooling coils would almost certainly be a preferred system for a vapor phase reactor utilizing a multifunctional catalyst.

5.1.3 Tube-Wall Reactor

The conceptual design prepared by the R. M. Parsons Company (17) for a Fischer-Tropsch complex was used as a starting point for the tube-wall reactor design used in this comparison. The Parsons yield structure and reactor design were modified to be consistent with information from the kinetic model, and also to reflect changes considered necessary from an operations standpoint.

The Parsons tube-wall reactor design incorporates flame-sprayed iron catalyst on external extended-surface heat exchanger tubes. The reactor was designed for operation at 606°F and 400 psig, with a recycle ratio of 1.5 and a space velocity "J" factor of 10. Based on these conditions, Parsons predicted a very attractive process. However the predicted yield structure was based on an experiment (54) using potassium-promoted steel lathe turnings catalyst at a gas recycle ratio of 27 and a J factor of 1.5. It is doubtful that a flame-sprayed catalyst could be produced with the activity of magnetite (Parsons activity basis) and at the same time with the yield structure of the potassium-promoted lathe turnings. In addition, a critical review of the reactor design reveals other shortcomings.

The chief advantages claimed for the tube-wall reactor are isothermal operation, high thermal efficiency, and efficient utilization of a small

amount of catalyst. The kinetic model for the tube-wall reactor supports the claim of good temperature control and isothermal operation, predicting catalyst temperatures never exceeding the coolant temperature by more than two degrees. Removal of the heat of reaction by steam generation in the reactor does give a good thermal efficiency for the reactor. This can be done in all the reactors included in this study, so the thermal efficiency is mainly dependent on the recycle-to-fresh feed ratio, as discussed elsewhere in this report. Catalyst activity is related to surface area, and compared to pelleted catalyst the flame-sprayed catalyst does have more surface area per pound; therefore, less is required. Compared to the finely divided catalyst used in the slurry and entrained bed reactors, however, our computer modeling work shows no advantage in activity per pound of catalyst.

When the kinetic model was run at conditions simulating those used for the Parsons reactor design, but with a catalyst considered to be more representative, it showed only 35% CO conversion compared to the 89% used in their basis. In order to get predicted CO conversion back up to 90%, it was necessary to raise reactor temperature to 640°F and almost double the catalyst surface area. With the excellent temperature control possible in the tube-wall reactor, recycle gas is not needed for temperature control. By operating without recycle the catalyst requirement is reduced. The present reactor is, therefore, intended to operate at 640°F at 400 psia, with no recycle gas and a J factor of 9. However, there are some doubts about the ability to operate for an extended time at this high temperature due to free carbon formation. Reducing the temperature would, of course, require more catalyst. The reactor could also require a higher H_2/CO ratio for extended operation.

While the Parsons reactor utilized catalyst on external extended-surface heat exchanger tubes, the reactor used for this comparison has the flame-sprayed catalyst on the inside of the heat exchanger tubes. This is done in order to make in-situ catalyst replacement feasible. In-situ flame-spraying was demonstrated in the tube-wall reactor process development unit (16). Circulation of coolant during the flame-spraying prevented warping of the reactor. For the case of catalyst on external fins,

catalyst replacement would require complete dismantling of the reactor. This would be prohibitively expensive and time-consuming. Applying the catalyst on the inside of 2-inch tubes (the minimum diameter for internal flame-spraying) does result in less surface area per reactor volume. The present conceptual design requires five to six times as many reactors as does the Parsons design, for a given amount of catalyst, or 42 reactors for 28.05 MM SCFH of CO + H_2 conversion.

For the purpose of this study, the yield structure was based on Hot-Gas-Recycle Experiment 26C (54), as was the yield structure in the Parsons conceptual design. As discussed in a later section of this report, this yield structure, modified to reflect higher methane yield due to the higher operating temperature, appears to be reasonable for the present reactor design. The assumption implicit in this choice of data base is the ability to flame-spray a promoted taconite catalyst and retain the properties associated with the lathe turnings catalyst used in Experiment 26C. To date, this ability has not been proven. Typical tube-wall reactor experiments (61) have shown a very low degree of polymerization, yielding only 10 to 15 wt-% gasoline compared to the 48 wt-% theoretical maximum. This yield structure is not attractive if liquid fuels are the objective.

As one might expect from the relative reactor size and the number required, the tube-wall reactor system is quite expensive, costing twice as much as the entrained bed reactor system. In addition, the flame-sprayed catalyst, due to the method of application, is much more expensive than the forms used in the other reactors. The development of a different catalyst, perhaps one which could be applied as a chemical wash on the inside of small-diameter tubes, could reduce the cost to an economically attractive range. However, for the tube-wall reactor as presently defined, the high cost, the lack of a proven flame-sprayed catalyst, and doubts about free carbon formation, all lead to the conclusion that the tube-wall reactor is not an attractive choice for the Fischer-Tropsch reaction.

5.1.4 Slurry Reactor

The slurry reactor described by Koelbel (2) was used as a basis for this reactor comparison. Since 400 psia operating pressure was selected for this study as compared to the 174 psia used by Koelbel, it was first necessary to check what effect this pressure change would have on space velocity requirements. The kinetic model described in Section 4 was used for this purpose. The model predicted that if the same linear velocity and catalyst concentration are used at 400 psia as at 174 psia, the conversion per pass will increase. Until further work has been done in fitting the kinetic model to slurry reactor data taken over a wide range of operating pressures, it is not believed justified to use the higher conversion predicted as a basis for this comparison. Therefore, it is assumed that the conversion will remain unchanged if the pressure is increased, providing the superficial gas velocity and gas feed composition are the same. Even with this assumption, the capacity of a given reactor is virtually proportional to the operating pressure and a given vessel can process more than twice the moles of syngas at 400 psia as at 174 psia. The kinetic model also indicates that if the same catalyst is used, the degree of polymerization will increase, but that this can be restored to the optimum degree of polymerization for gasoline by adjusting the hydrogenation rate constant. As this rate constant appears to be adjustable by changing the potassium concentration in the catalyst, it has been assumed that a suitable catalyst can be produced for the 400 psia operation.

A reactor superficial feed gas velocity of 0.3 ft/sec, and a reactor height of 27 feet (almost identical to Koelbel's demonstration unit) was selected for reactor sizing. With this superficial gas velocity, this type of reactor will require many reactors in parallel. Fourteen feet diameter was selected as the maximum diameter that will normally permit shop fabrication. With this diameter, 18 reactors in parallel are required to convert the 28.05 MM SCFH of syngas used as a basis for this study. The expanded liquid level was set at 21 feet, with 6 feet allowed for vapor disengagement. The gas hold up in the expanded liquid phase was taken as 30%, and the catalyst concentration in the liquid set at 10 wt-% of 30 μ catalyst.

The only internals included in the reactor design are a gas distributor and steam coils for the generation of 600 psig steam. No vertical baffles were included. There has been much discussion in the literature (2) on the possible scale-up problems of this type of reactor, but there is no documentation offered for the suggested channeling of bubbles. Scaling up from the 5 feet diameter used successfully in Koelbel's demonstration plant to the 14 feet diameter suggested in this study is not a large step. The cooling coils do provide vertical surfaces which reduce the hydraulic diameter of the system. Large diameter reactors are commonly used for bubbling slurry reactors without the need for internals to obtain good gas distribution (62).

With a gas velocity of 0.3 ft/sec, the degree of back-mixing of the liquid phase will be very high, and complete back-mixing of the liquid was assumed in the kinetic studies. With low viscosity liquids, there will be little gas back-mixing, and plug flow was, therefore, assumed in the kinetic studies. The superficial gas velocity is, however, in a region where some of the gas may travel through the reactor in slugs and, if this is the case, there will be some departure from plug flow; but more importantly, gas by-passing could result and conversion may suffer. The kinetic study did show that staging the slurry system will provide a significant increase in conversion from the same reactor volume. The use of baffles to reduce back-mixing and get some staging in the parallel reactors may be justified, but the utility of baffles to provide staging would need to be demonstrated. It is more likely that slurry reactors will be arranged with two or three reactors in series. The gas velocity in the first reactor will be higher, and the presence of some gas slugging will be tolerated. Subsequent reactors can be operated in the bubbling region and conversion could then be so high that recovery and recycling of residual CO and H_2, would not be justified. The potential of obtaining a conversion over 95% in one pass offers a considerable simplification of the Fischer-Tropsch process.

No means for temperature control beyond adjustment of steam pressure was provided in the reactor operated at Koppers. Most operators would probably prefer to keep the steam pressure constant, and an external,

adjustable circulating trim cooler for temperature control of the reactor is included in the present design. This is a much smaller system than the very large circulation required for the ebullating bed system, and causes an increase in reactor cost of about 3%.

As the reactors are intended to maximize gasoline yield, there will be negligible production of liquid product at reactor conditions and virtually all of the product will leave in the vapor phase. No liquid product filtering system has been included in the design, although a small system will be required for removal of reactor liquid for the maintenance of the quality of the catalyst and the liquid phase.

The maintenance of the quality of the liquid phase appears to be an important factor in obtaining successful operation of this type of reactor. The liquid must have a low viscosity at reactor conditions if good hydrodynamic characteristics are to be achieved. The oil should also have good stability, and some further experimentation to determine the optimum material is probably justified.

The choice of the right catalyst and operating conditions is essential to the maintenance of oil quality. The operating temperature should be low enough that the formation of free carbon is not encountered. The combination of operating conditions and catalyst formulation should also ensure that the product is removed in the vapor phase in order to minimize contamination of the reactor oil with high molecular weight olefins which have poor stability. The correct selection of the oil, catalyst and operating conditions, combined with an appropriate oil withdrawal and replacement rate should ensure a high on-stream efficiency.

The slurry reactor appears to be the most promising for the Fischer-Tropsch reaction. It can operate on syngas with a low H_2/CO ratio and provide high conversion per pass. Condensation of the high molecular weight "tail" of the product on cooling surfaces can be tolerated in this liquid phase system, which permits selection of the optimum degree of polymerization to fit the product needs. The use of high CO concentrations permits operation at low temperature while maintaining good conversion levels. Low temperature should avoid excessive methane production

and free carbon formation. Operation in an essentially once-through mode is also a possibility that could greatly simplify the overall process.

The slurry reactor has never been operated for Fischer-Tropsch synthesis on a commercial scale. It has been operated up to 5 feet diameter, and the scale-up from there to the 14 feet diameter suggested for commercial production should not be difficult. The system will require a much lower investment if it is operated at 400 psia, but this will require some experimental work to demonstrate that a suitable catalyst can be developed for this operating pressure, and also to determine what operating temperature can be used at this operating pressure to avoid free carbon formation and obtain a suitable catalyst life.

5.1.5 Ebullating Bed Reactor

Operating conditions for the ebullating bed reactor were chosen primarily on the basis of work at the U.S. Bureau of Mines (26, 28). Chem Systems, Inc. was subcontracted under Task Order No. 15 to prepare an ebullating bed reactor conceptual design, using the specified operating conditions as a design basis. Chem Systems was chosen to do the design work because of their experience in the design and operation of ebullating bed reactors for production of methane and methanol (3, 29).

The ebullating bed reactor is a three-phase reactor in which the heat of reaction is removed by cooling oil circulated through an external heat exchanger, then returned to the reactor. Liquid and gas rise cocurrently through the reactor, at velocities sufficient to expand the bed of granular catalyst without carrying it out of the reactor. Liquid and vapor leave the reactor at the top and are separated in a disengaging vessel. Means for adding or withdrawing oil from the reactor can be incorporated in the liquid circulation loop.

The liquid phase provides excellent temperature control and eliminates concern over the formation of local hot spots in the reactor. The good temperature control and low temperature operation allow the use of a CO-rich syngas without excessive carbon formation. In turn, a high

conversion per pass is made possible even at low temperature, by the use of CO-rich syngas. In addition, methane production is lower than in gas-phase reactors, as observed in work carried out at the Bureau of Mines (27).

The circulating oil method of heat removal is advantageous in several respects. In addition to the good temperature control discussed above, the method provides ease in adjustment of the amount of heat removal by varying the liquid circulation rate. While the range over which the liquid velocity can be varied is restricted by catalyst fluidization requirements, the maximum allowable velocity being approximately twice the minimum will allow good temperature control over a wide range of feed rates. By expanding the catalyst bed and providing some scrubbing action, the circulating oil prevents agglomeration of the catalyst particles. The expanded bed also makes more efficient use of catalyst than does a packed bed. (26)

As with the slurry reactor, stability of the cooling oil is critical to the operation of the ebullating bed reactor. An oil that becomes very viscous due to excessive free carbon or high molecular weight wax content does not allow adequate transport of gas-phase reactants and products to and from the liquid phase. The paraffins produced in the Fischer-Tropsch reactor have been used for this purpose and performed satisfactorily when used with the proper catalyst and in the correct temperature range. As with the slurry reactor, the selection and maintenance of the most suitable fluid will be an important part of the reactor development.

The ebullating bed reactor is very simple in design, containing no internals except for the gas distributor. This type of reactor does not present a scale-up problem as the flow behavior is expected to be the same in a 14-foot diameter commercial reactor as in a small pilot-scale reactor. The amount of oil circulation required to limit temperature rise in the reactor to about 20°F is very large, and the oil circulation pumps increase the cost of the reactors by almost 25% over that of the slurry system. Several reactors in parallel will be required for a large scale

plant, and for the 28.05 MM SCFH of syngas conversion used as a basis in this study, twenty 14-foot diameter reactors in parallel would be required.

The liquid phase behavior in an ebullating bed reactor is nearer to plug flow than in a slurry reactor. As discussed elsewhere in this report, the kinetic model predicts that staging a three-phase reactor gives higher conversion for the same reactor volume and catalyst activity than a totally back-mixed system. This is not a great advantage over the slurry reactor, as the slurry reactor could be designed with two or three reactors in series. With either liquid system, one-pass conversion over 95% should be possible.

The largest obstacle to commercial development of the ebullating bed reactor is one of catalyst development. A granular catalyst (this study assumes 1/16-inch diameter) is required to allow liquid circulation without catalyst carryover, as well as the other operational advantages listed in preceding paragraphs. The only Fischer-Tropsch catalysts to have demonstrated the ability to withstand the constant agitation in an ebullating bed reactor over a reasonable period of operation are the massive iron catalysts developed by the U.S. Bureau of Mines. (28) These catalysts have no internal surface area and are, therefore, much less active than a typical ammonia synthesis catalyst. The use of these less active catalysts would require more catalyst and more reactors, and the system would be unattractive economically.

In order to keep the reactor size reasonable, use of the more active fused-iron catalysts has been assumed. In the Bureau of Mines experience (58), the fused-iron catalysts disintegrated within two to three months. Such frequent catalyst replacement could be very expensive. In addition, in the Bureau of Mines reactor, the catalyst fines settled out in the heat exchanger (27) and no doubt would eventually have caused a plant shutdown.

If a catalyst with high activity and good physical strength could be developed, this type of reactor could be considered for the Fischer-Tropsch reaction. The potential advantages over the slurry reactor are:

- Higher conversion for a given catalyst activity
- If high middle distillate yield is required, it would be easier to produce and separate a liquid product.

These are not very significant advantages. The second does not apply in a maximum gasoline case because operating conditions can be selected that allow the product to be removed as vapor. The first may not be significant because arranging slurry reactors in series would give the same result.

The lack of physical stability of the catalyst may be the result of changes in catalyst composition during operation, causing the particles to fracture. The use of a support that is stable in this reaction environment may be required to overcome this problem. A supported catalyst is likely to be expensive compared to the finely divided iron used in the slurry system. This combined with the expensive oil circulation system leads to the conclusion that the ebullating bed reactor is unlikely to be used for the Fischer-Tropsch reaction.

5.2. COMPARISON OF SYSTEMS

5.2.1 Basis of Comparison

5.2.1.1 General

In order to set a common basis for comparison of product yields, investment costs and thermal efficiencies, conceptual designs were prepared for criticial portions of each of the reactor systems. The basis used for the designs was conversion of 73,900 pound-moles per hour (28.05 MM SCFH) of CO + H_2. This quantity corresponds to approximately 25,000 barrels per day of hydrocarbon products, and is considered to be a typical size for an indirect liquefaction plant. The moles of CO + H_2 converted is thought to be a fair basis of comparison because it eliminates the effect of the water-gas shift reaction. In the shift reaction, one mole of CO reacts with water to form one mole of H_2, and the total moles of CO + H_2 remains constant.

The synthesis gases shown in Table 5.2-1 indicate the H_2/CO ratio considered optimum for each reactor type. As the compositions are based on work reported in the literature (4, 2, 54), they also reflect variations in minor components due to the different syngas sources. The quantities shown are those required to give the design conversion of CO + H_2, on a once-through basis for the tube-wall and slurry reactors, and in a recycle operation in the entrained bed reactor. In practice the CO and H_2 in the reactor effluent would presumably be recovered and recycled, resulting in conversions similar to that shown for the entrained bed reactor. (See Table 5.2-6). The effect of using some recycle gas is to reduce the quantity of fresh feed required, and to change the H_2/CO ratio in the feed gas. The resulting syngases and combined feeds are given in Table 5.2-2.

The operating pressure was set at 400 psia for all four reactor systems. This is a pressure at which syngas can be supplied from a modern gasifier without requiring additional compression. Other operating conditions were set according to the requirements of the individual systems, and are discussed separately.

A conceptual design and cost estimate were prepared for the ebullating bed reactor; however, there is no indication in the literature (27, 28) of a significant difference bewteen the ebullating bed and slurry reactors in fresh feed requirements or product yields. Both reactors are three-phase systems and as such are expected to produce similar yields under similar operating condtiions. In addition, thermal efficiencies will be similar. Therefore, when discussing syngas requirements, product yields and thermal efficiencies, references to the slurry reactor apply equally to the ebullating bed reactor, and the ebullating bed reactor is not discussed separately.

5.2.1.2 Entrained Bed Reactor

The Kellogg Synthol Feasibility Study (4) was the primary source used in the entrained bed reactor design. Where information given by Kellogg was insufficient for design purposes, it was supplemented by Sasol publications (9, 12, 63) and by standard engineering design practice.

With few modifications, the Kellogg design was scaled to the quantity of feed set for the conceptual design basis. The fresh feed shown in Table 5.2-1 is of a composition indicated by Kellogg, with the CO_2 content reduced to a level intermediate to that claimed by Kellogg and by Sasol (63). With the same exception, the product distribution given in Table 5.2-3 parallels that claimed by Kellogg. The ratio of recycle gas to fresh feed is the same as indicated in Kellogg. Although information published by Sasol is less specific, the ranges of feed composition, product distribution and recycle ratio they report are in general agreement with those used for this study.

The design pressure of 400 psia is higher than that used in the Kellogg design. In order to allow for the increased conversion attainable at higher pressure, gas hourly space velocity was increased in the same ratio as the pressure. The reactor diameter was set to give a superficial gas velocity of 8 feet per second, which is apparently in the range used by Sasol (12, 37). The operating tempearture of 600 to 635°F is the same as shown in the Kellogg design. It was decided, however, to use steam

generation in the reactor cooling coils for heat removal instead of circulating oil. This decreases the length of the cooling section somewhat, and eliminates the need for a second heat transfer step from the oil to steam.

Very little information is available on the design used for the catalyst separator, quench tower and heat exchangers. These items were sized according to standard practices, and are included in the equipment list given in Appendix E.

5.2.1.3 Tube-Wall Reactor

In designing the tube-wall reactor consideration was given to the conceptual design prepared by R. M. Parsons (17) and data from the U.S. Bureau of Mines (1, 54) were also used. Due to apparent discrepancies (see Section 4.3.2) in the Parsons design, the reactor model developed in the kinetic modeling portion of this study was used to set the temperature and space velocity "J" factor to get the specified conversion of CO + H_2.

In order to predict a reasonable gasoline yield, it was necessary to run the reactor model with catalyst characteristics attributed to a hypothetical potassium-promoted flame-sprayed taconite catalyst. This catalyst would have the activity of flame-sprayed taconite, and a yield structure associated with potassium-promoted catalyst made from steel lathe turnings. With this catalyst, the model predicts that at a temperature of 640°F, pressure of 400 psia, and J factor of 9, a once-through CO + H_2 conversion of 90% will be achieved. The predicted yield structure is similar to that observed in Hot-Gas-Recycle Experiment 26C (54) and also claimed by Parsons (17).

The syngas shown in Table 5.2-1 for the tube-wall reactor has a composition typical of that used in tube-wall reactor experiments (28); however, it is not known with any degree of certainty what H_2/CO ratio would be required to prevent free carbon formation at the temperature selected for this design. Operation with minimal recycle gas was selected because it decreases the size of reactor required.

The heat removal scheme uses boiling oil in the reactor instead of steam because, in the temperature range required for this operation, oil temperature is more easily controlled by pressure changes than is steam temperature.

The catalyst is applied to the inside of 2-inch diameter tubes. This results in a larger reactor section than shown in the Parsons design, where the catalyst was applied to external extended surfaces. The reason for this significant departure from previous practice is discussed in Section 5.1.3. The reactor sizes and other equipment details are listed in Appendix E.

5.2.1.4 Slurry Reactor

The conceptual design for the slurry reactor is based entirely on information published by Koelbel (2) on the Koppers-Rheinpreussen demonstration unit. The syngas shown in Table 5.2-1 has an average composition used in the demonstration unit. The product yield structure shown in Table 5.2-6 is that claimed by Koelbel. The demonstration unit was generally operated without recycle gas, and the conceptual design is also based on once-through operation. The one significant modification to the demonstration plant design consists in setting operating pressure at 400 psia instead of the 174 psia used in the demonstration unit. The operating temperature is also slightly higher at 527°F instead of 514°F. The effect of temperature and pressure on reaction rate is compensated by increased space velocity: the space velocity in the conceptual design is 772 hr^{-1} while that used in the demonstration unit was 270 hr^{-1}. The catalyst concentration is that which Koelbel claims is optimum -- 10 wt-%. The total reactor cross-sectional area is set to give a superficial gas velocity of 0.3 feet per second, which is the same as typically run in the demonstration unit.

When the computer model of the slurry reactor was run at the operating conditions of the conceptual design, it predicted CO conversion of over 93%, and a high degree of polymerization. It is assumed the degree of polymerization could be corrected to give a maximum yield of gasoline, by using a catalyst with lower potassium content.

The surface area required for the cooling coils located in the reactor was calculated on the basis of the heat transfer coefficient claimed by Koelbel (2). Very little additional equipment is required for the reactor section of a slurry reactor Fischer-Tropsch plant. The complete equipment list is in Appendix E.

5.2.1.5 Ebullating Bed Reactor

As stated previously, the literature (26, 27, 28) indicates the ebullating bed and slurry reactors are very similar in terms of general operating conditions and yield patterns; therefore, the synthesis gas composition, average temperature and pressure for the ebullating bed reactor conceptual design are the same as those set for the slurry reactor. The yield structure is also expected to be similar.

The most significant difference between the two three-phase systems is in the size of the catalyst particles used. The slurry reactor uses a very finely divided catalyst, while the ebullating bed catalyst is large enough to remain in the reactor and not be carried overhead by the circulating oil. For the conceptual design, the catalyst diameter was set at 1/16 inch, typical of that used in U.S. Bureau of Mines work (26). The difference in size affects the activity of the catalyst, which in turn affects the amount required and the space velocity.

Based on their experience in the design and operation of ebullating bed reactors (3, 29), Chem Systems was requested to prepare a conceptual design for an ebullating bed Fischer-Tropsch reactor. The operating conditions specified for the design were 500°F, 315 psia, and fresh feed space velocity of 300 hr^{-1}, based on settled volume of catalyst. Two feed gas compositions were specified: one with a H_2:CO ratio of 2.0 and a second with H_2:CO ratio of 0.64. Their report is included as Appendix F.

As more information became available through more thorough literature review, new design specifications were set, and a new conceptual design was prepared based on information from Chem Systems. The final design specifications are based on U.S. Bureau of Mines oil-recycle Experiment

26A (26). In this experiment 90% conversion of CO + H_2 was achieved at a space velocity of 600 hr^{-1}, temperature of 492°F, and pressure of 415 psia. Syngas with 0.7 H_2:CO ratio was used and the recycle-to-fresh feed ratio was 1. A fused iron catalyst was used and over 2 months operation was achieved. For the conceptual design, the temperature was increased to 527°F, and space velocity (based on settled catalyst volume) was increased to 750 hr^{-1}. The resulting reactor and other equipment sizes are discussed in Section 5.2.3.5 and listed in Appendix E.

5.2.2 Product Yield Comparison

5.2.2.1 Introduction

Product yield structures for the entrained bed, tube-wall, slurry and ebullating bed reactor systems are given in this section along with a discussion of how each of the yield structures was determined.

In order to obtain as realistic a yield structure as possible for each of the systems, experimental data were used. The kinetic models were used as a guideline for determining the degree of shift activity and for making adjustments due to changes in operating conditions. The number of moles of H_2 + CO converted was held constant for all of the systems. The figures presented are net yields from the reactors based on a recycle operation of 2.3:1 for the entrained bed system, and once-through yields for the tube-wall and slurry systems. Moles of H_2 + CO converted is considered to be the best basis of comparison, because it eliminates the effect of internal versus external shift by giving yields per mole of syngas converted.

Synthesis gas feeds are shown in Table 5.2-1. Their compositions are based on those given in the literature pertaining to each particular reactor type (1, 2, 4). The feed shown for the slurry reactor is also applicable to an ebullating bed reactor. While initial design work for the tube-wall and liquid-phase reactors was based on once-through operation, it is presumed that the hydrogen and carbon monoxide in the effluent streams will in all cases be recovered and recycled, resulting in similar

overall conversions. Syngas feeds, modified to reflect the effect of recycle operation in the tube-wall and slurry reactors, are shown in Table 5.2-2. The feed composition for the entrained bed reactor does not change and is shown only for comparison.

5.2.2.2 Entrained Bed Reactor

The product yield structure for the entrained bed reactor is shown in Table 5.2-3. The yield structure is based on data from Kellogg (4). The yield parallels that given in the Kellogg study with adjustments for a different CO_2 composition in the feed. The concentration of CO_2 in the synthesis gas was set at 4.0 mol-% which is intermediate to that used in the Kellogg study and concentrations reported by Sasol (63). Product properties were based on the hydrocarbon types given in the Kellogg study. For calculation purposes, the acid component was considered to be a mixture of acetic and propionic acid, and the non-acid chemical component was considered to be a mixture of ethanol and propanol, as reported by Sasol (11).

C_8 and heavier mixtures were broken down into individual alkanes and alkenes which were then regrouped to give the gasoline, diesel and heavy cuts as shown in the product yield in Table 5.2-3. The ratio of components within each cut was selected in such a way that the molecular weight of each cut was maintained after splitting into its individual components. Once the relative amounts of alkanes and alkenes were set, the product distribution was calculated so that gasoline contained C_5 to C_{11}, diesel C_{12} to C_{25}, and heavies C_{26} to C_{40}.

If the product yield is plotted, it shows that there are more high molecular weight materials (i.e., above C_{26}) than would be present if the C_5+ yield structure followed a Schulz-Flory distribution. This departure from Schulz-Flory not only increases the yield of heavy product but also increases the hydrocarbon dew point of the reactor effluent (see discussion in Section 5.1.2). An estimate was, therefore, made of what the yield structure would be if all of the C_5+ material fell on a Schulz-Flory line, with an overall degree of polymerization of 3.3 and an olefin-to-paraffin ratio of 2. This is shown as the modified yield structure in

Table 5.2-3. The degree of polymerization of 3.3 was determined by reference to Figure 4.3-3, using the method described in Section 4.3.1.2 of this report. The quantities of H_2, CO, CO_2 and H_2O in this product structure were calculated by making an overall material balance and holding the molar ratio of CO_2 and H_2 to CO and H_2O in the reactor effluent constant.

A product yield structure reported by Sasol (12) is also shown in Table 5.2-3, for comparison with the others.

5.2.2.3 Tube-Wall Reactor

The basis for the yield structure from the tube-wall reactor is U.S. Bureau of Mines Experiment 26C (54). This yield structure was also the basis for the yield shown in the R. M. Parsons study, "Fischer-Tropsch Complex Conceptual Design/Economic Analysis" (17) and is shown in Table 5.2-4. Some modifications were made to this data in order to make it consistent with the particular catalyst and operating conditions selected for this reactor.

Experiment 26C was a Hot-Gas-Recycle experiment using potassium-promoted lathe turning catalyst operating at 586°F and a J factor of 1.5. The tube-wall reactor design uses a potassium-promoted taconite catalyst on the inside of 2-inch diameter tubes, having a J factor of 9, operating at 640°F, once-through mode of operation. When these conditions were used in the kinetic model, it predicted a degree of polymerization of 4.3 which is the same as Experiment 26C. This suggests that the yield structure for Experiment 26C is a reasonable estimate for the tube-wall reactor yield at 640°F.

One difference that can be expected and which the kinetic model does not account for is methane formation via the free carbon mechanism discussed previously. It is necessary to distinguish between the increase in methane due to the main Fischer-Tropsch mechanism and that due to the free carbon mechanism. When the kinetic model was run at 590 and 640°F, keeping the reactor configuration constant, the C_1 content, expressed as mol-%

of the hydrocarbon product, increased by 4.5%. However, when the yields from Experiment 26C at 586°F and 26H at 640°F are compared, the methane yield has increased by 5.9 mol-%. The difference of 1.4 percentage points was attributed to the free carbon mechanism, and the mole fraction of methane estimated for the tube-wall reactor product was increased by this amount. The quantities of H_2, CO, CO_2 and H_2O in the product were determined from the tail gas analysis and adjusted as necessary to maintain an overall material balance. To make this adjustment, the molar ratio of CO_2 + H_2 to CO + H_2O was kept equal to that shown by the kinetic model for the same operating conditions. The resulting product is shown as the modified yield structure in Table 5.2-4.

The syngas feed for the tube-wall reactor shown in Table 5.2-1 does not include nitrogen. This is because the experimental syngas composition did not contain N_2, and this was carried through the design. The effect of including N_2 in the feed would be to increase the size of reactors required. The modified yield structure for the tube-wall reactor is used for the yield comparison in Table 5.2-6 because it is believed to be more realistic.

5.2.2.4 Slurry Reactor

The slurry reactor yield structure used for this study is based on data from Koelbel and Ralek (2). The hydrocarbon yield they report is shown in Table 5.2-5, scaled to a quantity consistent with the design basis of 28.05 MM SCFH CO + H_2 converted. For comparison with yields from the other reactors, the C_5+ material was broken into the individual components and then regrouped into the standard gasoline, diesel and heavy cuts shown. The H_2, CO, CO_2 and H_2O in the reactor effluent were determined by making an overall material balance on the reactor, using the feed shown in Table 5.2-1. This syngas feed composition represents an average of the range of compositions reported by Koelbel (2). The kinetic model was used to determine the correct ratio of CO_2 + H_2 to CO + H_2O in the reactor effluent at the operating conditions used in this study.

As the conceptual reactor operating pressure is 400 psia and the demonstration unit was operated at 174 psia, this could have a significant effect on yield structure. The kinetic model predicts that a given catalyst will produce a much higher degree of polymerization at 400 psia than at 174 psia. For the purpose of this comparison, it is assumed that the catalyst and operating conditions can be selected which will produce a yield structure similar to Koelbel's.

The slurry reactor yield structure reported by Koelbel shows a gasoline yield higher than the maximum of about 48 wt-% that is possible with a Schulz-Flory distribution of hydrocarbon products. A modified yield structure was, therefore, prepared in which the products follow a Schulz-Flory distribution with a degree of polymerization of 4 and an olefin-to-paraffin ratio of 2. The degree of polymerization of 4 was chosen by comparing Koelbel's yield structure with the plot in Figure 4.3-3, as discussed in Section 5.2.2.2. The olefin-to-paraffin ratio is the average ratio shown in Koelbel's slurry reactor product. This modified yield structure is shown in Table 5.2-5. The main differences between the two yield structures are the lower gasoline and higher diesel yield for the Schulz-Flory product, compared to the experimental data.

5.2.2.5 Ebullating Bed Reactor

It is expected that, due to the similarity of operating conditions in the two liquid-phase reactors, the product yield structures will also be very similar. The low H_2/CO ratio syngas feed (shown in Table 5.2-1) as recommended for the slurry reactor, is also an appropriate feed for the ebullating bed reactor. The slurry reactor product yield structure shown in Table 5.2-5 also represents the product expected from an ebullating bed reactor.

The belief that slurry and ebullating bed reactors will give similar product yield structures is supported by work done at the U.S. Bureau of Mines (10). Under operating conditions similar to those used in Koelbel's demonstration unit, a similar product slate was achieved. During Experiment 37, Period 7, the reactor temperature was the same as reported for

the slurry reactor. The effect of higher operating pressure and higher H_2/CO ratio on degree of polymerization would tend to cancel each other, and, indeed, the observed degree of polymerization is very close to that observed in the slurry reactor.

The main differences between the slurry and ebullating bed reactors are catalyst particle size and method of heat removal. It is possible that pore diffusion effects in the larger catalyst particles could cause a shift in product distribution. This is not believed to be a significant effect with the type of catalysts used for ebullating bed Fischer-Tropsch synthesis.

The method of heat removal, by oil circulation in the ebullating bed reactor as compared to internal coils in the slurry reactor, is more likely to have an effect on product yield structure. The external oil circulation as well as the presence of larger catalyst particles results in a system in which the liquid phase is no longer totally back-mixed. The kinetic model, operated in a manner representing less back-mixing, showed a small effect on both conversion and degree of polymerization. While the understanding of the ebullating bed reactor is not sufficient to predict these effects with great precision, the differences appear to be of a magnitude that could easily be adjusted by changes in catalyst composition.

5.2.2.6 Yield Comparison

Yield structures for the entrained bed, tube-wall and slurry reactors are presented for comparison in Table 5.2-6. The entrained bed and slurry yields are those represented by Kellogg (4) and Koelbel (2), respectively.

In Tables 5.2-3 and 5.2-5, it has been shown that the gasoline yields would be 22% higher and 17% lower for the entrained bed and slurry reactors, respectively, if the yield structure followed Schulz-Flory distributions. However, there is no clear evidence that Schulz-Flory will be followed and, therefore, the published yields are used for comparison purposes. The tube-wall reactor design selected is so far from any

experimental data with respect to operating conditions, recycle ratio and J factor, that an estimated yield has been used for comparison purposes.

Despite some remaining uncertainties with respect to yield structure, some broad conclusions can be drawn:

1. Yields should be compared on the basis of moles of hydrogen plus carbon monoxide converted.

2. The entrained bed and tube-wall reactors require high hydrogen content syngas feeds. The high operating temperatures require high hydrogen partial pressures to suppress carbon formation. The high hydrogen partial pressure reduces hydrogen production via internal shift. In the case of the entrained bed reactor, the high level of carbon dioxide in the recycle gas virtually eliminates the shift reaction. The slurry reactor operates with the lowest hydrogen partial pressures and can provide the internal shift reaction necessary to operate with a synthesis gas feed having a low hydrogen-to-carbon monoxide ratio, such as would be produced by the Texaco or Shell gasifiers.

3. The higher operating temperature of the tube-wall and entrained bed reactors will result in a considerably higher methane yield than with the slurry reactor.

4. The gasoline yield will be highest for the slurry reactor. The comparative yields in Table 5.2-6 show the slurry reactor to have almost twice the gasoline yield of the entrained bed reactor, with the tube-wall intermediate between the two. If all of the reactors produced a Schulz-Flory yield pattern, the slurry reactor would still produce the most gasoline, but the ratio would now be about 1.36 times the entrained bed. This higher gasoline yield is due to flexibility of the slurry system allowing the selection of operating conditions that minimize methane production and maximize gasoline production. This reflects a combination of high catalyst activity allowing lower temperature operation, and the inherent advantage of the liquid phase systems ability to tolerate the higher dew point product.

5.2.3 Investment Cost Comparison

5.2.3.1 Introduction

This section compares sizes and investment costs of the four reactor systems. Since annual catalyst replacement costs proved to be significant, a comparison of catalyst costs is also included. The investment cost comparison is restricted to the reactor section of each Fischer-Tropsch plant. The impact of the reactors on upstream and downstream requirements is discussed in a separate section of this report.

A conceptual design for a reactor system capable of converting 28.05 MM SCFH of $CO + H_2$, was prepared for each reactor type under consideration. The complete design basis is included in Section 5.2.1 of this report. Based on the conceptual designs, in-house estimating procedures were applied in determining relative costs of the four reactor systems.

The items of equipment included in the designs are shown schematically in Figures 5.2-1 through 5.2-4. A complete list of equipment sizes is given in Appendix E. The decision as to which items to include in each design was based on items inherently a part of the particular reactor, plus additional heat exchange equipment required to recover usable heat from the reactor effluent. Due to the height of the entrained bed reactor, structural steel is a significant item. Thus the steelwork was included in the design and cost estimate for the entrained bed reactor but not for the other three.

The cost estimates include only major items of equipment, i.e., reactors and other vessels, heat exchangers, and pumps, plus labor for installation. Specifically excluded from the cost estimates are piping and instrumentation, foundations, insulation, painting, site preparation, land and buildings. As these are not complete cost estimates, actual dollar figures would be misleading and thus relative rather than absolute dollar amounts are presented in Table 5.2-7. The entrained bed reactor is the only commercial system and the cost of this operation is set at 100; all other items are compared against this figure.

The items in Table 5.2-7 are grouped into the following categories: reactor and receiver, other vessels, heat exchangers, and pumps. The reactor cost includes internals, if any are required. This category also includes, for the entrained bed reactor, the catalyst receiver and structural steelwork; for the tube-wall reactor, the hot oil receiver; and for the ebullating bed reactor, the product separator. The "heat exchange" category includes all heat exchangers external to the reactors.

Differences in reactor inventory and catalyst life contribute to significant differences in catalyst replacement costs. Based on available information, catalyst life for the entrained bed (4, 9) and ebullating bed (26) reactors is set at two months. Slurry reactor catalyst life is set at 38 days (10), and tube-wall reactor catalyst life is set at six months (64). There is some doubt about the ability to achieve a six month catalyst life in the tube-wall reactor for the reasons discussed in Section 5.2.3.4. Based on quotes from Kellogg and catalyst suppliers, it appears that catalyst for the entrained bed and ebullating bed reactors will cost about the same per pound. Koelbel used a precipitated iron catalyst for his slurry reactor which has been estimated to cost approximately 4.5 times the fused iron catalyst used in the entrained bed. The cost figures shown in Table 5.2-8 are based on on-site catalyst production. The cost of purchased catalyst is approximately three times this amount. The cost of application of the flame-sprayed catalyst for the tube-wall reactor was obtained from PETC.

While the investment and catalyst costs are only approximate, some definite trends can be observed. On the basis of initial investment and catalyst replacement costs, the slurry reactor is far superior to the other three.

5.2.3.2 Entrained Bed Reactor

The Synthol reactor design prepared by Kellogg (4) formed the basis for the conceptual design used in this comparison. While Sasol claims that 20 years experience has allowed them to improve on the design, published information indicates that the basic reactor design is still quite similar. Two modifications to the Kellogg design are the use of 400 psig

operating pressure, and the use of direct steam generation instead of hot oil in the reactor cooling coils. Figure 5.2-1 illustrates the items included in the entrained bed reactor conceptual design and cost estimate.

For the design basis of 28 MM SCFH CO + H_2 conversion, two entrained bed reactor trains are required. The reactors themselves are 13-feet diameter by 111-feet overall height; each contains two sets of internal cooling coils. A 30-foot diameter by 40 foot tall catalyst receiver with cyclones is required to separate the catalyst from the product. A transfer line from reactor to catalyst receiver and a 50-inch standpipe with two slide valves are also included as part of the reactor. Due to the height and size of these vessels, extensive structural steelwork, amounting to about 10% of the cost of the reactor section, is required. As shown in Table 5.2-7, the reactor is about one-third of the cost of the entrained bed reactor system. The cost of two entrained bed reactors alone is comparable to the cost of 18 slurry or 20 ebullating bed reactors.

The "other vessels" in Table 5.2-7 include a quench tower and catalyst hoppers. The catalyst hoppers, one for fresh and one for spent catalyst, are considered necessary for catalyst addition and withdrawal. The 27-foot diameter by 80-foot tall quench tower is unique to the entrained bed reactor system, and is included in the design because it is required for separation of catalyst fines carried over from the catalyst receiver, from the reaction products. The quench also is an integral part of the heat recovery system and so cannot be excluded. The quench tower contributes about one-third of the total system cost. Moreover, the investment cost difference between the entrained bed reactor system and the two liquid-phase systems is due primarily to the quench section.

The final portion of the entrained bed reactor investment cost is for heat exchangers. The heat exchange section is different for this reactor system than for the others, due to the quench oil circuit. Quench oil is exchanged against combined feed and the cost of this exchanger is on a par with the feed/effluent exchangers for the other reactor systems. Heat exchange of a portion of the quench oil against boiler feed water allows

further heat recovery and also provides a means of temperature control for the quench tower. Finally, heat exchange of the quench vapor against boiler feed water allows recovery of useful heat of the reactor effluent down to 250°F.

The annual cost for catalyst replacement in the entrained bed reactor system is double that in the slurry reactor system. This difference results entirely from the difference in catalyst inventory. The bulk of the 900 ton catalyst inventory in the entrained bed reactor is contained in the catalyst hopper and standpipe. The quantity of catalyst actually in the reactor is similar to that contained in the slurry reactors.

The entrained bed reactor catalyst inventory must be replaced quite frequently; every two months is typical (4, 9). In addition approximately 1% of the inventory must be added daily to make up for catalyst loss due to attrition. This high rate of catalyst replacement is necessitated by the high operating temperatures and consequent free carbon formation. Deposition of product wax on the catalyst also creates more of a problem in the gas phase system.

The entrained bed reactor is the only Fischer-Tropsch reactor operating on a commercial scale. While the cost of the reactor section is more than that of some of the potential systems, the reactor section is a relatively small part of the overall cost of a complete coal liquefaction plant. Until an alternative system has been demonstrated on a commercial scale, investors in indirect liquefaction may choose to go with the proven system.

5.2.3.2 Tube-Wall Reactor

The tube-wall reactor is a heat exchanger with catalyst flame-sprayed on the tube surface. The Parsons conceptual design called for applying the catalyst on external fins. It appears that recoating the tubes in a reactor of that design would require completely dismantling the reactor, an operation which seems unrealistic on a commercial scale. For the

present design, it was decided to apply the catalyst to the inside of the tubes; with this design, it is possible to reapply catalyst without dismantling the reactor. The design also makes it possible to design a flame-spraying unit which can coat multiple tubes simultaneously. One drawback to the design is the 2-inch minimum diameter which can be flame-sprayed with currently available techniques (developed at PETC). Because present Fischer-Tropsch catalysts have little useful internal surface area, catalyst activity is mainly dependent on external surface area, and this increases the size of the reactors over what would be required if smaller diameter tubes were used.

More than with the other reactor types, the kinetic model was used in the design of the tube-wall reactor. This was necessary in order to predict the effects of changes in geometry and operating conditions, as most of the experimental work was done at different operating conditions than the design. All of the modeling work was based on properties of taconite catalyst. The reactor design is also based on taconite catalyst. As discussed in Section 4 of this report, the Parsons study used an activity based on tests with a flame-sprayed magnetite and a yield structure based on tests with a taconite catalyst. It is possible that the magnetite is more active catalytically than taconite, although the available data are inconclusive on this point. If this more active catalyst were used, the tube-wall reactor would be smaller. As the reactors alone are nearly twice as expensive as the entire entrained bed reactor system, a more active catalyst could result in significant savings. However, it has not been demonstrated that a magnetite catalyst can give the same yield structure as the potassium-promoted taconite, and this is still the primary consideration.

The tube-wall reactor design used in this comparison calls for 4 parallel trains of 13 reactors each. The reactors are 16-foot diameter by 64-foot long heat exchangers, containing bundles of 2-inch diameter tubes with taconite catalyst flame-sprayed on the inside of the tubes. The heat of reaction is removed by boiling oil. The temperature of the oil can be controlled by adjusting the pressure on the hot oil receiver. Oil is

preferred over steam because the steam temperature is relatively insensitive to pressure in the temperature range required for this application. Given the high heat transfer coefficients in the tube-wall reactor, the catalyst temperature is very close to the oil temperature and, therefore, close control of coolant temperature is essential. The hot oil goes to a steam generator where it is condensed, and 600 psig steam can be produced.

The numerous large reactors, with the associated hot oil receivers, comprise over 90% of the cost of the tube-wall reactor system illustrated in Figure 5.2-2. Four parallel feed/effluent heat exchangers add modestly to the cost of the system, and allow recovery of sensible heat from the reaction products. Cost of the steam generators is also included in the "exchangers" cost figures. As shown in Table 5.2-7, the tube-wall reactor system as presently conceived represents an investment cost more than twice that of the entrained bed reactor system. This figure could be improved considerably by the development of a more active catalyst but it is unlikely that it would ever be significantly better than the entrained bed reactor.

Catalyst replacement costs for the tube-wall reactor are the highest of the four systems studied. The estimated annual cost for catalyst replacement shown in Table 5.2-8 is based on an assumed catalyst life of 6 months. This assumption is based on an experiment in which PETC operated a bench-scale unit with flame-sprayed taconite catalyst for 6 months before it began to rapidly deactivate. Regeneration allowed an additional 2 months operation (64). Even with a 6-month catalyst life, catalyst replacement costs for the tube-wall reactor are twice those for the entrained bed reactor. This high cost is due entirely to the expensive and labor-intensive flame-spraying method of catalyst application. In addition, six month catalyst life may be overly optimistic at the high temperature and relatively low H_2/CO ratio called for in this design. The ability to achieve this operation would have to be proven before building a tube-wall reactor. This additional work may not be justified, however, for a reactor system which shows the potential for only marginal, if any, improvement over the entrained bed reactor.

5.2.3.4 Slurry Reactor

The slurry reactor conceptual design is based on information published by Koelbel and others (2, 20), on the Koppers-Rheinpreussen demonstration unit. In addition comments received in direct correspondence with Professor Koelbel were helpful in setting design parameters.

The reactor system as illustrated in Figure 5.2-3 consists of a reactor with steam generation coils located internally, a feed/effluent heat exchanger, and a small trim cooling system. The trim cooler was not a part of the demonstration unit, where temperature control was achieved by adjusting the pressure (and thus the temperature) of steam generation in the coils. As most operators would probably prefer to produce steam at constant pressure, the small oil circulation system is included for fine temperature control. For the design basis of 28 MM SCFH CO + H_2 conversion, at 400 psig, 18 of these reactor units in parallel are required. The reactors are 14 feet in diameter by 27-feet tall, the diameter being set by limits of shop fabrication and transport. Koelbel (2) mentioned a possible requirement for baffles in a large-size reactor to ensure good contacting between gas and liquid. Baffles are not included in the present design, and some additional study would be required to determine if they are truly needed. One catalyst hopper supplies fresh catalyst to all 18 reactors. A filtering system, the size of which is dependent on the type of product and operating conditions, is required to separate catalyst from the net product. The filter was not included in the cost estimate, but would not contribute significantly to the total system cost.

As shown in Table 5.2-7, the reactor accounts for three-quarters of the total cost of the slurry reactor system and is approximately equal to the entrained bed reactor cost. With the major heat-removal taking place in the reactor, very little additional heat exchange is required. The simplicity of the system then contributes to keeping the investment cost of the complete system low, equal to about half that for the entrained bed reactor system.

The catalyst consumption of the slurry reactor is very low (Table 5.2-8) representing a catalyst consumption of about 11% of the entrained bed system. However, as Koelbel used a precipitated catalyst for the slurry reactor while fused iron is used in the entrained bed and assumed for the ebullating bed reactor, a higher catalyst price ($1.80 per lb) has been used for estimating the annual catalyst cost of the slurry reactor. This results in an annual catalyst cost that is about 51% of that of the entrained bed system. This estimated annual cost shown in Table 5.2-8 is also based on a catalyst life of 38 days, based on Poutsma (10). This is the shortest of any of the systems, and under the mild operating conditions (low temperature, low CO concentration) in the slurry reactor, it would not be unreasonable to expect longer catalyst life.

The reason for the low catalyst costs in the slurry reactor is the small inventory required. The kinetic modeling work has shown the catalyst activity to be closely related to surface area and, therefore, the very small catalyst particle size results in a high activity per pound. In the slurry reactor system there is no lower limit on catalyst particle size other than that imposed by the ability to separate the solids by filtration. For this study, an average particle size of 30 microns was assumed. This results in the slurry reactor requiring roughly half as much catalyst as is contained in the entrained bed reactor. (The total entrained bed system inventory is several times that, due to the catalyst receiver inventory, as discussed in Section 5.2.3.2.)

Thus the slurry reactor is very attractive in terms of both investment and catalyst cost.

5.2.3.5 Ebullating Bed Reactor

An ebullating bed reactor conceptual design was prepared by Chem Systems, Inc. based on their experience in the design and operation of ebullating bed reactors for the production of methane and methanol. The design as received from Chem Systems is included in Appendix E. Based on this information, a design scaled-up to the common basis was prepared.

The system shown in Figure 5.2-4 includes a reactor, a product separator, a circulating oil cooling system, and a feed/effluent heat exchanger.

For the design rate of 28 MM SCFH CO + H_2 conversion at 400 psig, 20 parallel reactor trains are required. The reactors are empty shells, 14-feet diameter by 30-feet tall. The product separators are 14-feet diameter by 15-feet long, horizontal vessels. They serve the dual purpose of allowing vapor/liquid disengaging and providing overflow capacity for the liquid inventory. As shown in Table 5.2-7, the cost for 20 ebullating bed reactors plus product receivers is about the same as for two entrained bed reactors plus catalyst receivers.

A very high rate of oil circulation is required to hold the temperature rise in the reactor within reasonable limits. For this conceptual design, the maximum ΔT was set at 20°F. To achieve this, an oil circulation rate of about 20,000 gpm is required for each reactor. With this large oil circulation system, pumping costs become considerable. The pumps account for 25% of the cost of the reactor system. The circulating oil is cooled by heat exchange in a steam generator. This heat exchange adds 15% to the total system cost. It is the cost of the oil circulation system, including the pumps and the oil-versus-steam heat exchanger, that sets the cost of the ebullating bed reactor system above that of the slurry reactor system. Otherwise investment costs for the two systems are about equal.

It is in catalyst replacement costs that the slurry and ebullating bed reactors are notably different. As discussed in Section 5.2.3.4 of this report, catalyst costs for the slurry reactor are low due to the low inventory. The ebullating bed reactor, on the other hand, has a much higher catalyst replacement cost. For the ebullating bed reactor, a catalyst life of 2 months is assumed. This assumption is based on work at the U.S. Bureau of Mines (26), where over two months operation was possible with fused iron catalysts. The two month catalyst life is on the same order as that achieved in the slurry and entrained bed reactors. However, there could be mechanical difficulties due to the effect of fines in the oil circulation system. This potential problem has not been addressed in this study.

Because catalyst activity is largely dependent on surface area, the ebullating bed reactor requires much more catalyst than is contained in the slurry reactor. On a per pound basis, the 30 micron slurry catalyst has about 50 times as much surface area as the 1/16 inch ebullating bed catalyst. Catalyst replacement cost is 4 times that for the slurry reactor, and similar to that for the tube-wall reactor.

While the ebullating bed reactor is more attractive in terms of investment costs than the entrained bed reactor, there is as yet no catalyst with the structural strength to withstand the constant agitation in the ebullating bed. The slurry reactor, so similar in many ways, is less costly to build and operate and, therefore, there is little incentive to develop an ebullating bed catalyst.

5.2.4 Thermal Efficiency Comparison

For the purpose of this discussion the term "thermal efficiency" is defined as that portion of the heat of reaction which is recovered in some useful form. The heat of reaction in a Fischer-Tropsch system is equal to 20 to 25% of the heat of combustion of the CO and H_2 converted.

The conceptual designs used for the cost estimates, and shown in Figures 5.2-1 through 5.2-4, also form the basis for determination of thermal efficiencies of the units. In order to compare the units on a consistent basis, the envelope is drawn to include introduction of feed to the system at 120°F. As far as possible the enthalpy of the reactor effluent is recovered by heat exchange against the cold feed, or in the case of the entrained bed system, against quench oil and boiler feed water. The actual amount of heat that can be recovered differs according to the requirements of the individual systems. Heat recovery for each system is shown in Table 5.2-9. The ebullating bed reactor is considered to have the same thermal efficiency as the slurry reactor.

In the entrained bed reactor, 36% of the heat of reaction is recovered by steam generation in the reactor cooling coils. The reactor effluent is taken to the quench tower, where circulating oil removes

catalyst fines and also cools the vapor product from 635 to 280°F. The quench vapors are exchanged against boiler feed water, where another 164 MM Btu/hr, or 8.6% of the ΔH_R, is recovered. The temperature of the quench oil is maintained by the heat exchange of the oil against combined feed to the reactor and by boiler feed water heating. Thus 30% of the heat of reaction is recovered by heating boiler feed water. This low temperature heat is generally considered to be less valuable than high temperature steam; however, the quench system leaves no option for additional steam generation. The total heat recovery, or thermal efficiency, of the entrained bed reactor system then is 66%. The difference between the enthalpy of the quench vapor at 250°F and the combined feed at 120°F represents an enthalpy loss of 640 MM Btu/hr. This constitutes the remaining 34% of the heat of reaction.

In the tube-wall reactor, 85% of the heat of reaction is removed by boiling oil in the reactor. This heat is recovered from the oil by external steam generation. The reactor effluent is cooled by heat exchange against feed, to 220°F. The difference in enthalpy between the products at 220°F and the feed at 120°F is 300 MM Btu/hr, or 15% of the heat of reaction. The large amount of steam in the tube-wall reactor effluent causes a pinch point in the exchanger and thus sets the limit of heat exchange for this system.

Direct steam generation in the slurry reactor removes 91% of the heat of reaction, for a thermal efficiency of 91%. The reactor effluent is heat exchanged against fresh feed, and thereby cooled to 180°F. Because the slurry reactor produces primarily CO_2 and very little water, the difference in enthalpy between feed and products is considerably less than in the tube-wall system.

The ebullating bed conceptual reactor recovers the heat of reaction by allowing a 20°F temperature increase in the circulating oil. This heat is then recovered by generation of high pressure steam in the external steam generator. If feed and product similar to those of the slurry reactor are assumed, the overall thermal efficiency for the system is also similar to that of the slurry reactor.

The conceptual designs for the three-phase reactors are based on operation near the product dew point, and the thermal efficiencies shown are valid only for this case. If operating conditions are such that a significant quantity of the liquid phase is vaporized with the effluent vapor, the net thermal efficiency will be lower.

5.2.5 Upstream and Downstream Processing

While the scope of this study is restricted to a comparison of Fischer-Tropsch reactors, the synthesis section accounts for only 20 to 25% of the cost of all processing units in an indirect liquefaction plant. It is important, therefore, to consider what possible impact the choice of reactor will have on upstream and downstream processing requirements. These requirements are discussed in a qualitative fashion in this section.

The most important difference in upstream processing is caused by varying requirements for syngas H_2/CO ratio. The three-phase systems operate preferably with a H_2/CO ratio of 0.6 to 0.7. This ratio is supplied by modern gasifiers directly, without the need for a shift reactor. The gas-phase reactors on the other hand require a considerably higher H_2/CO ratio. The tube-wall reactor conceptual design is for a H_2/CO ratio of 2.0, and the entrained bed reactor requires a H_2/CO ratio of 2.4 in the fresh syngas. Use of either of these reactors thus mandates the inclusion of a shift reactor upstream of the synthesis section. Depending upon the particular reactors chosen, the cost of the shift reactor may be one-tenth or more of the cost of the Fischer-Tropsch section.

An additional cost when using an external shift reactor is for an extra Acid Gas Removal (AGR) system upstream of the Fischer-Tropsch reactors. One AGR unit is required before the shift reactor and a second one after it. This reduces the CO_2 content of the shifted syngas. For operation without a shift reactor, only one AGR system is required before the Fischer-Tropsch reactor. If we assume, as a base case, that tail gas from the Fischer-Tropsch section is to be used as pipeline gas, then CO_2 must also be removed from this stream. The CO_2 content in the effluent from

the three-phase reactors is much higher than that from the entrained bed and tube-wall reactors, as shown in Table 5.2-6. Total CO_2 production, if that from the shift reactor is included, is the same for all four Fischer-Tropsch systems. The difference between whether the CO_2-producing shift reaction takes place in the reactor or externally, determines the number of acid gas removal units, and the liquid phase systems will always have one less.

The entrained bed reactor requires a large amount of gas recycle. As discussed in Section 5.1.2, the recycle gas serves three main functions:

- Reduces CO content in combined feed
- Aids in temperature control
- Improves fluidization

The other three reactor systems are capable of operation without gas recycle. As shown in Table 5.2-2, little or no gas recycle is required to achieve 90% CO + H_2 conversion in the three alternative reactor systems. The impact of the recycle system is to increase the size of separations facilities to handle the increased quantity of reactor effluent (the volume of recycle gas in the entrained bed reactor system is 2.3 times the volume of the syngas feed). The recycle gas must be separated from the reactor effluent and scrubbed to reduce CO_2 content. A compressor is required to increase the pressure of the recycle gas stream to that at the reactor inlet.

It is apparent from this analysis that a liquid phase system shows a significant advantage over a gas phase system in not requiring an external shift reactor. The entrained bed reactor is at a further disadvantage in requiring a large amount of gas recycle.

FIGURE 5.2-1

ENTRAINED BED REACTOR SYSTEM

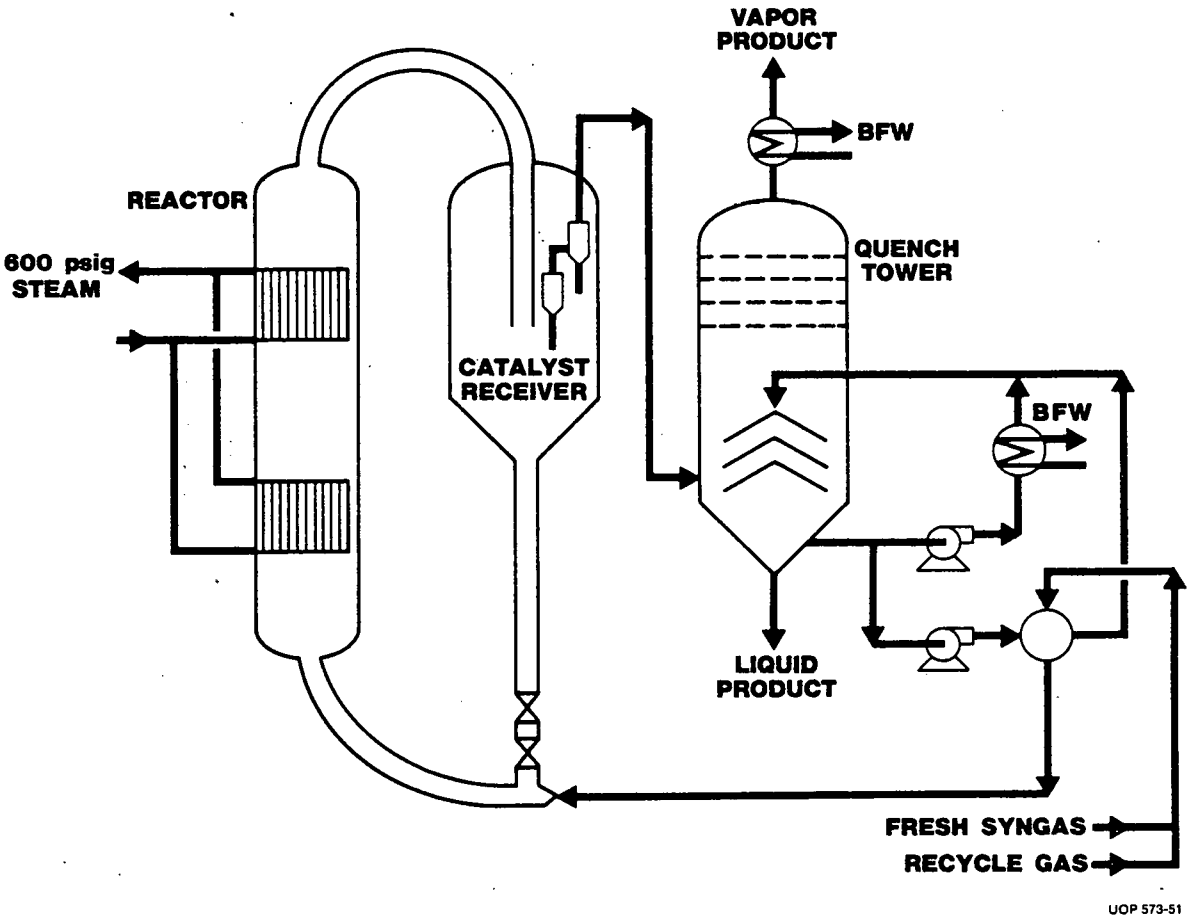

FIGURE 5.2-2
TUBEWALL REACTOR SYSTEM

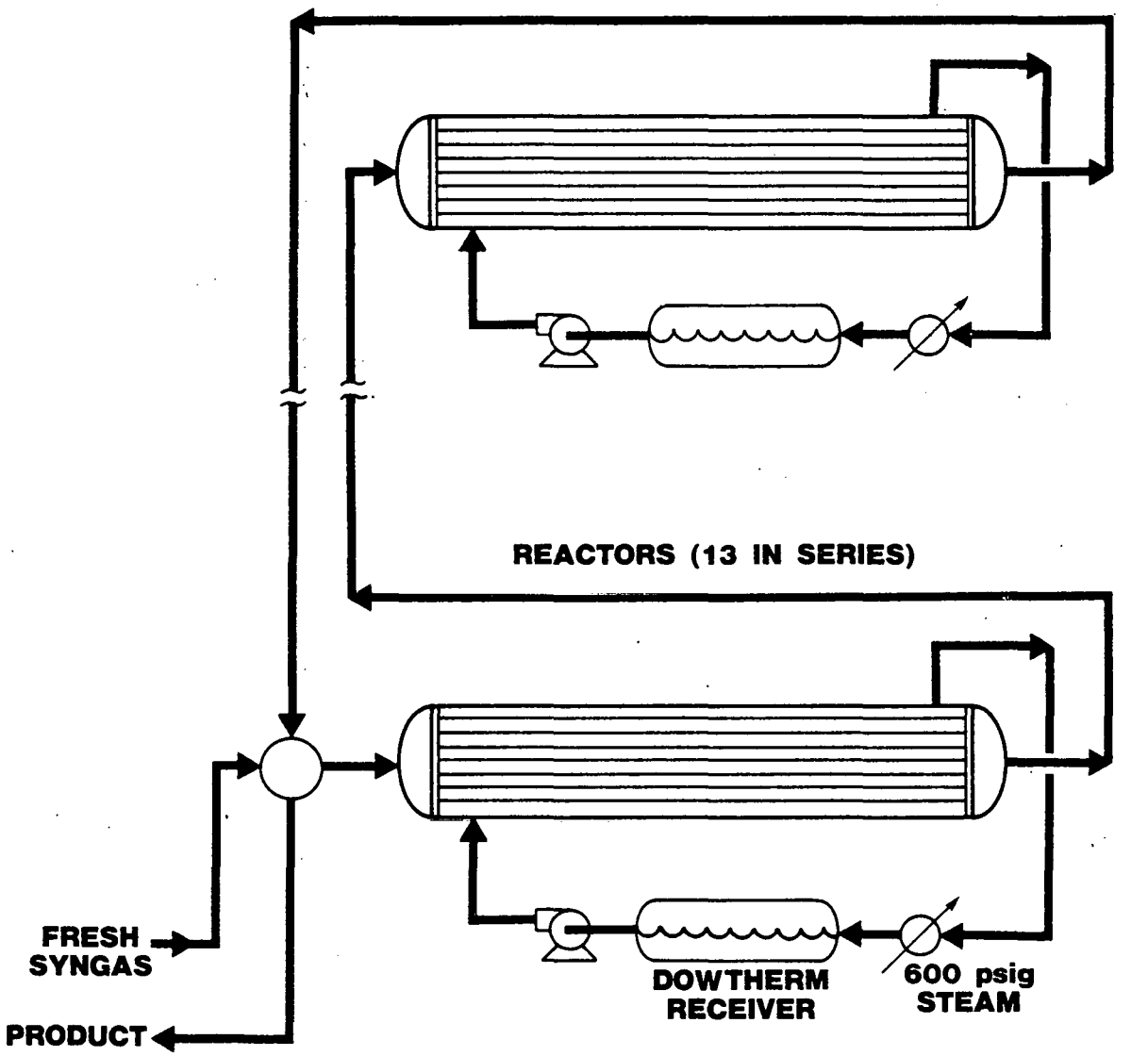

UOP 573-48

FIGURE 5.2-3

SLURRY REACTOR SYSTEM

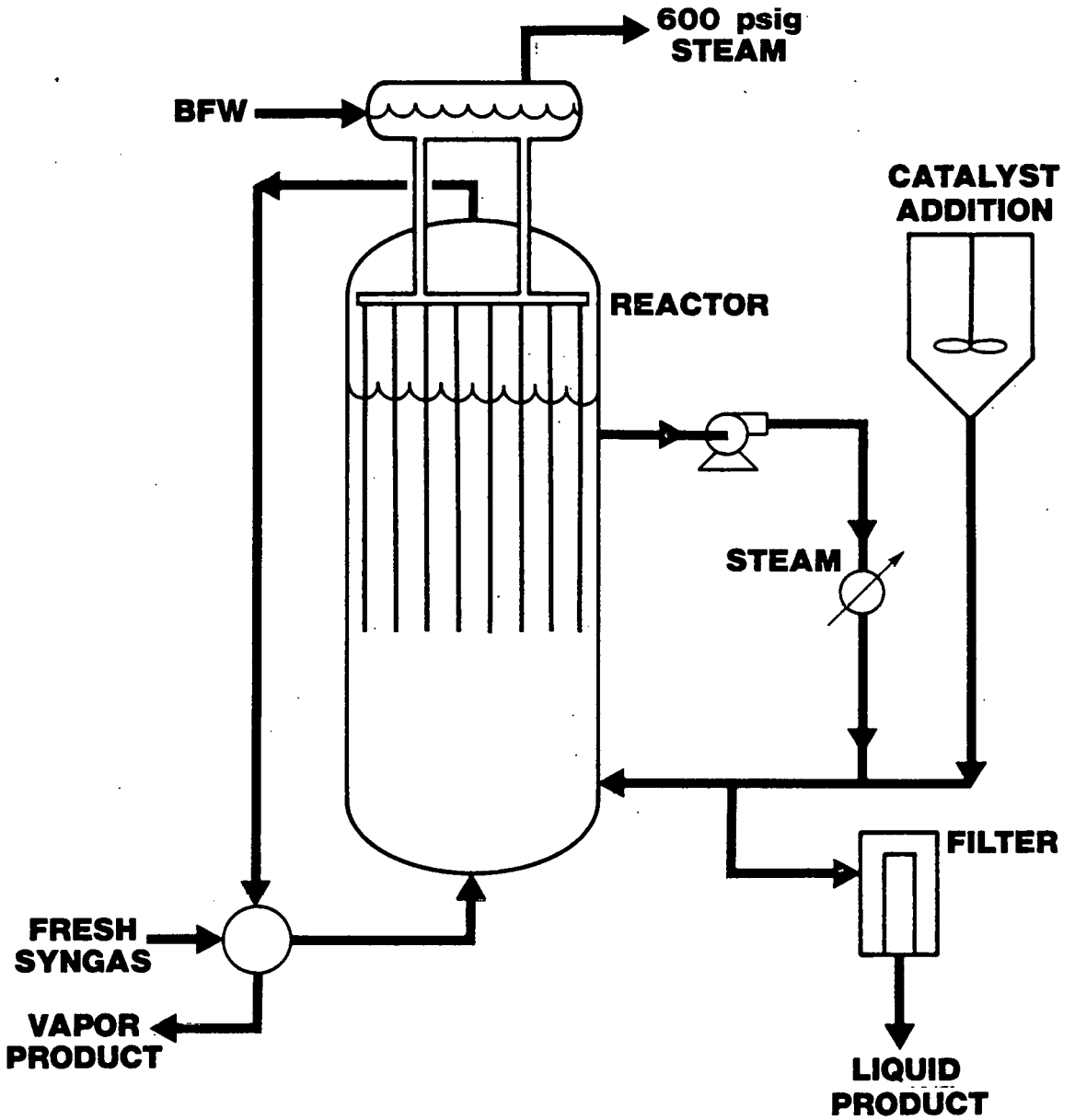

UOP 573-50

FIGURE 5.2-4

EBULLATING BED REACTOR SYSTEM

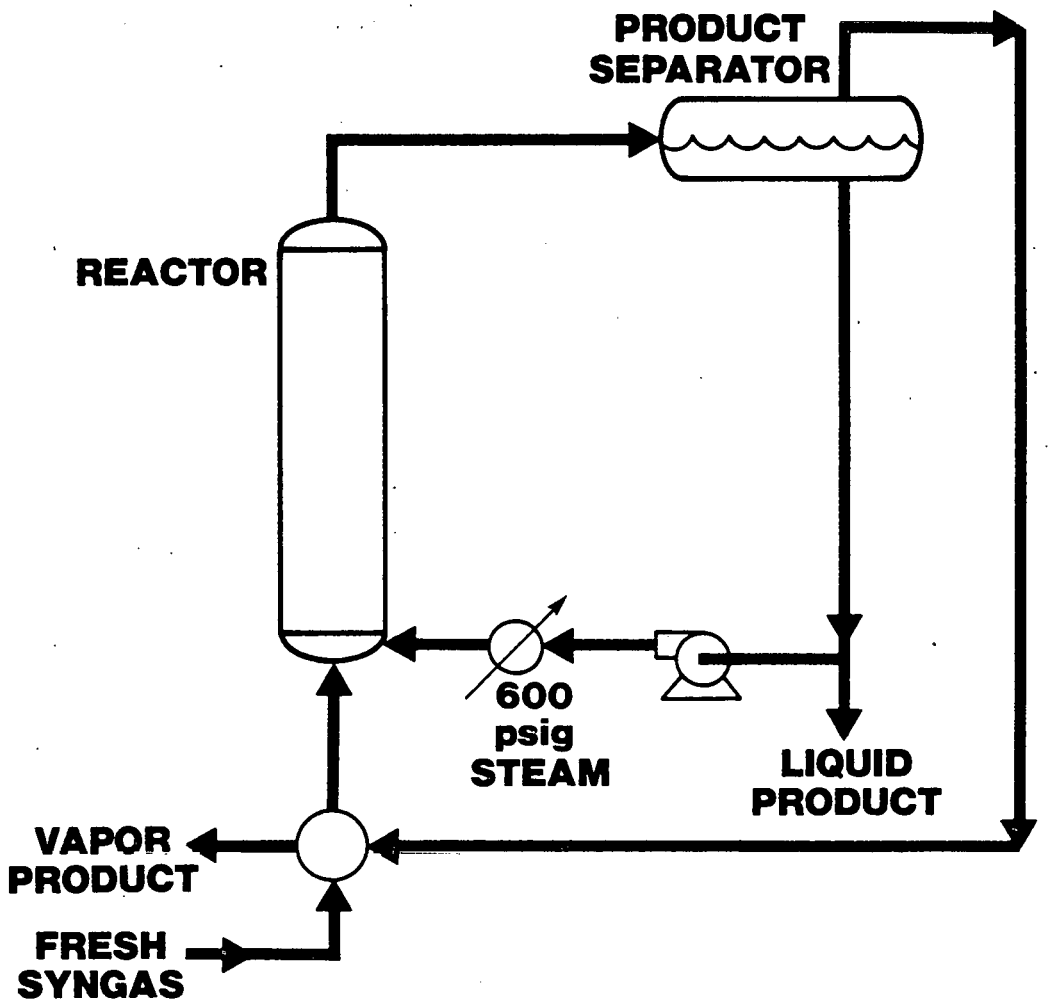

UOP 573-49

TABLE 5.2-1

Syngas Feeds for Fischer-Tropsch Reactor Systems

Component	Entrained Bed Reactor	Tube-wall Reactor	Slurry Reactor
H_2, MM SCFH	21.8	25.6	13.6
CO, MM SCFH	9.1	12.8	19.3
CO_2, MM SCFH	1.3	1.2	1.8
H_2O, MM SCFH	-	0.1	-
N_2, MM SCFH	0.3	-	1.1
H_2:CO ratio	2.4	2.0	0.7

Quantities required for conversion of 28.0 MM SCFH of CO + H_2:

once-through basis for tube-wall and slurry reactors,

recycle basis for entrained bed reactor.

TABLE 5.2-2

Fischer-Tropsch Reactor Feeds Recycle Operation

Component	Entrained Bed Reactor		Tube-Wall Reactor		Slurry Reactor	
	Syngas	Combined Feed	Syngas	Combined Feed	Syngas	Combined Feed
H_2, MM SCFH	21.8	52.1	18.7	25.6	12.4	13.6
CO, MM SCFH	9.1	11.1	12.2	12.8	18.5	19.3
CO_2, MM SCFH	1.3	15.9	1.0	1.3	1.6	1.8
H_2O, MM SCFH	-	0.2	0.1	0.1	-	-
N_2, MM SCFH	0.3	4.1	-	-	1.0	1.7
C_1 + HC's, MM SCFH	-	24.1	-	4.5	-	0.9
Total, MM SCFH	32.5	107.5	32.0	44.3	33.5	37.3
H_2:CO ratio	2.4	4.7	1.5	2.0	0.7	0.7

TABLE 5.2-3

Entrained Bed Reactor Product Yields

Kellogg Basis, lb/hr		Comparison Basis, lb/hr			
Component	Kellogg Yield	Component	Kellogg Yield	Modified Yield	Sasol Yield
H_2O	408,500	H_2O	408,500	403,800	
H_2	14,500	H_2	14,500	14,400	
N_2	24,900	N_2	24,900	24,900	
CO	13,400	CO	13,400	15,300	
CO_2	156,900	CO_2	156,900	159,400	
C_1	44,000	C_1	44,000	44,000	37,700
$C_2^=$	18,600	$C_2^=$	18,600	18,600	25,700
C_2	21,300	C_2	21,300	21,300	
$C_3^=$	35,900	$C_3^=$	35,900	35,900	44,600
C_3	10,000	C_3	10,000	10,000	
$C_4^=$	33,200	$C_4^=$	33,200	33,200	37,700
C_4	6,800	C_4	6,800	6,800	
C_5	26,200				
C_6	16,700				
C_7	14,000	Gasoline (C_5-11)	99,800	122,100	126,800
C_{8-9}	22,300				
C_{10-12}	28,200				
C_{13-18}	18,600	Diesel (C_{12-25})	32,800	22,300	37,700
$C_{19}+$	18,700	Heavy ($C_{25}+$)	12,100	300	12,000
NAC	27,900	Alcohols	27,900	27,900	20,600
Acids	4,300	Acids	4,300	4,300	
Total	964,900	Total	964,900	964,500	
Total HC's	346,700	Total HC's	346,700	346,700	342,800

TABLE 5.2-4

Tube-Wall Reactor Product Yields

Component	Parsons Yield, lb/hr	Modified Yield, lb/hr
H_2O	207,400	257,900
H_2	30,100	50,100
N_2	24,800	-
CO	123,800	63,600
CO_2	560,200	513,900
C_1	40,400	42,600
$C_2^=$	5,000	5,200
C_2	20,200	20,100
$C_3^=$	3,400	3,600
C_3	11,800	12,000
$C_4^=$	10,100	10,400
C_4	30,200	30,200
Gasoline	139,500	135,700
Diesel	54,000	52,100
Heavy	8,200	10,400
Alcohols	16,100	13,300
Acids	1,800	5,200
Total	1,287,000	1,226,300
Total HC's	340,700	340,800

TABLE 5.2-5

Slurry Reactor Product Yields

Literature Basis, lb/hr		Comparison Basis, lb/hr		
Component	Koelbel Yield	Component	Koelbel Yield	Modified Yield
		H_2O	59,800	57,200
		H_2	13,500	12,900
		N_2	79,200	79,200
		CO	171,000	171,600
		CO_2	1,117,600	1,120,200
$C_1 + C_2$	10,800	C_1	7,800	8,300
$C_2^=$	12,000	$C_2^=$	12,000	21,800
		C_2	3,000	11,700
$C_3^=$	61,200	$C_3^=$	61,200	24,500
C_3	15,300	C_3	15,300	12,900
$C_4^=$	13,000	$C_4^=$	13,000	24,500
C_4	4,300	C_4	4,300	12,700
104-356°F	181,300	Gasoline (C_{5-11})	193,900	166,600
356-428°F	13,500			
428-608°F	20,300	Diesel (C_{12-25})	25,100	53,500
> 608°F	6,300	Heavy (C_{26+})	2,300	1,400
		Alcohol	5,700	5,700
		Total	1,784,700	1,784,700
Total HC's	338,000	Total HC's	343,600	343,600

TABLE 5.2-6

Comparison of Product Yields for Fischer-Tropsch Reactors

Component	Entrained Bed, lb/hr	Tube-Wall, lb/hr	Slurry, lb/hr
H_2O	408,500	257,900	59,800
H_2	14,500	50,100	13,500
N_2	24,900	-	79,200
CO	13,400	63,600	171,000
CO_2	156,900	513,900	1,117,600
C_1	44,000	42,600	7,800
$C_2^=$	18,600	5,200	12,000
C_2	21,300	20,100	3,000
$C_3^=$	35,900	3,600	61,200
C_3	10,000	12,000	15,300
$C_4^=$	33,200	10,400	13,000
C_4	6,800	30,200	4,300
Gasoline (C_{5-11})	99,800	135,700	193,900
Diesel (C_{12-25})	32,800	52,100	25,100
Heavy ($C_{26}+$)	12,100	10,400	2,300
Alcohols	27,900	13,300	5,700
Acids	4,300	5,200	-
Total	964,900	1,226,300	1,784,700
Total HC's	346,700	340,800	343,600

TABLE 5.2-7

Investment Cost Comparison for Fischer-Tropsch Reactor Systems

Reactor Type	Entrained Bed	Tube-Wall	Slurry	Ebullating Bed
No. of Reactors	2	52	18	20
Relative Investment Costs:				
Reactor and Receiver	34	189	33	28
Other Vessels	30	-	<1	-
Heat Exchangers	32	15	10	21
Pumps	4	4	2	16
Total	100	208	45	65

TABLE 5.2-8

Catalyst Replacement Costs for Fischer-Tropsch Reactors

Reactor	Entrained Bed	Tube-Wall	Slurry	Ebullating Bed
Catalyst Inventory, tons (ft^2)	900	(4.4×10^6)	100	3000
Catalyst Usage, tons/yr (ft^2/hr)	8,400	(8.8×10^6)	950	18,000
Catalyst Cost, 10^3 $/yr	6,720	14,200	3,420	14,400

TABLE 5.2-9

HEAT RECOVERY IN F-T REACTORS

- Entrained Bed Reactor (ΔH_R = 1900 MM Btu/Hr)

	MM Btu/Hr	% of ΔH_R
Steam Generation	690	36%
BFW Heating	570	30%
$H_{Products} - H_{Feed}$	640	34%

- Tube-Wall Reactor (ΔH_R = 1960 MM Btu/Hr)

	MM Btu/Hr	% of ΔH_R
Steam Generation	1660	85%
$H_{Products} - H_{Feed}$	300	15%

- Slurry Reactor (ΔH_R = 1960 Btu/Hr)

	MM Btu/Hr	% of ΔH_R
Steam Generation	1790	91%
$H_{Products} - H_{Feed}$	170	9%

5.3 CONCLUSIONS OF THE PHYSICAL COMPARISON

5.3.1 General

Phase I of this study has undertaken a comparison of four reactor systems for the production of gasoline via the classic Fischer-Tropsch synthesis. Certain generalizations can be made as to the most desirable mode of operation.

1. The Fischer-Tropsch section is a small part of an indirect liquefaction plant and, therefore, the most important economic consideration is that of product yield. With the objective being transportation fuel, especially gasoline, this means the ideal process should maximize gasoline production and minimize the amount of methane produced. A Schulz-Flory degree of polymerization near 4 corresponds to maximum gasoline production.

2. Because the Fischer-Tropsch reaction is highly exothermic, the reactor must be designed to control the temperature by removing the heat generated. To improve thermal efficiency, the heat of reaction should be recovered in a form that is useful elsewhere in the plant.

3. Use of a low H_2/CO ratio synthesis gas as feed to the Fischer-Tropsch reactor eliminates the need for a separate shift reactor. This decreases investment cost and increases thermal efficiency for the total indirect liquefaction plant.

5.3.2 Entrained Bed Reactor

1. This is the only one of the four reactor systems studied which is operating commercially. In light of the inevitable problems encountered when commercializing a new process, this is a significant advantage.

2. In order to minimize condensation of heavy products in the reactor, the entrained bed reactor is operated at a degree of

polymerization around 3.3. Thus the gasoline production is considerably less than the theoretical maximum. In addition, the high temperature operation results in a large methane yield.

3. The entrained bed reactor consists of three adiabatic reaction sections in series, with cooling sections between. This method of heat removal does hold the temperature increase across the reactor to a reasonable limit. The amount of temperature increase is very sensitive to changes in catalyst circulation rate, reactant concentration and quantity of recycle gas. The interrelationships between all these variables limit the flexibility of the process.

4. The entrained bed reactor must use a high H_2/CO ratio feed. In addition, the CO_2 in the recycle gas prevents the shift reaction from occurring in the reactor. Therefore, all the hydrogen (above that produced in the gasifier) must be produced in an external shift reactor.

5. Fluidization characteristics as well as other operating requirements unique to the entrained bed reactor, mandate the use of a large volume of recycle gas. This decreases thermal efficiency of the process and increases operating costs.

6. The entrained bed reactor typically operates at temperatures above 600°F where free carbon formation becomes a significant problem. This is presumably a key factor in limiting useful catalyst life to two months. As a result, catalyst replacement is a significant operating expense in this system.

5.3.3 Tube-Wall Reactor

1. Operational requirements should not prevent operating the tube-wall reactor at a degree of polymerization of 4. However, all flame-sprayed catalysts tested to date have produced a large amount of light gases and very low gasoline yields. The high temperature proposed in the conceptual design will also result in additional methane production.

2. The tube-wall reactor achieves excellent temperature control and isothermal operation. In addition, 85% of the heat of reaction is recovered as high pressure steam, resulting in a good thermal efficiency.

3. A high H_2/CO ratio is required to limit free carbon formation. This necessitates the use of an external shift reactor.

4. The flame-sprayed catalyst should be applied on the inside of the catalyst support tubes in order to facilitate replacing the catalyst. This results in a much larger reactor section than envisioned in the Parsons design.

5. The investment cost for major equipment items is more than twice that of the entrained bed reactor system. The annual catalyst replacement cost is also expected to be more than twice that for the entrained bed reactor.

5.3.4 Slurry Reactor

1. The slurry reactor is able to operate at conditions which produce a gasoline yield equal to, or possibly even greater than, the maximum predicted by a Schulz-Flory product distribution. Methane yield is minimized by the low temperature operation.

2. The slurry reactor design allows very good temperature control and high thermal efficiency. In addition, the presence of the liquid phase provides a margin of safety in case of operational difficulties.

3. A syngas feed with a H_2/CO ratio typical of that produced in a modern gasifier presents no problem in slurry reactor operation. The water-gas shift reaction produces the necessary H_2 within the reactor.

4. Once-through conversion of over 95% should be possible with the proper choice of operating conditions. This potentially can lead to a much-simplified process.

5. Maintenance of oil quality is essential to the successful operation of a slurry reactor. Further study is required to determine the best liquid for this use, and the conditions which will allow continuous operation.

6. It should be possible to select a catalyst that will make operation at 400 psia feasible, however, further study is required to prove that this is the case. Operation at 174 psia, as in the German demonstration unit, would adversely affect the investment cost.

7. Major equipment items for a slurry reactor system cost only half as much as those for an entrained bed reactor system of equal capacity. Catalyst replacement cost is expected to be only 51% of that for an entrained bed reactor, and other operating costs are also much lower.

5.3.5 Ebullating Bed Reactor

1. It was not possible to determine whether the ebullating bed reactor has a yield advantage over the slurry reactor. It is believed that the two liquid-phase reactors will give very similar product yield structures.

2. The liquid circulation system provides very good temperature control, though at considerable cost. Thermal efficiency is also high.

3. An external shift reactor is not required, as low H_2/CO ratio syngas can be used as feed to the reactor.

4. Once-through conversion of over 95% should be possible.

5. Maintenance of oil quality is critical to the success of this operation.

6. As with the slurry reactor, the choice of operating pressure will affect the overall economics of the system. Further study is required to determine whether continuous operation is possible at 400 psia.

7. It appears that major equipment items will cost more than for the slurry reactor, but still only a fraction of that for the entrained bed reactor. Catalyst costs are extremely high because a large quantity is required.

8. Developing a catalyst with the physical strength to withstand the constant agitation in an ebullating bed reactor appears to be difficult, if not impossible. The only catalysts that held together for a reasonable length of time had very low catalytic activity.

SECTION 6 - NOMENCLATURE

1) a = interfacial area of gas bubble (ft^2 bubble surface area/ft^3 expanded liquid)

2) A = cross sectional area of reactor (ft^2)

3) c = flame-sprayed catalyst thickness (ft)

4) $[\ ]$ = concentrations ($moles/ft^3$)

5) $[CAT]$ = catalyst concentration (lb cat/ft^3)

6) C_L = liquid molar concentration ($moles/ft^3$ liquid)

7) C_{Pi} = heat capacity of specie i (Btu/mole °F)

8) C_{Po} = heat capacity of coolant (Btu/mole °F)

9) C_{Ps} = heat capacity of solids (Btu/lb°F)

10) D = tube diameter (ft)

11) ΔE = activation energy

12) h_o = coolant film resistance [Btu/(hr)(ft^2)(°F)]

13) h_s = reactant side film resistance [Btu/(hr)(ft^2)(°F)]

14) H_{Rj} = heat of reaction j (Btu/mole)

15) k_G = gas phase reaction rate constant (ft/sec)

16) k_H = hydrogenation rate constant [$(ft^3_{Rx})^2$/lb cat-hr-mole]

17) k_L = liquid phase reaction rate constant (ft/sec)

18) $k_{L,i}$ = liquid film mass transfer coefficient for specie i (ft^3 liquid/ft^2 gas-bubble surface area - sec)

19) k_o = forward rate constant for olefin equilibrium [(ft^3_{Rx})/lb cat-hr]

20) k^o = frequency factor

21) k_P = polymerization rate constant [$(ft^3_{Rx})^2$/lb cat-hr-mole]

22) k_T = rate constant at temperature, T_a

23) k_{WG} = water-gas shift forward rate constant [$(ft^3_{Rx})^2$/lb cat-hr-mole]

24) k_c = catalyst thermal conductivity [Btu/(hr)(ft^2)(°F)(ft)]

25) K_e = olefin equilibrium constant

26) K_i = vapor-liquid equilibrium constant for specie i.

27) K_t = thermal conductivity of tube wall [Btu/(hr)(ft^2)(°F)(ft)]

28) $M(CH_2)_nH$ = active catalyst species with alkyl chain length n attached

29) M_i = molar flow rate of specie i (moles/hr)

30) M_o = molar flow rate of coolant (moles/hr)

31) N_c = number of components

32) NR = number of reactions

33) N_T = number of tubes

34) p = fraction of all monomers that have polymerized.

35) Q_L = heat removed (Btu/hr)

36) r = rate of formation (moles/hr-ft^3_{Rx})

37) r_j = rate of reaction j (moles/hr-ft^3)

38) R = gas constant

39) S_{ij} = stoichiometric matrix

40) t = tube-wall thickness (ft)

41) T = temperature (°F)

42) T_a = absolute temperature

43) T_W = temperature at the tube wall (°F)

44) U = overall heat transfer coefficient (Btu/hr-°F-ft^2)

45) V_G = gas molar flow (moles/sec)

46) W_S = weight flow rate of solids (lbs/hr)

47) X = unit length of reactor (ft)

48) X_n = mole fraction of carbon number species n.

49) $X_{b,i}$ = mole fraction of specie i in bulk liquid

50) Y_i = mole fraction of specie i in gas phase

SECTION 7 - BIBLIOGRAPHY

(1) Haynes, W. P., Baird, M. J., Schehl, R. R., and Zarowchak, M. F., "Fischer-Tropsch Studies in a Bench-Scale Tube-Wall Reactor Using Magnetite, Raney Iron, and Taconite Catalyst," ACS Meeting, Anaheim, March 12-17, 1978.

(2) Koelbel, H., and Ralek, M., "The Fischer-Tropsch Synthesis in the Liquid Phase," Catalyst Reviews -- Science and Engineering, 21 (2), 225-274 (1980).

(3) Blum, D. B., Sherwin, M. B., and Frank, M. E., "Liquid-Phase Methanation of High Concentration CO Synthesis Gas," ACS Adv. in Chem. Series 14C, 1974.

(4) Pullman Kellogg, "Synthol Feasibility Study for Standard Oil Company (Indiana) -- Base Case," J-5109, Revised Version, October, 1977.

(5) Rousseau, P. E., "The Conversion of South African Low Grade Coal to Oil and Chemicals," Transactions of the Commonwealth Mining and Metallurgical Congress, Vol. I, 1961, p. 375-393.

(6) Dry, M. E., "Predict Carbonation Rate of Iron Catalyst," Hydrocarbon Processing, 59, 2, 92-94 (1980).

(7) Koelbel, H., Ackerman, P., and Englehardt, F., "New Developments in Hydrocarbon Synthesis," Proceedings Fourth World Petroleum Congress -- Section IV/C, 1955.

(8) Farley, R., and Ray, D. J., "The Design and Operation of a Pilot-Scale Plant for Hydrocarbon Synthesis in the Slurry Phase," J. Inst. Petrol., 50, 482, p. 27-46, February, 1964.

(9) Hoogendoorn, J. C., and Salomon, J. M., "Sasol: World's Largest Oil from Coal Plant," Brit. Chem. Eng., June, 1957.

(10) Poutsma, M. L., "Assessment of Advanced Process Concepts for Liquefaction of Low H_2:CO Ratio Synthesis Gas Based on the Koelbel Slurry Reactor and the Mobil-Gasoline Process," Contract No. W-7405-eng-26, Oak Ridge National Laboratory, Feb., 1980.

(11) Deckwer, W. D., "F-T Process Alternatives Hold Promise," Oil & Gas Journal, 78, 45, p. 198-213 (1980).

(12) Hoogendoorn, J. C., "Experience with Fischer-Tropsch Synthesis at Sasol," Clean Fuels from Coal Symposium, Chicago, p. 353-365 (Sept., 1973).

(13) Hoogendoorn, J. C., "New Applications of the Fischer-Tropsch Process," Clean Fuels from Coal Symposium II, p. 343-358 (June, 1975).

(14) Garrett, L. W., Jr., "Gasoline from Coal via the Synthol Process," Chem. Eng. Prog., 56, 4, p. 39-43 (1960).

(15) Dry, M. E., "Advances in Fischer-Tropsch Chemistry," Ind. Eng. Chem., 15, 4, p. 282-285 (1976).

(16) Pennline, H., Schehl, R. R., and Haynes W. P., "Operation of a Tube-Wall Methanation Reactor," Joint ACS/Chem. Inst. Canada Mtg., Montreal (May, 1977).

(17) The Ralph M. Parsons Co., "Fischer-Tropsch Complex Conceptual Design/Economic Analysis," R&D Report No. 114, Interim Report No. 3, January, 1977, ERDA Contract No. E(48-18) (1975).

(18) Wei, V. T., and Chen, J., "Tube-Wall Methanator Scale-up for Bureau of Mines Synthane Coal Gasification Process," (Joint AIChE/CSChE Meeting, Vancouver, (Sept., 1973).

(19) Crowell, J. H., Benson, H. E., Field, J. H., and Storch, H. H., Ind. Eng. Chem., 42, 11 (1950).

(20) Koelbel, H., and Ackerman, P., "Hydrogenation of Carbon Monoxide in Liquid Phase," Proc. Third World Petroleum Congr., The Hague, Sect. IV, 1 (1951).

(21) Hall, C. C., Gall, D., and Smith, S. L., "Comparison of the Fixed-Bed, Liquid Phase ("Slurry") and Fluidized-Bed Techniques in the Fischer-Tropsch Synthesis," J. Inst. Petroleum, 38, p. 845 (1951).

(22) U.S. Bureau of Mines, Reports of Investigation 4470, 34 (1951); 4865, 50 (1952); 4942, 45 (1953); 5013, 3 (1954); 5118 (1955); 5236 (1956).

(23) Schlesinger, M., Crowel, M., Leva, M., and Storch, H., "Fischer-Tropsch Synthesis in Slurry Phase," Ind. Eng. Chem., 43, p. 1474 (1951).

(24) Schlesinger, M., Benson, H. E., et al. "Chemicals from the Fischer-Tropsch Synthesis," Ind. Eng. Chem., 46, p. 1322 (1954).

(25) Sakai, T., and Kunugi, T., "Characteristic Features of Oil-Slurry Process in the Fischer-Tropsch Synthesis," Sekiyu Gakkai Shi, 17 (10) 863 (1974).

(26) Benson, H. E., et al., "Development of the Fischer-Tropsch Oil Recycle Process," U.S. Bureau of Mines Bulletin 568 (1957).

(27) Kastens, M. L., Hirst, L. L., and Dressler, R. G., "An American Fischer-Tropsch Plant," Ind. Eng. Chem., 44, p. 450-466 (March, 1952).

(28) Bienstock, D., Forney, A. J., and Field, J. H., "Fischer-Tropsch Oil-Circulation Process: Experiments with a Massive-Iron Catalyst," U.S. Bureau of Mines, ROI, 6194 (1963).

(29) Blum, D. B., and Toman, J. J., "Three-Phase Fluidization in a Liquid Phase Methanator," AIChE Symposium Series, 73, 161, p. 115-120 (1977).

(30) Anderson, R. B., Schultz, J. F., Hofer, L. J. E., and Storch, H. H., "Physical Chemistry of the Fischer-Tropsch Synthesis," Bulletin 580, U.S. Bureau of Mines (1959).

(31) Vannice, M. A., "The Catalytic Synthesis of Hydrocarbons from Carbon Monoxide and Hydrogen", Sci. Eng., 14 (2), 153-191 (1976).

(32) Catalytica Associates, Inc., "Catalysis of CO-H_2 Reactions -- A Critical Analysis," Multiclient Study No. 1043, January, 1978.

(33) Oak Ridge National Laboratory Report, "Fischer-Tropsch Synthesis," March, 1979.

(34) Ponec, V., "Some Aspects of the Mechanism of Methanation and Fischer-Tropsch Synthesis," Catal. Rev. - Sci. Eng., 18 (1), 151-171 (1978).

(35) Flory, P. J., "Principles of Polymer Chemistry", Cornell University Press, Ithaca, N.Y., 1967.

(36) Caesar, P. D., Brennan, J. A., Gardwood, W. E., and Ciric, J., "Advances in Fischer-Tropsch Chemistry," Journal of Catalysis, 56, 274 (1979).

(37) Pichler, H., and Schulz, H., "Neure Erkemtnisse auf dem Gebiet der Synthese von Kohlenwasserstoffen aus CO and H_2," Chemie Ing. Techn., No. 18, 1162-1174 (1970).

(38) Schulz, Hans, Rao, B. Ramananda, and Estner, Manfred, "CI4 Stuides for the Evaluation of the Reaction Mechanism of the Fischer-Tropsch Synthesis," 23, Jahrgang, No. 10, p. 651-655 (1970).

(39) Schulz, H., and Zien El Deen, A., "New Concepts and Results Concerning the Mechanism of Carbon Monoxide Hydrogenation. II. Evolution of Reaction Steps on the Basis of Detailed Product Composition and Other Data," Fuel Processing Technology, 1, 45-56 (1977).

(40) Dwyer, D. J., and Somorjai, G. A., "The Role of Readsorption in Determining the Product Distribution during CO Hydrogenation over Fe Single Crystals," Journal of Catalysis, 56, 249-257 (1979).

(41) Henrici-Olive, G., and Olive, S., "The Fischer-Tropsch Synthesis: Molecular Weight Distribution of Primary Products and Reaction Mechanism," Angew. Chem., Int. Ed., (English, 15, 3 (1976).

(42) Smith, J. M., and Van Ness, H. C., Introduction to Chemical Engineering Thermodynamics, Second Edition, McGraw-Hill, (1959).

(43) Degnan, T. F., and Wei, J., "The Co-Current Reactor Heat Exchanger: Part I, Theory," AIChE Journal, 25, 2, p. 338-344 (1979).

(44) McAdams, W. H., Heat Transmission, Third Ed., McGraw-Hill, (1954).

(45) Franks, R. G. E., Modeling and Simulation in Chemical Engineering, Wiley-Interscience, N.Y., (1972).

(46) Satterfield, Charles N., and Huff, George A., "Effects of Mass Transfer on Fischer-Tropsch Synthesis in Slurry Reactors," Chem. Eng. Science, 35, p. 195-202 (1980).

(47) Zaidi, A., Louisi, Y., Ralek, M., and Deckwer, W. D., "Mass Transfer in the Liquid Phase Fischer-Tropsch Synthesis," Ger. Chem. Eng., 2, 94-102 (1979).

(48) Koelbel, H., and Langemann, H., "Steady and Unsteady State Concentration Distributions in Reactors with Different Properties from Stage to Stage," Verfahrenstechnik, 1, p. 5-18 (1967).

(49) Calderbank, P. H., and Moo-Young, M. B., "The Continuous Phase Heat and Mass Transfer Properties of Dispersions," Chem. Eng. Sci., 16, 39 (1961).

(50) Wilke, C. R., and Chang, P., "Correlation of Dissolution Coefficients in Dilute Solutions," AIChE Journal, 1, p. 264-270 (1955).

(51) Weitkamp, A. W., Seelig, H. S., Bowman, N. J., and Cady, W. L., "Products of the Hydrogenation of Carbon Monoxide over an Iron Catalyst," Industrial and Engineering Chemistry, 45, 2 (1953).

(52) Satterfield, C. N., and Way, P. F., "The Role of the Liquid Phase in the Performance of a Trickle Bed Reactor," AIChE Journal, 18, 2 (March, 1972).

(53) Field, J. H., Bienstock, D., Forney, A. J., and Demski, R.J., "Further Studies of the Fischer-Tropsch Synthesis Using Gas Recycle Cooling (Hot-Gas-Recycle Process)," U.S. Dept. of the Interior, Bureau of Mines, 1961.

(54) Forney, A. J., Bienstock, D., Demski, R. J., "Use of a Large Diameter Reactor in Synthesizing Pipeline Gas and Gasoline by the Hot-Gas-Recycle Process," U.S. Dept. of the Interior, Bureau of Mines, 1962.

(55) Storch, H. H., Golumbic, N., and Anderson, R. B., "The Fischer-Tropsch and Related Syntheses," John Wiley and Sons, Inc., New York, N.Y., 1951.

(56) Yerushami, J., and Chankurt, J. T., "Further Studies of the Regimes of Fluidization," Powder Technology, 13, 187-205 (1979).

(57) Deckwer, W. D., Louisi, H., Zaidi, A. K., and Ralek, M., "Gas Holdup and Physical Transport Properties for the Fischer-Tropsch Synthesis in Slurry Reactor," AIChE, 72nd Annual Meeting, San Francisco, November 25-29, 1979.

(58) Bienstock, D., Field, J. H., Forney, A. J., Myers, J. G., and Benson, H. E., "The Fischer-Tropsch Synthesis in the Oil-Circulation Process: Experiments with a Nitrided Fused-Iron Catalyst," U.S. Bureau of Mines, ROI 5603 (1960).

(59) Weisz, P. B., and Swegler, E. W., "Principles of Polystep Catalytic Conversion and the Transformation of Hydrocarbons," J. Phys. Chem., 59, p. 823-826 (1955).

(60) U.K. Patent Application GB 2 009 778 A, Shell Internationale (Nov. 29, 1978).

(61) Forney, A. J., Haynes, W. P., Elliott, J. J., and Zarochak, M. F., "The Fischer-Tropsch Process: Gasoline from Coal," Second Seminar on the Desulfurization of Fuels and Combustion Gases, Chicago (1975).

(62) Fair, J. R., "Designing Gas-Sparged Reactors," Chemical Engineering (NY), 74, 14, p. 67-74 (1967).

(63) Hoogendoorn, J. C., "Gas from Coal for Synthesis of Hydrocarbons," Ninth Synthetic Gas Symposium (Nov., 1977).

(64) Haynes, W. P., Schehl, R. R., Baird, M. J., Zarochak, M. F., Cinquegrane, G. J., and Strakey, J. P., "Synthesis of Liquids and Pipeline Gas by Fischer-Tropsch," Dept. of Energy/PETC Quarterly Report, July-Sept., 1978.

APPENDIX A

DERIVATION OF REACTION MECHANISM

APPENDIX A

DERIVATION OF PRODUCT RATE EQUATIONS

The derivation of product rate expressions proceeds as follows. The rate of formation of the active species, $M(CH_2)H$, can be described by the following equation:

$$r_{M(CH_2)H} = k_p[MH][CO][H_2] - k_p[M(CH_2)H][CO][H_2] - k_H[M(CH_2)H][H_2] \quad (1)$$

$M(CH_2)H$ can be defined in terms of MH with the assumption of steady state:

$$[M(CH_2)H] = \frac{k_p[CO][H_2]}{k_p[CO][H_2] + k_H[H_2]} \cdot [MH] \quad (2)$$

In order to simplify the equations, let $D = k_p[CO][H_2]$, $E = k_H[H_2]$ and $C = D/(D + E)$. This equation then simplifies to:

$$[M(CH_2)H] = C\,[MH] \quad (3)$$

In a similar manner, the rate of formation of $M(CH_2)_nH$ is described as:

$$rM(CH_2)_nH = 0 = D\,[M(CH_2)_{n-1}H] - D\,[M(CH_2)_nH] - E\,[M(CH_2)_nH]$$

$$- k_o\,[M(CH_2)_nH] + \frac{k_o}{K_e}\,[C_nH_{2n}][MH] \quad (4)$$

If one now collects terms and sets $A = D/(k_o + D + E)$ and $B = k_o/K_e(k_o + D + E)$, and solves for $[M(CH_2)_nH]$, the following equation results:

$$[M(CH_2)_nH] = A\,[M(CH_2)_{n-1}H] + B\,[C_nH_{2n}][MH] \quad (5)$$

Using the method of successive substitution, Equations 3 and 5 lead to:

$$[M(CH_2)_nH] = A^{n-1} C + B \sum_{i=2}^{n} A^{n-i} [C_iH_{2i}] \quad [MH] \tag{6}$$

Substituting Equations 6 and 3 into Equation 1 and rearranging gives:

$$[MH] = \frac{[CAT]}{1 + C + \sum_{j=2}^{n} \left(A^{j-1} C + B \sum_{i=2}^{j} A^{j-i} [C_iH_{2i}] \right)} \tag{7}$$

Rate expressions for the products can be written as follows:

Methane

$$r_{CH_4} = k_H[M(CH_2)H][H_2] \tag{8}$$

Paraffins $n \geq 2$

$$r_{C_nH_{2n+2}} = k_H[M(CH_2)_nH][H_2] \tag{9}$$

Olefins $n \geq 2$

$$r_{C_nH_{2n}} = k_o[M(CH_2)_nH] - \frac{k_o}{K_e} [C_nH_{2n}][MH] \tag{10}$$

Substitution for $[M(CH_2)_nH]$ in these expressions leads to the final product rate expressions:

Methane

$$r_{CH_4} = C\ k_H[H_2][MH] \tag{11}$$

Paraffins $n \geq 2$

$$r_{C_nH_{2n+2}} = \left(A^{n-1} C + B \sum_{i=2}^{n} A^{n-i}[C_iH_{2i}]\right) k_H[H_2] \; [MH] \qquad (12)$$

Olefins $n \geq 2$

$$r_{C_nH_{2n}} = \left[k_o \left(A^{n-1} C + B \sum_{i=2}^{n} A^{n-i} [C_iH_{2i}]\right) - \frac{k_o}{K_e} [C_nH_{2n}]\right] [MH] \qquad (13)$$

APPENDIX B

REACTOR MODELING INPUT CHECKLIST

APPENDIX B

INPUT PARAMETERS

Parameter	Tube-Wall	Entrained Bed	Slurry
I. Indicators			
A. Number of Components	X	X	X
B. Number of Stages in Gas Phase	X	X	X
C. Number of Stages in Liquid Phase			X
D. Number of Reactions	X	X	X
E. Number of Olefin Forming Reactions	X	X	X
F. Number of Paraffin Forming Reactions	X	X	X
G. Number of Reactors	X	X	X
H. Temperature Mode Indicator	X	X	
I. Kinetic Mechanism Selector	X	X	
J. Predict or Convergence Indicator	X	X	X
K. Type of Tubular Reactor	X		
L. Carbon Number Indicators for Degree of Polymerization Calculation	X	X	X
M. Carbon Number Indicator for Olefin-to-Paraffin Ratio Calculation	X	X	X
II. Reactor Information			
A. Number of Tubes	X	X	
B. Tube Diameter			
1) Inside	X		
2) Outside	X		
C. Tube Thickness	X		
D. Shell Diameter	X		
E. Reactor Diameter		X	X
F. Reactor Length	X	X	X
III. Operating Parameter			
A. Space Velocity	X		
B. J Factor	X		
C. Inlet Temperature	X	X	X
D. Inlet Pressure	X	X	X
E. Voidage	X		X
F. Mass Transfer Interfacial Area			X
G. Fresh Feed Rate and Composition	X	X	X
H. Recycle Rate and Composition	X	X	

APPENDIX B (Continued)

INPUT PARAMETERS

Parameter	Tube-Wall	Entrained Bed	Slurry
IV. Catalyst Information			
A. Thickness of Flame-Sprayed Catalyst	X		
B. Catalyst Skeletal Density	X		
C. Catalyst Porosity	X		
D. Ft^2 Catalyst/Ft^3 Reaction Space	X		
E. Slurry Catalyst Loading			X
F. Solids Circulation Rate		X	
V. Fitting Information			
A. CO Conversion	X	X	X
B. Degree of Polymerization	X	X	X
C. Olefin-to-Paraffin Ratio	X	X	X
D. CO_2 Molar Flow Rate	X	X	X
E. Number of Parameters Requiring Fitting			
1) Gas Phase	X	X	X
2) Liquid Phase			X
3) Predict Mode			X
VI. Heat Exchanger Information			
A. Coolant Temperature	X	X	
B. Coolant Designation		X	
C. Coolant Flow Rate		X	
D. Coolant Heat Capacity		X	
E. Exchanger Heights		X	

APPENDIX C

THERMODYNAMIC CONSTANTS

APPENDIX C

I. Heat of Reaction Calculations

A. Heats of Formation

Component	ΔH_F (Btu/Mole)
H_2O	-105193.16
H_2	0.0
CO	-47379.94
CO_2	-169414.66
C_1 Paraffin	-35542.60
C_2 Paraffin	-41526.08
C_3 Paraffin	-51122.31
C_4 Paraffin	-61967.80
C_5 Paraffin	-72024.86
C_6 Paraffin	-82267.32
C_n Paraffin n = 7 to 30	-82267.32 + (n-6)(-5.658)(3.9685)(453.5924)
C_2 Olefin	+19322.07
C_3 Olefin	+3929.58
C_4 Olefin	-6210.28
C_5 Olefin	-16402.34
C_6 Olefin	-26659.21
C_n Olefin n = 7 to 30	-26659.21 + (n-5)(-5.658)(3.9685)(453.5924)

B. Reactions

Paraffins: $(2n + 1)\ H_2 + nCO = C_nH_{2n+2} + nH_2$

Olefins : $2nH_2 + nCO = C_nH_{2n} + nH_2O$

Water Gas: $CO + H_2O = CO_2 + H_2$

C. Heats of Reaction

Paraffins: $HRxN_n = n\ \Delta Hf_{H_2O} + \Delta Hf_n - n\ \Delta Hf_{CO}$

$n = 1, 30$

Olefins : $HRxN_n = n\ \Delta Hf_{H_2O} + \Delta Hf_n - n\ \Delta Hf_{CO}$

$n = 2, 30$

Water Gas: $HRxN_{WG} = \Delta Hf_{CO_2} - \Delta Hf_{H_2O} - \Delta Hf_{CO}$

II. Heat Capacities

A. Equation

$$Cp_I = A + B\ \frac{T}{1.8} + C\left(\frac{T}{1.8}\right)^2 \quad \text{(Btu/mole °F)}$$

where:

$T = °R$

B. Values for A, B and C

Component	A	B	C
H_2O	7.256	2.298×10^{-3}	-0.283×10^{-6}
H_2	6.947	-0.200×10^{-3}	$+0.481 \times 10^{-6}$
CO	6.420	1.665×10^{-3}	-0.196×10^{-6}
CO_2	6.214	10.396×10^{-3}	-3.545×10^{-6}
C_1 Paraffin	3.381	18.044×10^{-3}	-4.300×10^{-6}
C_2 Paraffin	2.247	38.201×10^{-3}	-11.049×10^{-6}
C_3 Paraffin	2.410	57.195×10^{-3}	-17.533×10^{-6}
C_4 Paraffin	3.844	73.350×10^{-3}	-22.655×10^{-6}
C_5 Paraffin	4.895	90.113×10^{-3}	-28.039×10^{-6}
C_6 Paraffin	6.011	106.746×10^{-3}	-33.363×10^{-6}
C_7 Paraffin	7.094	123.447×10^{-3}	-38.719×10^{-6}
C_8 Paraffin	8.163	140.217×10^{-3}	-44.127×10^{-6}
C_n Paraffin	8.163 + (n-8)(1.097)	140.217×10^{-3} + (n-8)(16.667×10^{-3})	-44.127×10^{-6} + (n-8)(-5.338×10^{-6})
C_2 Olefin	2.830	28.601×10^{-3}	-8.726×10^{-6}
C_3 Olefin	3.253	45.116×10^{-3}	-13.740×10^{-6}
C_4 Olefin	3.909	62.848×10^{-3}	-19.617×10^{-6}
C_5 Olefin	5.347	78.990×10^{-3}	-24.733×10^{-6}
C_6 Olefin	6.399	95.752×10^{-3}	-30.116×10^{-6}
C_7 Olefin	7.488	112.440×10^{-3}	-35.462×10^{-6}
C_8 Olefin	8.592	129.076×10^{-3}	-40.775×10^{-6}
C_n Olefin	8.592 + (n-8)(1.097)	129.076×10^{-3} + (n-8)(16.667×10^{-3})	-40.775×10^{-6} + (n-8)(-53.380×10^{-6})

APPENDIX D

DERIVATION OF SLURRY MASS TRANSFER/MASS BALANCE

APPENDIX D

DERIVATIONS OF SLURRY MASS TRANSFER MASS BALANCE EQUATIONS

The basic mass balance equation is:

$$-\frac{1}{A}\frac{d(V_G Y_i)}{dZ} = k_{L_i}\, a\, C_L \left(\frac{Y_i}{K_i} - X_{b_i}\right) \qquad (1)$$

where:

A = reactor cross sectional area (ft^2)
V_G = molar flow rate (moles/hr)
Y_i = gas mole fraction of component i
Z = reactor length (ft)
k_{L_i} = mass transfer rate constant for component i (ft^3 liq/ft^2-hr)
a = interfacial area (ft^2/ft^3 reactor)
C_L = liquid molar concentration (moles/ft^3 liq)
K_i = vapor-liquid equilibrium constant
X_{b_i} = bulk liquid mole fraction of component i

This equation can then be written as:

$$V_G \frac{dY_i}{dZ} + Y_i \frac{dV_G}{dZ} = -k_{L_i}\, a\, C_L\, A\left(\frac{Y_i}{K_i} - X_{b_i}\right) \qquad (2)$$

The sum of all components from i = 1 to n result in:

$$\sum_{i=1}^{n}\left[V_G \frac{dY_i}{dZ}\right] + \sum_{i=1}^{n}\left[Y_i \frac{dV_G}{dZ}\right] = \sum_{i=1}^{n} - k_{L_i}\, a\, C_L\, A\left(\frac{Y_i}{K_i} - X_{b_i}\right) \qquad (3)$$

Since:

$$\sum_{i=1}^{n} \frac{dY_i}{dZ} = 0 \text{ and } \sum_{i=1}^{n} Y_i = 1$$

Equation 3 simplifies to:

$$\frac{dV_G}{dZ} = - A\ C_L \sum_{i=1}^{n} k_{L_i}\ a \left(\frac{Y_i}{K_i} - X_{b_i} \right) \tag{4}$$

Substitution of Equation 4 into Equation 2 results in:

$$V_G \frac{dY_i}{dZ} - Y_i\ A\ C_L \sum_{i=1}^{n} k_{L_i}\ a \left(\frac{Y_i}{K_i} - X_{b_i} \right) = - k_{L_i}\ a\ C_L\ A \left(\frac{Y_i}{K_i} - X_{b_i} \right) \tag{5}$$

Equation 5 can be rearranged to obtain:

$$\frac{dY_i}{dZ} = \frac{A\ Y_i\ C_L}{V_G} \sum_{i=1}^{n} k_{L_i}\ a \left(\frac{Y_i}{K_i} - X_{b_i} \right) - \frac{A\ C_L}{V_G} k_{L_i}\ a \left(\frac{Y_i}{K_i} - X_{b_i} \right) \tag{6}$$

APPENDIX E

MAJOR EQUIPMENT SUMMARY

MAJOR EQUIPMENT SUMMARY

ENTRAINED BED REACTOR SYSTEM

Description	Number Req'd.	Size	Design Temp., °F/Press., psig	Material
		Reactors		
F-T Reactor	2	13 ft ID x 111 ft T-T w/29,000 ft^2 cooling coils	640/450	C-1/2 Mo w/C-1/2 Mo tubes
		Other Vessels		
Catalyst Receivers	2	30 ft OD x 40 ft T-T w/cyclones	640/435	C-1/2 Mo
Catalyst Hoppers	4	15 ft OD x 30 ft 8 in T-T	640/450	C.S.
Quench Towers	2	27 ft OD x 80 ft T-T w/4 sieve trays and 3 pans	430/410	316L S.S.
		Heat Exchangers		
Comb. Feed vs. Circ. Oil	2	51,000 ft^2	410/450-Sh 430/450-T	316L-lined 316 tubes
BFW vs. Circ. Oil	2	47,500 ft^2	430/450-Sh 335/75-T	316L lined 316 tubes
BFW vs. Quench Vapor	2	27,500 ft^2	330/450-Sh 285/75-T	316L lined 316 tubes
		Pumps		
Circ. Oil to BFW Preheat	2	24,100 GPM - 1750 HP		
Circ. Oil to Comb. Feed Exch.	16	7,050 GPM - 450 HP		
		Other		
Structural Steelwork	2	350 tons		
Standpipe	2	50 in ID x 75 ft +2 Slide Valves	640/450	1-1/4 Cr-1/2 Mo
Transfer Line	2	80 in ID x 50 ft	640/450	1-1/4 Cr-1/2 Mo

APPENDIX E (Continued)

MAJOR EQUIPMENT SUMMARY

TUBE-WALL REACTOR SYSTEM

Description	Number Req'd.	Size	Design Temp., °F/Press., psig	Material
		Reactors		
F-T Reactors	52	16 ft ID x 60 ft T-T 106,300 ft^2 tube S.A.	690/60-Sh 690/450-T	C.S.-Sh C-1/2 Mo-T
		Other Vessels		
Dowtherm Receiver	52	10 ft ID x 12 ft 7 in T-T	690/100	C.S.
		Heat Exchangers		
Feed/Effluent	4	21,490 ft^2	630/450-Sh 690/450-T	C-1/2 Mo, 304L lined 316-T
Steam Generator	52	3,210 ft^2	690/60-Sh 540/650-T	C.S.
		Pumps		
Dowtherm Circ. Pump	52	1030 GPM - 20 HP		

APPENDIX E (Continued)

MAJOR EQUIPMENT SUMMARY

SLURRY REACTOR SYSTEM

Description	Number Req'd.	Size	Design Temp., °F/Press., psig	Material
		Reactors		
F-T Reactors	13	14 ft ID x 27 ft T-T w/9800 ft^2 cooling coils	580/450	C-1/2 Mo
		Other Vessels		
Catalyst Hopper	1	9 ft ID x 15 ft 9 in T-T	500/450	C.S.
		Heat Exchangers		
Feed Effluent	18	4530 ft^2	515/450-Sh 465/450-T	304L lined 316 S.S.
Steam Generator	18	1080 ft^2	640/650-Sh 580/450-T	C.S. K.C.S.
		Pumps		
Oil Circ. Pump	18	2000 GPM - 50 HP		

APPENDIX E (Continued)

MAJOR EQUIPMENT SUMMARY

EBULLATING BED REACTOR SYSTEM

Description	Number Req'd.	Size	Design Temp., °F/Press., psig	Material
		Reactors		
F-T Reactors	20	14 ft ID x 30 ft T-T	600/450	C-1/2 Mo
		Other Vessels		
Vapor/Liquid Separator	20	14 ft ID x 15 ft T-T	600/450	C.S.
		Heat Exchangers		
Feed/Effluent	20	4,740 ft^2	535/450-Sh 600/450-T	304L lined 316
Steam Generator	20	11,750 ft^2	640/650-Sh 600/450-Sh	C.S. K.C.S.
		Pumps		
Oil Circ. Pump	20	21,800 GPM - 1500 HP		

APPENDIX F

EBULLATING BED REACTOR DESIGN

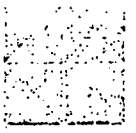

CHEM SYSTEMS INC.
747 Third Avenue, New York, N.Y. (10017)
Telephone (212) 421-9460 Telex 224649

September 15, 1979

Ms. Mary L. Reikena
UOP Process Division
20 UOP Plaza
Algonquin & Mt. Prospect Roads
Des Plaines, Illinois 60016

Dear Mary:

Chem Systems is pleased to submit herein two conceptual designs for liquid phase Fischer-Tropsch reactor systems per specifications in your letter of August 7. In the first case a Lurgi-type feed gas is processed, while a K-T type gas is employed in the second design. In both cases it is assumed that the reaction product slates provided by UOP are obtained in a single reactor pass instead of the 1/1 recycle/fresh feed scheme originally proposed by UOP. Two other assumptions that were incorporated into our design are:

- Catalyst volume was determined by employing a space velocity of 300 hr^{-1} for the once-through cases. This is one-half of the space velocity originally proposed for the recycle case.

- Circulating oil composition is the same for both cases and equivalent to the resulting equilibrium liquid obtained by flashing the K-T case product slate at the reactor conditions.

There are also two process options that are open to UOP's discretion. They are:

- Temperature of boiler feedwater charged to the oil cooler. This will ultimately set the quantity of 500 psig steam generation.

- The cooling medium(s) and flowscheme to be employed in the final cooling of the product gas stream.

The attached package includes process flow scheme, material balance, reactor effluent vapor cooling curve and major equipment descriptions for each of the two cases examined. Hopefully, the information provided here is in sufficient detail to enable preliminary review of the process, and also enable UOP to determine the proper way to cool the reactor effluent gases. Although a detailed analysis of gas recycle arrangements were not performed, a table

has been included that shows speculative process modifications that would be required to process the two feed gases in this manner. Interestingly enough, the same reactor could be employed for both feed gases whether operating in the once through mode or with recycle gas, namely 14' ID x 70' T-T. Also included is a possible flowscheme for catalyst reduction.

During the development of the two designs, communication between Chem Systems and UOP was quite helpful in arriving at the final flowschemes. Development of these final flowschemes is briefly described below.

Our development of the processes began with the Lurgi feed gas employing a once-through arrangement and assuming that the product slate of the recycle case could be obtained. When this product slate was flashed at the reactor exit conditions no liquid material resulted. In fact, computer results showed the gas stream to be superheated by 210°F. To insure that reactor product vapors would be at their dew point, and an equilibrium liquid (which would be used as circulating liquid) did exist, initially it was assumed that a portion of the liquid product stream was required as recycle back to the reactor. This situation would force more oil into the reactor vapor product until the dew point temperature was increased to 510°F. Under these conditions the oil cooler duty was only 25.0 instead of the 43.3 MM Btu/hr attained in the ultimate design. This represents a substantial reduction in the quantity of reaction heat that could be recovered at high temperature levels in the oil cooler and shifted a large portion of the reaction heat into the gas cooling train. Of course, increasing the reactor pressure would increase the vapor dew point temperature until it was 510°F. Although this would leave the bulk of reaction heat recovery in the oil cooler, the required operating pressure would be above the 500 psig design constraint given. Combinations of increased operating pressure with smaller recycle quantities of liquid product were envisioned but were not felt to be warranted since UOP assured that the reaction product would produce an equilibrium liquid.

Apparently, the actual breakdown of the reaction products contains some materials quite heavier than the average properties provided for the 750+ product cut. These are the materials that UOP has assured will not flash, and they also provided an equilibrium composition for circulating liquid. Production of this stream is extremely small. A review of this composition poses a new problem; is this material suitable as the circulating liquid? The liquid phase reaction system requires a seal flush return for pump seals and wear rings that would ultimately be returned to the circulating liquid. Although the required quantity of this stream is very small, (probably a small portion of the liquid product from the separator) it is much larger than the quantity of flash liquid produced and therefore the circulating would be much lighter than assumed. Thus, the circulating oil composition for the Lurgi case was assumed to be the same as for the K-T case.

Included below are some general comments in regard to the reaction catalyst. First, it may be necessary to install a sulfur guard chamber depending upon the resistance of the catalyst and the sulfur content of the feed gas. This unit could be put after the feed/effluent exchanger and may require an additional heater to attain an adequate temperature for the sulfur guard system. Gas temperature into the Fischer-Tropsch reactor is not that critical since the small sensible heat requirement for the feed gas required for heating or cooling this gas can easily be absorbed by the large bulk of circulating liquid. Feed/effluent exchanger surface could also be decreased if feed gas preheat is reduced below 470°F, without a noticeable change in the reactor system. This can be easily evaluated with the help of the enclosed reactor effluent cooling curves.

Also, a catalyst reduction system will be required and will need ample supply of hydrogen and nitrogen. The system will require as a minimum a feed/effluent exchanger and an additional heater to reach reduction temperatures. If large quantities of reduction gases are required it may be necessary to add a recycle compressor and cooler to insure adequate recycle of the reduction gas and also that this material is sufficiently dry enough for reuse. A typical scheme appears in Figure 5. The catalyst reduction will normally be started before oil circulation is initiated because reduction will take more time than system heat-up. After the reactor is isolated from the main circulating oil supply, process feed gas supply, and main reactor discharge lines, reactor heat-up can begin with nitrogen. Once a suitable temperature is reached (about 400°F), hydrogen flow is begun and nitrogen is shut off. The temperature is gradually increased to reduction temperature and maintained for the reduction period. Catalyst vendors will specify the hydrogen flow rates, reduction temperature and duration. The reduction is usually carried out at atmospheric pressure. At the end of the reduction period, nitrogen flow replaces the hydrogen, and the system temperature is lowered to reaction temperature. The catalyst is now reduced and ready for use. Simultaneously, the circulating oil system must be started up so that the system can be pressurized and the reaction started.

Depending upon the characteristics of the catalyst and the ultimate operation of the process, it may be necessary to install filters on the circulating oil to remove attrited catalyst.

The use of smaller catalyst particles was reviewed and found that they may not be economically justified for this system. By halving the catalyst particle diameter, to 1/32", the catalyst activity was assumed to increase fourfold; simply in direct proportion to surface area. Although this dramatically reduces the catalyst requirement, oil circulation, and possibly reactor diameter, the circulating oil ΔT and gas expansion in the reactor become too large.

We appreciated this opportunity to provide assistance to UOP as part of its support services contract to DOE. I hope sufficient information has been provided to carefully analyze the designs. Please do not hesitate to contact Marshall or myself should any additional information be required.

Very truly yours,

William A. Brophy
Process Technologist

WAB:mem

cc: MEF, RLM

Table of Enclosures

FIGURE I - CASE I PROCESS FLOW SCHEME

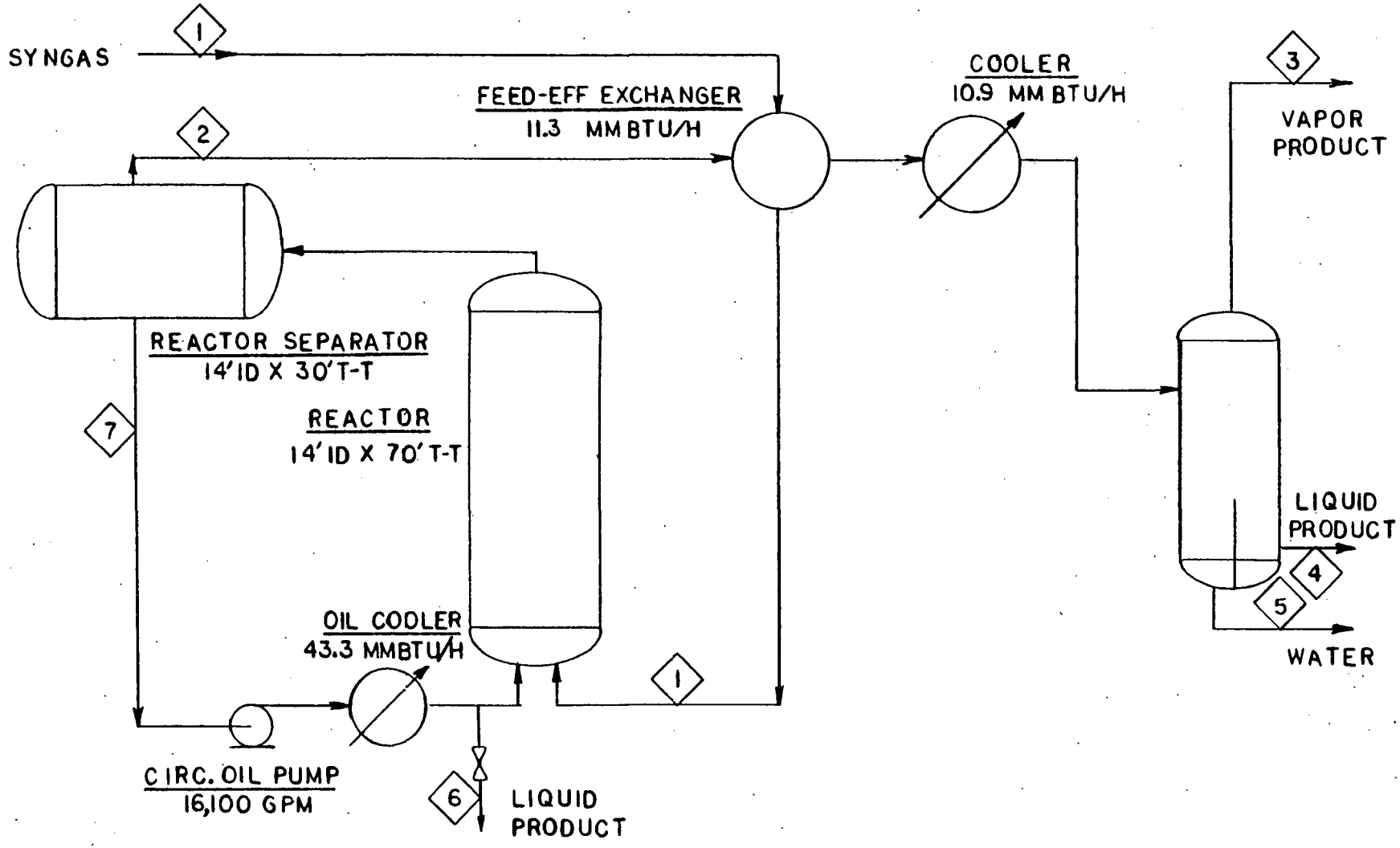

TABLE 1

Case I -- Lurgi Feed Gas - Once-Through-Material Balance (In Lb Mol/Hr)

Component	Mol. Wt.	1 Fresh Feed	2 Reactor Vapor	3 Vapor Product	4 Liquid Product	5 Water Product	6 Heavy Liq. Prod.	7 Reactor Liquid
Hydrogen	2.016	2,262.9	779.8	779.5	0.3			31.6
Carbon Monoxide	28.011	1,132.0	116.4	116.3	0.1			136.9
Carbon Dioxide	44.100	126.3	332.0	330.9	1.1			1,085.1
Methane	16,043	678.5	722.5	721.1	1.4			24.1
Ethylene	28.054		18.5	18.4	0.1			15.0
Ethane	30.070		20.0	19.8	0.2			18.8
Propylene	42.081		22.8	22.3	0.5			35.3
Propane	44.097		6.1	6.0	0.1			9.7
Butylene	56.108		18.2	17.1	1.1			48.9
Butane	58.124		3.5	3.3	0.2			9.7
C_5-375°F	98.7		56.36	28.52	27.84			637.6
375-750°F	209.8		8.53	0.01	8.52			3,350.0
750°F+	362.0		0.14	-	0.14			13,325.3
Water	18.016		593.9	11.9	0.1	581.9		287.2
Total, MPH		4,199.7	2,698.73	2,075.13	41.70	581.9	negligible	19,015.2

FIGURE 2 - CASE II PROCESS FLOW SCHEME

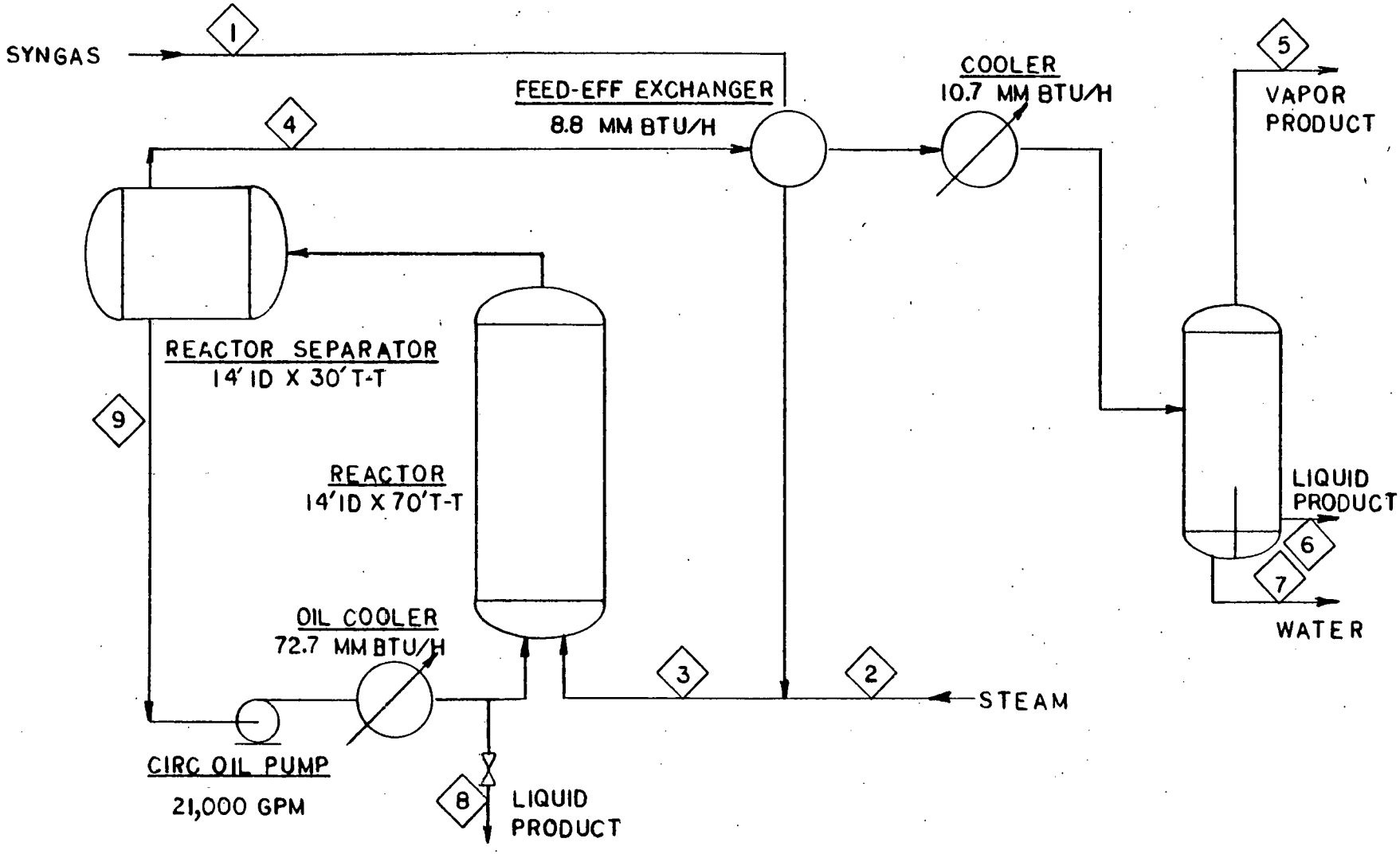

TABLE 2

Case II -- K-T Feed Gas - Once-Through-Material Balance (In Lb Mol/Hr)

Component	Mol. Wt.	1 Fresh Feed	2 Steam Addition	3 Combined Feed	4 Reactor Vapor	5 Vapor Product	6 Liquid Product	7 Water Product	8 Heavy Liq. Prod.	9 Reactor Liquid
Hydrogen	2.016	1,319.7		1,319.7	47.7	47.6	0.1			40.8
Carbon Monoxide	28.011	2,075.1		2,075.1	207.5	207.0	0.5			177.0
Carbon Dioxide	44.100	105.4		105.4	918.5	908.2	10.3		0.1	1,403.1
Methane	16,043				23.2	23.0	0.2			31.1
Ethylene	28.054				9.5	9.3	0.2			19.4
Ethane	30.070				10.3	10.0	0.3			24.3
Propylene	42.081				13.5	12.6	0.9			45.7
Propane	44.097				3.6	3.3	0.3			12.6
Butylene	56.108				12.3	10.2	2.1			63.2
Butane	58.124				2.3	1.9	0.4			12.6
C_5-375°F	105.44				57.7	14.7	43.0		0.1	824.5
375-750°F	225.92				24.9		24.9		0.4	4,331.7
750°F+	362.0				1.6		1.6		1.8	17,230.4
Water	18.016		350.0	350.0	530.8	7.2	0.2	523.4		371.4
Total, MPH		3,500.2	350.0	3,850.2	1,863.4	1,255.0	85.0	523.4	2.4	24,587.8

Figure 3
Reactor Effluent Cooling Curve
Case I - Lurgi Feed Gas

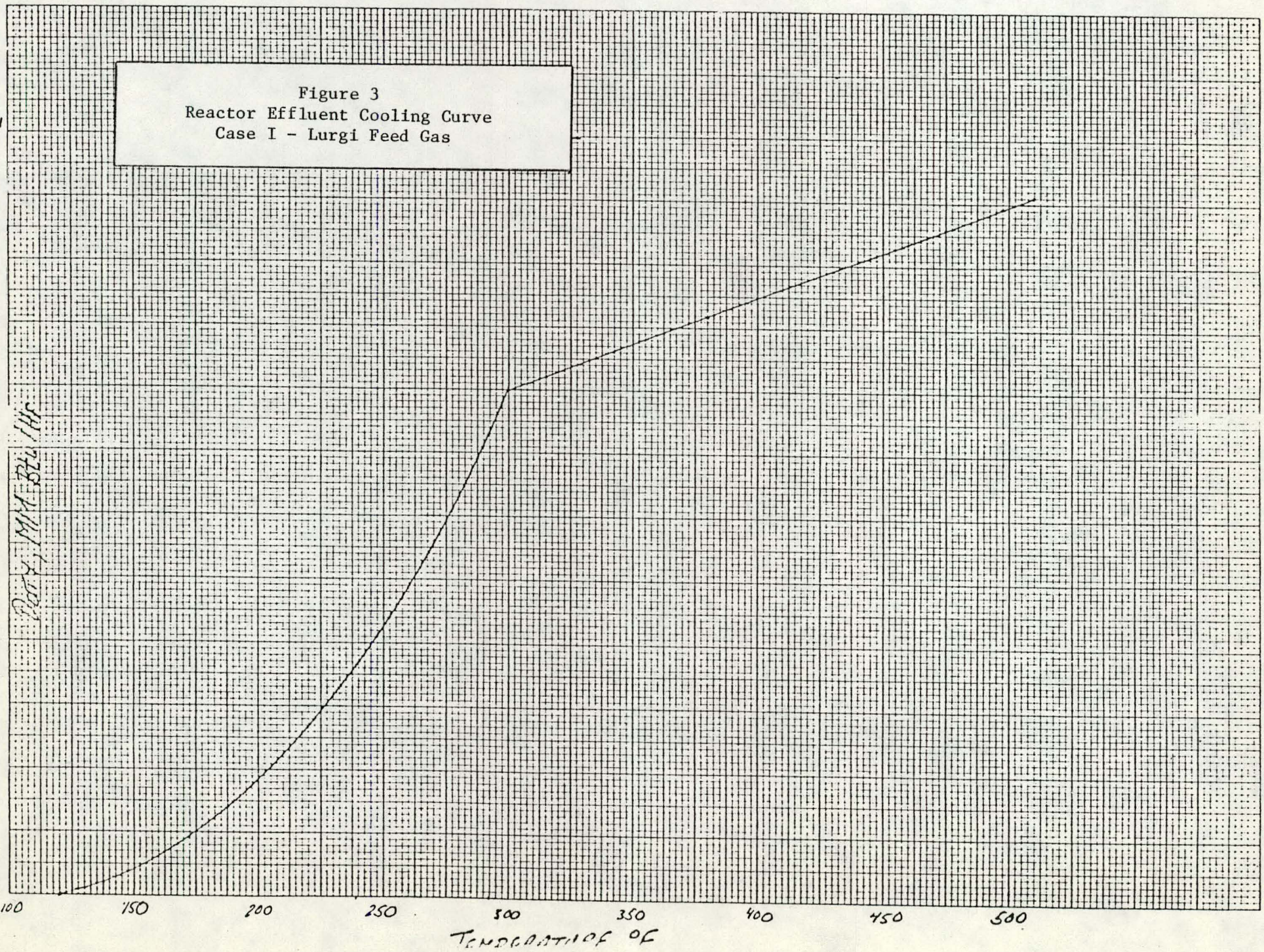

F-11

Figure 4
Reactor Effluent Cooling Curve
Case II - K-T Feed Gas

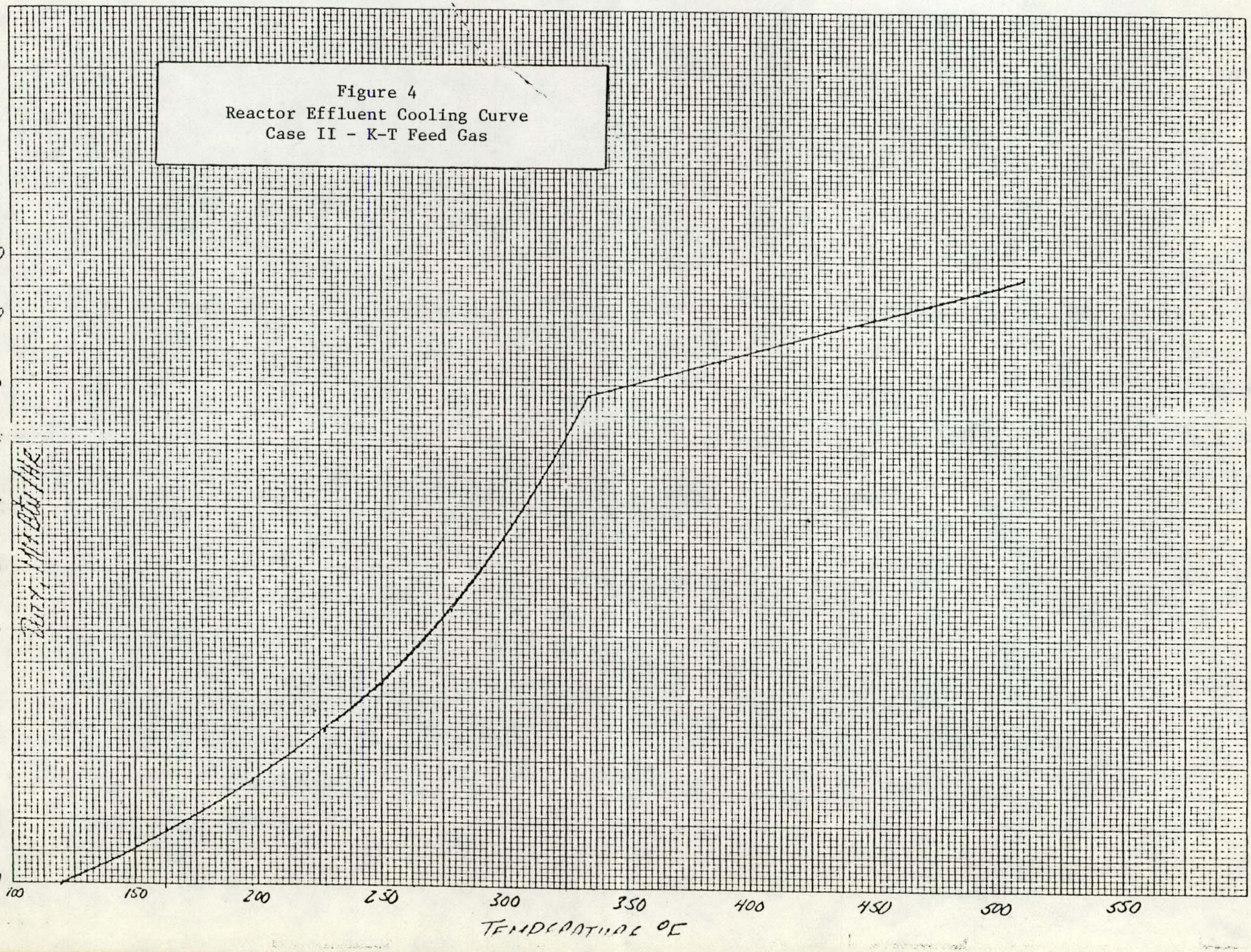

Table - 3
Major Equipment Description

Item	Case I Lurgi Feed Gas	Case II K-T Feed Gas
Reactor		
Dimensions	14'ID x 70' T-T	14'ID x 70' T-T
VHSV, hr^{-1}	300	300
Catalyst Size	1/16" Spheres	1/16" Spheres
Catalyst Volume, ft^3	5,305	4,864
Design Pressure and Temperature	350 psig @ 600°F	
Oil Cooler		
Duty, MM Btu/hr	43.3	72.7
Oil Temp In/Out, °F	510/499	510/496
Steam Generation Pressure	500 psig (470°F)	500 psig (470°F)
Design Pressure Oil/Steam Side	350/550 psig	350/550 psig
Design Temperature Oil/Steam Side	600/525°F	600/525°F
Circulating Oil Pump		
Quantity	1 + spare	1 + spare
Horsepower	750	1,000
Head	50 psi	50 psi
Flowrate, GPM	16,100 (17,700) Design	21,000 (23,000) Design
Reactor Separator		
Dimensions	14'ID x 30' T-T	
Design Pressure and Temperature	350 psig @ 600°F	
Feed/Effluent Exchanger		
Duty, MM Btu/Hr	11.3	8.8
Reactor Effluent Temp In/Out, °F	510/268	510/296
Cooling Curve, Figure #	3	4
Feed Gas Temp In/Out, °F	120/470	120/470
Design Pressure and Temperature	350 psig @ 600°F	
Final Cooler(s)		
Duty, MM Btu/hr	10.9	10.7
Reactor Effluent Temperature In/Out, °F	268/120°F	296/120°F
Cooling Curve, Figure #	3	4
Cooling Medium	BFW and/or CW	
V/L Separator		
Dimensions	4.5'ID x 12' T-T	
Design Pressure and Temperature	350 psig @ 150°F	

Table 4

Major Process Parameters Changes
(Speculative 1/1 Feed/Recycle Gas Case)

	Case I Lurgi Feed Gas	Case II K-T Feed Gas
VHSV, hr^{-1}	600	600
Oil Cooler Duty, MM Btu/hr	42.1	71.6
Oil ΔT, °F	10.7	13.8
Effluent Gas Cooling MM Btu/hr (510°F → 120°F)	33.7	37.0
Feed Gas Heating, MM Btu/hr (120 → 470°F)	11.3	8.8
Recycle Gas Heating, MM Btu/hr (120 → 470°F)	11.3	8.8
Recycle Compressor, HP (260 → 320 psig)	540.0	450.0
Steam Addition, Lbs/Hr		12,611